Gareth L Evans

Doctor of Philosophy in Medicine

RIG-I-like receptors (RLRs): Viral sensors that recognize Coxsackieviruses

Supervised by Dr Martha Triantafilou

and Professor Kathy Triantafilou

Submitted September 2012

Acknowledgements

To my supervisors, Dr Martha Triantafilou and Professor Kathy Triantafilou, thank you for your support and friendship throughout my PhD, I would not have achieved this without you. Thanks are also needed for my fellow lab members, particularly Edward Richer and Fred Gamper, who where a great help during the first few years of my thesis. And finally a big thank you to the University of Sussex and Cardiff University, both great institutions to have completed my studies.

Abstract/Summary

The innate immune system is a vital part of the body's defences against viral pathogens. RIG-I and MDA5 belong to the retinoic acid inducible gene-I (RIG-I)-like receptors (RLRs) family and function as cytoplasmic PRRs that are involved in the elimination of actively replicating RNA viruses. Their location and their differential responses to RNA viruses emphasises the complexity of the innate detection system. RIG-I and MDA5 contribute to antiviral signalling in different ways depending on the virus involved.

Coxsackieviruses are positive sense, single-stranded RNA viruses belonging to the *Enterovirus* genus of the Picornaviridae family. They cause many serious diseases, including viral myocarditis (which can lead on to dilated cardiomyopathy), aseptic meningitis, and pancreatitis. In order to identify which RLR recognises these viruses and which RNA species triggers RLR activation during Coxsackievirus infection, viral ssRNA and replicative intermediates of Coxsackievirus RNA as well as synthetic dsRNA were used in this study. The results revealed that MDA5 recognises not the genomic ssRNA but the dsRNA generated by the replication of these viruses. Confocal microscopy provided unique evidence between the relationship of viral dsRNA and MDA5 while cytokine assays using HEK-MDA5 cells showed a strong immune response to Coxsackievirus and the dsRNA intermediates. This shows very strong evidence that MDA5 is a key sensor of the dsRNA intermediate of Coxsackieviruses.

As RIG-Is role in Coxsackie recognition still needs to be verified Huh7 and Huh7.5.1 cells were used and showed no difference in immune response in the absence of RIG-I to Coxsackievirus infection, as well as the isolated ssRNA, suggesting that the VPg group present on the RNA blocks recognition. Furthermore immunoprecipitation experiments showed that in response to Coxsackievirus stimulation, RLRs

homodimerise as well as heterodimerise with LGP2, potentially upregulating their activity as a possible mechanism for viral detection.

The data presented here show a much clearer role for RLRs in Coxsackievirus infection, while opening new questions as to MDA5s role in the diseases caused by Coxsackieviruses, as well as the specifics behind dimerisation of the RLRs.

Contents Page

Chapter 1: Introduction

Chapter 2: Materials and Methods

Chapter 1: Introduction

1.1: Coxsackie Virus

Coxsackieviruses are part of the enterovirus genus in the picornavirus family, along with Poliovirus, Echovirus and others. Infection with enteroviruses usually results in an asymptomatic infection without causing any significant disease. However infection can lead to serious illness, especially in infants and immuno-compromised individuals.

In 1948 an unknown virus was isolated from the faeces of a child with febrile illness during a poliomyelitis epidemic in the Hudson River town of Coxsackie, New York [5;6]. The isolates were obtained by inoculating suckling mice with the virus and showed a pathogenesis clearly different of that of Poliovirus, replicating readily in the mice [7]. The virus was named Coxsackievirus and later became part of the group A Coxsackieviruses (CVA). The following year the first Coxsackievirus group B (CVB) member was isolated from a case of aseptic meningitis [8]. The isolated CVA caused myositis with flaccid hind limb paralysis in newborn mice, while the new isolate was separated into the new group CVB as it resulted in spastic paralysis and generalised infection with myositis as well as involvement of the heart, pancreas, brain and brown fat [9]. The two groups were separated primarily by the ability to induce flaccid paralysis in suckling mice (Group A), or not (Group B).

1.1.1: Symptoms and Diseases Associated with CVB

Enterovirus transmission is via the faecal oral route or respiratory. The faecal-oral route is more likely in areas with poor sanitary conditions, while respiratory transmission is more prominent in more developed countries. While the major route of CVB infections in infants and children is faecal-oral, vertical transmission from mother to the infant is

also possible [10]. CVB infections in humans range from asymptomatic infections to chronic, debilitating diseases and are associated with inflammatory disorders of the heart, pancreas and central nervous system (CNS) and are mostly associated with pleurodynia and myocarditis [11]. The specific symptoms and their rate of occurrence of CV in infants include lethargy, vomiting, anorexia, fever (90%), aseptic meningitis (50%), irritability (35%), non-specific rash (20%) and encephalitis, myocarditis, pancreatitis and pneumonia (1-3%) [12]. Of all enteroviruses CVB causes 20-30% of neonatal infections in industrialised countries [13].

In the heart CVB3 can produce myocarditis that can lead to chronic dilated cardiomyopathy. Myocarditis is inflammation of the myocardium associated with damage unrelated to ischemic injury. Evidence that CVB causes myocarditis comes from isolation of the infectious virus as well as its nucleic acid from hearts of patients with myocarditis, in particular neonatal and paediatric cases [14;15]. Lesions on the heart appear to be due to both direct viral lysis and the immune response to the virus. Persistent viral infection triggers an immune response that damages the cells and leads to myocarditis. Auto-antibodies and auto-reactive T-cells have both been implicated in heart disease induced by enteroviruses, with cases of pathogenic immune responses being directed at myocytes that contain the virus as well as antigenic mimicry. In antigenic mimicry T-cells or B-cells that are directed against the virus cross-react with cardiac antigens that are exposed later in the infection. Lymphocytes that recognise virus-positive cardiocytes may also play an important role in myocardial injury [16]. The damage contributed by viral lysis and the immune response varies between cases. The CVB3 RNA persists in the heart of patients with chronic myocarditis even in the absence of the virus. It is hypothesised that the non-productive genome of the virus remains in the myocardium until a subsequent insult associated with cellular

proliferation activates gene expression [17]. Viral myocarditis can also mimic acute myocardial infarction by producing direct inflammation o the myocardium [18].

Acute viral myocarditis leads to dilated cardiomyopathy in a significant number of cases. The infecting virus initiates the disease and then persists, inciting ongoing cardiac damage [19]. Part of what may cause dilated cardiomyopathy in CVB infection is that the CVB 2A protein cleaves dystrophin, a key protein component in the heart muscle that is frequently mutated in inherited forms of cardiomyopathy. In dilated cardiomyopathy the heart becomes large with impaired function and leads to heart failure. One of the characteristics is little or no inflammation. Enteroviruses are capable of persisting in patients with developmental cardiomyopathy until the end stage of the disease and persists in the myocardium in a significant proportion of patients with end-stage dilated cardiomyopathy in the absence of a continuing cell-mediated or humoral immune response [20]. CVB evolves into a slowly replicating form of the virus during infection capable of establishing a low-grade infection of the heart [21]. While one of the major symptoms associated with CVB, only 3.2% of CVB infections result in overt cardiac signs or symptoms. However children that die of CVB frequently have signs of myocarditis [22].

CVB3 infection also leads to acute and chronic pancreatitis in some patients and like myocarditis is due to both viral and host factors [23]. Infection of the pancreas induces a massive cellular infiltrate composed of natural killer cells, T-cells and macrophages and leads to the destruction of exocrine tissue. The physiological manifestations of pancreatic CVB infection are correlated to the viral tropism with the virus infecting acinar cells but sparing the islets of langerhans [24]. CVB3 can also infect neuronal

progenitor cells in the subventricular zone. This infection of the developing CNS leads to neurodevelopmental defects in foetal infection [25].

1.1.2: Structure of Picornaviruses

Enteroviruses differ from other picornaviruses based on physical properties such as their buoyant density in caesium and stability in weak acid. They are resistant to common laboratory disinfectants, including 70% ethanol, isopropanol, dilute Lysol and quaternary ammonium compound. They are also insoluble to lipid solvents including ether and chloroform and soluble in detergents at room temperature. Enteroviruses can be deactivated by formaldehyde, gluteraldehyde, strong acid, sodium hypochlorite and free residual chlorine, as well as by UV light. They are also relatively thermostable and most are inactivated at 42°C [26].

Picornaviruses are amongst the simplest RNA viruses with a highly structured capsid spherical in nature with a diameter of around 30 nm. The protein shell contains a naked single positive stranded RNA genome. They lack lipid envelopes and as a result their infectivity is insensitive to lipid solvents. Picornaviruses must be acid stable enough to pass through the stomach to reach the intestine so retain infectivity at pH 3.0 and lower [27].

The capsid of picornaviruses is composed of four structural proteins; VP1, VP2, VP3 and VP4, one copy of each together forming the protomer building block that makes the capsid. 60 copies of the four capsid proteins VP1-VP4 form an icosahedraly symmetric shell [28]. Each triangular protomer has VP1, VP2 and VP3 on the external face, with VP4 on the inner surface. While VP1, VP2 and VP3 show no sequence homology, they all have the same topology consisting of an 8-stranded anti-parallel β-barrel. At the 5-fold axis of symmetry in the icosahdral pattern there is a star-shaped plateau (or mesa) that is surrounded by a deep depression known as the canyon. There is also another protrusion at the 3-fold axis. The canyon of CVB3 is not as pronounced as that of Poliovirus and Rhinovirus. There is a large pocket factor at the base of the canyon that has been shown to contain a lipid in Coxsackieviruses and may be responsible for acid stability [29]. The main differences between VP1, VP2 and VP3 are the loops connecting the β-sheets and the N and C-terminal sequences that extend from the β-barrel domain. These amino acid sequences give each picornavirus its distinct morphology and antigenicity. Upon receptor binding at physiological temperatures the virus undergoes a conformational change from 160S into an altered form known as the 135S or A Particle (S is the sedimentation property) [30]. The A particle is not infectious and conformationaly altered with both the VP4 and the N-terminal of VP1 becoming externalised rather than being internal [31]. The antigenicity and sensitivity to proteases of the virus also changes [32]. The N-terminus inserts into the cell membrane, forming a pore through which its viral RNA can enter the cell, while

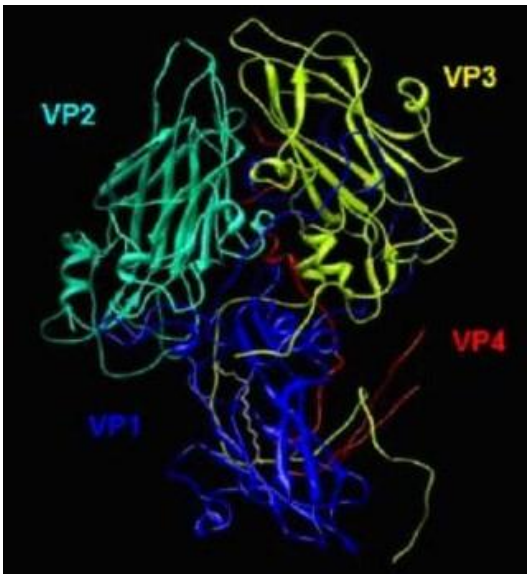

Figure 1.1 - Structure of CVB3 VP1 – VP4. VP1 (blue) VP2 (turquoise) and VP3 (yellow) lie on the surface of the capsid, with VP4 (red) being internal [2].

VP4 also partitions into the membrane. After conversion to 135S a second conformational change occurs in which the viral RNA is injected into the cell leaving an empty particle that sediments at 80S [33;34].

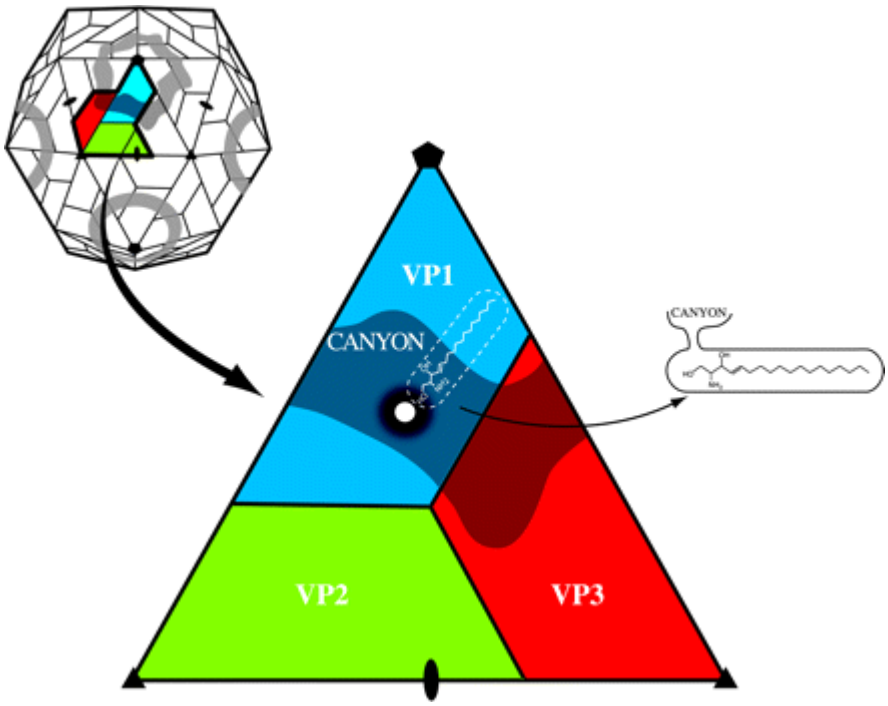

Figure 1.2 - Structure of the capsid surface. The diagram shows the positioning of VP1, VP2 and VP3 with the canyon displayed as the shadowed area, the white dot the location of the entry to the hydrophobic pocket and the hydrophobic pocket shown by the white dotted line. Inside the hydrophobic pocket is the pocket lipid factor [35].

The genome of picornaviruses is a single positive stranded RNA molecule that is infectious because it is translated into viral proteins required for viral replication upon entry into the cell. The length of picornaviruses genomes varies between 7209 to 8450 bases depending on the virus. The CVB genome is 7.4 kb in length and functionally equivalent to eukaryotic messenger RNA (mRNA) [36]. The picornavirus RNA is unique in that it has a Virion Protein, genome linked (VPg) covalently linked at the 5' end. An O4-(5' uridylyl)-tyrosine linkage covalently joins the VPg cap to the 5' uridylate moiety with the tyrosine always being the third amino-acid from the N-

terminus. The VPg molecule varies from 22-24 amino-acids in length and is not included in the viral mRNA which is the only difference to the genome. It is not involved in infectivity and is removed by a host protein called “unlinking enzyme”. It is also present on nascent RNA chains of the replicative intermediate and on negative stranded RNA, suggesting it may be a primer for RNA synthesis. There is a 5’ non-coding region of picornaviruses that is long and highly structured and contains sequences that control genome replication and translation. It also contains the internal ribosome entry site (IRES) that directs translation of the mRNA by internal ribosome binding. The 3’ non-coding region is shorter and contains a pseudoknot that has been implicated in controlling viral RNA synthesis and a 3’ poly(A) tail [37].

The viral protein is translated from a single open reading frame (ORF) to form a single 200 kD polyprotein that is processed by proteolytic cleavages to generate individual viral proteins in equimolar amounts [38]. The polyprotein is cleaved during translation by viral encoded proteins so the full length product is never observed. The polyprotein is first cleaved into three sections, P1, P2 and P3. P1 contains the viral capsid proteins and P2 and P3 encode protein processing ($2A^{Pro}$, $3C^{Pro}$ and $3CD^{Pro}$) and genome replication (2B, 2C, 3AB, $3B^{VPg}$, $3CD^{Pro}$ and $3D^{Pol}$) [39].

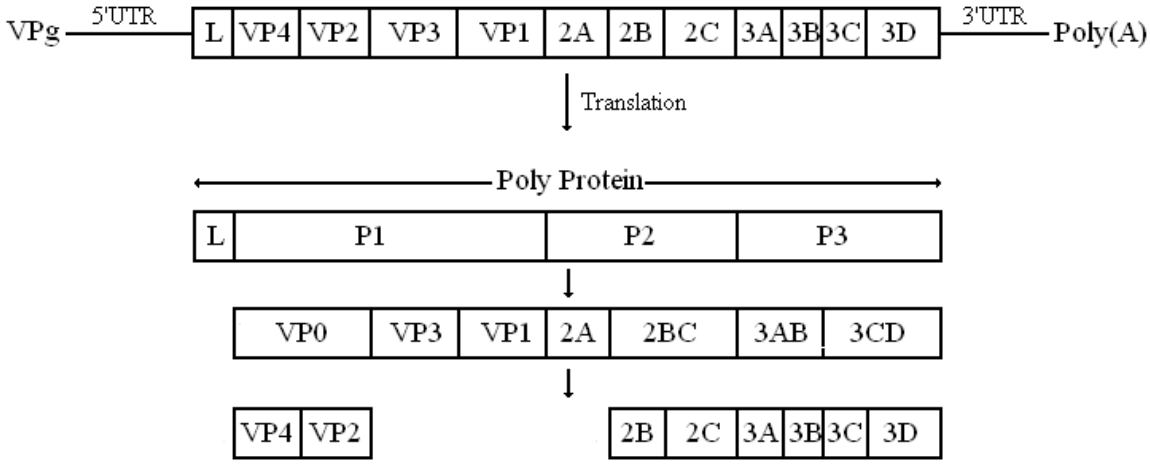

Figure 1.3 - Diagram to show processing of picornavirus viral genome. Adapted from [40].

1.1.3: Coxsackievirus and its Receptors CAR and DAF

The first step in viral infection is binding to specific receptors on cells and internalisation of viral components. CVB3 interacts with at least two receptors; Coxsackie-Adenovirus Receptor (CAR) and Decay Accelerating Factor (DAF also known as CD55). A receptor for CVB was first identified in 1985 by Mapoles *et al* which turned out to be CAR [41] and has since been determined as the main receptor for all 6 serotypes of CVB [42]. CAR is a member of the CTX family which promote cell adhesion and many of which are located in tight junctions so its role in the body appears to be in cell-cell contact formation [43]. In epithelial cells tight junctions control the flow of ions and macromolecules across the intact epithelium and divide the apical and basolateral compartments. CAR is absent from the apical surface of epithelial cells, but is located in these tight junctions where it associates with another tight junction protein ZO-1 [44]. Tight junctions are important as natural defence against invasion by microbial pathogens as many pathogens must breach the epithelial barrier to gain access

to the body and CARs location in the tight junction must act as an impediment to Coxsackie infection. The importance of localisation in the tight junction is highlighted by the number of pathogens that disrupt the tight junctions integrity such as *Clostridium perfringens, Helicobacter pylori* and Rotavirus [45]. CAR has high expression in the brain, pancreas and the heart with significant expression also in the testes and prostrate, which shows consistency with the tropism of CVB which infects via the GI tract and causes myocarditis, pancreatitis and meningeoencephalitis [46-48]. In the heart it is mainly expressed on intercalated discs, regions important to the hearts structural integrity and CAR is essential to normal development of the heart. Gene deletions lead to severe cardiac abnormalities and death in utero. It has also been suggested to be important in early development of the CNS and other tissues as well as being involved in cell proliferation [49]. There is a large amount of interest in CAR due its being a receptor for Adenovirus as increased expression could give greater sensitivity to Adeno-viral mediated gene therapy and make it more efficient [50].

DAF is a member of the Regulator of Complement Activation (RCA) gene family, which play a role in down regulation of complement activity at the cell surface [51]. It has been shown to be a cell surface receptor for CVB1, CVB3 and CVB5, as well as CVA21 and Echovirus 7 [52-54]. Some enteroviruses can also bind DAF and cause haemaglutination due to DAFs expression on erythrocytes [55]. DAF is expressed on the surface of polarized epithelial cells and like CAR is expressed in the heart [56;57]. Viral immunoprecipitation results have also shown that CVB3 and CVB5 can bind five other receptors, however, which receptors these are and their role in CVB infection remains unclear [59].

Both of the receptors are involved in binding CVB to the cell surface but their roles differ in comparison to each other and depend on the strain of virus. Binding of CVB to CAR and DAF creates a tight association that prevents acid elution of the virus. However only binding to CAR leads to A-particle formation of the virus, not though binding DAF, suggesting that CAR and not DAF is capable of triggering the conformational change that leads to uncoating and RNA release from the viral capsid. While CVB bound to DAF does not elute, neither does it undergo any form of conformational change and remains in its intact infectious state. However binding to DAF does increase susceptibility to infection suggesting that once bound to DAF the virus becomes available for further interactions with CAR that lead to infection [60]. Interestingly in Adenovirus infection CAR is insufficient for viral uptake, but facilitates attachment and uptake through Integrins avβ3 and avβ5 [61]. Most picornaviruses use the canyon-like feature on their surface to bind to cellular receptors such as CAR. Binding in the canyon causes destabilisation of the virus and thus initiates the uncoating process [62]. DAF binds outside of the canyon, lying across it and interacting with VP2 rather than entering the canyon and therefore does not cause the disruption required for uncoating to begin [63;64].

While CAR is the main receptor for binding and uncoating all strains of CVB, the role of DAF varies dependant on the strain. Rhabdo-myosarcoma (RD) cells are a cell line normally resistant to CVB3 infection, however passing CVB3 through RD cells creates a new strain (CVB3-RD) that is capable of infecting RD cells while still maintaining the ability to infect HeLa cells [65]. CVB3-RD is capable of binding DAF, while the wt CVB3 strain Nancy cannot bind DAF transfectants. As well as this, the use of anti-DAF does stop CVB3-Nancy from binding HeLa cells which have both DAF and CAR [66;67]. Haemaglutinating CVB3 (CVB3-HA) can be bound by CHO transfected with

DAF, while wt CVB3 does not become bound and in neither cases does infection occur, further demonstrating the importance of CAR in infection [68]. However strains of CVB that can bind DAF infect polarised cells more efficiently than those unable to attach to DAF [69]. The DAF binding ability of CVB strains appears to correlate with the presence of an epitope on the VP2 capsid protein [70].

CAR is a 46 kDa transmembrane glycoprotein of 365-amino acids in length with a short leader, a 222-amino acid extracellular domain, a single membrane spanning helical domain and a 107 amino acid intracellular domain [71;72]. The intracellular domain contains a site for palmitylation, potential sites for phosphorylation and furin cleavage and a C-terminal hydrophobic peptide motif that interacts with PDZ-domain proteins. The extracellular domain is composed of two immunoglobulin (IG)-like domains, D1 and D2 [73]. Both Coxsackie virus and Adenovirus bind the N-terminal D1 domain, however they recognise different parts of D1 [74]. It is the D1 domain that is inserted into the canyon of CVB [75] with capsid proteins VP1, VP2 and VP3 all interacting with D1, with the majority of the interactions being through VP1 [76]. The extracellular domain of CAR with the membrane tether is sufficient for CAR to support CVB infection [77]. DAF has 5 domains, four of which are short consensus repeats (SCRs) and a C-terminal serine/threonine (S/T)-rich region ending in a glycosylphosphatidyl inositol (GPI) anchor. The N-terminal SCR1 does not appear to be involved in CVB binding, while the other four domains are necessary. The S/T region is required for binding but does not bind the virus itself. SCR2 and SCR3 form the main interaction with VP2, with VP3 also mainly crossing the canyon. SCR4 also binds the virus at the carboxyl end [78;79].

1.1.4: Picornavirus and Coxsackievirus Replication and Life Cycle

Replication occurs in the cytoplasm so once the virus has bound CAR, become uncoated and its RNA genome inserted into the cell, the viral replication process can start. The single positive stranded RNA is copied to create a negative stranded intermediate and then additional positive strands are copied from the negative strand to build up the quantity of RNA for translation. There are three forms of RNA in picornavirus infections, single-stranded RNA (ssRNA), replicative intermediate (RI) and replicative form (RF). ssRNA is almost exclusively positive, negative stranded ssRNA has never been detected. RI is full length positive stranded RNA from which 6-8 nascent negative strands are attached, although a negative strand with positive nascent strands has also been detected. RF has a double stranded structure with one copy each of a positive and negative strand. This is essentially a dsRNA intermediate in the replication process. $3D^{Pol}$ is a primer-dependant enzyme that copies enterovirus RNA in the presence of an oligo (U) primer and VPg. Translation occurs through the 40S subunit binding the IRES. Both translation and replication of the mRNA into negative strands and the polyprotein can happen at the same time. It is hypothesised that cloverleaf structures in the 5' non-coding region regulate which occur with $3CD^{Pro}$ binding the cloverleaf and blocking translation while promoting RNA synthesis. However despite this there is evidence that the two mechanisms do occasionally collide [80].

The viral proteins are synthesised from the polyprotein precursor, which is cleaved nascently by $2A^{Pro}$ and $3C^{Pro}$ or $3CD^{Pro}$. Among the proteins synthesised are viral RNA-dependant RNA polymerase and accessory proteins for genome replication and mRNA synthesis. P1 is cleaved to form the immature protomers which assemble to form a

pentamer structure. New single positive stranded RNA associates with the pentamer to form an infectious virion. The overall life cycle is around 5 to 10 hours depending on the virus. As the cell loses its integrity the new viruses are released [81].

During the life cycle the host cell undergoes certain changes induced by the virus to create a more efficient state for viral replication. Proliferation and rearrangement of intracellular membranes in infected cells leads to the destruction of the endoplasmic reticulum (ER) and the Golgi as well as causing the cytoplasm to fill with double membrane vesicles. RNA replication occurs on the surface of these vesicles and localisation there ensures high levels of the replication components in the same location and promotes oligomerisation. Three CVB3 proteins inhibit protein secretion, 2B and 2BC by inhibiting protein trafficking through the Golgi while 3A also destroys the Golgi. This occurs early in the viral life cycle, with 2BC having stronger anti-secretory effects than 2B suggesting it may be important in early immune evasion [82]. 2B, when expressed, localises to the ER and also to the Golgi, although to a lesser extent. It modifies intracellular Ca^{2+} homeostasis by decreasing the Ca^{2+} of both the ER and Golgi without affecting is uptake [83]. 2B does this by forming pores in the ER and Golgi membranes resulting in conditions that favour the virus as well as suppressing apoptotic responses [84]. By disrupting the Golgi complex, viral protein 3A shuts of antograde MHC trafficking and the MHC class I not stopped by 3A are rapidly internalised which is induced by 2B and/or 2BC. This causes down regulation and inhibition of MHC Class I while leaving MHC Class II presentation relatively uninterrupted [85;86]. eIF4G is cleaved resulting in the termination of host mRNA translation as well as eIF4F modulation. Viral RNA translation continues unaffected due to the IRES. Host RNA synthesis is inhibited via inhibition of specific transcription factors such as TFIID, TFIIC, and TFIIIC. Nuclear import of proteins is inhibited due to

proteolysis of two components of the nuclear pore complex (Nup153 and p62). Transport of secretory and plasma membrane proteins is blocked through viral proteins 2B and 2BC which block protein secretion from the Golgi, and 3A which blocks vesicular traffic from the ER [87].

CVB3 causes cell arrest at G1 or G_1S indicated by reduced host DNA synthesis, decreased cyclin D1, cyclin E, CDK2 and CDK4, and reduced phosphorylation of Rb. This cell arrest creates an ideal environment for CVB3 replication due largely to CVB3s effect on the ubiquitin/proteosome system (UPS) [88;89]. CVB3 infection results in increased levels of ubiquitin activating enzyme E1A/E1B and ubiquitin-conjugating enzyme UBCH7, as well as decreasing de-ubiquitinating enzyme UCHL1. This leads to increased polyubiquitination and a subsequent decrease in free ubiquitin levels. Blocking the changes to the UPS that CVB3 causes by siRNA, proteosome inhibitors or Pyrrolidine dithiocarbonate (PDTC inhibits the ubiquitin/proteosome pathway) all lead to decreased viral replication and highlight the importance of the UPS [90-92]. One of the major determinants of the severity of the disease is due to the balance of pro and anti apoptopic pathways. CVB3 uses several methods of inhibiting the pro-apoptopic pathway so that it can continue to replicate before the cell undergoes full apoptosis. Akt is phosphorylated in a PI3K dependant mechanism during CVB3 infection modulating downstream signalling involving cell survival, proliferation, differentiation, migration and apoptosis. Inhibiting Akt during infection leads to enhanced cleavage of both caspase-3 and PARP, indicating its strong anti-apoptopic role in CVB3 infection [93]. Phosphorylation and activation of the extracellular signal-regulated kinase (ERK 1/2) participates in viral replication and suppresses caspase activity, protecting the cell from apoptosis and is necessary for efficient viral replication [94-96]. Cytopathic effects include condensation of chromatin, nuclear blebbing, proliferation of membrane

vesicles, changes in membrane permeability, leakage of intracellular components and shrivelling of the entire cell [97].

1.2: Pattern Recognition Receptors

Charles Janeway in the now famous paper "Approaching the Asymptote: Revolution and Evolution in Immunology", in 1989, coined two very important terms when dealing with the innate immune system. The first was the idea of Pattern Recognition Receptors (PRRs), molecules which would be capable of recognising pathogens. The second term was used to describe the molecules from the pathogens that the PRRs recognised, Pathogen Associated Molecular Patterns (PAMPs). He suggested that the PAMPs would be produced by broad classes of pathogens so that PRRs could recognise them [98]. As well as PAMPs a newer term has been coined, Danger-Associated Molecular Patterns (DAMPs), which are endogenous ligands associated with inflammation, which can also cause an immune response through certain PRRs. Recognition of PAMPs, or DAMPs by PRRs initiates signalling pathways that start the innate immune response necessary in killing infectious microbes.

Toll-Like Receptors (TLRs) were the first group of PRRs to be discovered as part of the hosts innate immune response to pathogens. They are a family of type I transmembrane proteins that have a large range of PAMPs as their ligands. There are 10 human TLRs that can be separated into two groups; cell surface TLRs that largely recognise bacterial and fungal PAMPs as well as viral capsid proteins, and cell surface TLRs that mainly recognise nucleic acid PAMPs.

The next major group are Retinoic Acid-inducible Gene (RIG)-Like Receptors (RLRs), whose main function is to recognise viral RNA. This is a family of cytosolic PRRs that is made up of RIG-I, Melanoma Differentiation-Associated Gene 5 (MDA5) and LGP2.

Nod-Like Receptors (NLRs) are a more diverse group of receptors that can be separated into either those that can form the inflammasome, or those that can't. The NLRs have been shown to recognise a large array of PAMPs, particularly highlighted in NLRP3 which has been suggested to recognise DAMPs caused by various pathogens or defects, rather than specific PAMPs.

1.2.1: Toll-Like Receptors

Toll was first discovered in the Drosophila in 1985 by Nusslein-Volhard *et al* as an important part in developing dorsal-ventral polarity in the embryo [99]. At the time it was not linked at all to immunity, however in 1991 Gay *et al* showed that the cytoplasmic domain of Drosophila toll was related to that of human inerleukin-1 receptor (IL-1R), a protein involved in human inflammation [100]. The question arose, why would a protein involved in dorsal-ventral development in a fly be similar to a protein involved in the innate immune system in humans? It wasn't until 1996 that Lemaitre *et al* discovered that in Drosophila Toll protects against fungi after Toll deficient adult flies were infected with *Aspergillus fumigates* and died after 2-3 days [101]. It appeared that Toll was involved in embryonic development as well as adult immunity. The first human homologue of Toll was discovered by Medhitzhov and Janeway in 1997, named hToll, then in 1998 Rock *et al* discovered 5 homologues of Toll, TLRs 1-5, the 4th of which was hToll, TLR4 [102;103]. A major breakthrough occurred later the same year when Poltorak *et al* discovered that TLR4 was activated by lipopolysaccharide (LPS), a component of the outer membrane of gram negative

bacteria [104]. For the first time a molecular mechanism was revealed for inflammation during sepsis. TLR6 was discovered in 1999 by Takeuchi *et al*, followed by TLRs 7, 8 and 9 in 2000 and TLR10 in 2001 by Chuang and Ulevitch [105-107]. Over the last decade the molecular components and pathways of the innate immune response through TLRs has developed significantly giving a much more detailed view of this important system.

TLRs are Type I transmembrane proteins, with their ectodomains containing leucine rich repeats (LRRs) that are responsible for recognising their ligand, a single transmembrane domain and an intracellular Toll-intereukin-1 receptor (TIR) domain for signalling. So far ten TLRs have been discovered in humans, while there are 12 TLRs in mice. TLR1 through TLR9 are conserved in both while TLR10 is non functional in mice due to a retroviral insertion. TLR11, TLR12 and TLR13 have been lost in the human genome [108]. Each TLR recognises a different set of PAMPs ranging from components of bacterial cell walls to viral nucleic acids. TLRs can be split into two groups, those that are expressed on the cell surface and those expressed in intracellular vesicles. TLR1, TLR2, TLR4, TLR5 and TLR6 are all cell surface receptors and largely recognise microbial components. TLR3, TLR7, TLR8 and TLR9 are all expressed on intracellular vesicles and recognise pathogenic nucleic acids. Once the TLR binds its ligand it dimerises, either with itself or another TLR, and recruits a single, or combination of, TIR domain containing adaptor proteins. The signalling cascade that ensues results in the production of proinflammatory cytokines as well as type-I interferon (IFN) with some TLRs [109].

TLRs are widely expressed throughout the body, including immune cells such as dendritic cells (DCs), T cells, B cells and macrophages. However this does not mean

expression is uniform throughout all cell types, even within subsets of immune cells expression can vary. As an example Myeloid DCs express TLR1 through TLR9, while plasmacytoid DCs (pDCs) express TLR7 and TLR9 strongly, while TLR2 and TLR4 are only expressed weakly [110].

1.2.2: Cell Surface TLRs and their Ligands

There is a large list of PAMPs for TLR2 including lipoproteins from both gram-positive and negative bacteria, lipotechoic acid (LTA), peptidoglycan, fungal phospholipo-mannans and zymosan as well as viral components such as haemaglutinin from measles virus [108;109]. TLR2 functions mainly by forming heterodimers with either TLR1 or TLR6. The TLR1/2 heterodimer recognises triacylated lipopeptides as its main PAMP, while the TLR2/6 heterodimer recognises diacylated lipopeptides [108;110]. Some PAMPs require accessory molecules to be detected, for example in TLR2s case CD36 and Dectin1 have been shown to be required. Upon ligand binding the TLR2 heterodimers, the receptor complex is translocated to lipid rafts where it associates with CD36, a double-spanning membrane protein and class B scavenger receptor. CD36 is required for recognition of LTA as well as diacylated lipopeptide MALP-2. Dectin1 binds fungal β-glucans such as zymosan and enhances TLR2s response to the PAMP [111]. Interestingly TLR2 does not cause type-I IFN response in macrophages and DCs, but does in inflammatory monocytes when infected with Vaccinia virus. This highlights that not only does expression of TLRs vary between cell types, but the specific role of certain TLRs may also vary [108].

As mentioned earlier TLR4 was identified as the PRR for LPS, a component of the outer-membrane of gram-negative bacteria that is associated with septic shock. Like TLR2 it appears to have a large range of PAMPs including LPS, fusion protein of

respiratory Syncytial virus, envelope protein of Mouse mammary tumour virus, fungal mannans and zymosan and glycoinositolphospholipids from the parasite *Trypanosoma* [108;109;112]. TLR4 forms a complex on the cell surface with a soluble protein called MD-2 in order to recognise LPS. TLR4 does not appear to bind LPS directly, rather MD-2 binds LPS and then binds itself to TLR4. Also involved in LPS detection is CD14, a glycosylphosphatidylinositol (GPI) anchored protein expressed on the cell surface, and LPS binding protein (LPB) a soluble plasma protein. CD14 binds LPS and facilitates its transfer to the TLR4/MD-2 complex, while LBP also binds CD14 and LPS [111].

Another accessory molecule is RP105, a type-1 transmembrane protein with 22 LRRs, which was the first LRR containing receptor reported on the B-cell surface. RP105 is required for both TLR2 and TLR4 signalling in B-cells and RP105 deficient B-cells have defective TLR2 and TLR4 responses. It associates with MD-1, a homologue of MD-2. The RP105/MD-1 complex is assumed to positively regulate the responses of both TLR2 and TLR4, however negative regulation has been reported in response to LPS in macrophages and DCs [111].

TLR5 detects flagellin of bacterial flagella. Mouse TLR11 is a close relative of TLR5 and recognises uropathogenic bacterial components and protozoan parasite proteins. Human TLR11 is non-functional due to a stop codon in the gene [109].

1.2.3: Intracellular TLRs and their Ligands

The intracellular TLRs recognise pathogenic nucleic acids, DNA, ssRNA and dsRNA. TLR3 is responsible for dsRNA recognition including genomic RNA from dsRNA viruses and dsRNA intermediates created during replication of ssRNA viruses as well as some dsDNA viruses [109;113]. ssRNA is recognised by TLR7 and TLR8. They were

originally identified as recognising imidazoquinoline derivatives and guanine analogues, they also recognise ssRNA from RNA viruses including Vesicular stomatitis virus, Influenza A virus and Human immunodeficiency virus. TLR7 is highly expressed in pDCs in order to produce large quantities of type-1 IFN upon RNA virus infection as well as cytokine production. In DCs TLR7 recognises bacterial RNA to induce type-1 IFN. TLR8 is expressed highly in monocytes and mediates recognition of R-848 as well as viral ssRNA [108;109]. TLR9 detects CpG-DNA, fungal DNA as well as hemozoin from parasites [109].

Expression of nucleic acid sensing RNAs in intracellular vesicles aids in distinguishing between host and pathogen nucleic acids. Cellular nucleic acids present in the extracellular environment are rapidly degraded by nucleases and thus do not access the vesicles. Localisation in the intracellular vesicles also enables recognition of viruses as soon as uptake of the virus occurs. Viruses fuse with the membrane and are taken up into endosomes by autophagy. Once a virus is mature it may also use endosomes for uptake and release. Uptake of microbes into the endocytic pathway occurs via receptor-mediated endocytosis, phagocytosis or on-specific fluid phase endocytosis [113].

Other ways of avoiding self nucleic acid recognition are still debatable. The CpG DNA motif that TLR9 recognises is four times less abundant in mammalian DNA than in bacterial or viral DNA. However it has been shown that the 2' deoxyribose phosphate backbone is recognised by TLR9, not necessarily specific sequences such as CpG DNA. It could be that compartmentalisation of TLR9 in vesicles is still the main way of avoiding self DNA recognition [113]. With TLR3 it is possible that it avoids self dsRNA, partially because dsRNA is very rare in mammalian cells, but also because it

can only bind dsRNA longer than 40bp, while any dsRNA that does occur in mammalian cells is shorter than this.

Intracellular TLRs are present in the endoplasmic reticulum (ER) in unstimulated cells and are rapidly trafficked to endolysosomes upon infection via the common secretory pathway through the Golgi. A 12-membrane spanning protein, Unc93B interacts directly with the transmembrane domain of TLR3, TLR7 and TLR9 mediating their translocation to the endolysosome [111;113]. PRAT4A, a TLR4-binding chaperone that translocates it to the plasma membrane and also associates with TLR1, is required for immune responses from both TLR7 and TLR9, but not TLR3. It has been shown to be required for TLR9s translocation to lysosomal compartments. TLR9 translocation is also facilitated by High-mobility group box1 protein (HMGB1). Gp96 is a more general chaperone for TLRs, both cell surface and intracellular, and associates with TLRs in the ER and acts as a chaperone for protein folding as well as being required for TLR maturation [111].

1.2.4: TLR Signalling Pathways

Once their particular PAMP has been recognised TLRs form a homodimer or, in the case of TLR1, TLR2 and TLR6, a heterodimer. This is believed to bring together the TIR domains of the TLRs which allows recruitment of TIR domain containing accessory molecules such as Myeloid differentiation primary response gene-88 (MyD88), TIR-domain-containing adapter-inducing interferon-β (TRIF), TIR-domain containing adaptor protein (TIRAP) and TRIF-related adaptor molecule (TRAM). MyD88 is used by all of the TLRs except TLR3 and activates Nuclear factor kappa-light-chain-enhancer of activated B cells (NF-κB) and mitogen-activated protein kinases (MAPKs) to induce inflammatory cytokine production. This pathway is known as the

MyD88-dependant pathway. The other pathway used by TLRs is the TRIF-dependant pathway. TRIF is used by TLR3, as well as by TLR4, which can utilize both pathways. As well as leading to NF-κB and inflammatory cytokines, it also leads to Interferon regulatory factor 3 (IRF3) activation and type-I IFN production. TLR4 also requires TRAM to use the TRIF pathway and both TLR2 and TLR4 use TIRAP to recruit MyD88. TLR4 is the only TLR to use all TIR accessory molecules and both pathways. It recruits TIRAP at the plasma membrane which facilitates recruitment of MyD88 leading to the usual activation of NF-κB and MAPKs. Then, via dynamin dependant endocytosis, TLR4 is trafficked to endosomes where it recruits TRAM and TRIF and activates the TRIF-dependant pathway. This leads to IRF3 as well as MAPKs and NF-κB. Both pathways appear to be necessary for TLR4 to activate expression of inflammatory cytokines [108].

1.2.5: MyD88-Dependant Pathway

After MyD88 activation by TLRs it recruits IL-1 receptor-associated kinases IRAK4, IRAK1, IRAK2 and IRAK-M. MyD88 contains an N-terminal death domain (DD) that interacts with the DD of IRAK4. IRAK4 then phosphorylates IRAK1 and IRAK2, which go on to activate TNF receptor associated factor 6 (TRAF6). IRAK-M is an inhibitor of TRAF6. TRAF6 is an E3 ubiquitin ligase which, along with Ubc13 and Uev1A, catalyses the synthesis of polyubiquitin linked to Lys63 on target proteins including itself and IRAK1. The poly-ubiquitin chains then bind to novel zinc finger-type ubiquitin-binding domains of TAK1 binding protein 2 and 3 (TAB2 and TAB3) which are the regulatory components of TGF-β activated kinase 1 (TAK1), activating TAK1. As well as binding and activating TAK1, the Lys63 polyubiquitin chains also bind the ubiquitin binding domain of NF-κB essential modulator (NEMO), a regulatory

component of the IKK complex required for NF-κB activation. As TRAF6 binds both the IKK complex and the TAK1 complex, the two are brought together and TAK1 phosphorylates IKKβ of the IKK complex. This leads to IκB phosphorylation and subsequent degradation of the protein and the resultant NF-κB nuclear translocation and activation. The IKK complex also phosphorylates p105, which becomes degraded leading to the activation of MAP3K8. This activates MKK1 and MKK2, which then activate extracellular single related kinases (ERK) 1 and 2, as well as Jun Kinases (JNKs). TAK1 also activates mitogen-activates kinase (MAPKs) leading to phosphorylation of JNKs, p38 and CREB. Together this culminates in transcription factors AP-1 and the IRFs activation and with NF-κB induces gene transcription of proinflammatory cytokines [108;113;114].

1.2.6: TRIF-Dependant Pathway

Once TLR3 binds its ligand, or TLR4 is internalised after ligand binding, TRIF is recruited to the TLR. TRIF associates with TRAF3 and TRAF6 as well as receptor-interacting proteins (RIP) 1 and 3. TRAF6 and RIP1 are required to activate TAK1, as well as other adaptors such as TRADD and Pelino-1, which bind RIP1. TRAF6 is thought to bind TRIF in the same ubiquitin-dependant mechanism as it binds MyD88. RIP1 binds TRIF through its RIP homotypic interaction motif and also undergoes Lys36 polyubiquitination. Once activated TAK1 goes on to activate NF-κB and MAPKs and the subsequent induction of proinflammatory cytokines in the same manner as in the MyD88-dependant pathway. As well as this pathway TRIF also recruits the IKKs, TBK1 and IKKi through TRAF3. This causes phosphorylation and activation of IRF3, leading to IFNβ production [108;113].

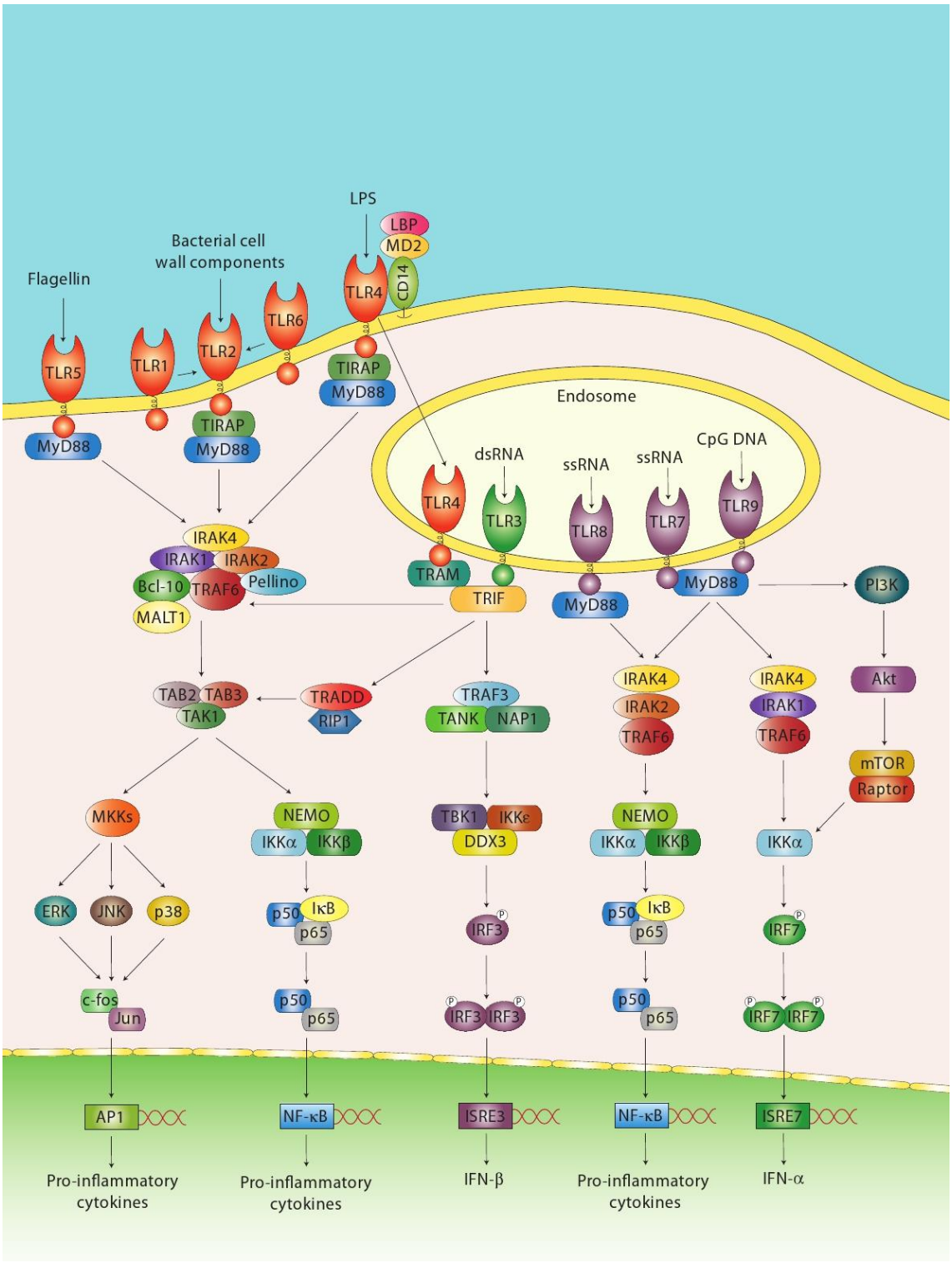

Figure 1.5 - Diagram to show the signalling pathways of the TLRs. Shown are both the MyD88 dependant pathway leading to NF-κB, AP1 and IRF3 and the TRIF dependant pathway utilized by TLR3 and TLR4. Adapted from [115;115].

1.2.7: Structure of the TLRs

TLRs are type-I integral membrane receptors with an N-terminal ligand recognition domain, known as the ectodomain, a single transmembrane helix and a C-terminal cytoplasmic signalling domain. The signalling domain is known as the TIR domain due to its homology with the signalling domain of the interleukin-1 receptor family members. The TIR domain (as mentioned above) is also found on many adaptor proteins and homotypic interactions between the TIR domains of the TLRs and the adaptors are the first step of signalling. The TIR domain is approximately 160 amino acid residues in length and the primary sequence is characterised by three conserved sequence boxes known as Box 1, Box 2 and Box 3. The transmembrane domain is typically an alpha helix of around 20 amino acid residues that are uncharged and mostly hydrophobic.

The N-terminal, or ectodomain, of the TLRs are either extracellular or in endosomes and are glycoproteins of around 550-800 residues in length. It is in this region that the TLRs bind their specific PAMPs and thus an important region in understanding how TLRs bind their ligand. The ectodomain is made up of leucine-rich repeats (LRRs), which are typically 20-30 amino acids in length. They consist of a conserved "LxxLxLxxNxL" motif and a variable region. Typically in LRR structures there are around 24 LLRs in a row, each LRR forming a loop structure with consecutive LRRs forming a "solenoid" structure. Side chains of conserved leucines point inwards, creating a stable hydrophobic core. The conserved asparagines are important in maintaining the overall shape of the protein. Beta sheets built by parallel beta strands provided by the "LxxLxLxxN" motif are more compact than the rest of the LRR loop structure and cause the solenoid shape to form a distinctive "horseshoe" shape, with the

beta sheet forming the concave part. A characteristic feature of TLR ectodomains is that there are often more than the standard 24 LRRs in a row, producing loops that protrude from the horseshoe structure, most commonly on the concave side. This is most noticeable in TLR7, TLR8 and TLR9. There are also "cap" structures on the C and N terminals of the ectodomain, cysteine rich regions known as LRR-CT and LRR-NT respectively. The LRR-CT is connected directly to the transmembrane domain. Dimerisation of TLRs occurs at the C-terminal of the ectodomain, with the N-terminals extending in opposite directions creating a characteristic "M" shape. Dimerisation of the ectodomains would likely bring together the TIR domains as well, with TIR domain containing adaptors recognising the dimerisation of the TLR TIR domains.

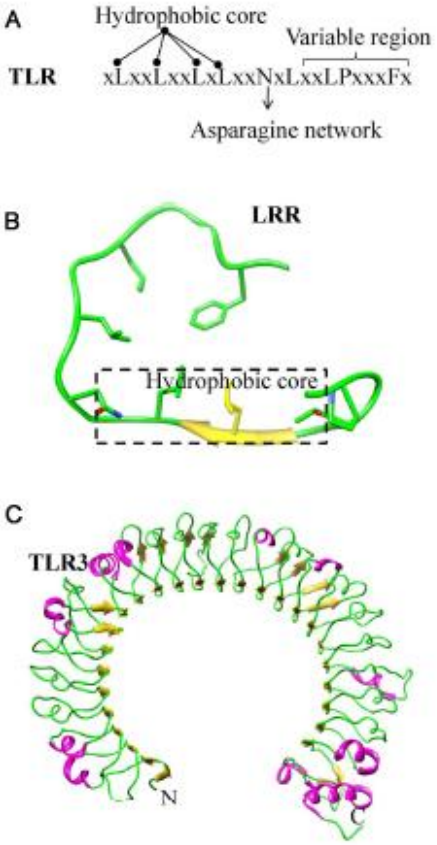

Figure 1.5 - Diagram to show ectodomain structure of TLRs. A. Conserved LxxLxLxxN motif and variable region. B. Loop structure of LRR with beta sheet. C. Horseshoe structure of the ectodomain with betas heets making the concave backbone [3].

As would be predicted the ectodomain varies between each TLR as each binds a different and specific set of PAMPs. TLR2 forms heterodimers with TLR1 or TR6 with the binding site being where the convex curved edges meet (Figure 1.6-A+B.). The lipid binding pocket of the TLR2/6 complex is half the length of the TLR1/2 complex, explaining why there is selectivity of diacylated over triacylated lipopetides. There is also the possibility that TLR2 can form homodimers, however this has yet to be confirmed.

Unlike TLR2, TLR4 does not interact with its ligand directly, instead it forms a complex with MD-2. MD-2

binds LPS in a large hydrophobic pocket and then binds TLR4 allowing TLR4 to recognise LPS. Dimerisation of TLR4 only occurs when its ligand is recognised, forming a TLR4/MD-2/LPS dimer. Five lipid chains of LPS are contained within the MD-2 hydrophobic pocket, while a sixth chain is presented to TLR4 and forms hydrophobic interactions with the second TLR4 in the homodimer. LPS phosphate groups form ionic interactions with positively charged residues on both MD-2 and TLR4. As well as this MD-2 interacts with the second TLR4s ectodomain upon ligand stimulation, further stabilising the complex. The TLR4s also interact with each other in the homodimer complex. The structure of the complex and its binding sites can be seen in Figure 1.6-C with MD-2 binding the concave side of the "horseshoe" structure.

TLR3 is a monomer in solution and forms a homodimer upon ligand binding, forming the typical "M" structure. It interacts with dsRNA at two sites on each ectodomain as can be seen in Figure 1.6-D once near the C-terminal and once near the N-terminal of the ectodomain. Once dsRNA has bound the TLR3s interact with each other at the LRR-CT, positioning the four binding sites to correctly bind dsRNA. All three of the ectodomain binding sites (two for dsRNA, one to form the dimer) are required for stable dsRNA binding and signalling. The site at the LRR-CT at which the TLR3s bind each other is minimal, suggesting that dsRNA binding is the main dimerisation force. Interestingly TLR3 binds the phosphate backbone of the dsRNA which explains the lack of specificity between dsRNAs. It also means that mutation of the RNA sequence to avoid detection is not a factor and prevents escaping detection by mutation. There is also a distance of 120Å between the two N-terminal binding sites, which means that any dsRNA shorter than 40bp is incapable of being bound by the TLR3 dimer. As most 'self' dsRNA is rarely longer than 25bp this would seem a likely mechanism to avoid recognition of 'self' dsRNA.

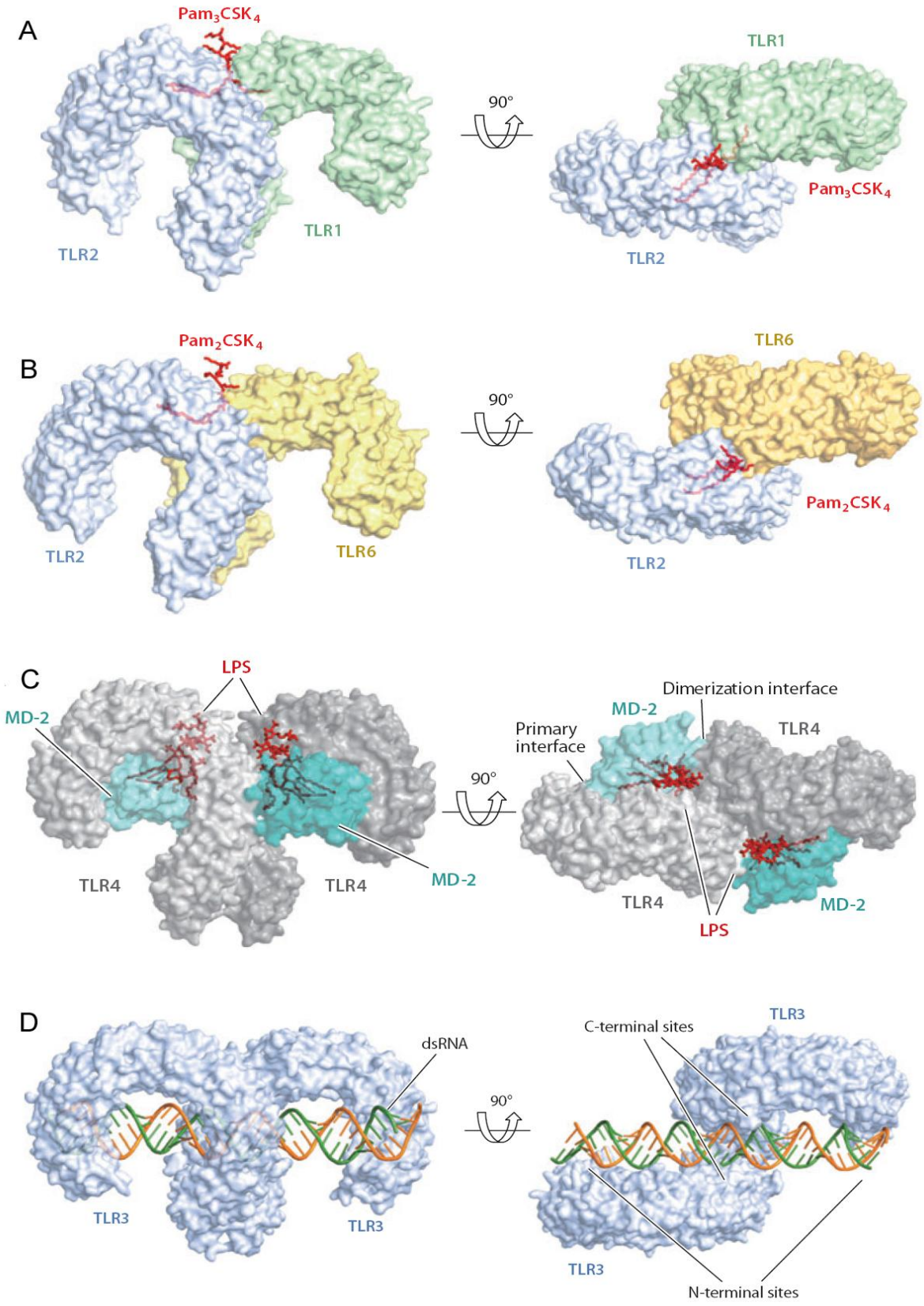

Figure 1.6 – Diagrams to show the 3D structure from the side and from above of TLRs in their dimers binding their ligands. A. TLR1/2 complex binding Triacylated lipopeptide. B. TLR2/6 complex binding diacylated lipopeptide. C. TLR4/MD-2 complex binding LPS. D. TLR3 binding dsRNA. [116]

No structure is available for TLR5, but its ectodomain is estimated to contain 20 LRRs with an important role of the 9th LRR in flagellin recognition. Likewise there has been no structure reported for TLR7, TLR8 and TLR9. Their amino acid sequence suggests that they are noticeably different from TLR3. The ectodomain of each of the three TLRs contains 25 LRRs and importantly have stretches of amino acids around 40 residues in length between LRRs 14 and 15 that have an undefined structure. It has been reported that TLR9 undergoes conformational change upon ligand binding that could be dependent on this undefined region as well as evidence that TLR9 may be cleaved in this region between LRRs 14 and 15,. Both cleavage and conformational change could be required for TLR9 to be active; something which it seems is not required by TLR1, TLR2, TLR3, TLR4 and TLR6 [3;116;117].

1.3.1: Nod-Like Receptors

Nod-Like Receptors (NLRs) can be considered as another part of the trinity of pathogen sensors as suggested by Creagh and O'Neill [118] alongside the TLRs and RLRs and like the RLRs are located in the cytosol. The NLRs can be split into four different groups based on their structure, or two separate groups based on their function. There are 23 different NLRs known within the human genome, while there are over 34 in mice [119] and they can be defined by a nucleotide binding/oligomerisation domain (NBD, or NACHT) followed by a leucine rich repeat (LRR) domain. The C-terminal is the LRR domain, which like TLRs is thought to be the ligand binding domain, although this has yet to be proven, as well as having an auto-repression function when not binding a ligand [120]. The NBD is the central domain capable of binding ribonucleotides which regulates oligomerisation of the NLRs. The N-terminal is more variable and is the domain through which the NLRs can be separated into sub families through their

structure, known as NLRA, NLRB, NLRC and NLRP. This domain is the effector domain and mediates homotypic protein-protein interaction for downstream signalling. NLR Class II Transactivator (CIITA) is the only NLRA in humans and has an acid transactivation domain as it N-terminal. NLRBs contain a baculovirus inhibitor repeat (BIR) domain and in humans the only NLRB is NAIP. NLRCs have a caspase recruitment domain (CARD) and include Nulceotide-binding Oligomerisation Domain-containing (NOD) 1, NOD2, NLRC3, NLRC4, NLRC5 and NLRX1. The final group, NLRPs, have a pyrin domain (PYD) and include 14 members, NLRP1 through to NLRP14 [121-124]. Functionally NLRs can be separated on their ability to form a complex known as the inflammasome. Inflammasome formation mainly leads to IL-1β activation, while other NLRs lead to NF-κB, MAPK activation and type-I IFN induction.

1.3.2: Inflammasome forming NLRs

The inflammasome was named due to its similarity to the apoptosome and its ability to cause inflammation [125] and can be activated by members of the NLRs as well as certain PYTHIN protein families. Like the apoptosome, which activates apoptotic caspases, the inflammasome complex controls the release of inflammatory caspases upon formation and activation [126]. As well as caspase activation the inflammasome can lead to pyroptosis, a form of inflammation induced cell death. The basic components of the inflammasome are the activated receptor molecule, apoptosis-associated speck-like protein containing CARD (ASC) and pro-caspase-1 [127]. It has been suggested that pyroptosis is mediated by direct CARD-CARD interaction between CARD containing NLRs and pro-caspase-1 without the involvement of ASC. In these

cases activation of caspase-1 requires ASC and the formation of a larger inflammasome complex [128].

In their inactive state the NLR is kept inactive by the fold-back of its LRR domain onto the NDB. They are kept in this inactive state with the help of chaperone proteins SGT1 and HSP90, which help stabilise the fold-back, while at the same time leaving the NLR capable of recognising and binding its ligand. Once the NLR binds its specific ligand a conformational change occurs releasing the LRR from the NBD, allowing a ribonucleotide (ATP or NTP) to bind a Walker A motif on the NBD. This enables NLR oligomerisation and recruitment of other members of the inflammasome complex [129]. NLRs bind ASC through either PYD-PYD homotypic interaction or through CARD-CARD homotypic interaction, while NLRCs can also interact directly with pro-caspase-1 through their CARD domains. ASC then binds pro-caspase-1 via CARD-CARD homotypic interactions. The inflammasome activates caspase-1 by bringing the inactive pro-caspase-1 together in the complex, which undergoes proximity induced dimerisation and autocatalytic activation by cleavage [130-132]. The main role of caspase-1 is to cleave the inactive pro-IL-1β into the active IL-1β inflammatory cytokine. This is the second step in the activation of IL-1β, the first (priming signal) is the transcription and expression of the pro-IL-1β gene which is promoted by TLR and RLR recognition of their ligands, as well as other NLRs. Pro-IL-18 is also cleaved into its active form, however unlike IL-1β, it is constitutively expressed and doesn't need a priming signal. Caspase-1 activation also results in the release of leaderless proteins that may facilitate in tissue repair [133].

It has been shown that NLRP1, NLRP2, NLRP3, NLRP6, NLRP12, NLRC4, NOD2 as well as the PYTHIN receptor Absent in Melanoma-2 (AIM2) can activate caspase-1 and

lead to IL-1β processing when over expressed with pro-caspase-1 and ASC, suggesting roles in inflammasome formation. While certain NLRs have definitively been shown to form an inflammasome, such as NLRP1, NLRP3, NLRC4 and AIM2, other NLRs roles in inflammasome formation remain more unclear.

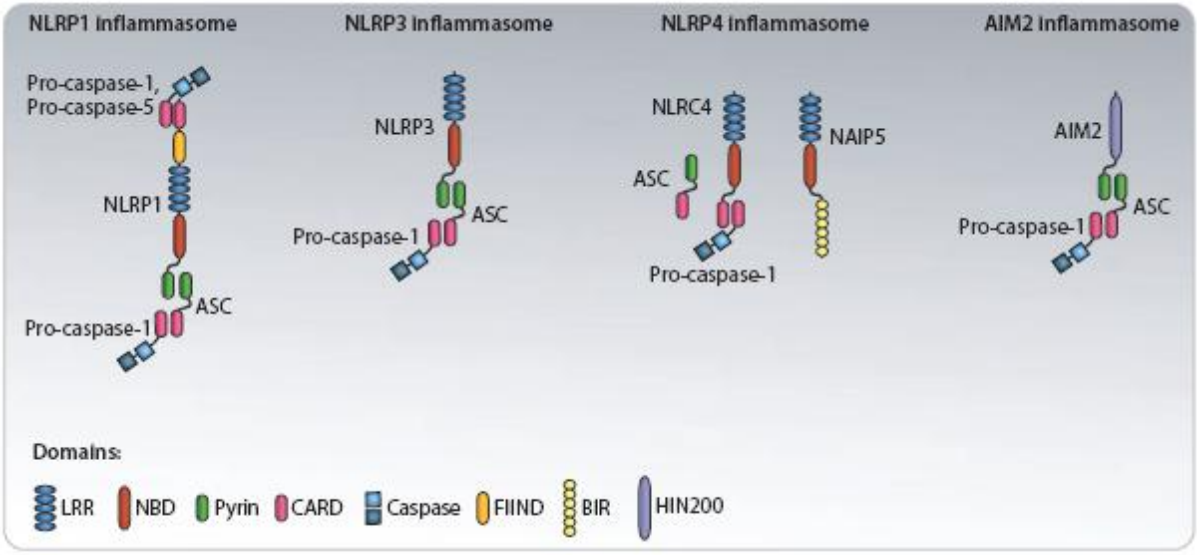

Figure 1.7 - Diagram to sow the structure of certain inflammasomes. NLRP1, NLRP3 and AIM2 use ASC through PYD-PYD interactions to bind Pro-caspase-1 through CARD. NLRP1 can also bind Pro-caspase-1 as well as pro-caspase-5 directly through a CARD domain on its C-terminal. NLRC4 (incorrectly labelled s the NLRP4 inflammasome) can bind directly Pro-caspase-1, or via ASC [134].

In 2002 Tschopp *et al* discovered a caspase-1 activating multimolecular complex that contained caspase-1, caspase-5, ASC and NLRP1, which they called the inflammasome [135]. NLRP1 was the first NLR to be shown to form an inflammasome. It was shown by Reed *et al* that the minimum components of the NLRP1 inflammasome were NLRP1, pro-caspase-1 and NTP and not ASC, however ASC enhanced assembly. They also showed that NLRP1 recognised diacyl muramyl dipeptide (MDP) from bacterial peptidoglycan and suggested that upon binding MDP, NLRP1 undergoes a conformational change that allows binding and hydrolysis of NTP by the NBD causing self-oligomerisation [136]. Other stimuli for NLRP1 are *Bacillus anthracis* via its lethal

toxin and *Toxoplasma gondii* [137;138]. NLRP1 is not widely expressed, with its main expression being in T-cells and Langerhans cells, with a lower expression level in stomach epithelial cells, gut and lungs [139].

It is a unique member of the NLRP sub-family as, in addition to its PYD domain at its N-terminal, it has a FIIND motif and a CARD at its C-terminal. While it can interact with ASC through PYD-PYD homotypic interactions it can also bind caspase-1 and caspase-5 in an ASC independent manner through its C-terminal CARD [140;141]. The interaction with caspase-5 may contribute to IL-1β processing in human cells. Surprisingly, despite being the first NLR discovered that could form the inflammasome, it is one of the least studied and understood. This is likely due to its differences between itself and its three murine homologues, NLRP1a, NLRP1b and NLRP1c. The murine homologues only have the CARD domain at the C-terminal and lack the PYD domain. As well as this the human NLRP1 has been shown, as mentioned above, to recognise MDP, a trait that has not been shown in the murine homologues [142]. NRLP1s ability to recognise very distinct ligands such as MDP and lethal toxin also raises questions as to how it can detect such differing ligands.

NLRP3 has a more standard structure than NLRP1, with the atypical LRR C-terminal, NBD and PYD N-terminal. Its NBD binds ATP upon stimulation causing the receptor to oligomerise and recruit ASC via its PYD. This then activates caspase-1 resulting in IL-1β and IL-18 processing and can lead to pyroptosis [143;144]. NLRP3 is not expressed in most tissues, except peripheral blood leukocytes. NLRP3 RNA expression is highest in monocytes with detectable levels in T-cells and granulocytes, as well as expression in brain microglia, lungs and testes [145].

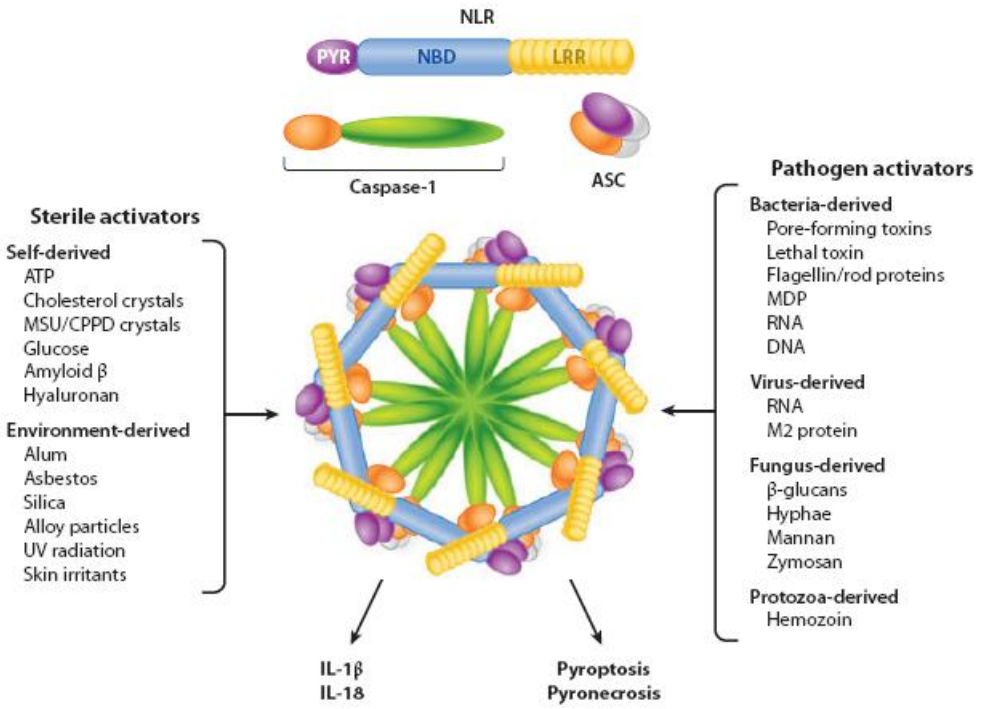

Figure 1.8 - Diagram showing the inflammasome which forms a pentamer or heptamer structure. Inflammasome activators can be separated into sterile or pathogen activators. The majority of these are capable of activating NLRP3 [146].

There are a plethora of different NLRP3 activators including viral, bacterial, fungal and protozoan PAMPs, as well as DAMPs, all very different in physical and chemical structure. NLRP3 can also act as a sensor for tissue damage. Following cell death after tissue damage, ATP can appear extracellularly and is sensed by the P2X7 receptor, activating NLRP3. Cell death can also release uric acid into the extracellular environment which can precipitate to form monosodium urate (MSU) crystals that are capable of activating NLRP3. MSU crystals can also cause gout as well as chronic arthritis, thus NLRP3 may have a role in the inflammation in these diseases. The NLRP3 inflammasome also activates in response to fibrillar ameyloid-β undergoing phagocytosis by microgilia. The resultant release of pro-inflammatory cytokines and neurotoxic factors could play an integral role in the pathogenesis of Alzheimer's disease. Cholesterol crystals are also recognised, forming early in atherosclerotic lesions

and leads to severe inflammation. As well as these self-derived activators, environmental hazards that form crystals or inorganic fibrils such as asbestos and silica crystals can cause the NLRP3 inflammasome to become activated leading to pulmonary fibrosis and silicosis. It also appears to become active due to UVB in sunburn and skin irritants in contact hypersensitivity. There is also a link to type-II diabetes and obesity due to the fact that NLRP3 can function as a sensor of glucose levels, islet amyloid polypeptide (IAPP) deposits and saturated fatty acids from high-fat diets. With all these diseases, mice lacking components of the NLRP3 inflammasome have milder forms of the disease. However, the detrimental role of NLRP3 in these disease contrasts with its necessary involvement in protection against certain pathogens as well as its protective role in inflammatory bowel disease (IBD) and colorectal cancer [147;148]. It would be impossible for the LRR of NLRP3 to detect all of these very different stimuli, so direct binding of any of these activators seems unlikely. Instead it would seem indirect recognition would be more likely with three main hypotheses on how NLRP3 activates.

The first of these hypotheses is that NLRP3 recognises Potassium efflux. In 1994 Perregaux *et al* demonstrated that efficient secretion of active IL-1β in response to LPS/ATP or LPS/nigericin required a K^+ efflux. The physiological homeostatic K^+ concentration within a cell does not allow the NLRP3 inflammasome to form, but requires the P2X7 receptor to form pores upon sensing extracellular ATP, as occurs in tissue damage [149]. Recognition of most bacteria by NLRP3 is also likely due to pore forming bacterial toxins causing a K^+ efflux [150]. This appears to be a common initiator for the inflammasome as several NLRs are inhibited by hyperosmotic K^+ [151].

The second hypothesis suggests that reactive oxygen species (ROS) can activate NRLP3 and adding reactive oxygen compounds such as hydrogen peroxide can induce the

formation of the NLRP3 inflammasome. Inhibiting or scavenging of ROS has also been shown to suppress NLRP3. It is unclear whether ROS is sensed directly or indirectly by NLRP, as it could be possible that ROS directly modifies NLRP3, or NLRP3 recognises a ROS-modified or induced intermediate molecule. Certain PAMPs, including some recognised by TLRs, known to activate ROS are insufficient for inflammasome formation. For example fungal pathogens can cause IL-1β cleavage in response to ROS as well as K^+ efflux [152]. It has also been shown that over expression of ROS can also inactivate caspase-1 by oxidation and glutathionylation, suggesting a very tightly controlled method of caspase-1 control through ROS [153]. ROS is also involved in the priming stages as well, promoting proinflammatory cytokines and up-regulates NLRP3, prerequisites of NLRP3 inflammasome formation [154].

Cathepsin B release upon lysosomal damage activating NLRP3 is the third hypothesis [155]. Lysosomal damage is possible with all NLRP3 activators and pharmacological disruption of lysosomes has been shown to activate NLRP3. Furthermore proton pump inhibitors used to prevent lysosomal acidification, which in turn inhibits acid dependant proteases, completely stops NLRP3 inflammasome activation and lack of just cathepsin B, a lysosomal protein, causes substantial inhibition of the NLRP3 inflammation [156]. Recognition of asbestos silica in silicosis by NLRP3 has been shown to be dependent on ROS, however silicosis has also been shown to cause lysosomal damage [157]. It is possible that more than one of the three hypotheses may be required in certain cases and it certainly seems that all three are involved to some degree.

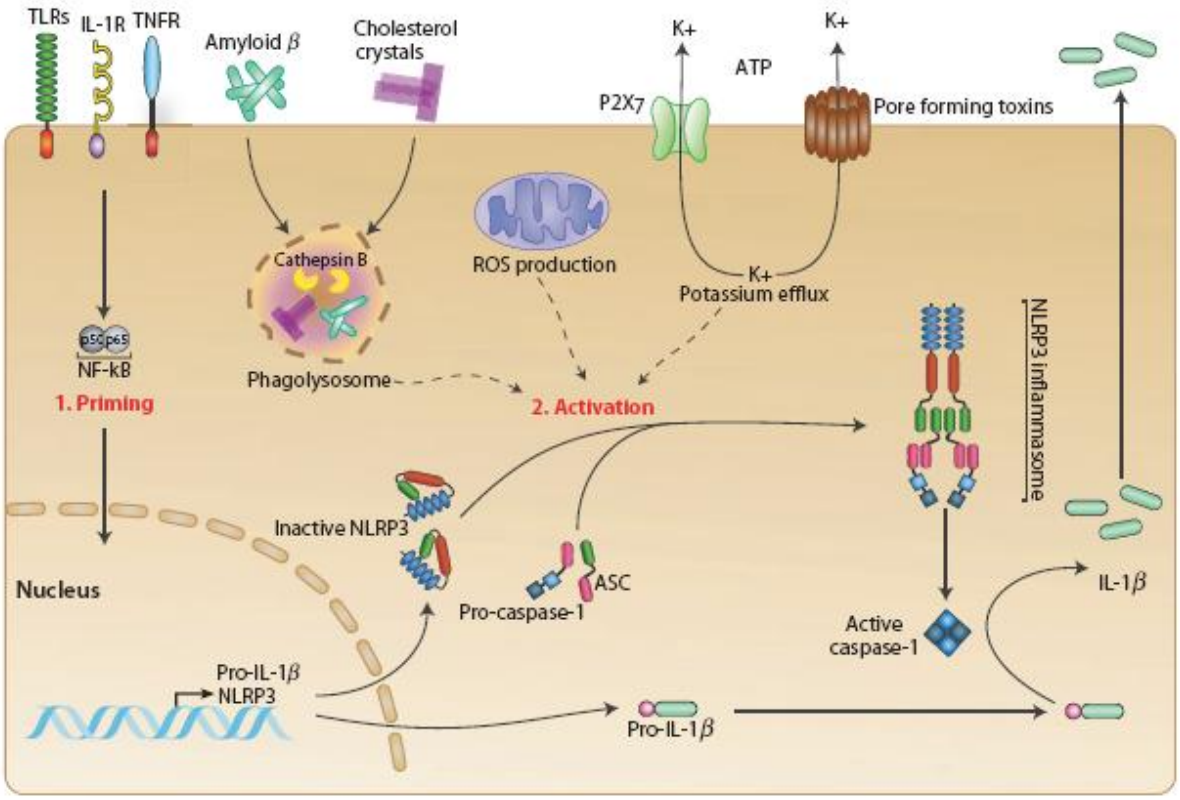

Figure 1.9 - Diagram to show the three models of NLRP3 activation, as well as the priming and activation stage. Other PRRs result in the expression of Pro-IL-1β in response to stimuli, known as the Priming stage. The activation stage involves the cleavage of Pro-IL-1β by caspase-1 into IL-1β. This occurs in response to either ROS production, potassium efflux, or release of cathepsin B in response to lysosomal damage and causes inflammasome assembly with NLRP3, pro-caspase-1 and ASC [158].

NLRC4 is the only NLRC currently known to form an inflammasome. As its N-terminal structure contains a CARD, not a PYD it is capable of recruiting pro-caspase-1 via CARD-CARD homotypic interactions without recruiting ASC. However in order to actually form an inflammasome and for a full and more robust IL-1β response ASC is required, which it binds through its CARD domain [159-161]. It is expressed predominately in hematopoietic tissues and cells as well as in the colon epithelia [162;163]. The main ligand for NLRC4 is flagellin, a major component of bacterial flagella. The receptor has been shown to recognise *S. Typhimurium, Shigella flexneri, Pseudomonas aeruginosa* and *Legionella pneumophilia* all of which are gram-negative

bacteria. In order to deliver virulence factors into the cell *P. aerugiosa*, *S. Typhimurium* and *S. Flexneri* use a type III secretion system (T3SS) while *L. Pneumophilia* uses a type IV secretion system (T4SS). As well as flagellin NLRC4 is able to recognise the T3SS basal body rod component that is believed to be secreted by accident into the host cytoplasm by active T3SS and T4SS [164;165]. There is evidence that NAIP5 may work alongside NLRC4 in order to recognise flagellin [166-168]. As with the other inflammasomes NLRC4 activation leads to IL-1β and IL-18 processing and pyroptosis.

AIM2 is an interferon inducible gene and a member of the PYTHIN family that is localised in the cytosol [169] and is expressed in the small intestine, spleen and peripheral blood leukocytes [170]. AIM2 does not have an NBD, but has a HIN200 domain and a PYD through which it can interact with ASC to form an inflammasome [171]. It senses dsDNA through its HIND200 domain from both bacteria and viruses. Interestingly it does not appear to recognise all dsDNA viruses, recognising Cytomegalovirus, but not Adenovirus, whose recognition is dependent on NLRP3. It is possible that the dsDNA viruses that are not recognised by AIM2 have a life cycle that keeps its DNA out of the cytosol and thus away from AIM2 [172]. With no NDB, AIM2 forms oligomeric complexes due to clustering of AIM2 when binding dsDNA and through ASC. As with the NLR inflammasomes, the AIM2 inflammasome converts pro-caspase-1 into the active caspase-1 and processes IL-1β and IL-18 and can cause pyroptosis.

Other inflammasome forming NLRs include NLRP6 which can form an inflammasome with ASC. The NLRP6 inflammasome is important in the colonic epithelium where it is essential in preventing recurring colitis and is protective against IBD and colorectal cancer. Its role in these conditions can be explained by the fact that it controls the

composition of gut microbiota, preventing harmful bacteria from colonisation as well as suppressing proliferation of intestinal epithelial cells following injury [173;174]. NLRP12, like NLRP6, has been shown to co-localise with ASC and both can induce capase-1 dependent IL-1β secretion [175].

1.3.3: Non-Inflammasome forming NLRs

Nod1 and Nod2 were the first NLRs that were discovered to regulate NF-κB and MAPK. Both recognise fragments of peptidoglycan from the bacterial cell wall. Nod1 recognises meso-diaminopimelic acid (DAP) found in gram-negative bacteria and some gram-positive. It has also been demonstrated that Nod1 contributes to host defence against *Trypanosoma cruzi* which is a protozoan parasite and does not have peptidoglycan so Nod1 must be capable of recognising another PAMP, or maybe even DAMP. Like NLRP1, Nod2 recognises MDP, which forms a part of peptidoglycan in both gram-positive and gram-negative bacteria, making Nod2 a more general bacterial sensor than Nod1. Nod2 appears to be more adapted to recognising bacteria such as *M. tuberculosis* that convert their MDP from its N-acetylated form to its N-glycosylated form, which is a stronger activator of Nod2. Nod2 may also have a role in sensing ssRNA from viruses as Nod2 deficient mice were shown to be more susceptible to respiratory syncytial virus (RSV) due to a less robust type-I IFN response. It has also been implicated in the initiation of autophagy which results in bacterial confinement to autphagosomes and restriction of infection [176;177].

After the peptidoglycan PAMPs are internalised through bacterial membrane vesicles, bacterial secretion systems, or host cell mediated pH-dependant endocytosis, Nod1 and Nod2 are translocated to the plasma membrane at the site of ligand entry. As Nod1 and Nod2 are NLRCs their structure consists of an LRR which binds the ligand, an NBD

and CARD through which they recruit RIP2. This causes autophosphorylation of RIP2 to occur as well as Lys63 ubiquitin chain formation via the E3 ubiquitin ligase cIAP1/2 allowing recruitment of the TAK1-TAB2/3 complex. Nemo is also recruited to RIP2, bringing together the IKK complex (of which Nemo is a part) close to the TAK1 complex. This causes phosphorylation of IKKβ by TAK1 and its subsequent activation. IκB is then phosphorylated by IKKβ and degraded, allowing the release of NF-κB [178;179].

RIP2 can also recruit TRAF3 which activates TBK1 and IKKi. This leads to type I IFN production through IRF3 and IRF7 activation. While Nod2 has been shown to use this pathway it only appears to be in response to infection with ssRNA viruses such as RSV, VSV and influenza A virus. Nod2 also appears to interact, when translocated to the mitochondria, with MAVS, a signalling molecule downstream of the RLRs located at the mitochondria. Although not very well described or understood, Nod2 appears to utilise a RIP2-independant mitochondrial signalling complex, at the core of which is MAVS, and is not known to be used by any other PRR [180]. However while Nod2 does appear to interact with MAVS, it is unclear as to whether it directly or indirectly associates with viral ssRNA. It is possible that immunoprecipitation of Nod2 only has ssRNA present due to co-immunoprecipitation of RIG-I through MAVS [181].

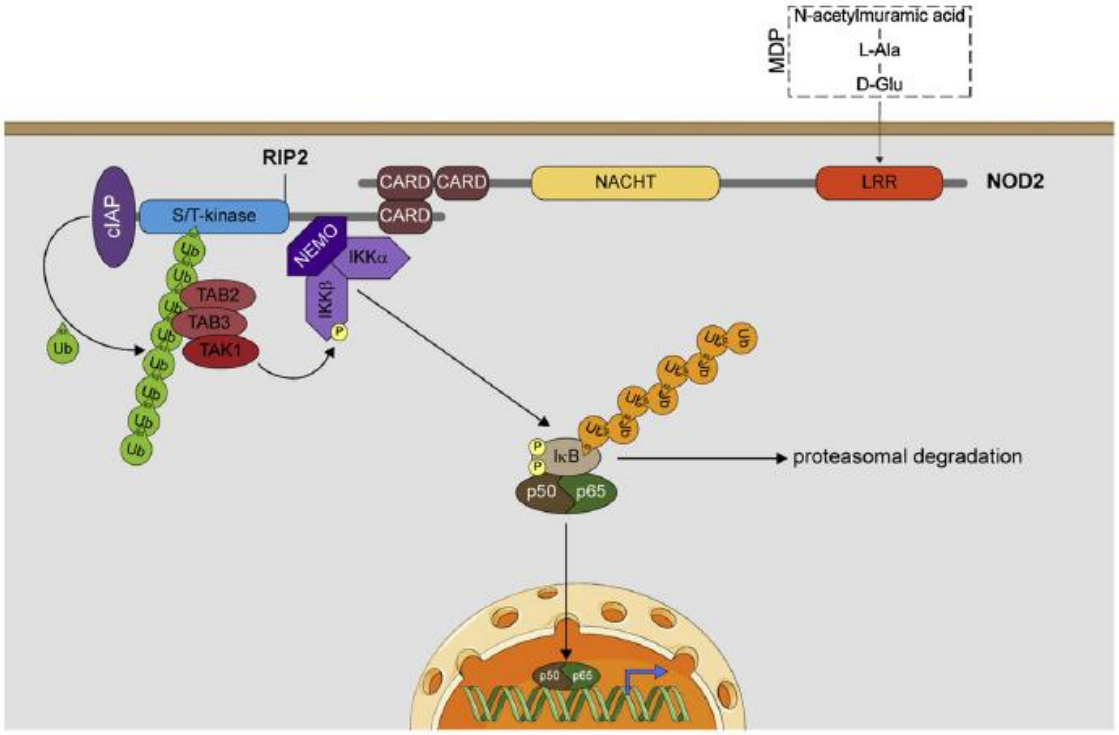

Figure 1.10 - Diagram to show the NF-κB activation pathway after Nod2 is activated. Nod2 recruits RIP2 through CARD-CARD homotypic interaction. cIAP forms a ubiquitin chain on RIP2 that allows association with the TAK1 complex. The IKK complex binds RIP2 directly through Nemo. Tak1 then phosphorylates IKKβ allowing the IKK complex to phosphorylate IκB. IκB is then ubiquitinated causing it to undergo proteasomal degradation. This frees NF-κB to move to the nucleus and start transcription of genes.

Other non-inflammasome NLRs include NLRX1, a unique NLR due to its mitochondrial targeting sequence at its N-terminal which causes it to be located at the mitochondria. Its N-terminal effector domain is similar to CARD or PYD but can't quite be categorised as either. It has been shown to interact with MAVS, impeding its association with RIG-I, and thus acting as a negative regulator in viral responses. It also positively regulates ROS production in response in intracellular bacterial pathogens [182-184]. NLRC5 has also been shown to act as a negative regulator. Like NLRX1 its N-terminal bears no similarity to other NLRs, however its LRR and NBD are most similar to those of Nod1 and Nod2. It has been shown to negatively regulate NF-κB through IKKα/β and type-I IFN through RIG-I and MDA5 [185].

1.4.1: RIG-Like Receptors

RIG-Like Receptors (RLRs) are PRRs located within the cytosol and have been shown to have an important role in sensing pathogenic nucleic acids. There are three members of the RLRs, Retinoic-acid Inducible Gene-I (RIG-I), Melanoma Differentiation-Associated-gene 5 (MDA5) and Laboratory of Genetics and Physiology 2 (LGP2). The RLRs belong to the superfamily 2 (SF2) helicases/ATPases and contain a C terminal domain, believed to be the main ligand recognition site, a central DExD/H box helicase domain with ATPase activity and two N-terminal CARDs. LGP2 differs from the other two RLRs in that it lacks the two CARDs in its structure.

RIG-I was originally identified as a gene that was induced in retinoic acid-treated acute promyelocytic leukaemia [186] and was first associated with viral infection when a porcine homolog was displayed to be induced by porcine reproductive and respiratory syndrome virus [187]. In 2004 RIG-I was shown to activate IRF-regulated reporter gene expression in response to Poly(I:C), a synthetic dsRNA and known strong inducer of IFN. RIG-I knock-out mice showed RIG-I as being essential for virus-induced type-I IFN expression in fibroblasts and conventional DCs and is thus critical in regulation of adaptive immunity as well as its major role in innate immunity [188]. MDA5 was originally isolated as a gene induced by mezerin, an IFN and protein kinase C activating compound, in a melanoma cell line [189]. LGP2 was first identified as the gene adjacent to the STAT3/5 locus [190]. All three have since been shown to have vital importance the production of type I IFNs and inflammatory cytokines in the innate immune response to viral pathogens, although their roles do differ and each recognises a different set of viruses and nucleic PAMP structures.

1.4.2: RLRs and their Ligands

Both RIG-I and MDA5 have been shown to recognise viruses and cause an innate immune response due to their ligands, but the viruses recognised differ. LGP2s role is more complicated as it has been shown to be both a negative and positive regulator in response to viral infection. RIG-I detects both negative and positive stranded RNA viruses including Japanese Encephalitis virus, Sendai virus (SeV), Vesicular stomatitis virus (VSV), Influenza virus, Hepatitis C virus (HCV), Respiratory syncitial virus (RSV) and Newcastle disease virus (NDV). Mice deficient in RIG-I show no production of proinflammatory cytokines or type I IFNs in response to any of these viruses, while MDA5 knock-outs still show normal responses. RIG-I can also be activated by the DNA virus Epstein-Barr virus. MDA5 has been demonstrated to recognise Picornaviruses such as Encephalomyocarditis virus (EMCV), Mengo virus and Theilers virus, while the similarity in viral structure would suggest that other Picornaviruses, including CVB3, are recognised by MDA5 as well. Norovirus also appears to be primarily recognised by MDA5 as well as some other Hepatitis viruses. These viruses all showed diminished response in MDA5-deficient mice, but not RIG-I deficient mice. Both can detect Rotavirus, Paramyxoviruses, Herpes simplex virus and Flaviviruses while Reovirus is recognised by MDA5 but also slightly by RIG-I [191;192]. Over-expression of LGP2 causes lowered IFN production in response to viral infection, however LGP2 knock-out cells have an attenuated IFN response to VSV and EMCV, suggesting, that while it probably can't signal downstream due to its lack of CARDs, it may co-operate with MDA5 and RIG-I [193].

The synthetic dsRNA Poly(I:C) has been known to be a potent inducer of IFN for a relatively long time and is a ligand for TLR3 as well as the RLRs. It was initially

thought that MDA5 was the main RLR that recognised Poly(I:C), however it has since been shown that both RIG-I and MDA5 bind Poly(I:C) but differ in specificity based on the length of the Poly(I:C). Long Poly(I:C) (around 2 kbp) is recognised by MDA5, while shorter Poly(I:C) (around 70 bp) is recognised by RIG-I [194]. As most commercial Poly(I:C) is approximately 4-8 kbp this would explain why it was initially thought that MDA5 was the main Poly(I:C) receptor, however partial digestion by RNaseIII leads to smaller fragments of Poly(I:C) of roughly 300 bp that can be recognised by RIG-I and not MDA5 [195]. This would suggest that the same is true of viral nucleic acids and that long dsRNA is primarily bound by MDA5 and shorter dsRNA by RIG-I. dsRNA in most viruses is likely to be a replication intermediate or secondary structures formed such as hairpin structures. It is also possible that dsRNA in some viruses is not an intermediate but generated by defective interfering particles [196-198]. The ability to distinguish between different lengths of dsRNA and structures of RNA may be due to the ability of MDA5 to form a cooperative filamentous assembly along the length of the dsRNA. The filament is suggested to be a dynamic structure that uses ATP hydrolysis to determine its stability [199].

RIG-I also differs from MDA5 in that it recognises RNA with a 5'triphosphate (5'ppp) end. 5'ppp viral RNA is selectively recognised by RIG-I [200;201]. Host RNA is almost always either capped (such as adding a 7-methyl-guanosine cap in mRNA) or post-translationally modified to remove the 5'ppp (tRNA and rRNA), therefore recognising 5'ppp RNA is an excellent way of avoiding "self"-RNA recognition, while 5'ppp RNA is still common in the genomes of most RNA viruses recognised by RIG-I [202;203]. The 5'ppp facilitates dsRNA recognition but is in itself not sufficient for RNA binding by RIG-I. The 10-20bp region behind the 5'ppp is also thought to be essential in recognition by RIG of the viral RNA [204]. Certain viruses avoid RIG-I detection by

removing the 5'ppp structure or by having a cap structure instead. Hantaan virus (HTNV), Crimean Congo hemorrhagic fever virus (CCHFV) and Borna disease virus (BDV) all have the 5'ppp structure removed in infected cells [205], while Picornaviruses have a VPg molecule attached to the 5' end of the viral RNA, blocking the 5'ppp and thus preventing RIG-I from recognising its RNA [206]. As well as the 5'ppp RNA, RIG-I also requires dsRNA to either be blunt ended or have a 5' overhang. 3' overhang RNA becomes unwound and is unable to cause an IFN response, while the blunt end and 5'overhang appear to be resistant to helicase activity, preventing unwinding and can generate an efficient IFN response [207]. Findings on whether RIG-I recognises base sequence vary, with some studies showing that RIG-I recognising Hepatitis C virus requires AU rich sequences, while other groups have shown no involvement of the base sequence of the viral RNA whatsoever [208-210]. RIG-I has also been demonstrated to recognise RNase L cleavage products during viral infections including 5' and 3'monophosphate dsRNAs [211;212]. RIG-I is also capable of detecting DNA viruses through RNA polymerase III-derived 5'ppp RNA that can be generated from viral non CpG DNA [213;214].

As mentioned earlier initial reports showed LGP2 as a negative regulator of RIG-I, most likely through competitive inhibition and is not required for synthetic RNA ligands such as Poly(I:C). It has since been shown that LGP2 is required for IFN production in response to certain viruses recognised by RIG-I and MDA5. The CTD of LGP2 has been shown to bind the terminus of dsRNA regardless of the presence of 5'ppp and with higher affinity than which it is capable of binding 5'ppp ssRNA. It has been suggested that LGP2 may work by making the viral RNA more accessible for binding by RIG-I and MDA5 by removing protein from viral ribonucleoprotein complexes, or by unwinding of the viral RNA [215-217].

Both RIG-I and LGP2 appear to have auto-repression, most likely through the CTD blocking the ATPase/helicase activity as well as the CARDs on RIG-I. The same regions thought to be the repressor domain in LGP2 and RIG-I do not show any auto-repression function in MDA5. It seems likely that the viral RNA ligand binding RIG-I causes it to undergo a conformational change in the presence of ATP that releases the CARDs for downstream signalling [218;219]. Thus the ATPase activity appears to be required for conformational change rather than helicase activity [220]. CARD interaction with the CARD of downstream factors is also reliant on the conjugation of Lys63 linked ubiquitin to RIG-I by E3 ubiquitin ligase tripartite motif protein 25 (TRIM25) [221]. As with auto-regulation this TRIM25 dependant ubiqutination does not occur with MDA5 suggesting that there is differential regulation of RLRs [222]. However both MDA5 and RIG-I are both dependant on the formation of Lys 63 polyubiquitin chains for IRF3 activation [223]. RIG-I then forms an oligomer (possibly a tetramer [224]) allowing its CARDs to interact with the CARDs of Mitochondrial antiviral signalling (MAVS) on the outer membrane of the mitochondria [225].

1.4.3: MAVS and Downstream Signalling

The adaptor molecule for the RLRs, used by both RIG-I and MDA5, was discovered in 2005 by four different groups who identified a CARD containing adaptor molecule located on the mitochondrial outer membrane. Each group gave the molecule a different name, Mitochondrial antiviral signalling (MAVS) [226], Interferon-β promoter stimulator-1 (IPS-1) [227], Virus-induced signalling adaptor (VISA) [228] and CARD adaptor inducing IFN-β (Cardif) [229]. MAVS contains an N-terminal CARD domain, a proline rich region in its centre and a transmembrane domain at its N-terminal. The transmembrane domain is attached to the outer membrane of the mitochondria and

MAVS localisation there appears to be critical. Both forced translocalisation to the ER or plasma membrane as well as C-terminal truncation result in signal activation being stopped [230]. Both RIG-I and MDA5 form oligomeric complexes with MAVS through CARD-CARD interaction upon activation. MAVS was thought to form a dimer which is crucial to its signalling and Baril *et al* showed that blocking MAVS oligomerisation inhibits signal transduction [231]. In 2010 Onoguchi *et al* [232] showed data to suggest that MAVS may form an aggregate in response to viral infection. New data from Hou e*t al* [233] demonstrated that upon viral infection MAVS does indeed aggregate on the mitochondrial membrane and that aggregation is required for IRF3 activation. Upon Lys63 bound CARD terminals from RIG-I or MDA5 binding the MAVS CARD domain, the CARD of MAVS forms protease-resistant and prion-like fibrils. This causes aggregates to form in a progressive manner, with the MAVS aggregates formed from binding the RLR CARDs being capable of inducing other MAVS molecules to form these prion-like aggregates. Of note is that the RIG-I CARD can form Lys63 polyubiqutin chains, which the MAVS CARD is incapable of forming and that the MAVS CARD can form the prion-like fibrils, which the RIG-I CARD is incapable of. It is thought that the region between the CARD and the trans-membrane domain is responsible for recruiting downstream signalling factors.

Once this has occurred MAVS recruits tumour necrosis factor (TNF) receptor associated factor 3 (TRAF3), an E3 ligase for Lys63-linked polyubiquitination which interacts with the TRAF-interacting motif (TIM) in MAVS proline rich region. This then activates two IκB kinase (IKK) related kinases, IKKi and TANK-binding kinase 1 (TBK1) which phosphorylate IRF3 and IRF7 causing their translocation from the cytoplasm to the nucleus. Once activated and in the nucleus IRF3 and IRF7 activate transcription of genes encoding Type I IFNs and IFN-inducible genes. TRAF3 also

signals to the IKK complex which consists of IKKα, IKKβ and NF-κB essential modulator (NEMO) which phosphorylates IκB. This phosphorylation signals IκB for proteosome dependant degradation and allows functional NF-κB to translocate to the nucleus and activate transcription of cytokines. Other molecules that are involved are TRAF2 and TRAF6 which may interact with MAVS in a similar manner to TRAF3. Fas-associated death domain (FADD and receptor interacting protein 1 (RIP1) are both death domain (DD) containing molecules and are both involved by interacting with MAVS at the C-terminal and activate NF-κB through caspase 8 and caspase 10. Another DD molecule, TNFR-associated DD (TRADD), also forms a complex with MAVS, TRAF3, TANK, FADD and RIP1 and is involved in activation of both NF-κB and IRF3 and 7 [234-236].

Type-I IFNs play a crucial role in antiviral responses in the host by inducing transcription of IFN-induced genes (ISGs). Type-I IFNs consist of IFNβ, multiple sub-types of IFNα as well as IFNκ and IFNω. Type-I IFNs activate the transcription of ISGs by engaging the IFNα receptor 1/2 (IFNAR1/2) heterodimer which are present on most cell types and induces the JAK-STAT pathway. There are more than 1000 ISGs, many of which are uncharacterised, however many have shown to possess antiviral effects such as ISG15, myxovirus resistance 1, the 2'-5' oligodenylate synthetases/ribonuclease L system that induces RNA breakdown and protein kinase R (PKR) that phosphorylates the eukaryotic translation initiation factor 2α, resulting in the inhibition of protein synthesis. In addition, Type-I IFNs also enhance the immune response by inducing maturation of dendritic cells, activation of monocytes and natural killer cells, and by promoting T-cell responses and antibody production [237;238].

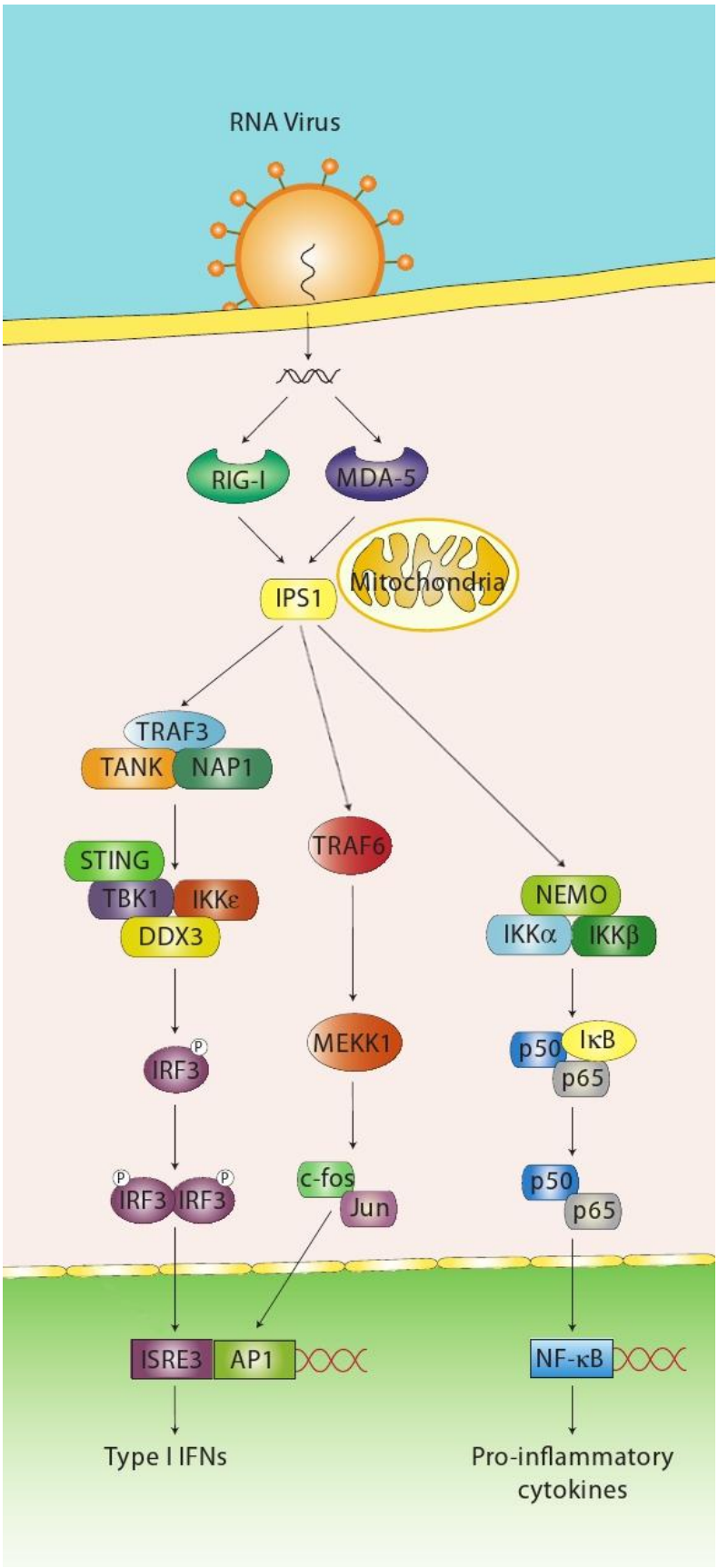

Figure 1.11 - Diagram to show signalling from MDA5 and RIG-I. The RLRs create a signalling cascade through MAVS (IPS1) to activate IRF3 and NF-κB, leading to the release of Type-I IFNs and pro-inflammatory cytokines. Adapted from [115].

1.4.4: RLR Signalling Pathway Regulation by Host and Viruses

There are numerous ways through which both the host and the virus can affect the RLR signalling cascade. Firstly RIG-I and MDA5 are themselves ISGs and are induced by Type-I IFNs. As mentioned earlier TRIM25 aids in RIG-I binding MAVS through polyubiquitination, dependant on caspase 12. Another caspase, caspase 8, while involved in NF-κB activation also cleaves RIP-I and negatively regulates RIG-I, possibly acting as a negative feedback mechanism. Stimulator of interferon genes (STING) appears to have a role in RIG-I signalling as STING deficient mice are more susceptible to VSV, normally recognised by RIG-I. STING is located on the ER and appears to aid RIG-I recognising viral RNA from ER-attached ribosomes and the subsequent association with MAVS [239]. STING also facilitates in recruitment of TBK1 and phosphorylation of IRF3. STING interacts with RIG-I, but does not bind MDA5 [240].

Other molecules that induce IFNs are also capable of inducing the RLRs due to their being ISGs. On top of the NLRs and TLRs that cause Type-I IFN expression there are also DNA sensors such as the cytoplasmic DNA-dependant activator of IFN-regulatory factors (DAI). DAI is highly cell specific in its role, but can detect pathogenic DNA and lead to Type-I IFN production. IFI16, a PYTHIN member like AIM2, detects non-AT rich DNA like VACV DNA and another DExD/H box-containing helicase DHX36 selectively binds CpG-A and both elicit Type-I IFN production in pDCs.

Many viruses have methods of evading detection by the RLRs. V proteins of paramyxoviridae including NDV and SeV can interact with MDA5 and interfere with its activity to transmit a signal. While RIG-I is the usual receptor to detect SeV, and hence the reason for evading MDA5 may seem strange, defective interfering (DI)

particles of SeV contain dsRNA species as a result of abnormal copy back genome synthesis and could be detected by MDA5 if SeV did not utilise this evasion strategy. With Influenza A non-structural protein 1 (NS1) has been reported to interact and inhibit RIG-I. It may also bind RNA sequestering it from RLR recognition. NS3/4a of HCV inhibits RIG-I mediated IRF3 activation by cleaving MAVS and disrupting its mitochondrial activation [241]. Ebola virus VP35 protein serves as a competitor for dsRNA, disrupting RIG-I mediated Type-I IFN production, while SeV V protein selectively binds MDA5 and inhibits dsRNA induced activation of Type-I IFNs [242].

1.4.5: Picornaviruses and RLRs

Finberg *et al* [243] have shown that Type-I IFN production in response to CVB3 is reliant on MAVS, while the cytokine production is not. This is due to MDA5 being essential for the IFN response, although it is probably aided to some degree by TLR3, while other PRRs may have a larger role in cytokine production than MDA5. They showed an increased mortality rate and disrupted Type-I IFN response pathway in MAVS-MDA5 deficient mice. However they did not show whether RIG-I played a role (even if small), or the method by which the RLRs detected CVB3.

The role of TLR3 and MDA5 in Picornaviruses seems to be non-redundant, but rather a complementary role in controlling infection by RNA viruses, by each being predominant in differing cell tissues. TLR3 is required for the survival of mice infected with CVB, with TLR3 deficient macrophages in mice resulting in increased cardiac and liver damage during an acute infection. Loss of MDA5 resulted in faster viral replication, increased liver and pancreas damage and heightened mortality. The IFN response, particularly IFNα, appears to be MDA5 dependant. Results with EMCV-D which causes severe heart pathology showed increased viral titers in the heart and

elevated troponin levels in the serum in MDA5 deficient mice. TLR3 deficient mice have only moderately augmented viral titers in the heart, suggesting MDA5 has the dominant role in protecting against myocarditis in EMCV-D infection. TLR3 appears to be more prominent than MDA5 in the pancreas where it has been shown that TLR3 deficient mice develop diabetes. Mice deficient in MDA5 die due to severe myocarditis before diabetes can occur, but $MDA5^{+/-}$ mice do develop transient hyperglycemia [244]. The MDA5 gene is also a strong candidate for a gene locus associated with type-I diabetes, which would suggest the involvement of MDA5 in auto-immune disorders [245].

Picornaviruses also have evasion strategies to avoid RLR detection. Cleavage of RIG-I by $3C^{Pro}$ from Picornaviruses has been demonstrated with cleavage products appearing 6 hours post infection for Poliovirus, Echovirus type-I and EMCV. The cleavage product was only detected after 14 hours post infection for Rhinovirus type 16 [246]. Cleavage of MDA5 was also found in Picornaviruses with MDA5 cleavage starting at 4 hours post infection with Poliovirus causing a gradual decline in MDA5 levels. The same was not found in Rhinovirus type 16 or Echovirus type 1. For Rhinovirus type 1 and EMCV levels of MDA5 started to decline 6 hours post infection. The cleavage involves caspases and the cellular proteosome. In Poliovirus infection MDA5 has been shown to undergo caspase-dependant cleavage in cells induced to enter apoptosis. Whether this is part of the pathway leading to apoptosis or whether poliovirus induces apoptosis and MDA5 cleavage is a result is unknown [247]. MAVS can also be cleaved by Picornaviruses as Hepatitis A cleaves it though its 3ABC protease [248].

1.4.6: Structure of RLRs and MAVS

The RLRs comprise of three main domains, the CTD, the helicase domain and the two tandem CARDs. The two main RNA binding sites are contained in the CTD and the helicase domain and binding in the CTD is required for the molecule to undergo a conformational change that both releases the CARDs for downstream signalling and activates the ATPase activity in the helicase domain. RIG-I is a 925 residue, 106 kDa protein, while MDA5 is 117 kDa and LGP2 is 60 kDa.

The helicase domain of RIG-I is comprised of two Hel domains, Hel1 (242-456) and Hel2 (458-469, 609-745). The region in the centre of Hel2 is an insertion domain known as Hel2i (470-608). The C-terminal of Hel1 links to Hel2, while a bridging domain from Hel2 links to the CTD. The bridging domain is an elbow like helical structure, forming a long alpha helix that bridges back to Hel1 before connecting the CTD. Without the presence of an RNA ligand Hel2 and Hel2i form a single rigid structure. However upon ligand presentation Hel1, Hel2 and Hel2i all move in relation to each other with Hel1 rotating 60’ and Hel2i by around 23’ if Hel2 is taking as the stable position. This brings together two RecA domains creating mature dsRNA and ATP binding sites as well as causing disordered loops in the RecA domains to become more structured so that they can take part in ATP binding. The bridging domain also becomes involved in stabilising ATP binding. The helicase domain preferentially binds the 3’ end of dsRNA forming a 1:1 dsRNA/RIG-I complex for short dsRNA (around 20bp), while longer dsRNA can form a 2:1 complex with a separate RIG-I binding each end of the dsRNA. The helicase binds the dsRNA with the 3’ backbone coming into the most contact with RIG-I [249].

The tandem CARDs are linked directly to one another and most likely form a rigid structure. They are bound to the Hel2i domain of the helicase with CARD2 bound to Hel2i and in close proximity to Hel1. The close proximity to these Hel domains means that there is enough steric hindrance to stop polyubiquitin chains from forming on the CARDs by TRIM25 [250].

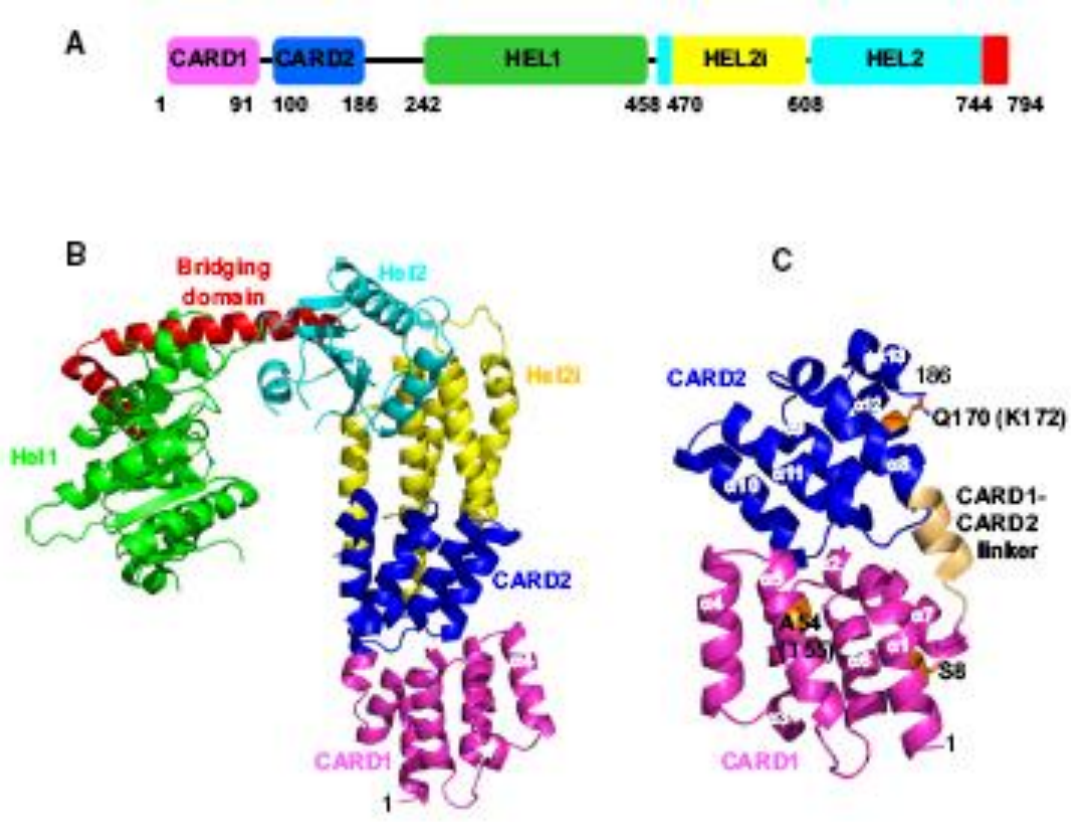

Figure 1.12 - Diagram to how the structure of RIG-I. (A) Domain structure of RIG-Is helicase and CARD domains. (B) Ribbon diagram of the RIG-I helicase and CARD structure. Colours are from A. The Bridging Domain links the helicase domain to the CTD. (C) Tandem CARDs of RIG-I with the linker between the two CARD coloured straw [251].

The CTD interacts primarily with the 5’ strand of the dsRNA, with the opposite strand making only very limited contributions to the binding of the RNA. This could explain why RIG-I is capable of binding ssRNA as well as dsRNA. There are three groups of residues on the CTD that bind RNA, the first interacting with the 5’ppp, the second binds the phosphate backbone and the third interacts with exposed bases at the dsRNA terminus as well as forming hydrogen bonds with the phosphate backbone. The first only interacts with 5’ppp RNA, while the second two interact with both 5’ppp and blunt end RNA. While RIG-I can recognise 5’ppp ssRNA, dsRNA and 5’ppp dsRNA it has a stronger binding affinity for 5’ppp dsRNA [252]. So while the helicase domain binds the 3’ end of the dsRNA, the CTD binds the 5’ end including the triphosphate group. Essentially the binding sites in the CTD and helicase domain complement each other and the receptor encircles the RNA. Unlike the rest of the protein, which is rigid when no ligand is present, the CTD is more flexibly linked to the helicase domain without strong interactions with the rest of the protein so remains available for binding dsRNA. Auto-regulation appears to work through the CARDs which are bound to Hel2i in such a way that it blocks the dsRNA binding site on the helicase domain. dsRNA competes with CARD for the binding site so once dsRNA binds the CTD it can compete with the CARD for the binding site causing the conformational change that releases the CARDs and allows ATP to bind [253].

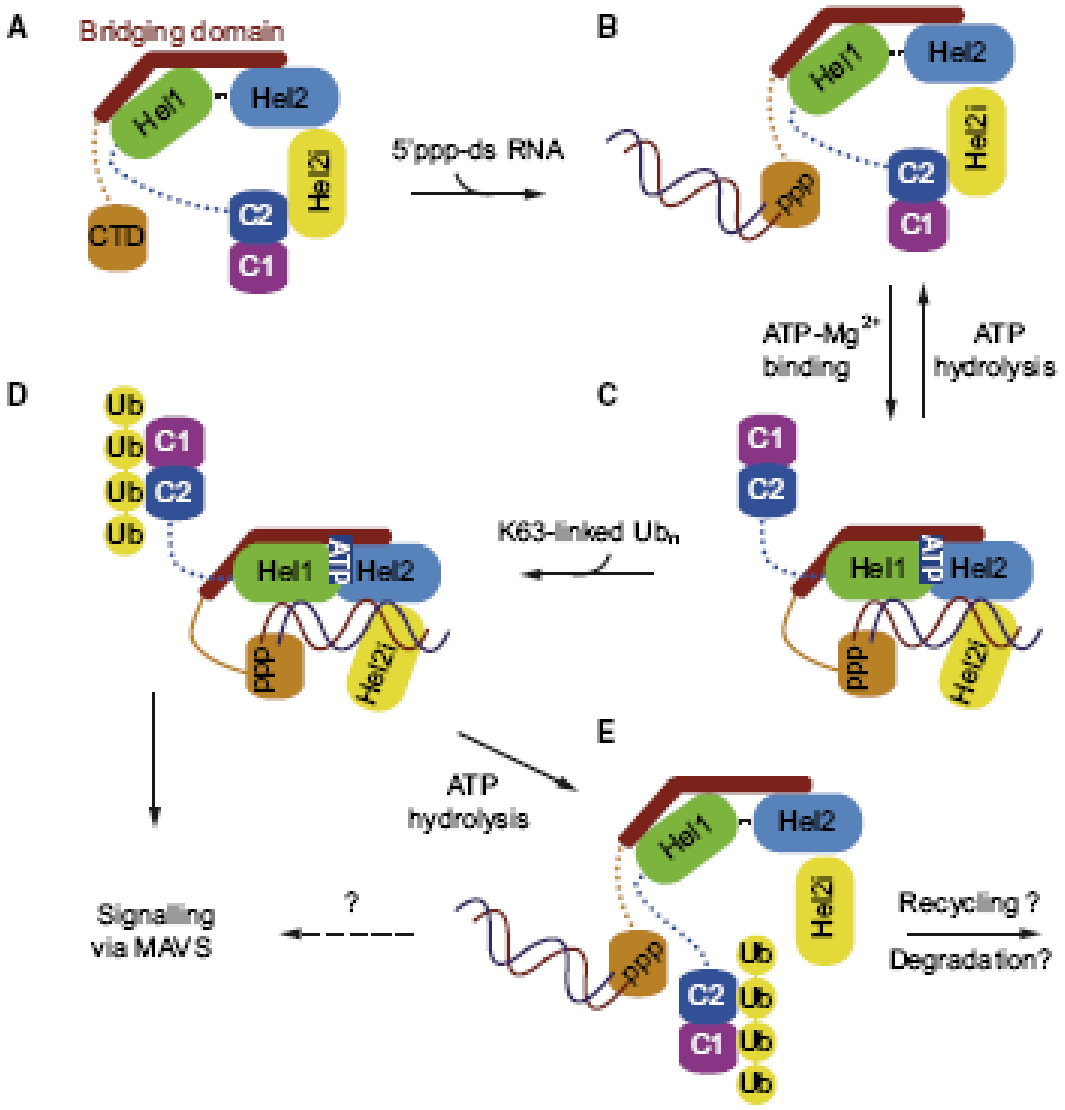

Figure 1.13 - Model from Kowalinski *et al* [254] to show the structure of RIG-I without its ligand and the conformational change upon binding the ligand. (A) RIG-I in an auto-repression state. (B) 5'ppp dsRNA binds the CTD of RIG-I. (C) ATP binding as well as ligand binding causes a conformational change that exposes the CARDs. The CARDs become polyubiquinated leading to (D). The helicase domain also becomes exposed allowing the dsRNA to bind fully. (D) Polyubiquitination allows downstream signalling to MAVS. (E) ATP hydrolysis leads to re-opening of RIG-I either for further use or degradation.

The CTD of RIG-I structure consists of three-leafed β-sheet structure with short connecting helices. The three leaves create a shallow groove on the concave side of the CTD carrying a positive electrostatic potential and forms the main binding site for the

RNA 5’ terminus, mainly interacting with the phosphate backbone. The MDA5 CTD consists of two four stranded β-sheets, one at the end terminus and one in the centre of the CTD and linked by a β-hairpin. They are also joined by four highly conserved Cys residues that coordinate a zinc ion crucial in maintaining the CTDs fold. A long loop known as the specificity loop between β-strands 5 and 6 is similar between RIG-I and MDA5, but absent in LGP2 and is responsible for recognising the RNA end structures. The β-sheet containing β5-8, the β hairpin, the specificity loop and loops between β8-9 and β9 to the C-terminal helix have a positive charge and thus form the RNA binding site in MDA5 similar to RIG-I and LGP2. RIG-I contains an extra positively charged area that could be responsible for binding the 5’ppp, counteracting the negative charge of the triphosphate moiety [255;256]. There is also a CTD binding loop that is critical in P2 and RIG-I but less so in MDA5 that could also explain why MDA5 binds slightly different ligands to RIG-I and LGP2 [26].

MAVS consists of an N-terminal CARD, a proline rich domain involved in protein interactions and a c-terminal transmembrane domain. It has three TRAF interacting motifs (TIMS), with the first two being in the proline rich region, one that binds TRAF6 and one that binds TRAF2. The third TIM is located close to the C-terminal and binds both TRAF6 and TRAF3. Both the C-terminal and N-terminal binding sites are required for TRAF6 to bind and for TRAF6 mediated activation of NF-κB. The C-terminal TIM binding of TRAF3 is essential for mediating the induction of IFN and ISG expression [257].

1.3: Aims and Objectives

While Finberg et al have shown that MDA5 is the RLR that recognises and creates a Type-I IFN response to CVB3, it remains unclear as to RIG-Is role in Coxsackievirus recognition, whether the same is true of CVA viruses and what the specific ligand is. Using both CVA9 and CVB3 the aim is to isolate RNA structures from both viruses and determine if any are recognised by either RLR and if in doing so activate the type-I IFN response.

It has been shown that during the Coxsackievirus life cycle, as well as the positive ssRNA genome of the virus, there are also the RF dsRNA intermediate and the RI dsRNA which is a single strand of RNA with nascent strands attached. By isolating these and infecting cells it should be possible to determine which of the natural Coxsackievirus RNAs activates the RLRs. By infecting cells with synthetic dsRNAs it will also be possible to determine the effect of having end-group structures on dsRNA. Using confocal microscopy should allow visualisation of any PAMP/PRR binding that may occur, while the innate immune response can be determined by measuring the activation of IRF3 or NF-kB and through cytokine assays. It is expected that as MDA5 recognises poly(I:C) that the RF form of the dsRNA intermediates will cause an immune response, while the ssRNA will not be bound by the RLRs. Due to its partial dsRNA, partial ssRNA structure, the RI could potentially be recognised by either RLR, however is most likely bound by MDA5 if at all.

Using Huh7 (wt) and Huh7.5.1 cells which have a mutation causing a defective RIG-I it can be determined whether the removal of RIG-I has any effect on the immune response to Coxsackie virus. While the most plausible outcome is that RIG-I is prevented from binding the ssRNA due to its VPg end group, its role needs to verified. Specifically the

possibility that the VPg end group is removed during replication allowing RIG-I to bind the ssRNA, but also whether any of the dsRNA intermediates are recognised. The RI may allow RIG-I to bind its nascent strands for example.

Other PRRs have been shown to form dimers, or large oligomeric structures (such as the inflammasome), as well as evidence that MAVS forms a homodimer. The same may therefore be true of the RLRs and using immunoprecipitation of the RLRs from infected cells may allow an insight, not just into whether RLRs form oligomeric structures, but also into the role of LGP2. The main aim is to see whether LGP2 binds RIG-I or MDA5 before and during Coxsackie infections, as well as looking for RIG-I or MDA5 homodimerisation.

Chapter 2: Materials and Methods

2.1: Chemicals

All fine chemicals were obtained from Sigma (UK). The mAb J2 used for dsRNA detection recognises double-stranded RNA (dsRNA) provided that the length of the helix is greater than 40 bp. dsRNA-recognition is independent of the sequence and nucleotide composition of the antigen [258]. The J2 antibody was obtained from English & Scientific Consulting Bt (Hungary). Alexa 488-Ulysis reagent was obtained from Molecular Probes Inc (Cambridge Biosciences, Cambridge, UK). Viral RNAs were labelled with Alexa-488-Ulysis reagent according to the manufacturer's instructions.

Synthetic RNAs:

The Synthetic RNAs used were the following:

- Poly (I:C) purchased from Invitrogen USA
- 5'OH-dsRNA 25-mer has a 5'OH modification, molecular weight of 8.31 kDa and a GCAGAGGGUGGCGCUCCCGACAAGC sequence. Purchased from Eurogentec.
- 5'ppp-dsRNA has a 5'ppp modification, molecular weight of 6.47 kDa and a GCAUGCGACCUCUGUUUGA sequence. Purchased from Eurogentec.

Antibodies:

The antibodies used were the following:

- Donkey Anti-Goat IgG (H+L) TRITC (Rhodamine), purchased from Jackson Immuno Labs 705-025-003.
- IRF-3 (FL-425) Rabbit Polyclonal IgG, purchased from Santa Cruz Biotechnology sc-9082.

- LGP2 Goat pAb to DHX58, purchased from Abcam ab82151.
- LGP2 (H-159) Rabbit Polyclonal IgG, purchased from Santa Cruz Biotechnology sc-134667.
- MAVS (T-20) Goat Polyclonal IgG, purchased from Santa Cruz Biotechnology sc-70096.
- MDA5 (C-16) Goat Polyclonal IgG, purchased from Santa Cruz Biotechnology sc-48031.
- MDA5 (H-61) Rabbit Polyclonal IgG, purchased from Santa Cruz Biotechnology sc-134513.
- Phospho-IkappaBalpha (Ser32) (14D4) Rabbit mAb, purchased from Cell Signaling Technology #2859L.
- Rabbit Anti-Goat Polyclonal Immunoglobulins FITC, purchased from DAKO F0250.
- RIG-I (C-15) Goat Polyclonal IgG, purchased from Santa Cruz Biotechnology sc-48929 .
- RIG-I (H-300) Rabbit Polyclonal IgG, purchased from Santa Cruz Biotechnology sc-98911.
- Streptavidin-HRP conjugate, purchased from Amersham Biosciences 1058765.
- Swine Anti-Rabbit Polyclonal Immunoglobulins FITC, purchased from DAKO F0205.
- Swine Anti-Rabbit Polyclonal Immunoglobulins HRP, purchased from DAKO P0217.

2.2: Tissue Culture

The following basic tissue culture techniques were used on all the cell lines utilised throughout the project. All tissue culture (TC) was performed in a Microflow Class 2 laminar flow hood in a sterile environment. Aqueous Virkon was used to clean the work area before use, and to clean all the equipment before placing it inside the cabinet, to ensure sterility. A lab coat and disposable gloves and shoes were worn. 25cm^2 Nunclon^{TM} Surface Flasks and Nunc Falcon tubes were used throughout.

2.3: Cell Lines

2.3.1: Human Cardiac Cell Line

Human Cardiac (Girardi) cell line (ECACC – European Collection of Animal Cell Cultures), maintained in 1g/L Glucose Dulbecco's Modified Eagle's Medium (DMEM), containing GlutaMAX, 10% heat-inactivated Foetal Calf Serum (FCS), and 1% non-essential amino acids (Invitrogen (UK)).

2.3.2: Huh 7.0 and Huh 7.5.1 Cell Lines

Human Hepatocellular (Huh) 7.0 cell line (Kindly donated by Dr Chisari, Scripps Research Institute, USA), maintained in 4.5g/L glucose DMEM, containing GlutaMAX, 10% heat-inactivated FCS, and 1% non-essential amino acids (Invitrogen (UK)).

Huh 7.5.1 cell line (Kindly donated by Dr Chisari, Scripps Research Institute, USA), maintained in 4.5g/L glucose DMEM, containing GlutaMAX, 10% heat-inactivated FCS, and 1% non-essential amino acids (Invitrogen (UK)). They contain a RIG-I mutation that leads to a defect in IFN production.

2.3.3: Human Embryonic Kidney (HEK) 293 Cell Line

HEK 293 cell line (ECACC), maintained in 1g/L DMEM, containing GlutaMAX, 10% heat-inactivated FCS, and 1% non-essential amino acids (Invitrogen (UK)).

Transfections of HEK/MDA5 and HEK/RIG-I cells with puno-hMDA-5, or puno-RIG-I (Invivogen) were performed using Lipofectamine 2000 according to the manufacturer's recommendations. HEK/MDA5 and HEK/RIG-I were maintained in DMEM containing 4.6 g/L glucose with 10% FCS and 100μg/ml Ampicillin.

2.3.4: HEK-Blue IFN-α/β Cells

HEK-Blue IFN-α/β cells were purchased from Invivogen USA and maintained in DMEM, 4.5 g/l glucose, 2-4 mM L-glutamine, 10% (v/v) fetal bovine serum, 50 μg/ml penicillin, 50 μg/ml streptomycin, 100 μg/ml Normocin.

These cells allow the detection of human type I IFNs by monitoring the activation of the ISGF3 pathway. These cells were generated by stable transfection of HEK293 cells with the human STAT2 and IRF9 genes to obtain a fully active type I IFN signalling pathway. The other genes of the pathway (IFNAR1, IFNAR2, JAK1, TyK2 and STAT1) are naturally expressed in sufficient amounts. The cells were further transfected with a SEAP reporter gene under the control of the IFN-α/β inducible ISG54 promoter. Stimulation of HEK-Blue IFN-α/β cells with human IFN-α or IFN-β activates the JAK/STAT/ISGF3 pathway and subsequently induces the production of SEAP. Levels of SEAP in the supernatant can be easily determined with QUANTI-Blue.

QUANTI-Blue is a colorimetric enzyme assay developed to determine any alkaline phosphatase activity (AP) in a biological sample, such as supernatants of cell cultures. It

detects and quantifies secreted embryonic alkaline phosphatase (SEAP), a reporter widely used for in vitro and in vivo analytical studies.

In the presence of alkaline phosphatase, the colour of QUANTI-Blue changes from pink to purple/blue. The intensity of the blue hue reflects the activity of AP. The levels of AP can be determined quantitatively using a spectrophotometer at 620-655 nm.

2.3.5: Primary Cardiac cells

Primary human cardiac cells were obtained from an adult male (TCS cell works) and maintained in the cell medium provided from TCS.

2.3.6: LLC Cell Line

LLC (Lewis Lung Carcinoma) cell line (ATCC – American Type Culture Collection), maintained in 1g/L DMEM, containing GlutaMAX, 10% heat-inactivated FCS, and 1% non-essential amino acids (Invitrogen (UK)). The LLC is a monkey cell line that is susceptible to nearly all viruses so it is extensively used for virus propagation.

2.4: Coxsackievirus B3 (CBV3) / Coxsackievirus A9 (CAV9)

2.4.1: Propagating CBV3/CAV9

A prototype strain of CBV3 (Nancy strain) or CAV9 (Griggs strain) was obtained from the ATCC, and propagated on LLC cells. 100 µl of virus was added to a flask of 1.5 ml LLC cells and incubated at 37^{o}C 5% CO_2 for approximately 24 hours. Once all the cells had been killed, the flasks were freeze-thawed three times, to break open the cells and release the virus. The cell supernatant was then transferred to 50 ml Falcon tubes and centrifuged at 12,000 rpm for 5 minutes at RT. The supernatant containing the virions was then added to fresh 50ml Falcon tubes and frozen at -80^{o}C.

2.4.2: Purifying CBV3 and CAV9 using a Sucrose Density Gradient

Both of the viruses were purified using a sucrose gradient purification procedure, prepared in 40 ml Beckmann SW28 ultra-centrifuge tubes. The sucrose solutions were layered into the tubes in the following order (with the boundary between them marked): 7 ml 60% sucrose in PBS; 6 ml 30% sucrose in PBS; and 3 ml 10% sucrose in PBS. 15 ml virus was gently loaded onto the gradient, and the tubes were centrifuged at 25,000 rpm for 90 minutes at 4°C. The virus settles in a band at the interface between 30% and 60% sucrose. The top layers of sucrose were carefully removed, and the purified virus was pipetted into 15 ml Falcon tubes and frozen at -80°C.

2.4.3: Isolating Single-Stranded RNA (ssRNA) from Purified virus

In tissue culture, 300 µl of purified CBV3 or CAV9 was added to sterile eppendorfs. Each eppendorf will end up containing 80 µl ssRNA, enough for two indirect immunofluorescence stimulations of 40 µl each. From this point on, all work was performed in a fume hood with sterile eppendorfs and tips, to ensure the purity of the ssRNA.

2 µl vanadyl ribonuclease complex (an RNase inhibitor, which stops the breakdown of RNA) was added to each eppendorf, followed by 300 µl ultra-pure phenol (the bottom layer). Phenol dissolves any proteins present. After vortexing for 5-10 seconds, the eppendorfs were centrifuged at 13,000 rpm for 10 minutes at RT. The upper layer was then transferred to new eppendorfs. 300 µl chloroform / isoamyl alcohol (chloroform dissolves lipids present, and isoamyl alcohol ensures deactivation of RNase) was added to each eppendorf, followed by another round of vortexing and centrifugation. The upper layer was again transferred into new eppendorfs. 15 µl ($1/20^{th}$) sodium acetate 2M pH 6.5 and 750 µl (2.5x vol) of 95% ethanol were added, mixed, and the eppendorfs

were then frozen at -80^{o}C for at least 60 minutes. Afterwards, the eppendorfs (straight from the freezer) were centrifuged at 13,000 rpm for 30 minutes at RT. The excess supernatant was removed, the eppendorfs were centrifuged at 13,000 rpm for a further minute, and the remaining supernatant was removed, leaving just a pellet of ssRNA. 80 µl sterile water (ddH_2O), or LAL water, was added to each eppendorf, and the ssRNA was frozen at -80^{o}C.

2.4.4: Isolation of dsRNA

The replicative intermediate dsRNA and the high order RI-RNA containing dsRNA with nascent ssRNA strands of CAV9 or CBV3 was isolated from infected cells, where the infection had proceeded for 5 hrs and dsRNA was purified from the cytoplasm of these cells using a protocol similar to Richards and Ehrenfeld [259-261]. Girardi cardiac cells ($5x10^{8)}$ were infected with virus at a multiplicity of 50 PFU/cell. Cells were lysed with lysis buffer (0.5% Nonidet P-40, 10 mM Tris-Hcl, 10 mM NaCl, 1 mM $MgCl_2$, 0.5 mM $CaCl_2$. Cell debris was removed and the supernatant was extracted with an equal volume of buffer A (0.15 M NaCl, 0.01 M Tris-HCl pH 8.3, 5 mM EDTA in saturated phenol). After centrifugation the aqueous phase was removed and again treated with buffer A. The aqueous layer was removed and precipitated with 0.2 M sodium acetate and 95% ethanol at -20^{o}C. The ethanol precipitate was dissolved in 10 mM EDTA-1% SDS and fractionated in 2 M LiCl at -20^{o}C. The suspension was centrifuged at 16,000 and the LiCl soluble fraction containing replicative dsRNA and RI-RNA was chromatographed through a CF11 cellulose column. The material eluted was ethanol precipitated and further purified by analytical zonal sedimentation in a 15% to 30% sucrose gradient (On 15% to 30% sucrose gradients RF RNA sedimented at 20S and banded at a density of 1.63g/ml, whereas viral ssRNA sedimented at 35S and banded at

a density of 1.68 g/ml). The precipitated RNA from appropriate fractions was further fractioned on a FPLC Superdex 200 column. The fractions containing dsRNA were pooled and ethanol precipitated.

2.5: Indirect Immunofluorescence

Immunofluorescence is a technique that uses a fluorescent dye (fluorochrome) conjugated to an antibody that binds a specific protein or antigen [262]. For example in these experiments fluorescein isothiocyanate (FITC) was used as the fluorescent dye. There are two major types of immunofluorescence, direct and indirect. In direct immunofluorescence the antibody that binds the antigen/protein is directly conjugated to the fluorochrome. In indirect immunofluorescence a primary and a secondary antibody are used. This method can be seen in Figure 2.1 and was the type used in these experiments. The primary antibody binds the antigen/protein for which it is specific, but does not have a fluorochrome conjugated to it (A). Any unbound primary antibody is then washed away, leaving just the primary antibody bound to the specific antigen/protein (B). The secondary antibody is specific for the primary antibody and does have a fluorochrome conjugated to it, binding the primary antibody that is bound to the antigen/protein (C). Again

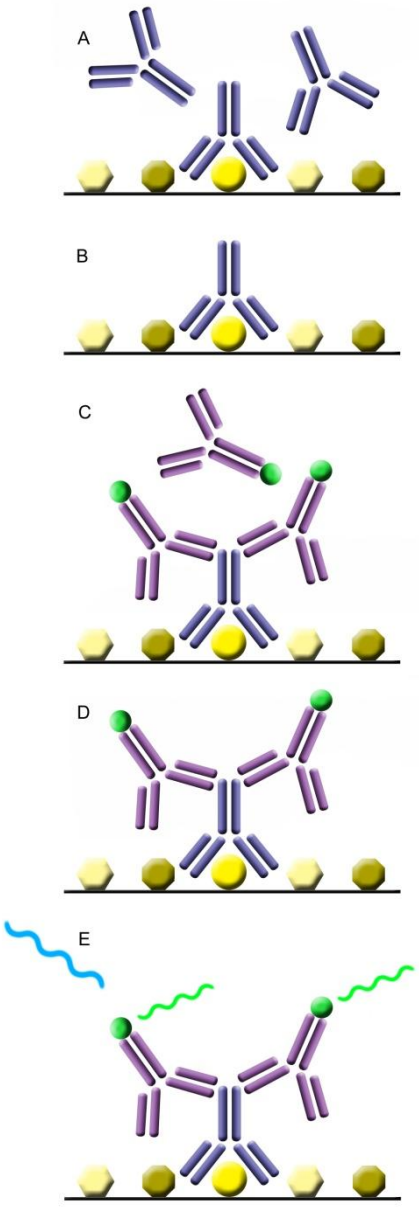

Figure 2.1 - Diagram to show the mechanics of indirect immunofluoresence.

unbound secondary antibody is washed away (D). Finally a laser is used to excite the fluorochrome and causes it to emit a different wavelength light which can be detected (E). The main advantage of indirect over direct is that several of the secondary antibodies can bind each primary antibody thus creating a brighter fluorescence than in the direct method [263].

The fluorochrome absorbs and emits different wavelengths of light as follows. At a normal temperature a molecule is at its ground state, however upon excitation using a photon of light an electron can jump to an excited state. Collision with surrounding molecules dissipates some of the excited energy however it quickly undergoes spontaneous emission, losing the remaining energy by emitting light of a longer wavelength. Fluorescein for example emits a green light upon being excited by blue light. This allows specific labelling of certain proteins within a sample as well as labelling different proteins by using molecules that absorb and thus emit different wavelengths of light from each other [4].

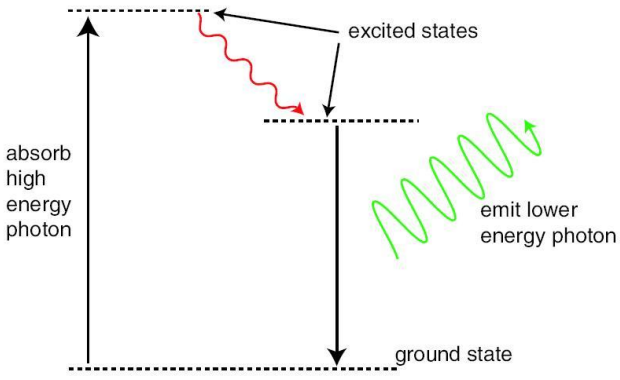

Figure 2.2 – Diagram of fluorochrome absorption and emission. The dotted lines show quantum energy levels within a molecule. Upon absorption of a high energy photon the energy level of the molecule is raised to an excited state. The red arrow indicates the dissipation of some of the energy by colliding with surrounding molecules, causing the molecule to be in a lower energy excited state. The green arrow shows the spontaneous emission of a longer wavelength light causing the molecule to fall back to its ground state energy level [4].

2.6: Flow Cytometry

Flow cytometry is a way of measuring characteristics of a single cell at a time as they flow past detectors using means such as light excitation, light scattering and fluorescence [264;265]. In order to measure a single cell at a time the sample of cells is injected into a sheath flow known as the fluidics system [1]. The fluidics system has a central core section through which the sample is passed and a surrounding section of sheath fluid which is travelling in the same direction at a higher speed. As well as this the diameter of the flow is reduced forcing the cells into the centre of the stream [265]. Together this creates a drag effect on the sample in the central core and changes its velocity causing the cells to be arranged in a single file [1]. This allows the cells to pass one at a time through a laser. As the cells pass through the laser they scatter light as well as fluorescing if labelled with fluorochrome molecules. The fluoresced light wavelength depends on the fluorochrome used [265].

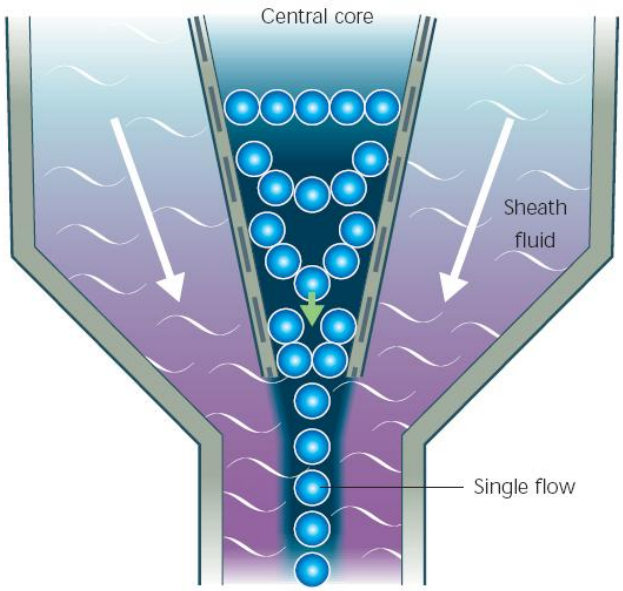

Figure 2.3 - Diagram of the mechanics by which the flow cytometer uses sheath fluid to force cells to pass before the laser one cell at a time [1].

Light scattered in the forward direction is detected by a photomultiplier tube (PMT) that converts the intensity of light into voltage. An obscuration bar is placed in front of the PMT stopping the intense light from the laser beam reaching the PMT, only the forward scatter light that is scattered around the obscuration bar reaches the PMT and is detected. The forward scatter detected correlates to the size of the cell with small cells

producing a small amount of forward scatter and with larger cells creating larger amounts of forward scatter [266].

The side scatter produced is dependent on the granular content and structural complexity of the cell [1]. The side scatter is detected by a different PMT than the forward scatter (often at 90’ to the laser) and is focused via a lens system [266].

Combining the forward and side scatter data allows differentiation between different types of cells within the cell sample population. For example in a blood sample the lymphocytes, monocytes and neutrophils can be distinguished from one another.

As in our experiments only one cell type was used at a time the amount of fluorescence is of more interest. As explained before when the laser hits the cell it causes the fluorochrome antibody to emit light of a different wavelength. The emitted light travels along the same path as the side scatter light and passes through a series of dichroic mirrors and filters, separating different wavelengths of light for detection. The intensity of fluoresced light is detected by a PMT and converted to voltage. There are three major types of filter used, long pass which allows light of a wavelength above a certain point to pass through, short pass which allows light of a wavelength below a certain point to pass through and band pass which allows only a narrow range of wavelengths to pass through [1]. These filters absorb the light not of the permitted wavelength while the dichroic mirrors are set at a 45’ angle to the light. Dichroic mirrors permit a certain wavelength or range of wavelengths through however instead of absorbing the non-permitted light it is reflected. Thus a specific wavelength of light can be separated and detected by a PMT and the fluoresced light from each cell measured.

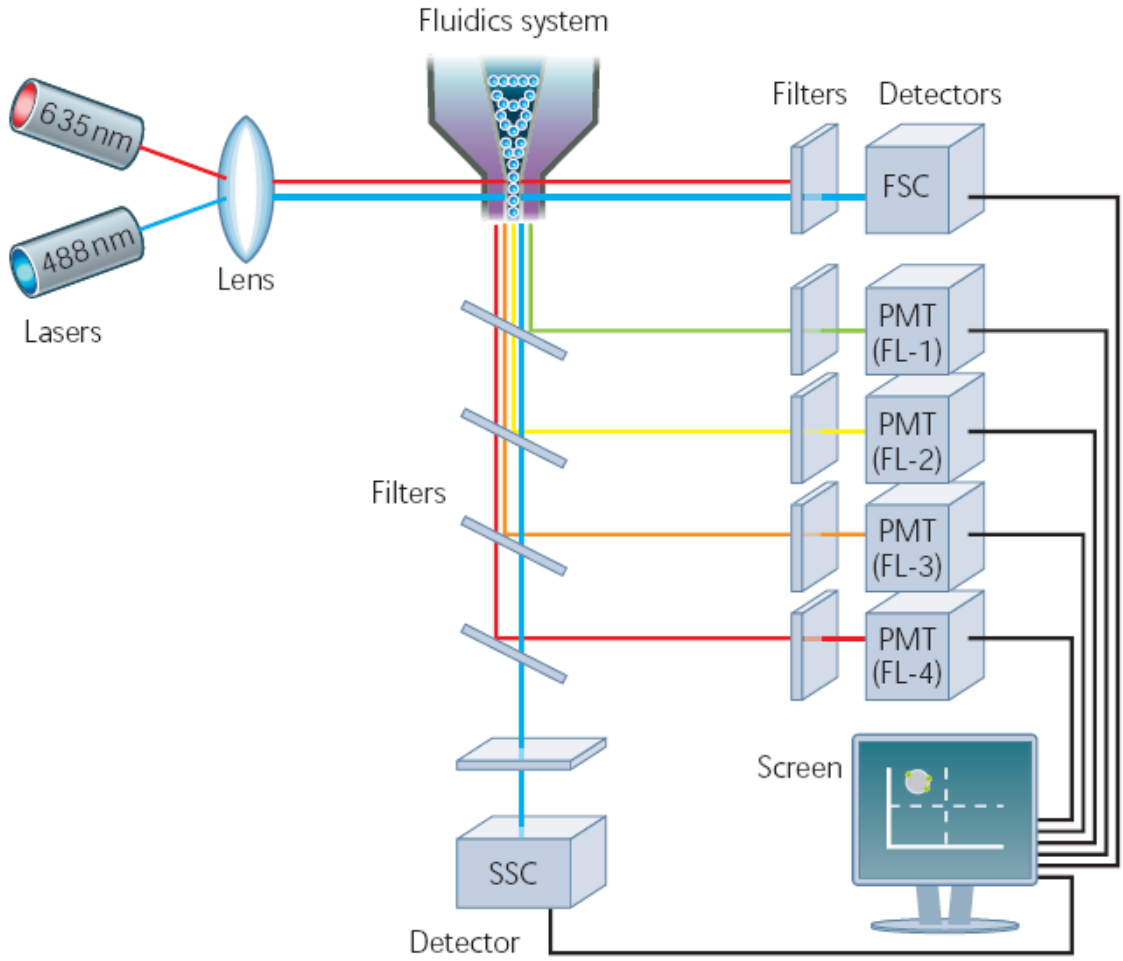

Figure 2.4 - A diagram of the overall setup of a flow cytometer. The fluidics system channels the cells so they pass through the laser one at a time. The forward scatter light is detected by a PMT (labelled FSC) and the side scatter is detected by a second PMT (labelled SSC). The fluoresced light passes through a range of dichroic mirrors reflecting first shorter wavelength light for detection, then longer and longer wavelengths so that each range of wavelengths is detected by a separate PMT. They also pass through a filter to make sure the correct wavelength light is being detected. The voltages created upon detected are sent to a computer and processed as data [1].

2.6.1: Determining RIG-I and MDA5 Expression Levels

Indirect immunofluorescence followed by flow cytometry was used to investigate the expression levels of RIG-I and MDA5 before and after stimulation. Confluent cells were stimulated with either 5 moi CBV3 or 20 μg/ml ssRNA, dsRNA or synthetic RNAs and incubated for 1, 2, 4, or 6 hours. Three flasks were needed per stimulation per time point. At each time point, 2 ml of the supernatant was added to screw-top

eppendorfs and frozen at -20°C, for use in the Cytometric Bead Array assay. The cells were then scraped off, washed with PBS and fixed with 4% Paraformaldehyde (PFA).

After centrifuging at 13,000 rpm for 2 minutes at RT, the cells were resuspended in 1 ml PBS / 0.02%$_{(w/v)}$ Bovine Serum Albumin (BSA) / 0.02%$_{(w/v)}$ Saponin / 0.02%$_{(w/v)}$ Sodium Azide (NaN_3). BSA is used as a carrier protein to antibodies and as a general protein blocking agent. The amphipathic nature of Saponin makes it act as a surfactant, enhancing the penetration of proteins through the cell membrane. NaN_3 prevents the internalisation of surface antigens, which could produce a loss of fluorescent intensity. The cells were then centrifuged and the supernatant aspirated off again, followed by resuspension in 100 µl PBS / BSA / Saponin / NaN_3, and incubation with 2 µl of primary antibody (MDA5 (C-16) Goat pAb or RIG-I (C-15) Goat pAb) for one hour or greater at RT.

After incubation in primary antibody, the cells were washed and resuspended in 100 µl PBS / BSA / Saponin / NaN_3, followed by incubation with 2µl of secondary antibody (pAb Rabbit anti-Goat FITC) for 45–60 minutes in the dark (to prevent photobleaching) at RT. The cells were then washed twice in PBS / BSA / Saponin / NaN_3, then resuspended in 500 µl PBS and transferred to flow tubes and run on the FACSCalibur™. 10,000 cells not gated were analysed for each sample.

2.7: SDS-PAGE and Western Blotting to detect pIκB, total IκB and IRF3

2.7.1: SDS-PAGE

SDS-PAGE stands for Sodium Dodecyl Sulphate Polyacrylamide Gel Electrophoresis. Electrophoresis is the separation of macromolecules in an electric field [267]. SDS is an anionic detergent used to denature proteins leaving them in their primary structure. The negative charge of SDS destroys most of the protein bonds as well as giving the protein a uniform negative charge making the protein travel to the positive pole in an electrical field [267;268]. The denaturation of the protein into its primary state is caused by heating the sample in a buffer containing soluble thiol reducing agent (such as β-mercaptoethanol in this case), which destroys all disulphide bonds on cysteine residues as well as SDS [269]. This results in proteins being separated by their primary structure size alone, having been given a uniform negative charge and removing all secondary, tertiary and quaternary structure of the proteins.

If the proteins are all denatured and with equal charge they will move in an electrical field towards the positive pole at the same rate. For this reason the medium used through which the protein moves is polyacrylamide. Polyacrylamide is porous and allows smaller molecules to pass through faster than larger ones, thus separating proteins based on their molecular mass [267]. The more concentrated the acrylamide, the smaller the pores in the gel are and the slower the proteins move through the gel. Polyacrylamide is a polymer of monomeric acrylamide, crosslinked with N,N'-methylene-bis-acrylamide (BIS). Together they do not polymerise but require ammonium persulphate (APS) for free radicals and -N,N,N',N'-tetramethylethyline diamine (TEMED) as a catalyst to start polymerisation [269].

When setting up a gel, a resolving gel is created and then a stacking gel on top. The reason for this is that the stacking gel, to which the proteins are loaded, is a low concentration polyacrylamide gel and so all the proteins move through it quickly and at relatively the same speed. When they reach the boundary of the resolving gel, the resolving gel is a higher concentration and essentially forces the protein to line up at the border and start moving more slowly through the higher concentration gel. It is in the resolving gel that the proteins are separated based on mass, when an electrical current is passed through the gel.

2.7.2: Western Blotting

Western blotting is a technique used to transfer the proteins that have been separated by SDS-PAGE onto a nitrocellulose membrane, and then probe them with antibodies for further analysis. Using the electroblotting method, a sandwich of the gel (with the stacking gel trimmed off) and the nitrocellulose membrane was compressed in a cassette between two layers of blotting paper and pads pre-soaked in transfer buffer. The gel holder cassette was then placed into a tank transfer system together with an ice block, and the tank filled with transfer buffer. A constant current of 210 mA was applied for 60 minutes, electrophoretically transferring the proteins from the gel to the membrane [270;271]

2.7.3: Immuno-Blotting membranes with Antibodies

A blocking reagent is used on the membrane, usually a source high in protein (in this case a milk powder solution), to prevent the antibodies from binding parts of the membrane which do not have protein bands. As nitrocellulose has a high binding affinity for all proteins, antibodies would naturally bind to it, however by using a

protein rich liquid, protein will bind the rest of the membrane ‘blocking’ the antibodies from binding [270].

Once blocked the membranes are incubated first with a primary antibody specific for the protein being detected and then with a secondary specific for the primary and conjugated to horseradish peroxidise (HRP). To detect the bands the membrane has electrochemiluminescence (ECL) reagent added to it causing the HRP to emit light. In a dark room the membrane has photographic film placed onto it which forms dark bands where there has been luminescence after developing.

2.8: Immunoprecipitation of RIG-I, MDA5 and LGP2

Immunoprecipitation is used to isolate an antigen using a specific antibody, usually from a complex solution such as cell lysate. The lysate is incubated with the antibody, before an insoluble support is added (in this case protein-A sepharose beads) which immobilises the antibody and bound antigen. Before adding the antibody, the cell lysate was mixed with protein-A sepharose beads as a pre clear. Pre-clearing is used to remove proteins that bind the immunoglobulin non-specifically, lowering the background and signal to noise ratio [272]. The sample is mixed thoroughly before being centrifuged. The supernatant is removed and new lysis buffer added and then the cycle repeated so that all the non-bound parts of the lysis have been washed out, leaving only the antibody and bound protein with the protein-A sepharose beads. The lysis buffer used is dependent on the target protein being immunoprecipitated and has many important functions including stabilising the native protein conformation, inhibiting enzymatic activity, minimising denaturation of the antibody binding site and increasing protein release from the cell lysate [273]. Once washed the protein is eluted using the reducing

sample buffer used in SDS-PAGE and once the sample buffer had been left for 15 min it can be added to the SDS-PAGE set up to be run.

To test whether RIG-I, MDA5, and LGP2 homo- or heterodimerise together, immunoprecipitation experiments were performed. The technique can be used to isolate a particular protein, as well as determine if dimerisation between two proteins has occurred. In this project, RIG-I, MDA5, or LGP2 antibodies were used to precipitate out their respective protein, and SDS-PAGE was then used to detect a different protein, i.e. precipitate out MDA5 and perform SDS-PAGE to detect LGP2.

Cardiac cells were stimulated with CBV3 for 1, 2, 4, and 6 hours, or left unstimulated (0 hour). At each time point, the cells were washed, lysis buffer was added for over 2 hours, followed by centrifugation and transferral of the supernatant to new eppendorfs. The cell lysate was then pre-cleared twice in Protein A Sepharose (PAS) beads, to prevent non-specific binding of the antibody to unwanted proteins, followed by incubation with primary antibody and more PAS beads.

The reason Protein A is used is that it binds specifically to the heavy chains in the Fc region of antibodies. This results in the antibody being oriented so that the antigen binding site faces outwards, immobilising the antibody while also allowing it to effectively bind the antigen [273].

After washing the resulting pellet in lysis buffer, the samples were analysed using SDS-PAGE and western blotting, using X2 SDS-PAGE Non-Reducing Sample Buffer.

2.9: Confocal Microscopy

Confocal microscopy is a technique used to visualise the interaction and location of different proteins within cells. A confocal microscope can create sharp images of

specimens by excluding out-of-focus light in specimens which are thicker than the focal plane by using a spatial pinhole. This increases the micrograph contrast and enables reconstruction of three-dimensional images.

Originally developed by Minsky in 1955 it sequentially focused a point of light across a specimen, point by point, and collected the returning rays. He reduced background light by firstly only focusing light on a single point and also by passing the collected light through a second pinhole aperture that removed unwanted light. To scan the specimen the stage that held the specimen moved, rather than the light source.

In fluorescence confocal microscopy a molecule absorbs light of one frequency and emits light at a different frequency. The sample is dyed and a suitable wavelength light is used to illuminate it. The resulting emitted light is collected and an image is formed. A dichroic mirror is used that reflects lower wavelength light buts transmits longer wavelength light. This allows light from the source to be reflected through the objective onto the sample, while the fluorescent light passes through the objective and the mirror as it is a longer wavelength. This method is called epifluorescence.

At a basic level, confocal microscopy works by having two lenses that focus the light from the focal point of one lens to the focal point of the other. The aim is to see only the focal point of one of the lenses on the specimen so a pinhole is created at the focal point of the other lens stopping light from any other point than the focal point from passing through. The specimen is also only illuminated by a single beam of light at the focal point using a pinhole system, reducing the amount of light from out of focus parts. This is unlike fluorescent microscopy where the entire section of the specimen is illuminated. The focal point forms an image at the pinhole thus the two points are known as conjugate points. The pinhole is conjugate to the focal point, hence ‘confocal’.

In Figure 2.5 it can be seen that the laser emits a blue light, which is reflected off the dichroic mirror and onto a pair of scanning mirrors, one horizontal the other vertical. These are motor driven and scan the laser across the specimen creating a full 2D image. The laser excites the fluorescent molecule in the specimen and the green light is emitted, which is descanned by the same mirrors that scan the excitation light (the blue laser) and passes through the dichroic mirror. It is then focused onto the pinhole and the light that passes through is detected, such as by a photomultiplier tube. The detector is connected to a computer that creates a full image from all the points one pixel at a time. [4;274;275;275]

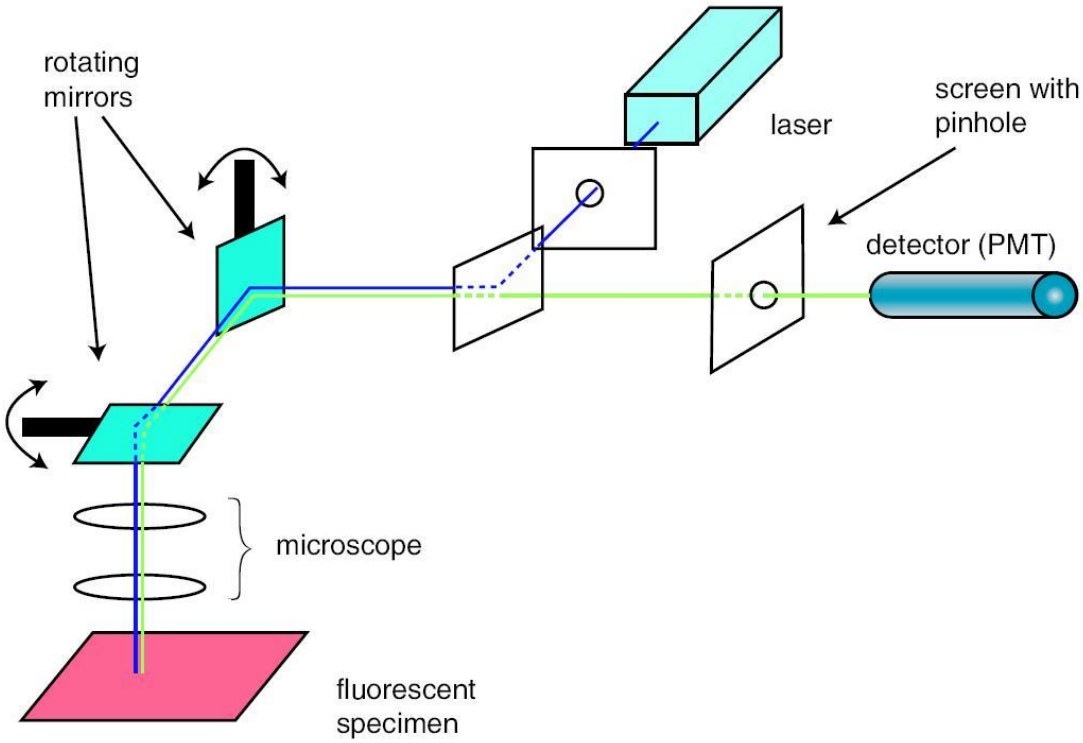

Figure 2.5 - Diagram to demonstrate how a confocal microscope works. This shows the path of the laser in the confocal microscope (blue) as it is reflected off the dichroic mirror and then the rotating (scanning) mirrors. This is then focused onto the specimen via the microscope lenses. The green line indicates the path of light emitted by the fluorescent label in the specimen, as it passes back through the microscope and is descanned by the rotating mirrors. It then passes through the dichroic mirror and then the light from the focal plane of the lenses passes through the pinhole and can be detected [4].

2.9.1: Labelling procedure for confocal microscopy

Cardiac cells grown on microchamber culture slides (Lab-tek, Gibco), were incubated with Alexa 488-ssRNA (20 μg/ml) or dsRNA for different time points, and were subsequently rinsed twice in PBS/0.02% BSA, prior to fixation with 4% formaldehyde for 15 min. The cells were fixed in order to prevent potential re-organisation of the proteins during the course of the experiment. Cells were permeabilised using PBS/0.02% BSA/0.02% Saponin and labelled with antibodies for RIG-I, MDA5 and MAVs directly labelled with the appropriate fluorophore. Cells were imaged on a Carl Zeiss, Inc. LSM510 META confocal microscope (with an Axiovert 200 fluorescent microscope) using a 1.4 NA 63x Zeiss objective. The images were analysed using LSM 2.5 image analysis software (Carl Zeiss, Inc.).

2.10: Cytometric Bead Array / IFN assays

A cytometric bead array (CBA) human soluble protein flex set bead system (Becton Dickinson) was used to quantitatively measure IFN-β production in cells. The flex set bead system is a bead-based immunoassay capable of measuring soluble IFN-β in cell culture supernatant samples. The beads, of known size and fluorescence, are coated with a capture antibody specific for IFN-β. The detection reagent is a mixture of phycoerythrin (PE)-conjugated secondary antibodies, which provides a fluorescent signal in proportion to the amount of bound IFN-β. When the beads are incubated with cell supernatant, sandwich complexes (capture bead, IFN-β, and PE) are formed, and can be measured using flow cytometry.

2.10.1: IFN Assay Procedure

The standards and detection reagents were prepared according to the BD CBA Human Soluble Protein Master Buffer Kit manual. 50 µl of the tissue culture supernatant prepared previously was added to flow tubes, followed by the addition of 50 µl of the IFN-β beads, mixed, and incubated for 1 hour at RT. 50 µl of the PE detection reagent was then added and mixed, followed by a further 2 hour incubation at RT in the dark. 1ml of Wash Buffer was added to each tube, centrifuged at 200 g for 5 minutes, and then the supernatant was carefully aspirated off and discarded. The bead pellets were resuspended in 300 µl of Wash Buffer, and the samples were analysed using flow cytometry, with the data acquired being analysed using the FCAP Array software (Becton Dickinson).

Chapter 3: Determining the RNA Ligand for MDA5 using CAV9

3.1: Introduction

Human Coxsackieviruses are divided into two subgroups, Coxsackie B viruses (CBV) and Coxsackie A viruses (CAV). Subgroup division is mainly based on the pathogenicity of the virus serotypes in experimental animals. CAVs cause flaccid paralysis in newborn mice in contrast to CBVs which induce spastic paralysis. CAVs affect striated muscle while CBVs replicate in several tissues including the central nervous system [276].

Coxsackieviruses are obligate intracellular pathogens that need to hijack the host's machinery in order to produce progeny of viruses, but this is often limited by the host's antiviral response. Successful sensing of the viruses by the host leads to a rapid innate immune response. Viral RNA seems to be a molecular signature that the host recognises and is a potent inducer of the innate host response. Viral RNA is recognised by TLRs or RLRs, which are the two main families of pattern recognition receptors (PRRs) that play a key role in sensing viral RNA and activate inflammatory cytokines and type I interferons (IFNs) [277;278].

TLR7 and TLR8 have been shown to detect genomic ssRNA from Coxsackie B viruses as well as from Human Parechoviruses which are related to Enteroviruses and trigger a cytokine response [279;280]. Furthermore studies utilising mice have shown that MDA5 recognises Coxsackie B viruses and triggers Interferon type I production but do not reveal the specific RNA ligand recognised [281].

RLRs have been recently discovered to play a key role in sensing RNA virus invasion. They recognise viral RNA independently of TLRs and unlike TLRs, which are found

either on the cell surface or endosomes, RLRs are found in the cytoplasm [282]. The two main RNA helicases are RIG-I and MDA5.

RLRs were initially thought to recognise the same ligand, dsRNA, but it has since become apparent that the two receptors possess distinct virus specificities. It has been shown that RIG-I and MDA5 recognise different viruses and different viral RNAs [283;284], with RIG-Is main ligands being single-stranded RNA (ssRNA) containing a terminal 5 -triphosphate (ppp) [285], as well as linear dsRNA no longer than 23 nucleotides [286]. MDA5 recognises long strands of dsRNA but the mechanism by which this occurs is less clear [286].

RIG-I recognises negative sense ssRNA viruses including Influenza virus, Newcastle disease virus, Sendai virus as well as Hepatitis C virus, while positive sense ssRNA viruses such as Picornaviruses, and more specifically Encephalomyocarditis virus and Coxcackievirus B3 have been shown to activate MDA5 and trigger IFN response [281;283;284].

Despite the wealth of information on the types of viruses and RNA that can activate RIG-I and MDA5, the natural ligand responsible for triggering the response remains unclear. RNA recognition by RIG-I seems to require the presence of a free 5'-triphosphate structure [285;287;288], but much less is known about the nature of the RNAs that act as ligands for MDA5. It has been suggested that higher order RNA viral structures are required in order to activate MDA5 [289], but the specific agonist has not been identified. Using biochemical methods, Pichlmair *et al* [289] concluded that MDA5 does not recognise the replicative intermediate dsRNA but higher order RNA structures. Their results suggest that MDA5 activation requires an RNA web rather than simply long molecules of dsRNA, however that fails to explain why MDA5 can sense

Poly:I:C, which is an equivalent of long dsRNA or dsRNA viruses such as Reoviruses [286] or why it cannot sense Picornavirus genomic ssRNA that contains highly ordered secondary structures and tertiary RNA structures in the 3' and 5'UTR regions. Since not all MDA5 agonists seem to fit the model of an RNA web, or branches of RNA, there is a pressing need to identify what is the exact MDA5 ligand. Revealing how MDA5 becomes activated during infection will lead to the future development of new therapies to combat viral disease.

In order to identify the specific ligand for MDA5, we chose to utilise Coxsackie A9 virus which is genetically similar to Coxsackie B viruses which belong to the Picornavirus family. Although members of the family have been shown to trigger the innate immune response via TLRs [280;290;291] and by MDA5 [281;283;284], little is known about the exact ligand. In addition there is not a lot of information about CAV9 innate immune recognition so far.

3.2: Results

3.2.1: Studies with Different Types of RNA

Enteroviruses are positive-sense ssRNA viruses thus their replication follows a strategy common for all positive-sense RNA viruses. The viral genome is transcribed into complementary RNA (negative strand) which in turn is used as a template to synthesize new strands forming double-stranded RNA (dsRNA), replicative intermediate forms (RF), and a complex partially double stranded RNA intermediate (RI) which has double stranded core to which nascent strands of ssRNA are attached. Therefore during an Enteroviral infection, the host's innate immune system will be presented with a pool of

foreign RNA, such pools would contain whole viral genomes, viral transcripts as well as replication intermediates.

In order to determine whether viral replication is essential for MDA5 recognition and to characterize the RNA species responsible for MDA5 activation in cells infected with positive stand RNA viruses such as CAV9, cardiac cells were infected and the full length genomic ssRNA as well as the viral dsRNA replicative form (RF) and the high molecular weight RI-RNA were isolated from the cytoplasm of these cells using modified purification procedures for the isolation of viral ssRNA and poliovirus replicative intermediates (RF) and (RI) similar to Richards and Ehrenfeld [261;292] and purified by Fast Performance Liquid Chromatography (FPLC) (Figure 3.1).

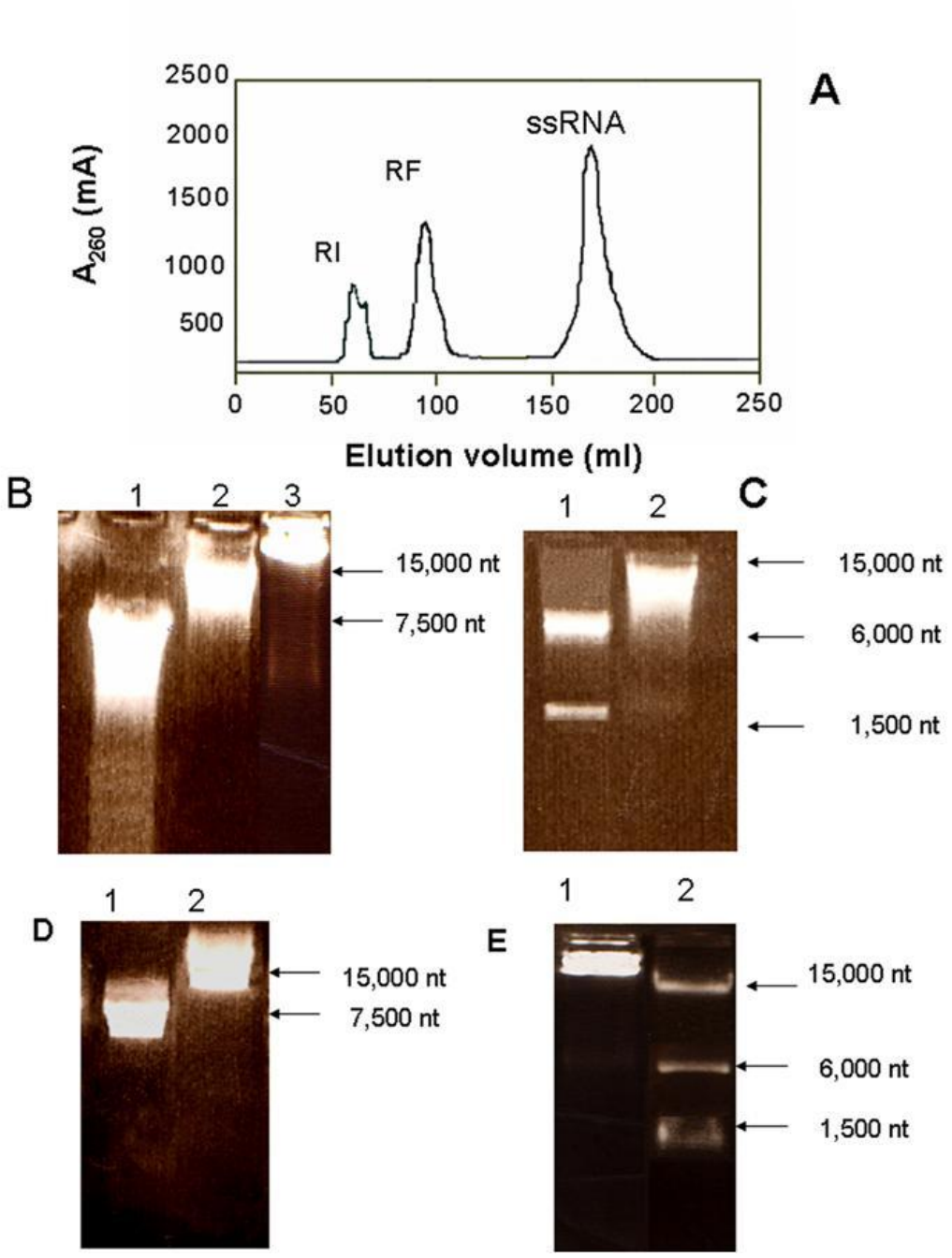

Figure 3.1 - Purification of RNA by size exclusion chromatography. (A) The standard elution curves for RNA oligonucleotides of various lengths on the Superdex 200 column size exclusion column was used for calibration. The elution profile of viral ssRNA and viral RF and viral RI obtained from the size exclusion chromatography step on the Superdex 200 column is shown. (B) FPLC was performed at 3mL/min. CAV-9 ssRNA (lane 1) and replicative intermediate RF-RNA (lane 2) and high order replicative intermediate RI-RNA (lane 3) were isolated and analysed by agarose gel electrophoresis. (C) The RNA samples ssRNA (lane 1) and RF-RNA (lane 2) were treated with pancreatic RNase (1μg/ml). (D) ssRNA (lane 1) and RF-RNA (lane 2) were treated with DNase I (20μg/ml). (E) RI-RNA was treated with with DNase I (20μg/ml) (lane 1) or pancreatic RNase (1μg/ml) (lane 2) and analysed by agarose gel electrophoresis.

The purified ssRNA was resistant to DNase I and digested by pancreatic RNase into two bands of 6,000 bases and 1,500 bases (Figure 3.1C). RF RNA was resistant to DNase I and over 99% resistant to pancreatic RNase indicating that there was no contamination by DNA or sensitive ssRNA (Figure 3.1D). The purified RI RNA was resistant to DNase I and over 50% resistant to pancreatic RNase (Figure 3.1E)

3.2.2: RLR Involvement in Recognition of Enteroviruses

In order to investigate the involvement of RIG-I and MDA5 in the innate recognition of enteroviruses, HEK-RIG-I and HEK-MDA5 cells were used. These cells were infected with CAV9 as well as Influenza A virus (IFVA) (a negative-sense RNA virus) as a control. MDA5 and RIG-I expression levels were tested at different time points after infection (Figure 3.2A, B). Our data demonstrated that MDA5 was up-regulated in HEK-MDA5 cells infected with Coxsackie A9 virus (CAV-9), but not Influenza A virus while as expected in HEK-RIG-I cells RIG-I was only up-regulated in cells infected with Influenza A virus.

In order to determine the immuno-stimulatory effect of the viruses, IFNβ secretion in response to these viruses was also examined (Figure 3.2C, D). Our data demonstrated that CAV9 and IFVA viruses triggered a significant IFN response, confirming the involvement of RLRs in the sensing of RNA viruses.

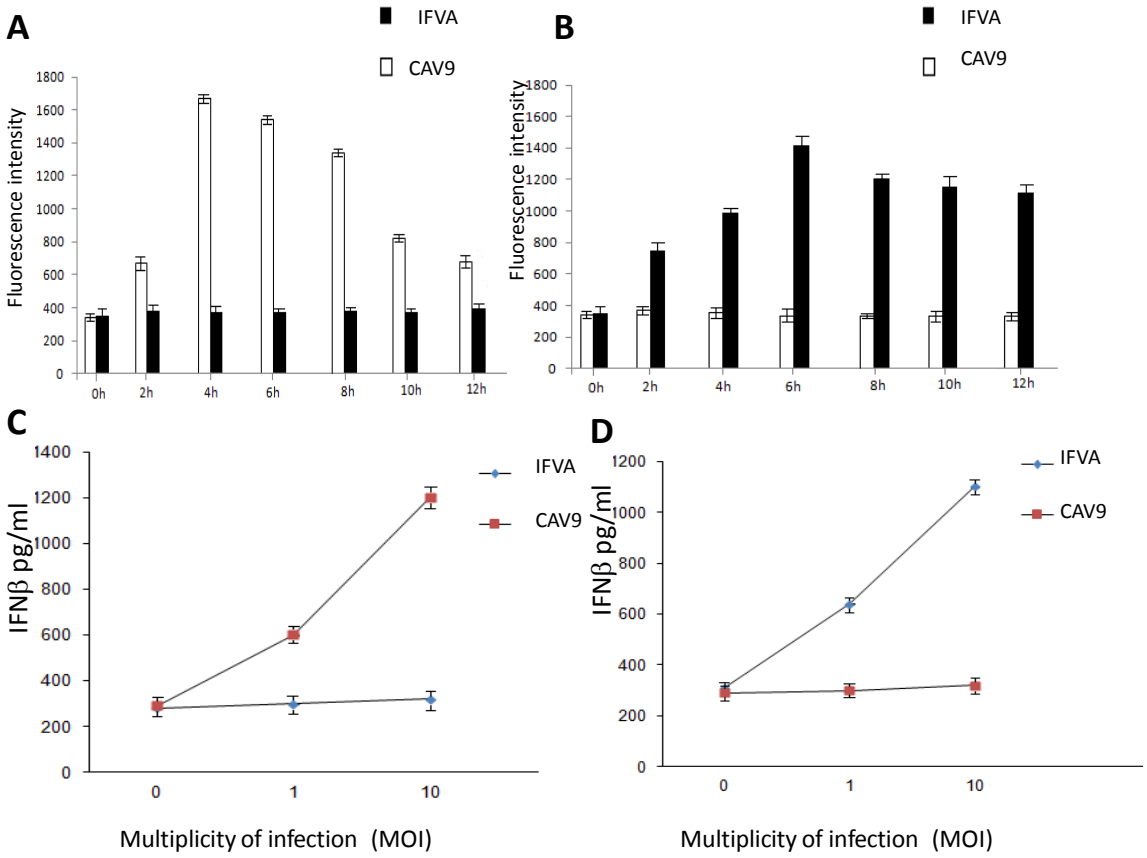

Figure 3.2 - RIG-I/MDA5 expression in HEK cells. HEK-MDA5 and HEK-RIG-I cells were either not stimulated (0 hour) or stimulated with CAV9 or IFVA at different time points (5 moi). The cells were fixed and permeabilised, followed by antibody staining against MDA5 in HEK-MDA5 cells (A) and RIG-I in HEK-RIG-I cells (B) followed by incubation with the appropriate secondary antibody conjugated to FITC. The supernatants were harvested and assayed for IFNβ secretion using the Flex set system (Becton Dickinson). In HEK-MDA5 cells (C) and HEK-RIG-I cells (D). Fluorescence was detected using a FACSCalibur (BectonDickinson). The data presented is the mean of three independent experiments.

3.2.3: MDA5 Senses the Viral Replicative Intermediate dsRNA

In order to determine which RNA species triggers MDA5 activation and induction of IFNα/β CAV-9 genomic ssRNA as well as the dsRNA replicative intermediates, RF-RNA and RI-RNA, were isolated (see Materials and Methods section) and transfected into cardiac cells. The data showed a small increase in IFNβ production when ssRNA was used possibly due to TLR7/8 detection and a very high IFNβ production in response to RF. The RI-RNA induced IFNβ response as well (Figure 3.3A), however it was lower than the response induced with RF-RNA.

In order to determine whether MDA5 was responsible for the IFNα/β response and to exclude other pattern recognition receptors such as TLR7 and TLR8 which recognise ssRNA or TLR3 which recognises dsRNA but trigger mainly IL6 and TNFα secretion, we used RNA interference to knock down expression of RIG-I and MDA5 in cardiac cells (Figure 3.3B). Following confirmation of knockdown we stimulated the cells with ssRNA, RF-RNA (dsRNA) and RI-RNA which contains both dsRNA and ssRNA and measured IFNβ production (Figure 3.3C). Our results showed that by knocking down RIG-I there was no down-regulation on IFNβ response, while knocking down MDA5 almost abrogated IFNβ production (figure 3.3C). These results confirmed that MDA5 senses CAV9 and more specifically the dsRNA formed during their replication in the cell cytoplasm.

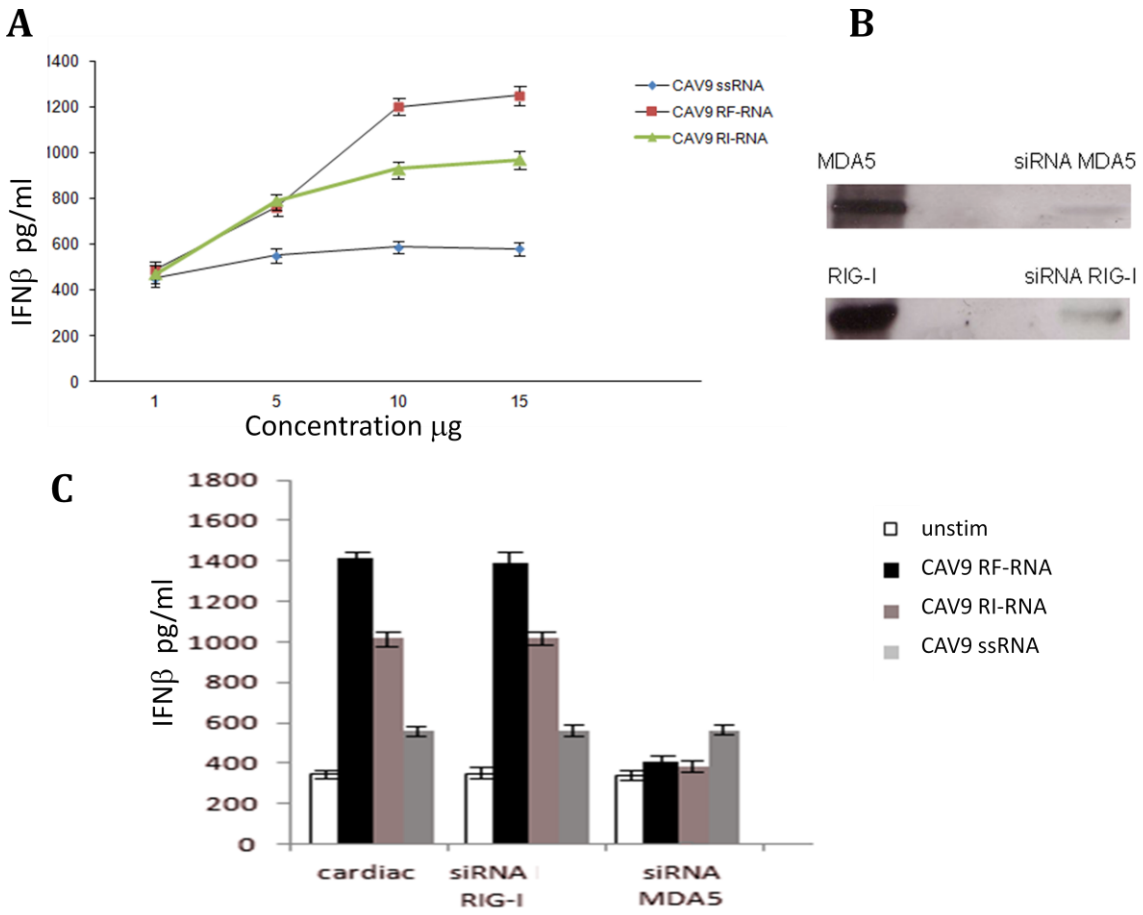

Figure 3.3 - IFNβ upregulation induced by viruses. Human cardiac cells were stimulated with different CAV9 RNAs, genomic ssRNA, replicative intermediate dsRNA (RF) and dsRNA-ssRNA replicative intermediate (RI). The supernatants were harvested and assayed for cytokine secretion using the Flex set system (Becton Dickinson). Fluorescence was detected using a FACSCalibur (BectonDickinson). IFNβ secretion is depicted in graph (A), and (C). RNA interference for MDA5, RIG-I, TLR3, TLR7 and TLR8 in cardiac cells is also depicted (receptor expression levels were reduced by 85% by RNA interference panel (B). Human cardiac cells were silenced for either RIG-I or MDA5, and either not stimulated (white bar charts), or incubated with ssRNA with RF-RNA or RI-RNA. The supernatants were harvested and assayed for IFNβ secretion at 4hr using the Flex set system (Becton Dickinson). The data represents the mean of three independent experiments.

3.2.4: Visualisation of MDA5 and Viral RNA

Our experiments revealed that MDA5 recognises not the genomic ssRNA but the dsRNA generated by the replication of these viruses. In order to confirm interaction between MDA5 and viral dsRNA intermediates we used confocal cell imaging. The ssRNA, dsRNA (RF), or RI-RNA were delivered directly into the cells' cytoplasm using streptolysin O (SLO), which is a pore-forming bacterial toxin, as a non endocytic delivery method in order to avoid TLR detection. This is a simple and rapid means of introducing nucleic acid into the cytoplasm of eukaryotic cells [293;294]. The ssRNA, dsRNA and RI-RNA were labelled with Alexa 488. MDA5 and RIG-I were labelled with Alexa 633-Fab goat specific Ig, while MAVs was labelled with Alexa 546-Fab rabbit specific Ig.

When we investigated MDA5-viral RNA interactions using confocal microscopy, a high level of co-localisation of dsRNA with MAVs and MDA5 was observed, whereas we saw no co-localisation of dsRNA with RIG-I (Figure 3.4 A+B). Furthermore when we used RI-RNA co-localisation of RI-RNA with MAVS and MDA5 was also shown (Figure 3.4 C+D). Interestingly, when we used CAV9 ssRNA, we found no co-localisation either with RIG-I or with MDA5 (Figure 3.5), suggesting that MDA5 does not engage the ssRNA of the viruses but only interacts and recognises the dsRNA intermediates that ae formed during the replication phase. As expected, when Influenza genomic 5' triphosphate ssRNA was used, we found co-localisation with RIG-I but not with MDA5 (Figure 3.6).

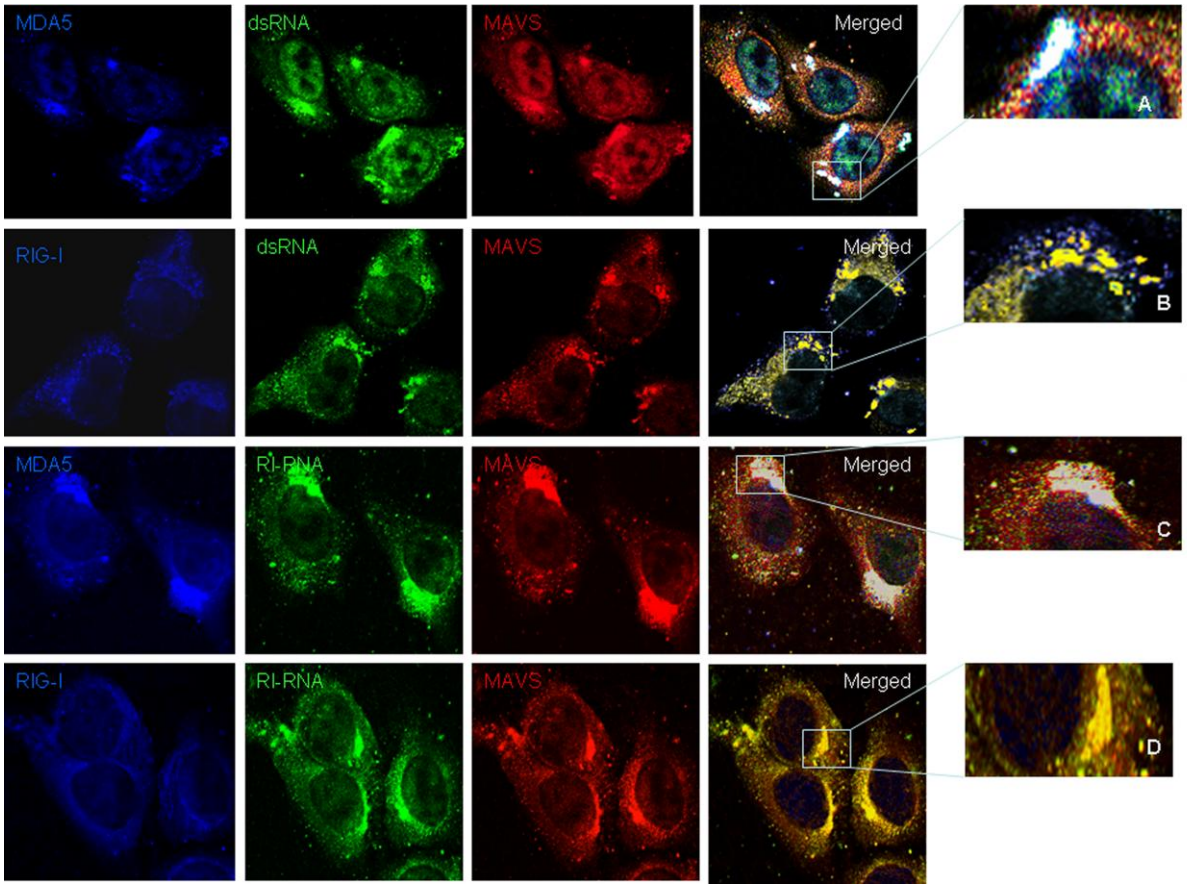

Figure 3.4 - Localisation of enteroviral dsRNA RF or RI-RNA and MDA5 in cardiac cells. Human cardiac cells containing CAV-9 ssRNA, dsRNA RF or RI-RNA directly conjugated to Alexa 488. MDA5 and RIG-I were labelled with Alexa 633-Fab goat specific Ig, while MAVs was labelled with Alexa 546-Fab rabbit specific Ig. The indicated regions in merged images are enlarged in panels A, B, C and D Yellow regions indicate localisation of MAVs with dsRNA RF and RI-RNA. White regions indicate localisation of MDA5, MAVs with dsRNA RF and RI-RNA. Bars 10 μm.

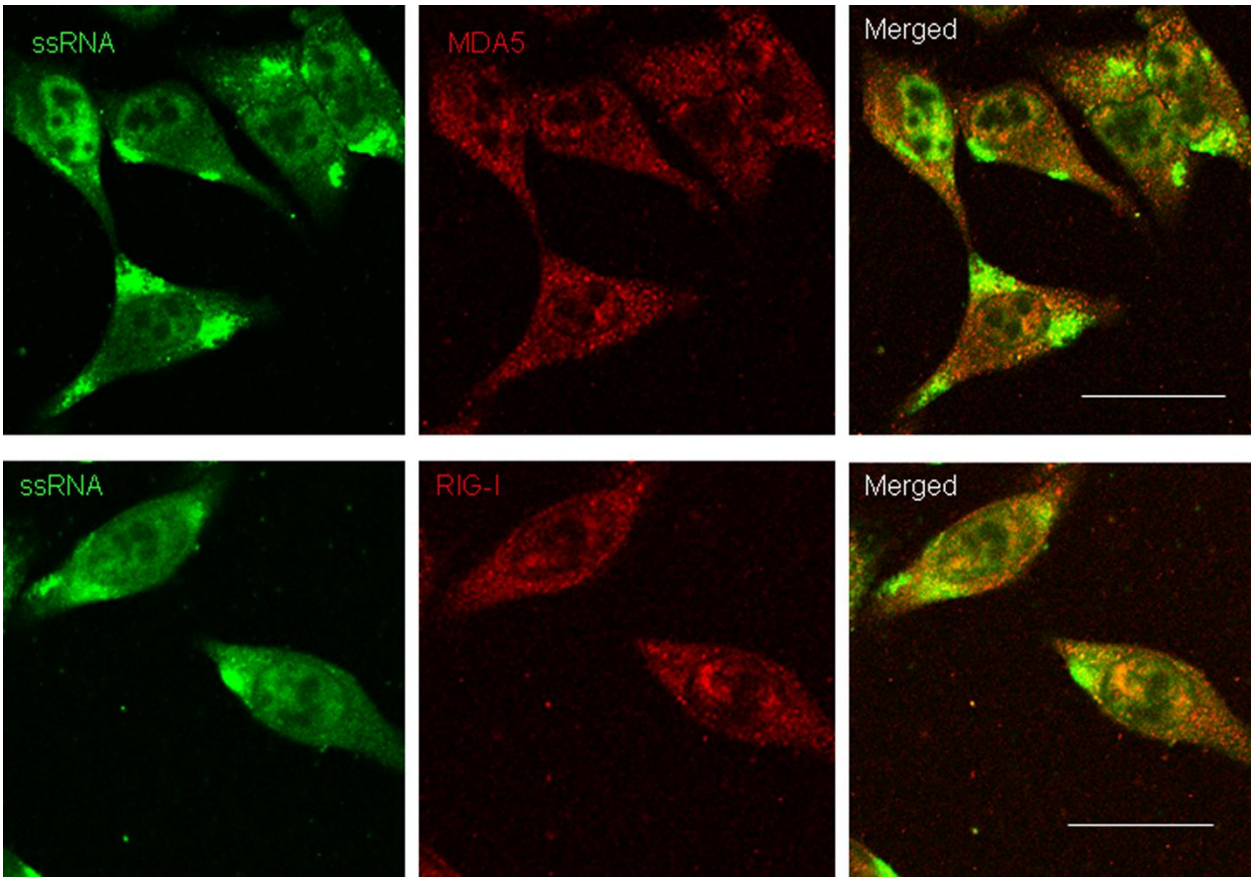

Figure 3.5 - There is no localisation of enteroviral ssRNA either with RIG-I or with MDA5. Human cardiac cells containing CAV-9 ssRNA conjugated to Alexa 488. MDA5 was labelled with Alexa 546-Fab goat specific Ig. RIG-I was labelled with Alexa 546 Fab goat specific Ig. We see no degree of localisation in the displayed images. Bars 10 μm

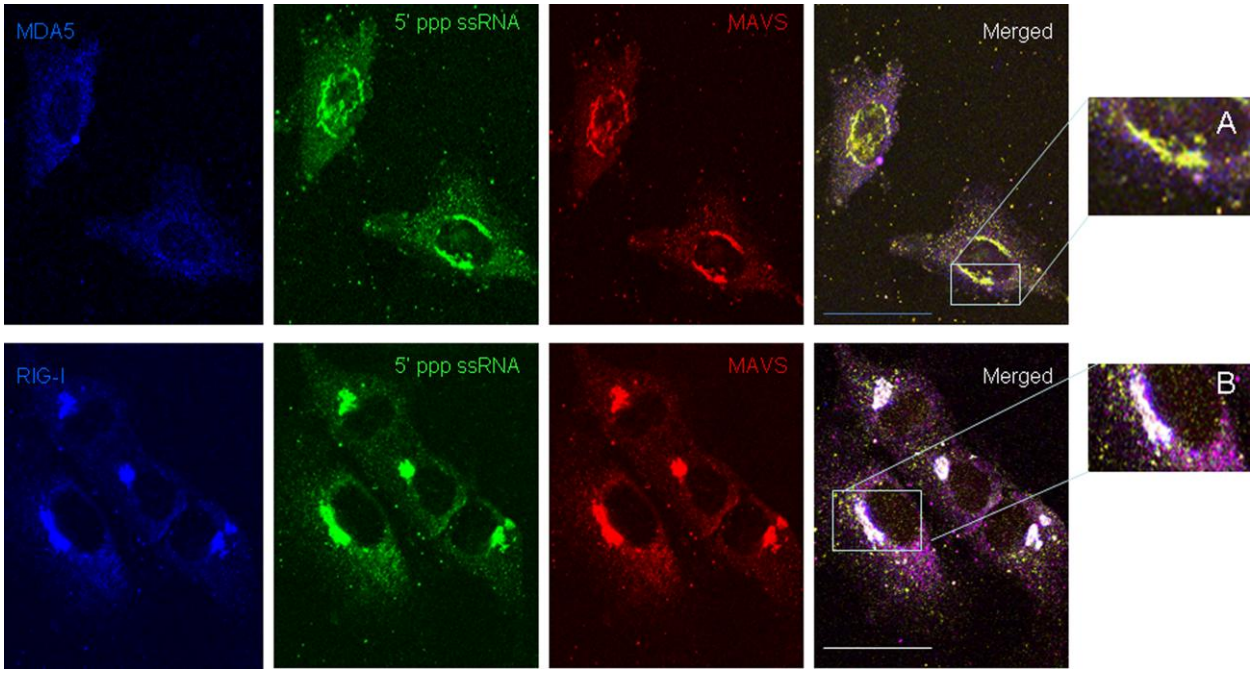

Figure 3.6 - Localisation of influenza ssRNA and RIG-I in cardiac cells. Human cardiac cells containing Influenza ssRNA (5'ppp ssRNA) conjugated to Alexa 488. MDA5 was labelled with Alexa 633-Fab goat specific Ig. while MAVs was labelled with Alexa 546-Fab rabbit specific Ig. RIG-I was labelled with Alexa 633-Fab goat specific Ig. Yellow regions indicate localisation of MAVs and ssRNA. White regions indicate localisation of RIG-I, MAVs and ssRNA. Bars 10 μm

3.2.5: Picornavirus replication is essential for MDA5 sensing

To gain more insight as to whether Picornavirus replication and the generation of dsRNA is a prerequisite for MDA5 sensing, confocal microscopy was once again used. This method helped us visualise dsRNA formed de novo during virus infection. Cardiac cells were infected with CAV9 for different time points during infection and the dsRNA was visualised using the monoclonal dsRNA-specific mouse antibody J2 Fab directly conjugated to Alexa 488. MDA5 and RIG-I were labelled with Alexa 546-Fab goat specific Ig, while MAVs was labelled with Alexa 546-Fab rabbit specific Ig. To verify that the dsRNA detected was indeed of viral not cellular origin, cells were also treated

with the DNA dependent RNA polymerase inhibitor actinomycin D and the dsRNA signal was still detected verifying that it was specific for viral dsRNA.

The experiments were consistent with our previous studies and highlighted that dsRNA co-localises with MDA5 and MAVs but not RIG-I (figure 3.7).

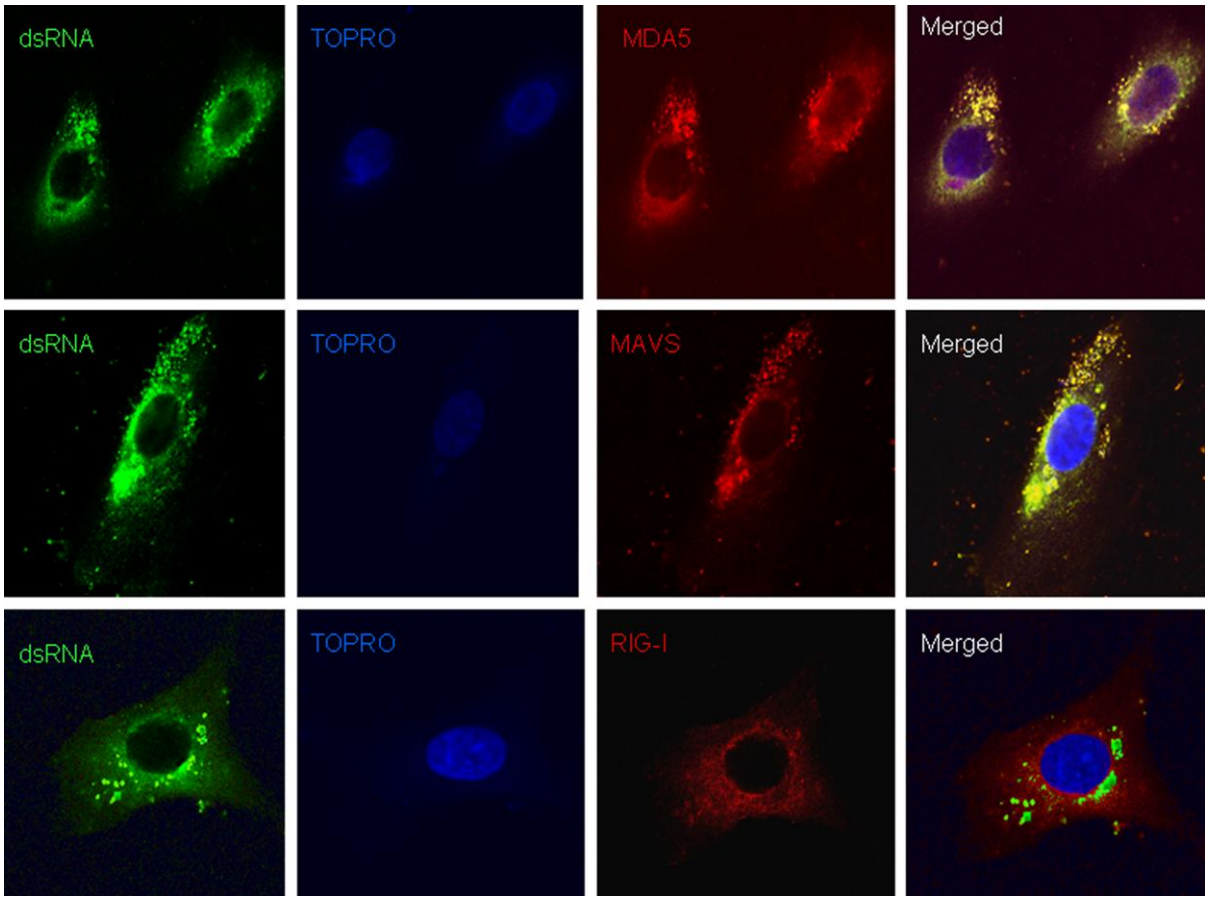

Figure 3.7 - Localisation of viral dsRNA and MDA5 in virus infected cardiac cells. Human cardiac cells infected with CAV-9 were stained with J2 Fab specific for dsRNA directly conjugated to Alexa 488. MDA5 and RIG-I were labelled with Alexa 546-Fab goat specific Ig while MAVs was labelled with Alexa 546-Fab rabbit specific Ig, RIG-I was labelled with Alexa 546 Fab goat specific Ig. Nuclear stain TOPRO was also used to label the nucleus. Yellow regions indicate localisation of MAVs or MDA5 with viral dsRNA. Bars 10 μm.

3.3: Discussion

The RNA helicases, RIG-I and MDA5, have been defined as essential PRRs for host detection of a variety of RNA viruses and activation of type I interferons. It has been widely known that RIG-I is a key sensor for negative strand ssRNA viruses such as Hepatitis C virus and Influenza viruses whereas induction of type I IFN by positive strand Picornaviruses, including Encephalomyocarditis virus, Theiler's virus and Mengo virus, is mediated by MDA5 and not RIG-I [283;284;295].

A large research effort has focused on understanding the ligands that are recognized by each of these RLRs since these new insights will help in the development of improved vaccines and new antiviral therapeutics to control virus infections.

Despite the wealth of information on the types of RNA that can activate RIG-I and induce IFN production there is not a lot of information on the viral RNA required for MDA5 activation. It has been shown that RIG-I recognizes single-stranded RNA (ssRNA) containing a terminal 5 -triphosphate (ppp), as well as linear dsRNA no longer than 23 nucleotides. MDA5 recognition is less clear, since it does not sense viral genomic ssRNA. It seems to recognise long strands of dsRNA but the mechanism by which this occurs has not been revealed. Pichlmair *et al* [289] using mainly biochemical methods had suggested that MDA5 senses high order structured RNA containing ssRNA and dsRNA, however that fails to explain why MDA5 can sense Poly(I:C), which is a synthetic long dsRNA, or dsRNA viruses such as Reoviruses [286] or why it cannot sense Picornavirus genomic ssRNA that contains highly ordered secondary structures and tertiary RNA structures in the 3' and 5'UTR regions. The inherent problem with the study by Pichlmair *et al* is that they rely on immunoprecipitations with a dsRNA-specific antibody in order to isolate RNA/MDA5 complexes. Using this

method they demonstrated that infected cells contained not only dsRNA but also ssRNA of high molecular weight, which was found to be immunostimulatory. The problem is that such biochemical isolations rely exclusively on the specificity of the antibody used and they are prone to artefactual associations.

The goal of the present study was to determine whether RIG-I or MDA5 participate in the induction of type I IFN in response to Coxsackie A9 virus infection and to determine the specific RNA ligand that was recognized and activated these sensors using non-invasive methods.

CAV9 is a positive ssRNA virus therefore in addition to its ssRNA genome there are also substantial amounts of cytosolic dsRNA produced during the replicative life cycle of these positive ssRNA viruses. Thus during an Enteroviral infection, there is a pool of viral RNA that trigger the host's innate immune response, raising the question of which viral RNA species is responsible for MDA5 activation. CAV9 ssRNA as well as the replicative intermediate dsRNA (RF) and the high order replicative intermediate (RI), which is basically a dsRNA RF with a nascent ssRNA viral strand, were isolated and used in this study. The data showed that although RIG-I acts as a sensor triggering interferon production in the presence of negative ssRNA virus such as Influenza A virus it cannot recognise the replicative intermediate dsRNAs of positive strand viruses.

The experiments have shown that there was no interaction of MDA5 with the genomic ssRNA. However MDA5 recognised the dsRNA produced during the CAV9 replication as well as RI-RNA which has a dsRNA core, highlighting the importance of dsRNA in MDA5 recognition. Thus providing unique evidence between the relationship of viral dsRNA and MDA5 and confirming that the dsRNA replicative intermediate form of CAV9 is the effective agonist recognised by MDA5 (Triantafilou, K. 2012).

While the confocal data does not prove direct interaction, the difference in co-localisation between MDA5 and RIG-I with the dsRNA intermediates and the difference between ssRNA localisation from CVA and IFVA with the RLRs is strong enough evidence to show interaction when combined with the IFN assay data. FRET or other methods could be used to show proximity of molecules and could be performed as further work to show evidence that MDA5 binds the dsRNA intermediate . However the evidence presented here is significant without the further work being neccesary.

Chapter 4: RIG-Like Receptor Involvement in CVB3 Infection of Cardiac Cells

4.1: Introduction

One of the most severe of CVBs symptoms is myocarditis, an infection of the heart muscle [296]. The cardiac Girardi cell line is a human heart cell line of epithelial morphology that is susceptible to CVB [297] thus making it a good base from which to understand the PRR response to CVB.

Recognition of CVB3 is most likely through MDA5, as has been shown for other Picornaviruses, rather than RIG-I [298;299]. Evidence thus far indicates that MDA5 is the main candidate for CVB3 recognition of the RLR family [300], however the extent of its role in relation to other PRRs and the exact nature of its recognition of CVB3 have yet to be elucidated. It has already been demonstrated in Chapter 3 that MDA5 recognises dsRNA intermediate when cells are infected with CAV9 and the same is likely true of CVB3, however this needs to be confirmed. To make matters more complicated there is evidence that suggests both RIG-I and MDA5 may be cleaved by the virus during its life cycle, likely towards the later stages of infection as has been shown in other Picornaviruses [301;302]. For this reason specific nucleic PAMPs have been used to stimulate the cells in order to determine specific structures that may influence MDA5 or RIG-I binding in CVB3 infections. Picornaviruses life cycle lasts from around 5 to 10 hours, with the Coxsackievirus life cycle estimated at around 6 hours [303], so for each stimulation time points of 2, 4 and 6 hours were used to create an idea of changes through the life cycle, as well as giving insight to any possibly cleavage of the RLRs that may occur.

The innate immune system is a vital part of the body's defences against viral pathogens. RIG-I and MDA5 function as cytoplasmic PRRs that are involved in the elimination of actively replicating RNA viruses. Their location and their differential responses to RNA viruses emphasises the complexity of the innate detection system. In order to identify which RNA species triggers MDA5 activation during infection, viral ssRNA and the replicative intermediate dsRNA were isolated from CVB3. Furthermore dsRNAs such as Poly(I:C) which is a mismatched double-stranded RNA with one strand being a polymer of inosinic acid, the other a polymer of cytidylic acid was used. Poly(I:C) is a known inducer of IFN response recognised by MDA5 [304]. It was later determined that MDA5 recognised Poly(I:C) around 2 kbp and RIG-I recognised cleaved Poly(I:C) products around 70 bp [305]. Viral dsRNA may follow the same rule of recognition with shorter dsRNA in secondary structures and the replicative intermediate and longer dsRNA in the replicative form which has a full copy of both the positive and negative strand RNA [306-309].

In addition synthetic dsRNAs with altered end structures were also used to determine their effect on RLR binding. Synthetic 5'ppp dsRNA was used as it has been linked as a possible factor in RIG-I binding to dsRNA structures [310], as well as RIG-Is known preference for 5'ppp ssRNA [311;312]. The synthetic 5'OH dsRNA was used as a second form of end structure for dsRNA. Using both could give a better insight into the end structures role in RLR recognition, whether changing the structure provides a better binding platform or acts as a hindrance.

To determine if CBV3 infection (and more specifically which CBV3 RNA constructs) triggers the innate immune response, cardiac cells were taken and stimulated with CVB3 as well as CVB3 ssRNA, CVB3 RF-RNA and synthetic RNA structures to determine which RNA constructs is immunostimulatory..

Ligand binding to either of the RLRs leads to signalling through MAVS that results in activation of both NF-κB and IRF3 [313-315]. This leads to the expression of type-I IFNs, including IFNα and IFNβ, which activate IFN-induced genes (ISGs) through the receptor IFNAR1/2 and inducing the JAK/STAT pathway. Therefore the presence of IRF3 and phosho-IκB (P-IκB) in cardiac cells in response to different RNA constructs were investigated.

P-IκB acts as a good determinant for the levels of NF-κB as the phosphorylation of total-IκB (T-IκB) releases NF-κB. For this reason T-IκB was also probed for as a control for the P-IκB.

The ligands used to stimulate the cells were CVB3 (figure 4.1), ssRNA and RF-RNA (dsRNA) both extracted from CVB3 infectious cycle, the synthetic dsRNA homolog Poly(I:C) and two synthetic RNAs with specific RNA structures shown here as RNA1 and RNA2 (see materials and methods). For each ligand the cells were stimulated for 2, 4 or 6 hours and unstimulated cells were used as a control.

4.2: Results

4.2.1: Immunostimulatory effect of CBV3 and different RNA constructs on cardiac cells

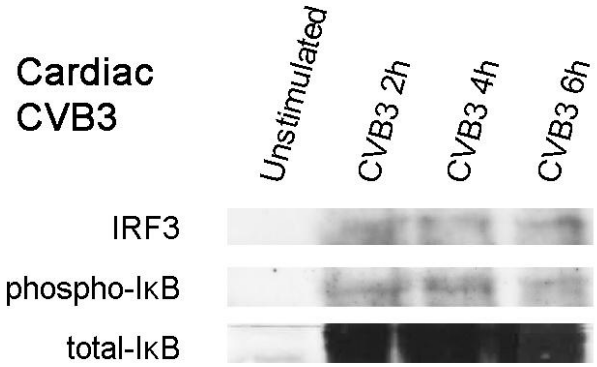

Figure 4.1 – Immunostimulatory effect of CBV3 on cardiac cells. Cells were either not infected or infected with 5 moi CVB3 for 2, 4 and 6 hours The cell lysate from each stimulation was used for SDS-PAGE gel electrophoresis and western blot analysis using primary antibodies specific for IRF3, phospho-IκB or total-IκB and followed by the appropriate secondary antibodies conjugated to HRP. The data represent the mean of three independent experiments.

Infection of cardiac cells with CVB3 triggers innate immune recognition since for IRF3, P-IκB and T-IκB were present upon viral infection This is consistent with previous studies showing CVB recognition by different PRRs such as TLR4, which recognises the virus capsid [290] as well as TLR7 and TLR8 which recognise CBV ssRNA [280] as well as MDA5 in CVB innate recognition [316].

To determine whether the CVB3 ssRNA is also immunostimulatory, CVB3 genomic RNA was used to stimulate cells (figure 4.2).

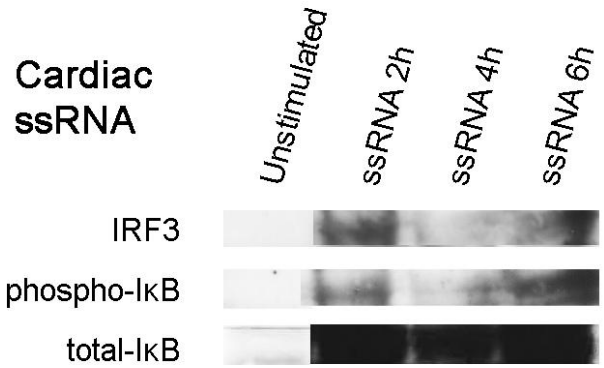

Figure 4.2 – Immunostimulatory effect of CBV3 ssRNA on cardiac cells. Cells were ustimulated or stimulated with 10 μg ssRNA for 2, 4 and 6 hours The cell lysate from each stimulation was used for SDS-PAGE gel electrophoresis and western blot analysis using primary antibodies specific for IRF3, phospho-IκB or total-IκB and followed by the appropriate secondary antibodies conjugated to HRP. The data represent the mean of three independent experiments.

As expected the data showed that CVB3 ssRNA is recognised by PRRs and triggers signalling cascades since IRF3, phospho-IκB or total-IκB are triggered upon ssRNA stimulation.

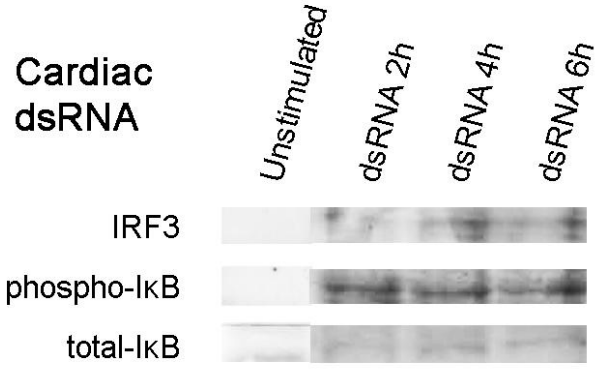

Figure 4.3 - Immunostimulatory effect of CBV3 RF-RNA (dsRNA) on cardiac cells. Cells were unstimulated or stimulated with 10 μg of CVB3 RF-RNA for 2, 4 and 6 hours The cell lysate from each stimulation was used for SDS-PAGE gel electrophoresis and western blot analysis using primary antibodies specific for IRF3, phospho-IκB or total-IκB and followed by the appropriate secondary antibodies conjugated to HRP. The data represent the mean of three independent experiments.

Stimulation with CVB3 RF-RNA appears to activate P-IκB evenly across all time points, but not IRF3, which appears to be expressed after 4 hours, indicating that it may utilise different PRRs for IRF3 and P-IκB (possibly TLR3 for P-IκB and MDA5 for IRF3). Again T-IκB is expressed uniformly across all time points (figure 4.3).

To determine the RNA ligand which triggers signalling in cardiac cells, different RNA synthetic constructs were used. Poly(I:C) is a synthetic dsRNA and was used to stimulate cells for different time points (figure 4.4).

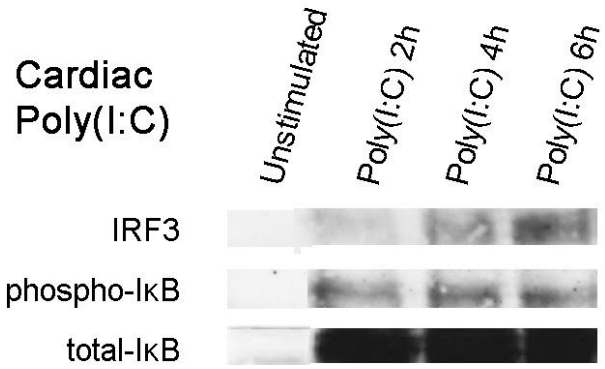

Figure 4.4 - Immunostimulatory effect of Poly IC on cardiac cells. Cells were unstimulated or stimulated with 10 μg of Poly IC for 2, 4 and 6 hours The cell lysate from each stimulation was used for SDS-PAGE gel electrophoresis and western blot analysis using primary antibodies specific for IRF3, phospho-IκB or total-IκB and followed by the appropriate secondary antibodies conjugated to HRP. The data represent the mean of three independent experiments.

Interestingly the results after stimulating cardiac cells with Poly(I:C) closely match those of stimulating with RF-RNA (dsRNA). Both have increased expression of IRF3 from 4 hours and uniform expression of P-IκB and T-IκB. This resemblance between the results would suggest that despite Poly(I:C) being a synthetic analogue of dsRNA they are both recognised by the same PRRs leading to similar innate immune responses.

Following Poly(I:C) synthetic RNA analogues with different end groups were used, first 5'OH synthetic dsRNA (RNA1) (figure 4.5) and then 5' ppp dsRNA (RNA2) (figure 4.6).

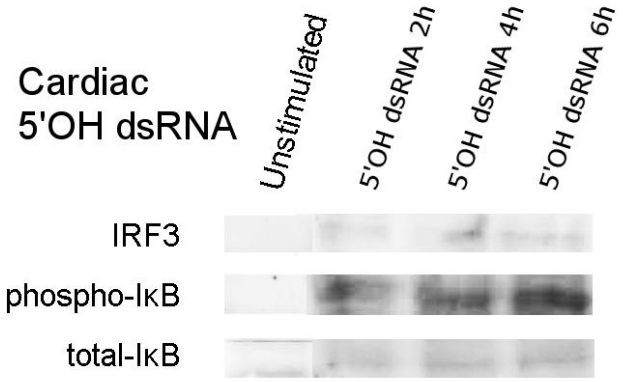

Figure 4.5 - Immunostimulatory effect of 5' OH dsRNA on cardiac cells. Cells were unstimulated or stimulated with 10 μg of 5' OH dsRNA for 2, 4 and 6 hours The cell lysate from each stimulation was used for SDS-PAGE gel electrophoresis and western blot analysis using primary antibodies specific for IRF3, phospho-IκB or total-IκB and followed by the appropriate secondary antibodies conjugated to HRP. The data represent the mean of three independent experiments.

Stimulation with 5'OH dsRNA creates a strong expression of P-IκB and T-IκB, however a diminished IRF3 response. This would suggest that unlike CVB3 ssRNA and RF-RNA it may not trigger all signalling cascades.

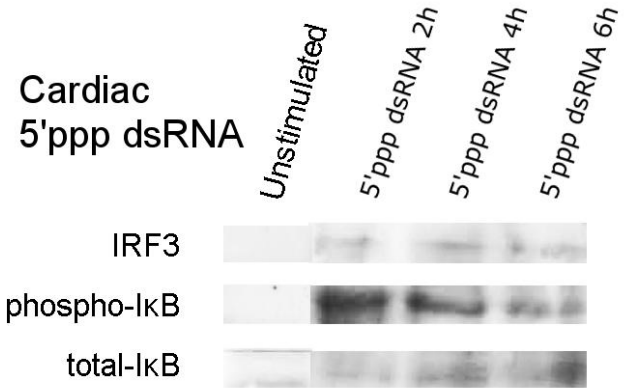

Figure 4.6 - Immunostimulatory effect of 5'ppp dsRNA on cardiac cells. Cells were unstimulated or stimulated with 10 μg of 5'ppp dsRNA for 2, 4 and 6 hours The cell lysate from each stimulation was used for SDS-PAGE gel electrophoresis and western blot analysis using primary antibodies specific for IRF3, phospho-IκB or total-IκB and followed by the appropriate secondary antibodies conjugated to HRP. The data represent the mean of three independent experiments.

Like 5'OH dsRNA, 5'ppp dsRNA has a diminished IRF3 response, while still having a good P-IκB and T-IκB response. However the P-IκB decreases after 2 hours, leaving a far less significant response by 6 hours.

4.2.2: IFN-β Production

Type I interferons IFNα/β are mainly triggered by RLRs such as RIG-I and MDA5. To determine the involvement of RLRs in CVB3 recognition IFNβ secretion was measured. Cardiac cells were stimulated with CVB3, CVB3 ssRNA, CBV3 RF-RNA, Poly(I:C) and synthetic 5'OH dsRNA and 5'ppp dsRNA. Time points of 2, 4 and 6 hours were used and the levels of IFNβ in the cells were measured.

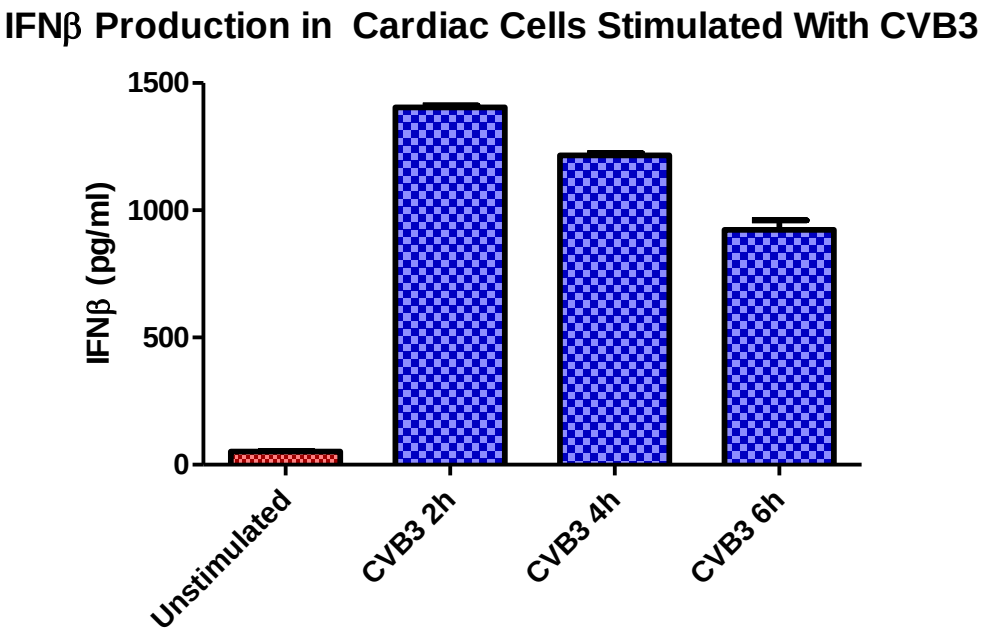

Figure 4.7 - CBV3 infection activates RLRs. Cardiac cells were either not infected or infected with 5 moi of CBV3 Supernatant was collected at 2 hr, 4 hr, 6 hr post infection and analysed for IFNβ secretion using the Flex set system on a FACSCalibur (Becton Dickinson). The data represents the mean of three independent experiments.

The results indicate an increase in IFNβ secretion (figure 4.7) when cells were infected with CVB3, thus implicating RLR involvement in CVB3 recognition. To determine the specific ligand that RLRs recognise, CBV3 ssRNA was used to stimulate cells (figure 4.8).

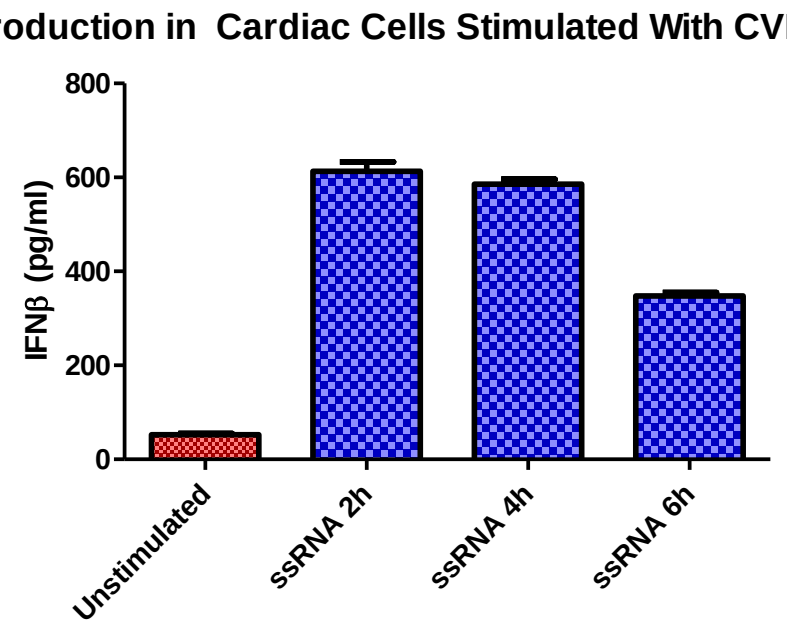

Figure 4.8 - CBV3 ssRNA stimulation on cardiac cells. Cardiac cells were unstimulated or stimulated with 10 μg of ssRNA. Cell Supernatant was collected at 2 hr, 4 hr, 6 hr post infection and analysed for IFNβ secretion using the Flex set system on a FACSCalibur (Becton Dickinson). The data represents the mean of three independent experiments

Expression levels of IFNβ are slightly elevated but are not as high as the expression levels triggered by CVB3. This probably suggests that ssRNA does not have as efficient an immunostimulatory effect on RLRs and the low levels of IFNβ are possibly triggered by TLR recognition.

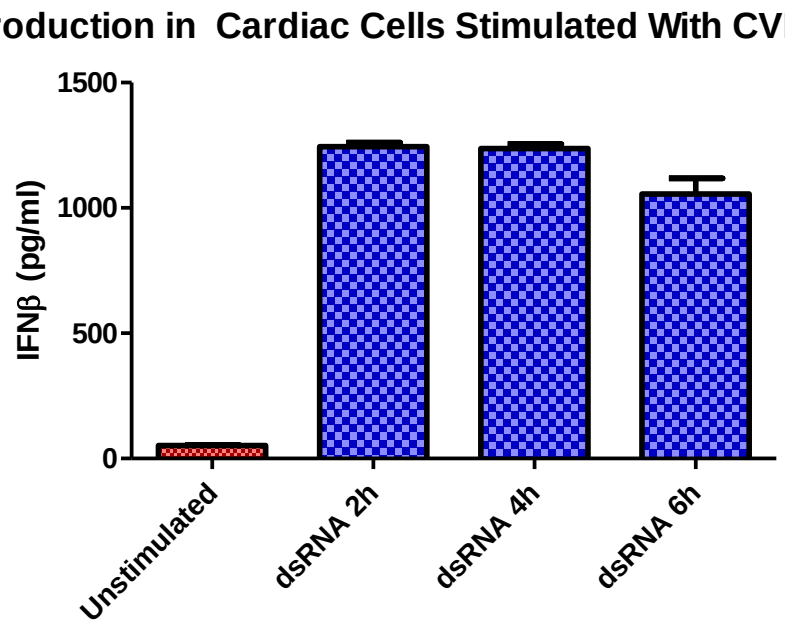

Figure 4.9 - CBV3 RF-RNA (dsRNA) stimulation on cardiac cells. Cardiac cells were unstimulated or stimulated with 10 μg of CBV3 RF-RNA Cell Supernatant was collected at 2 hr, 4 hr, 6 hr post infection and analysed for IFNβ secretion using the Flex set system on a FACSCalibur (Becton Dickinson). The data represents the mean of three independent experiments.

The stimulation with RF-RNA triggers high expression levels of IFNβ (figure 9), showing it to be a far greater inducer of the type-I IFNs than the viral ssRNA. The increase is nearly as high as the CVB3 results with a 25 fold increase over the unstimulated at 2 and 4 hours and a drop to just over 1000pg/ml at 6 hours. This indicates that the dsRNA intermediate is crucial in the PRR response to CVB3.

Synthetic dsRNA constructs were also used such as PolyIC (figure 4.10), synthetic 5'OH dsRNA (figure 4.11) and synthetic 5'ppp dsRNA (figure 4.12).

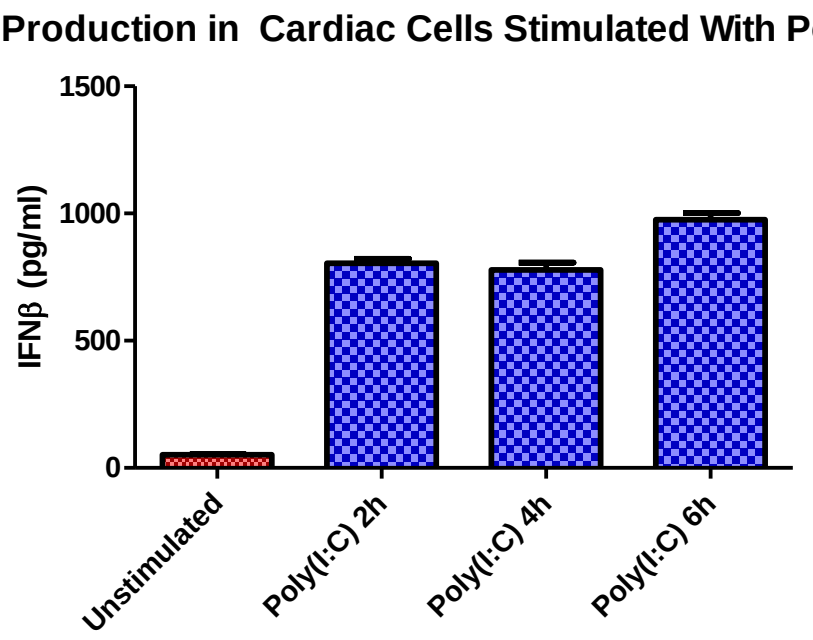

Figure 4.10 - Poly IC stimulation on cardiac cells. Cardiac cells were unstimulated or stimulated with 10 μg of Poly IC. Cell supernatant was collected at 2 hr, 4 hr, 6 hr post infection and analysed for IFNβ secretion using the Flex set system on a FACSCalibur (Becton Dickinson). The data represents the mean of three independent experiments.

The Poly(I:C) triggers IFNβ expression over time. Therefore confirming dsRNA recognition by RLRs.

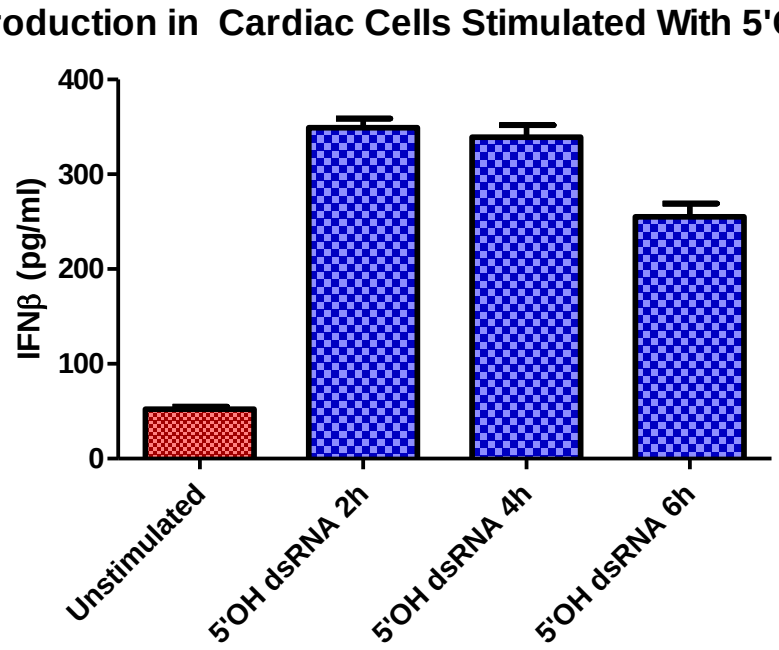

Figure 4.11 - Poly IC stimulation on cardiac cells . Cardiac cells were unstimulated or stimulated with 10 μg of 5' OH dsRNA. Cell supernatant was collected at 2 hr, 4 hr, 6 hr post infection and analysed for IFNβ secretion using the Flex set system on a FACSCalibur (Becton Dickinson). The data represents the mean of three independent experiments.

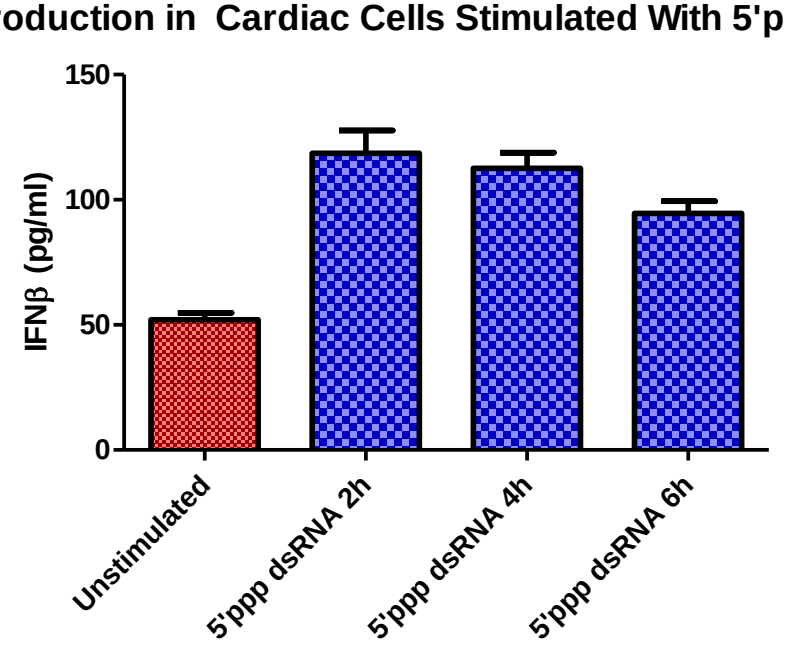

Figure 4.12 - 5'ppp dsRNA stimulation on cardiac cells. Cardiac cells were unstimulated or stimulated with 10 μg of 5'ppp dsRNA. Cell supernatant was collected at 2 hr, 4 hr, 6 hr post infection and analysed for IFNβ secretion using the Flex set system on a FACSCalibur (Becton Dickinson). The data represents the mean of three independent experiments.

In comparison with the other cardiac results, the 5' OH dsRNA construct triggers IFNβ production but not as high as Poly IC or RF-RNA. However 5'ppp dsRNA has by far the least increase in IFNβ expression, thus indicating that 5'ppp dsRNA does not have an immunostimulatory effect on RLRs.

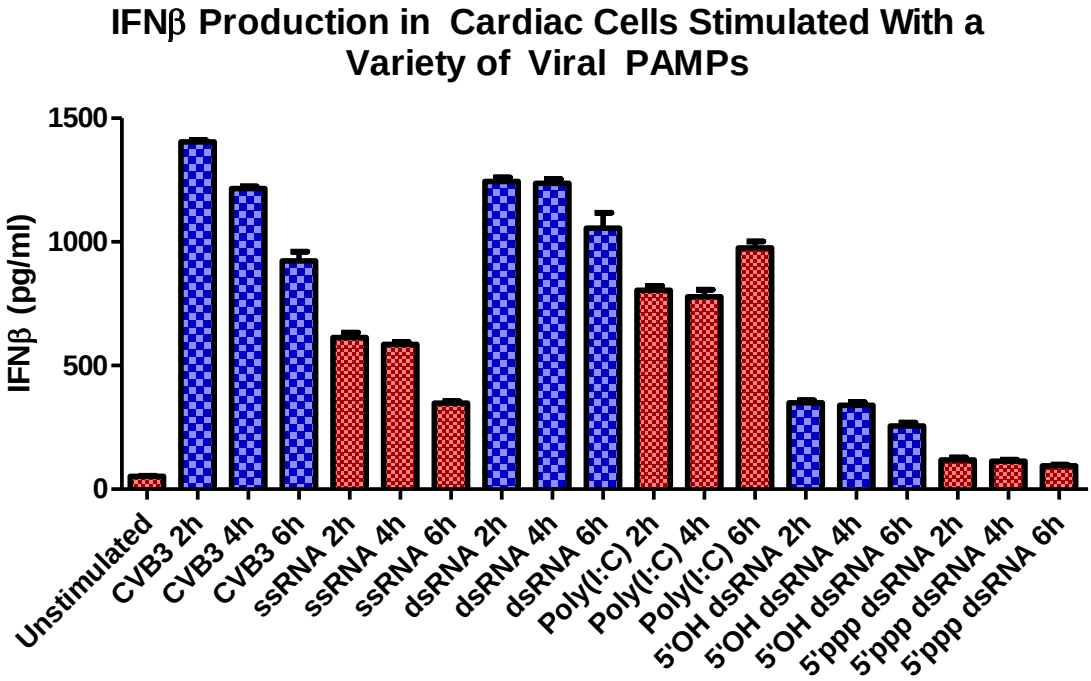

Figure 4.13 - RNA stimulations on cardiac cells. Cardiac cells were unstimulated or stimulated with 5 moi of CBV3 or with 10 μg of ssRNA, RF-RNA, Poly IC as well as 5'OH dsRNA or 5' OH dsRNA. Cell supernatant was collected at 2 hr, 4 hr, 6 hr post infection and analysed for IFNβ secretion using the Flex set system on a FACSCalibur (Becton Dickinson). The data represents the mean of three independent experiments

An overview of the cardiac stimulations (figure 4.13) shows that along with CVB, the RF-RNA creates the largest IFNβ response. The ssRNA is recognised but is not as potent an inducer of the immune response as the dsRNA. The 5'OH dsRNA is also clearly recognised while the 5'ppp seems to nearly completely negate any IFNβ response.

4.3: Innate Immune Response to CBV3 Infection in HEK and HEK-MDA5 cells

4.3.1: IFNβ Production in Stimulation with CBV3 and Genomic RNA as well as Synthetic RNA

In order to determine the specific role of MDA5 on RNA ligand recognition HEK293 cells transfected with MDA5 were also used. Measurements of IFNβ secretion determined the immunostimulatory effect of different RNA constructs (figure 4.14 and figure 4.15).

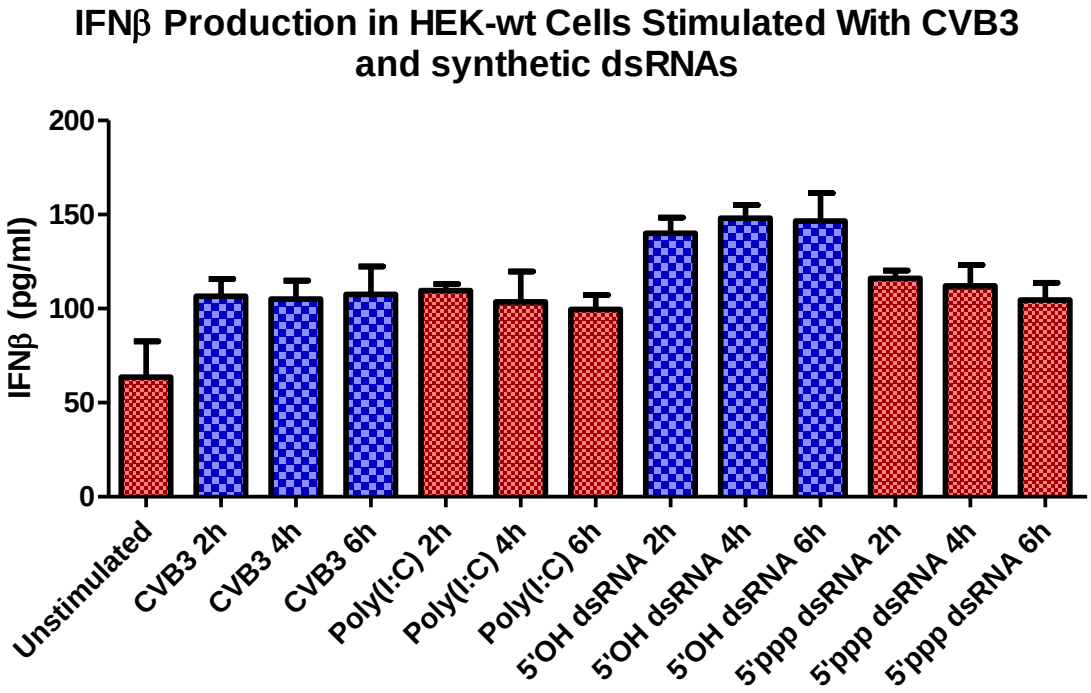

Figure 4.14 - RNA stimulations on HEK cells. HEK cells were unstimulated or stimulated with 5 moi of CBV3 or with 10 μg of ssRNA, RF-RNA, Poly IC as well as 5'OH dsRNA or 5'ppp dsRNA. Cell supernatant was collected at 2 hr, 4 hr, 6 hr post infection and analysed for IFNβ secretion using the Flex set system on a FACSCalibur (Becton Dickinson). The data represents the mean of three independent experiments

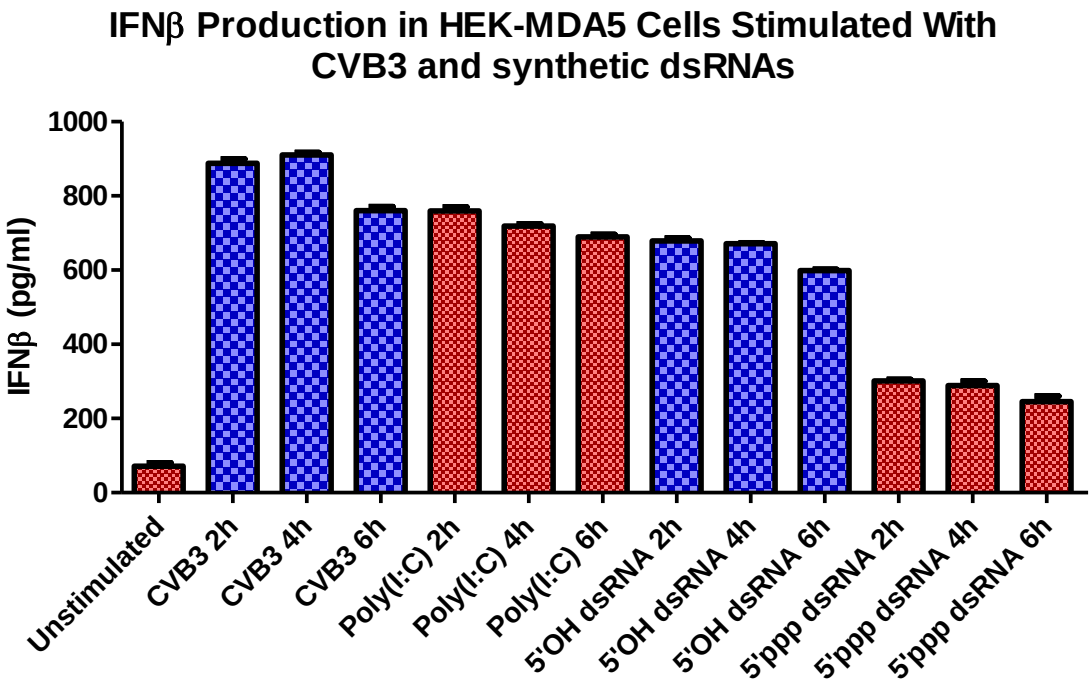

Figure 4.15 - RNA stimulations on HEK-MDA5 cells. HEK-MDA5 cells were unstimulated or stimulated with 5 moi of CBV3 or with 10 μg of ssRNA, RF-RNA, Poly IC as well as 5'OH dsRNA or 5'ppp dsRNA. Cell supernatant was collected at 2 hr, 4 hr, 6 hr post infection and analysed for IFNβ secretion using the Flex set system on a FACSCalibur (Becton Dickinson). The data represents the mean of three independent experiments.

Stimulation of HEK-wt cells showed no significant expression of IFNβ, as expected. However when HEK-MDA5 cells were used the data produced showed that the CBV3 virus as well as the synthetic dsRNAs created a strong IFNβ response. The addition of the 5'OH end group triggers an IFNβ response but obviously slightly lower than the RF-RNA since it is not as long as RF-RNA. Therefore the 5'OH end group may be a factor in dsRNA recognition. However The 5'ppp end group is not very immunostimulatory to RLRs since it stimulates a response but not very significant.

4.3.2: IRF3 Production after Stimulation with CBV3 and Genomic RNA as well as Synthetic RNA

The HEK cell line do not naturally express any PRRs so in order to determine the specific effect of MDA5 in recognising RNA constructs we used HEK-MDA5 cells.

Both HEK-MDA5 and HEK-wt cells were stimulated with CVB3, ssRNA and RF-RNA (dsRNA) isolated from CVB3, Poly(I:C), 5'OH dsRNA and 5'ppp dsRNA for 2, 4 and 6 hours as well as using unstimulated cells as the control. The cell extracts were analysed via SDS-PAGE electrophoresis and western blotting for the detection of IRF3 as the downstream signalling target to determine the strength of the innate immune response.

From the data (figure 4.16) we concluded that there is no IRF3 expression in HEK-wt type cells. However when HEK-MDA5 cells were used there was an IRF3 response to CVB3 infection as expected. Furthermore RF-RNA (dsRNA) as well as Poly(I:C) and 5' OH dsRNA triggered IRF3 response. We show no response when ssRNA was used and a very weak response when cells were stimulated with 5' ppp dsRNA.

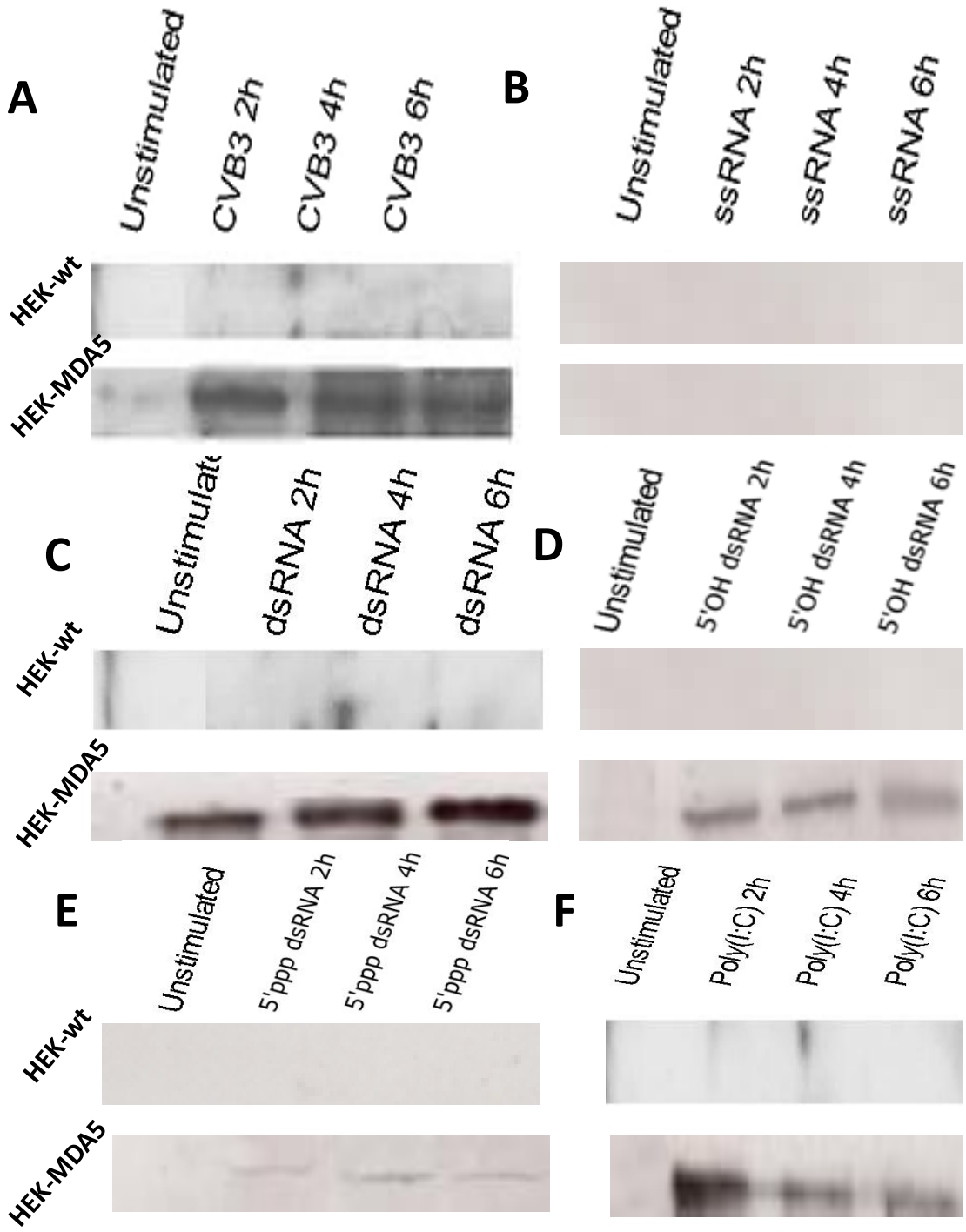

Figure 4.16 - IRF3 expression in rensponse to CBV3 and RNA constructs. Cells extracts from unstimulated HEK-wt or HEK-MDA5 cells as well as cells stimulated with 5 moi CVB3 (A) or with 10 µg of ssRNA (B), RF-RNA (C), as well as 5'OH dsRNA (D) or 5' ppp dsRNA (E) or Poly IC (F) were analysed for the presence of IRF3 by western blotting using an IRF3 Rabbit pAb and a Swine Anti-Rabbit Ig HRP secondary**.** The bands were visualised using the ECL procedure. The data represent the mean of three independent experiments.

4.3.3: Detection of Expression Levels of IFNα/β using HEK- IFNα/β reporter cells

As a second method of detecting the Type-I IFN response to CVB3 due to MDA5, HEK- IFNα/β reporter cells were used. One of the ISGs under the control IFNα and β causes expression of SEAP into the supernatant, which turns blue when Quanti-Blue is added. The more blue the supernatant, the more SEAP is expressed and the more IFNα and β are being expressed. A spectrophotometer was used to measure the level of SEAP at A630. Stimulations used CVB3, CVB3 ssRNA and dsRNA and the synthetic Poly(I:C), 5'OH dsRNA and 5'ppp dsRNA at 2, 4 and 6 hours.

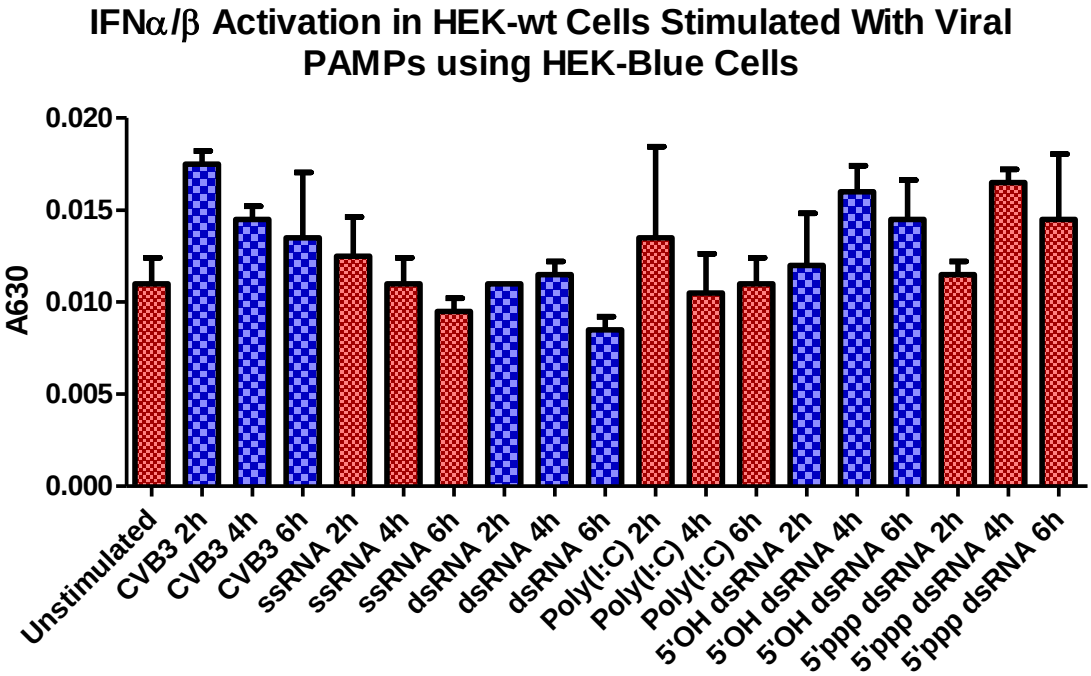

Figure 4.17 - IFN α/β response in HEK-wt cell infections. Supernatant from HEK wt infections with 5 moi of CVB3 as well as 10μg of ssRNA, dsRNA, Poly(I:C), 5'OH dsRNA or 5'ppp dsRNA for 2, 4 and 6 hours was added to HEK IFN α/β reporter cells and incubated for 24 hours. Quanti-Blue was added and the levels of SEAP measured using a spectrophotometer at 630nm. The SEAP levels correspond to the expression levels of IFNα/β.

As with the cytokine assay, the data overall show a negligible Type-I IFN response, which verifies that no PRRs are present in HEK-wt that can induce an innate immune response.

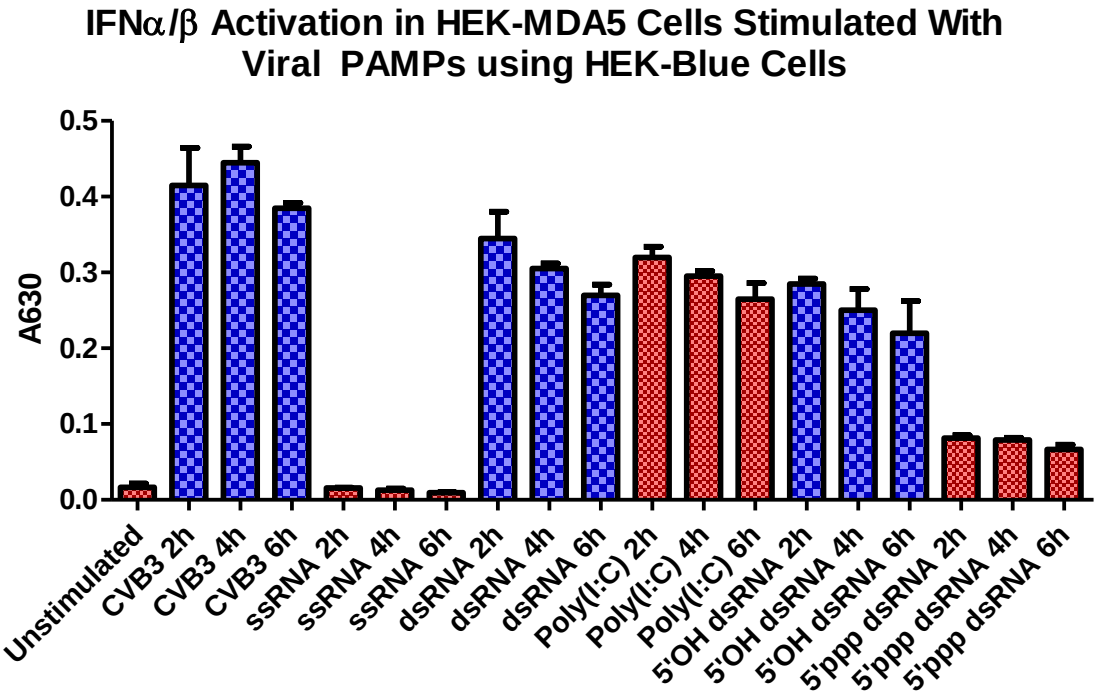

Figure 4.18 - IFN α/β response in HEK-MDA5cell infections. Supernatant from HEK MDA5 infections with 5 moi of CVB3 as well as 10μg of ssRNA, dsRNA, Poly(I:C), 5'OH dsRNA or 5'ppp dsRNA for 2, 4 and 6 hours was added to HEK IFN α/β reporter cells and incubated for 24 hours. Quanti-Blue was added and the levels of SEAP measured using a spectrophotometer at 630nm. The SEAP levels correspond to the expression levels of IFNα/β.

The overview of the HEK-MDA5 data shows that next to the expected strong response through MDA5 to CVB3, most of the dsRNAs create the next highest response. There is very little difference between the RF-RNA (dsRNA) and Poly(I:C) IFN expression levels when seeing the data. This indicates that the most crucial part of the viral dsRNA sensed by MDA5 is the double stranded nature of the RNA. The 5'ppp structure on the dsRNA appears to prevent the major portion of a Type-I IFN response to dsRNA, while 5'OH appears to have an effect in triggering IFNα/β response. Furthermore the data conclusively shows that ssRNA is not recognised by MDA5.

4.4: Co-localisation of RLRs and CVB3

Our experiments revealed that MDA5 recognises not the genomic ssRNA but the dsRNA generated by the replication of these viruses. In order to confirm MDA5 and viral RNA interactions we used confocal cell imaging.

When we investigated MDA5-viral RNA interactions using confocal microscopy, Cardiac cells were infected with CVB3 for different time points during infection and the dsRNA was visualised using the monoclonal dsRNA-specific mouse antibody J2 Fab directly conjugated to Alexa 488. MDA5 and RIG-I were labelled with Alexa 546-Fab goat specific Ig, while MAVs was labelled with Alexa 546-Fab rabbit specific Ig. A high level of colocalisation of dsRNA with MAVs and MDA5 was observed, whereas we saw no colocalisation of dsRNA with RIG-I (Figure 4.19).

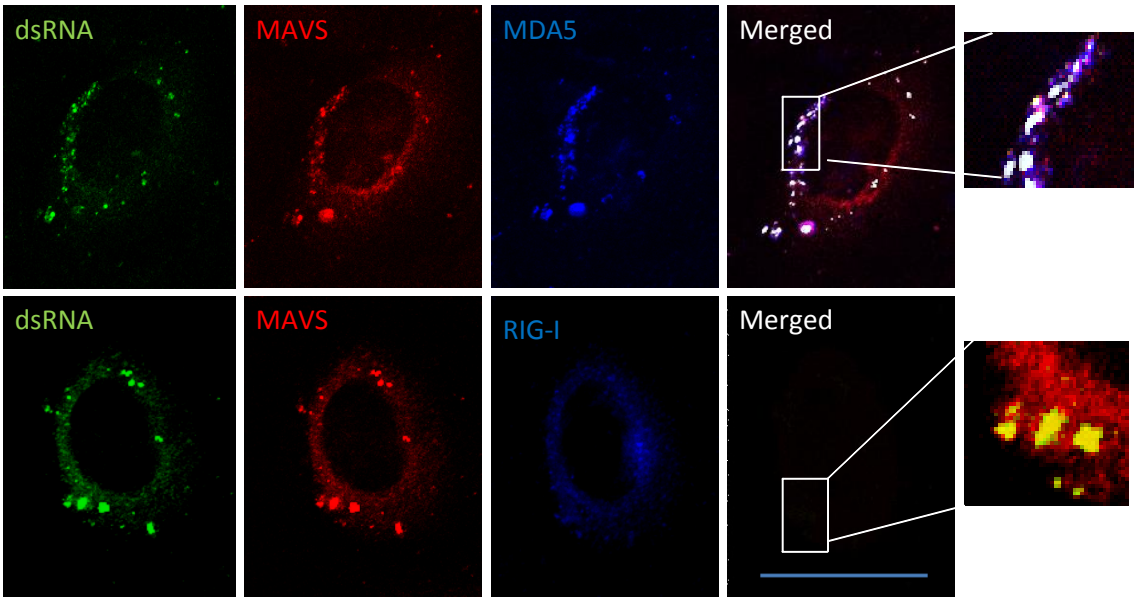

Figure 4.19 - Localisation of enteroviral dsRNA RF and MDA5 in cardiac cells. Human cardiac infected with CVB3 were stained with J2 Fab specific for dsRNA directly conjugated to Alexa 488. MDA5 and RIG-I were labelled with Alexa 633-Fab goat specific Ig while MAVs was labelled with Alexa 546-Fab rabbit specific Ig, Yellow regions indicate localisation of MAVs with dsRNA RF. White regions indicate localisation of MDA5, MAVs with dsRNA RF. Bars 10 µm.

4.5: Discussion

Effective immune defence against viral infection depends on accurate and robust detection of viral RNAs by pattern recognition receptors in the innate immune system. RIG-I and MDA5 function as cytoplasmic PRRs that are involved in the elimination of actively replicating RNA viruses.

Upon viral RNA recognition, RIG-I and MDA5 interact with a common signalling adaptor, MAVS and activate NF-kB and IRF3/7 signalling pathways, resulting in the expression of type I interferon and proinflammatory cytokines.

Despite the wealth of information on the types of RNA that trigger RIG-I, much less is known about the nature of the RNAs that act as agonists for MDA5. In order to identify the specific ligand for MDA5, we chose to utilise CVB3, which is a member of Picornaviridae. In order to identify which RNA species triggers MDA5 activation during infection, we isolated viral ssRNA and replicative intermediate of RNA as well as using synthetic dsRNAs. This work revealed that MDA5 recognises not the genomic ssRNA but the dsRNA generated by the replication of CVB3 and more specifically synthetic 5'OH dsRNA appears to have an effect in triggering IFNα/β response. Furthermore, using fluorescent imaging, visualization of dsRNA and MDA5 is achieved providing unique evidence between the relationship of viral dsRNA and MDA5 and gives strong evidence that MDA5 is the key sensor for the dsRNA replicative intermediate form of positive sense ssRNA.

Results from the cardiac cells are limited by the presence of other PRRs expressed within the cells and the SDS-PAGE data, while reliably showing expression of NF-κB or IRF-3, is not easily quantifiable. However alongside the IFN-assays, confocal work and the HEK-MDA5 data the evidence presented all points to the same conclusion.

Chapter 5: Determining the Role of RIG-I in CVB3 sensing using HUH Cells

5.1: Introduction

RLRs were initially thought to recognise the same ligand, dsRNA, but it has since become apparent that RIG-I and MDA5 possess distinct virus specificities. It has been shown that they each recognise different viruses and different viral RNAs [317;318]. RIG-I recognises single-stranded RNA (ssRNA) containing a terminal 5'-triphosphate (ppp) [319], as well as linear dsRNA no longer than 23 nucleotides in length [320]. MDA5 recognises long strands of dsRNA, but the mechanism by which this occurs is less clear [321].

In order to determine the involvement of RIG-I in CBV3 recognition, Huh cells were used. The Huh7 cells are a well differentiated human hepato-carcinoma cell line [322] that can be used to compare cell lines with or without RIG-I. The Huh 7.5.1 cell line is derived from the wt Huh7s and contains a mutation within the RIG-I gene. The T551 mutation within the gene is located in the CARD domain of RIG-I and prevents CARD-CARD homotypic interactions. This prevents RIG-I from transducing a signal through MAVS and essentially means that the RIG-I pathway is completely inhibited [323].

To elucidate the role of RIG-I in CVB3 infection both the Huh7 and Huh7.51 cell lines were used to compare the effect of a fully functioning RIG-I pathway. Stimulations used 2, 4 and 6 hour time points to cover the CBV3 life cycle and CVB3, CVB3 ssRNA and dsRNA and Poly(I:C) were used to infect the cells. The main point of interest is whether RIG-I plays any role in Coxsackievirus RNA recognition.

Phospho-IκB detection corresponds with NF-κB activation, which when coupled with IRF3 detection, gives an indication of MDA5 and RIG-I activity in response to different stimulations.

Huh7 and Huh 7.5.1 cells were stimulated with CVB3, ssRNA and RF-RNA (dsRNA) isolated from CVB3 and Poly(I:C). The Huh cell lines were used with the aim of determining the immunological difference of having a working RIG-I pathway present. The strength of the innate immune response was measured by probing for IRF3, phospho-IκB and total-IκB through SDS-PAGE and detecting via ECL. For each stimulus the cells were left for either 2, 4 or 6 hours as well as an unstimulated sample as the control.

5.2: Results

5.2.1.: Ligand recognition and Phospho-IκB and IRF3 signalling in Huh 7 and 7.5.1 Cells

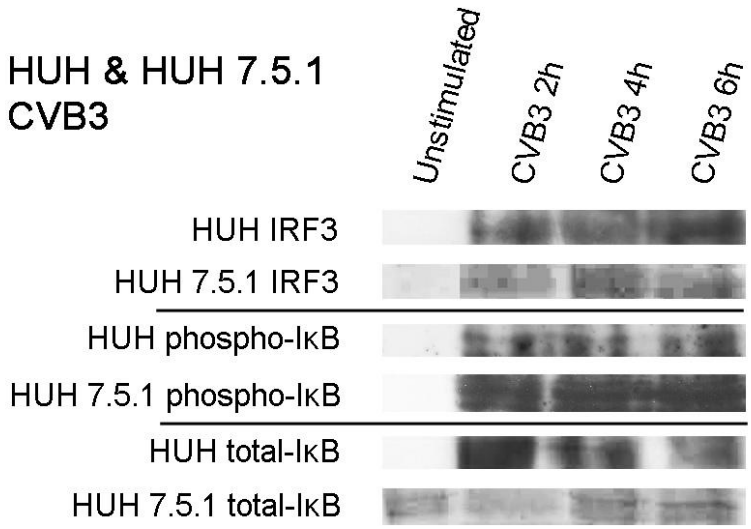

Figure 5.1 - CBV3 recognition by HUH cells. Huh7 and Huh7.5.1 cells were either left unstimulated or stimulated with CBV3 virions, for 2, 4, or 6 hour time points. Discontinuous SDS-PAGE followed by western blotting using specific phospho-Iκb, T-Iκb or IRF3 Rabbit pAb and a Swine Anti-Rabbit Ig HRP secondary antibody was used to detect their presence. The bands were visualised using the ECL procedure. This is a representative of three independent experiments.

Stimulation of both cell lines of Huh cells with CVB3 causes strong expression of IRF3, P-IκB and T-IκB through all three time points. There appears to be very little difference between the presence of RIG-I or not, most likely due to the fact that CVB3 is also detected by other PRRs such as TLR4, TLR3, TLR7, TLR8 or MDA5 [324-326].

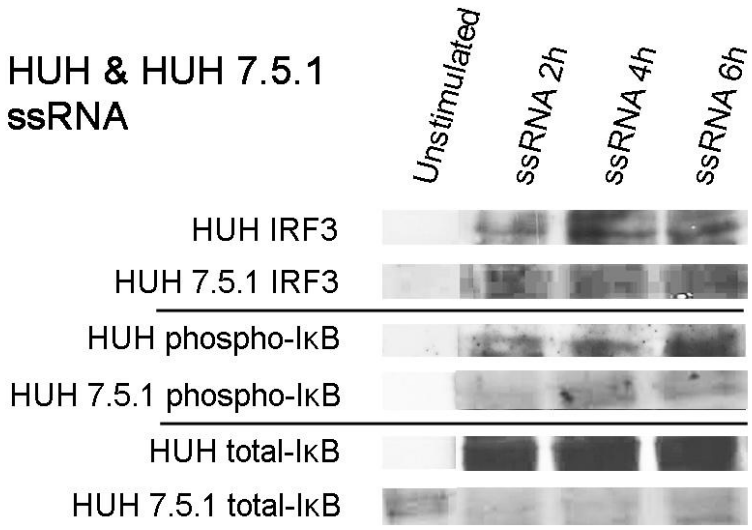

Figure 5.2 - CBV3 ssRNA recognition by HUH cells. Huh7 and Huh7.5.1 cells were either not stimulated or stimulated with, CBV3 ssRNA, for 2, 4, or 6 hour time points. Discontinuous SDS-PAGE followed by western blotting using specific phospho-Iκb, T-Iκb or IRF3 Rabbit pAb and a Swine Anti-Rabbit Ig HRP secondary antibody was used to detect their presence. The bands were visualised using the ECL procedure. This is a representative of three independent experiments.

Unlike the stimulation with CVB3, where there is no difference between the two cell lines, there is a slight difference in the expression of P-IκB with ssRNA stimulation. We have already seen in cardiac cells that RIG-I is not involved in CVB ssRNA recognition. This data could suggest that perhaps another PRR, (probably TLR7 which has been shown to recognize CVB ssRNA [327]) is responsible for IRF3 and P-IkB expression and could be more upregulated in the presence of RIG-I.

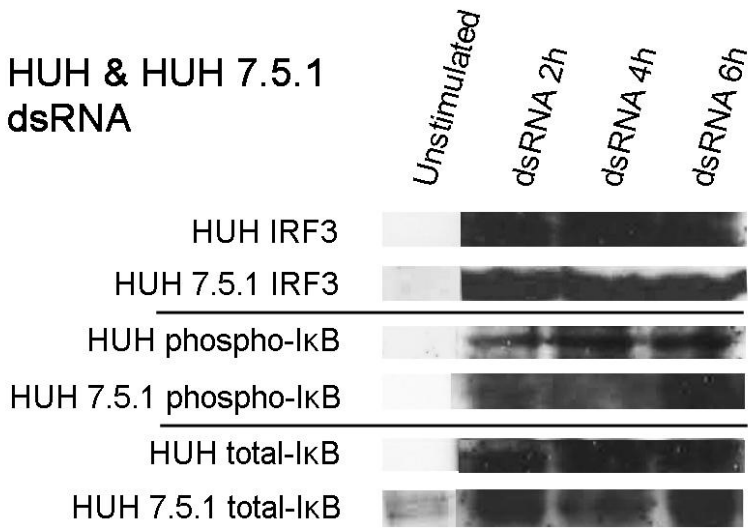

Figure 5.3 - RF-RNA (dsRNA) recognition by HUH cells. Huh7 and Huh7.5.1 cells were either not stimulated or stimulated with, CBV3 dsRNA, for 2, 4, or 6 hour time points. Discontinuous SDS-PAGE followed by western blotting using specific phospho-Iκb, T-Iκb or IRF3 Rabbit pAb and a Swine Anti-Rabbit Ig HRP secondary was used to detect their presence. The bands were visualised using the ECL procedure. This is a representative of three independent experiments.

Stimulation with RF-RNA (dsRNA) confirms that MDA5 is the main receptor for CVB3 and recognises the virus through its dsRNA intermediate as there is no difference in IRF3 and P-IkB expression in both cell lines. Huh7.5.1 cells lacking RIG-I still respond to dsRNA from CVB3. This data seems to corroborate that RIG-I is not important in CVB dsRNA recognition.

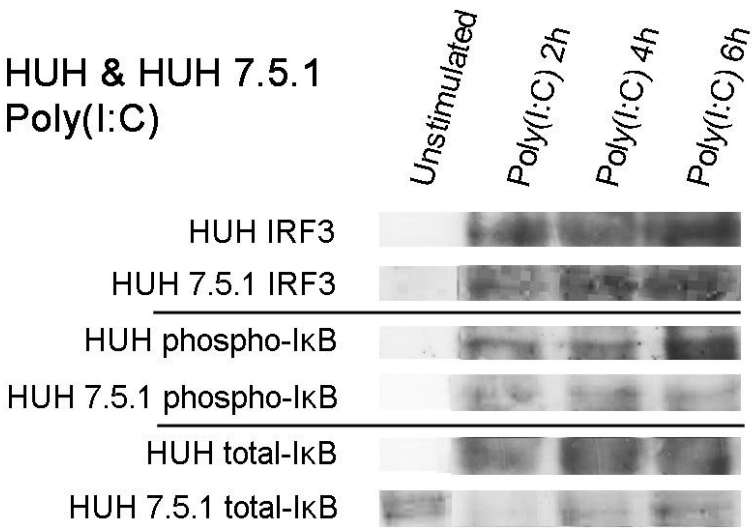

Figure 5.4 - Poly (IC) recognition by HUH cells. Huh7 and Huh7.5.1 cells were either not stimulated or stimulated with, Poly(I:C), for 2, 4, or 6 hour time points. Discontinuous SDS-PAGE followed by western blotting using specific IRF3, T-Iκb or P-IκB Rabbit pAb and a Swine Anti-Rabbit Ig HRP secondary antibody was used to detect their presence. The bands were visualised using the ECL procedure. This is a representative of three independent experiments.

Again the Poly(I:C) results are similar to those of dsRNA stimulations, Since Poly (IC) is a known ligand for MDA5 this results confirm that MDA5 is functional on both cell lines and that it recognises Poly(I:C) which is synthetic dsRNA.

To verify that RIG-I was functional in HUH 7.5.1 cells, ssRNA from Influenza A virus (IFVA) was used. IFVA genomic ssRNA has been shown to be recognised by RIG-I and triggers a strong IFNα/β via IRF3 [328] so IFVA ssRNA was used to stimulate HUH cells (see Fig. 5.5).

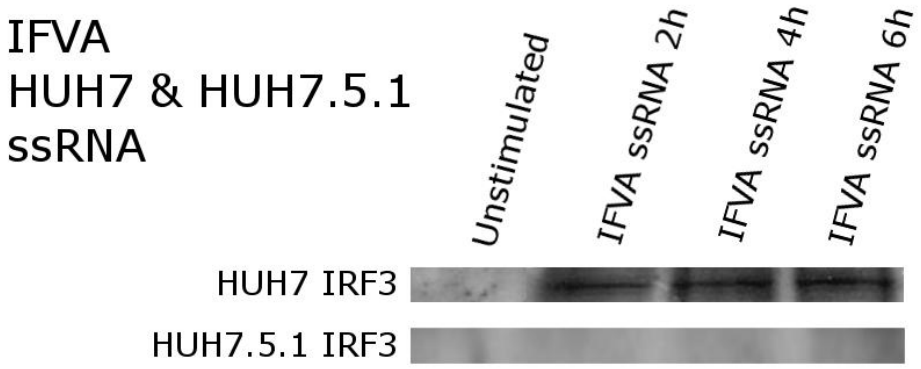

Figure 5.5 - IFVA ssRNA recognition by HUH cells. Huh7 and Huh7.5.1 cells were either not stimulated or stimulated with, IFVA ssRNA, for 2, 4, or 6 hour time points. Discontinuous SDS-PAGE followed by western blotting using IRF3 specific Rabbit pAb and a Swine Anti-Rabbit Ig HRP secondary antibody was used to detect the presence of IRF3. The bands were visualised using the ECL procedure. This is a representative of three independent experiments.

The data showed that although IFVA ssRNA triggered IRF3 signalling in Huh7 cells, in cells that did not have a functional RIG-I like the Huh7.5.1 there was no IRF3 signalling. Therefore confirming that RIG-I is functional in Huh7 cells and the data obtained for CVB3 were specific.

5.2.2: IFN-β Production

To determine the effect of inhibiting the RIG-I pathway on IFNα/β production Huh7 and Huh7.5.1 cells were used. They were stimulated with CVB3, CVB3 ssRNA and dsRNA for 2, 4 and 6 hours (Fig. 5.6)

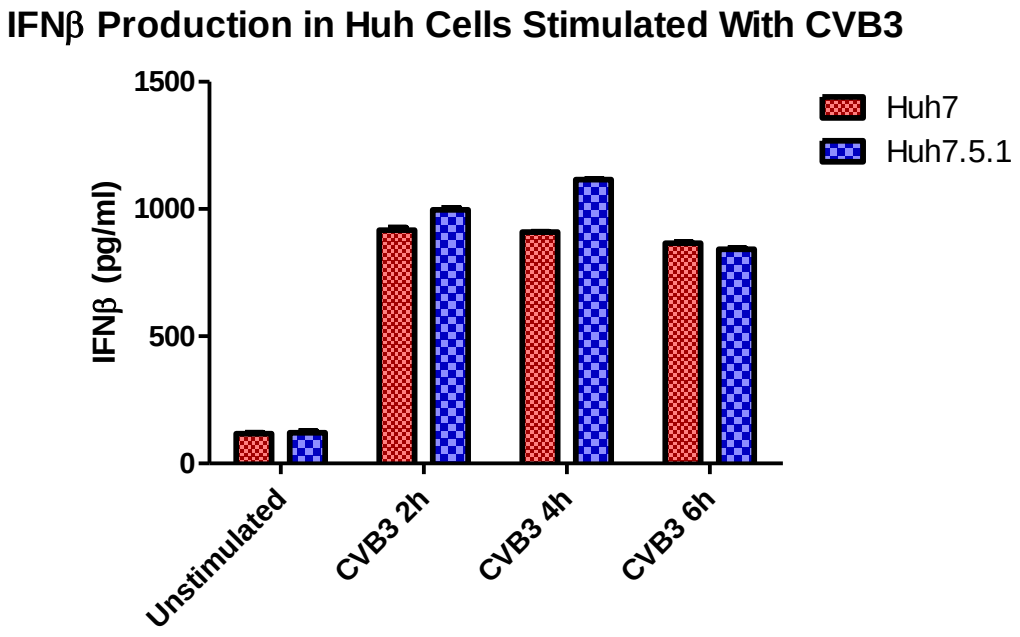

Figure 5.6 - CBV3 infection activates RLRs. Huh7 and Huh7.5.1 cells were either not infected or infected with 5moi of CBV3. Supernatant was collected at 2hr, 4h, 6h post infection and analysed for IFNβ secretion using the Flex set system on a FACSCalibur (Becton Dickinson). The data represents the mean of three independent experiments.

The difference between the IFN expression levels between the two cell lines is minimal which would suggest that RIG-I does not play a role in CVB3 recognition. The response is actually higher at 2 and 4 hours with 1000pg/ml over 915pg/ml for Huh7.5.1 and Huh7 at 2 hours respectively and 1115pg/ml over 910pg/ml for Huh7.5.1 and Huh7 at 4 hours respectively.

Cells were also stimulated with RF-RNA (dsRNA) for different time points (figure 5.7).

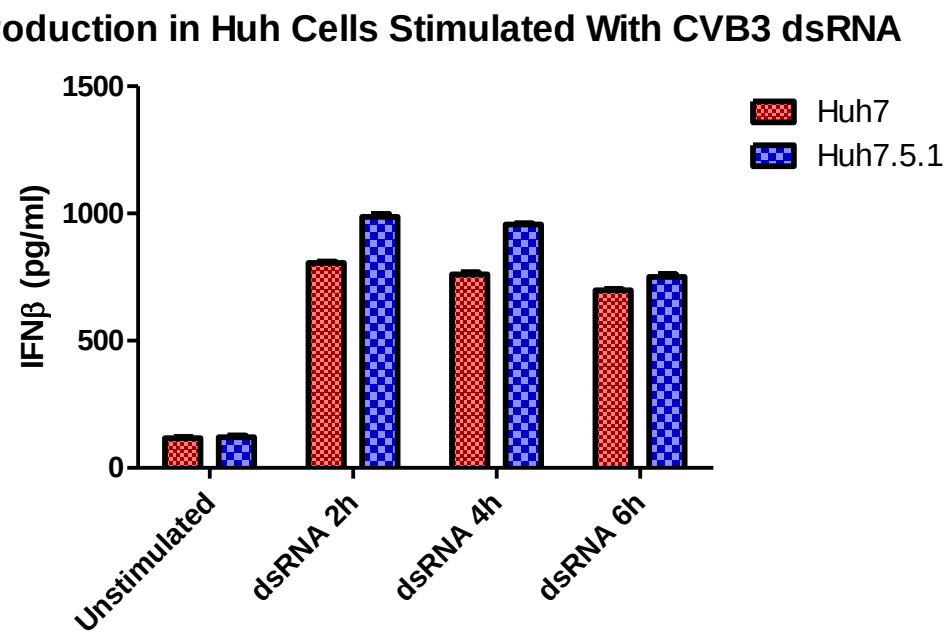

Figure 5.7 - CBV3 RF-RNA (dsRNA) stimulation on HUH cells. Huh7 and Huh7.5.1 cells were unstimulated or stimulated with 10 µg of CBV3 RF-RNA. Cell supernatant was collected at 2hr, 4h, 6h post infection and analysed for IFNβ secretion using the Flex set system on a FACSCalibur (Becton Dickinson). The data represents the mean of three independent experiments.

Stimulation with the CVB3 dsRNA creates IFNβ expression levels remarkably similar to those of the CVB3 stimulation. The Huh7 cells have a slightly lower expression when stimulated than the Huh7.5.1, verifying that RIG-I does not trigger a Type-I IFN response to CVB3 dsRNA,

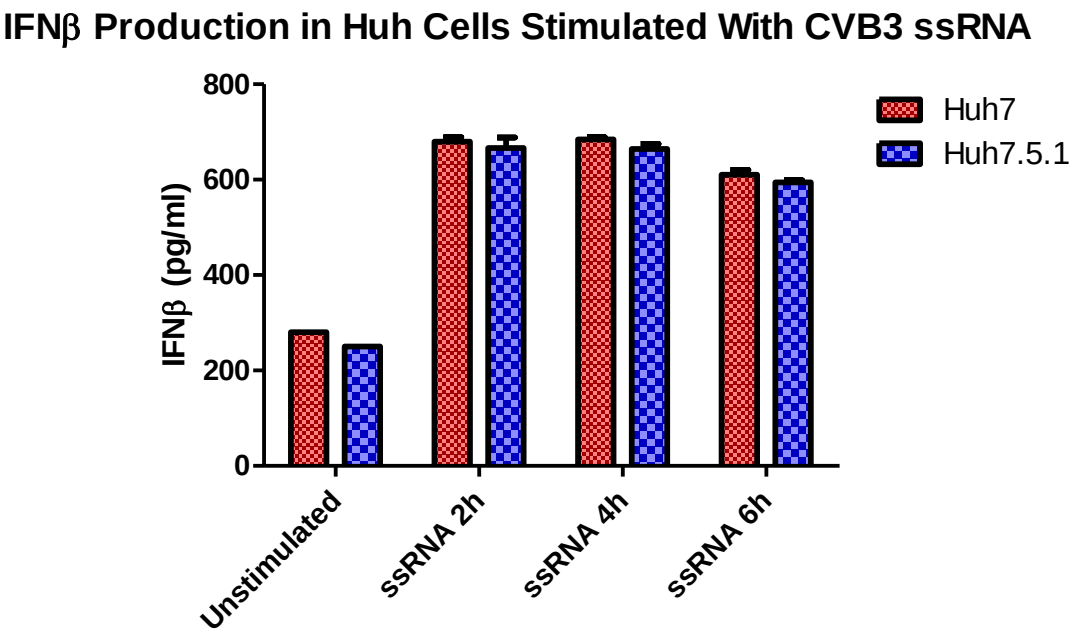

Figure 5.8 - CVB3 ssRNA stimulation on HUH cells. Huh7 and Huh7.5.1 cells were unstimulated or stimulated with 10 µg of CBV3 ssRNA. Cell supernatant was collected at 2hr, 4h, 6h post infection and analysed for IFNβ secretion using the Flex set system on a FACSCalibur (Becton Dickinson). The data represents the mean of three independent experiments.

The ssRNA isolated from CVB3 creates a much lower IFNβ than the full CVB3 virus and the dsRNA, with the highest expression still falling below 700pg/ml. This indicates that dsRNA is a far more prominent PAMP in CVB3 than the ssRNA. There is also very little difference between the IFNβ expression levels between the Huh7 and Huh7.5.1 showing that RIG-I is not capable of recognising and creating an immune response to CVB3s ssRNA.

5.2.3: Detection of Expression Levels of IFNα/β using HEK-blue cells

HEK IFNα/β reporter cells were also used to confirm the data obtained. Huh7 and Huh7.5.1 cells were stimulated with CVB3, CVB3 ssRNA and dsRNA and Poly(I:C) for 2, 4 and 6 hours and the IFNα/β measured using HEK-Blue cells.

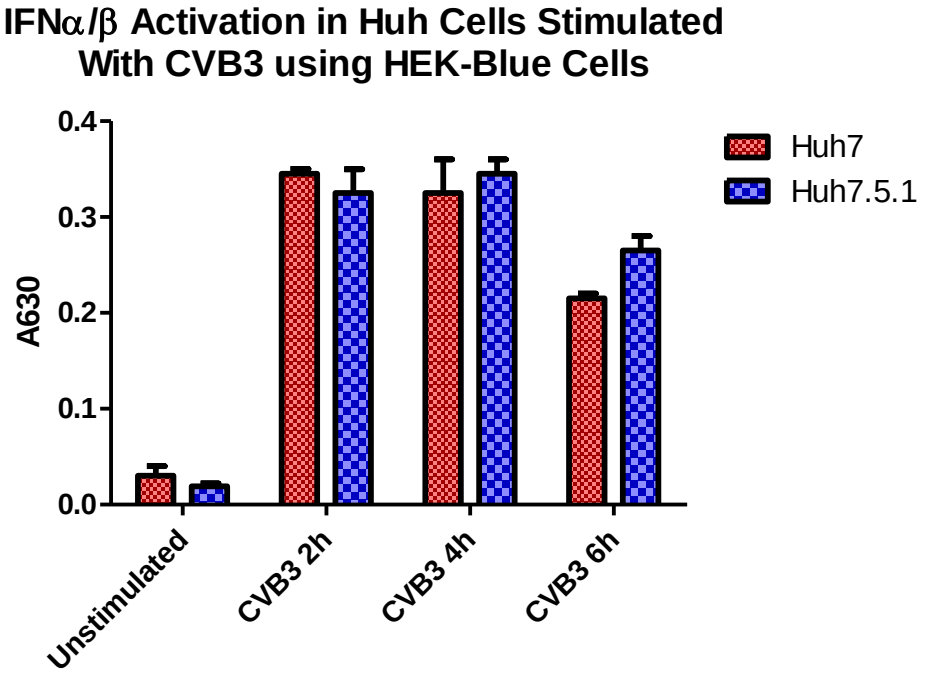

Figure 5.9 - IFN α/β response in CBV3 infections. Supernatant from HUH cell infections with 5 moi of CVB3 for 2, 4 and 6 hours was added to HEK IFN α/β reporter cells and incubated for 24 hours. Quanti-Blue was added and the levels of SEAP measured using a spectrophotometer at 630nm. The SEAP levels correspond to the expression levels of IFNα/β.

The Type-I IFNα/β response to CVB3 in both cell lines is strong, over 10 fold the unstimulated values for both in the first two time points. There is not much difference between expression levels at 2 and 4 hours (0.35/0.33 and 0.33/0.35 respectively) however by 6 hours there is a drop in expression levels on both the Huh7 and HUH7.5.1 leaving a stronger IFN response in the Huh7.5.1. The Type-I IFN α/β response, despite the loss of the RIG-I pathway, is not affected and complements the cytokine assay data.

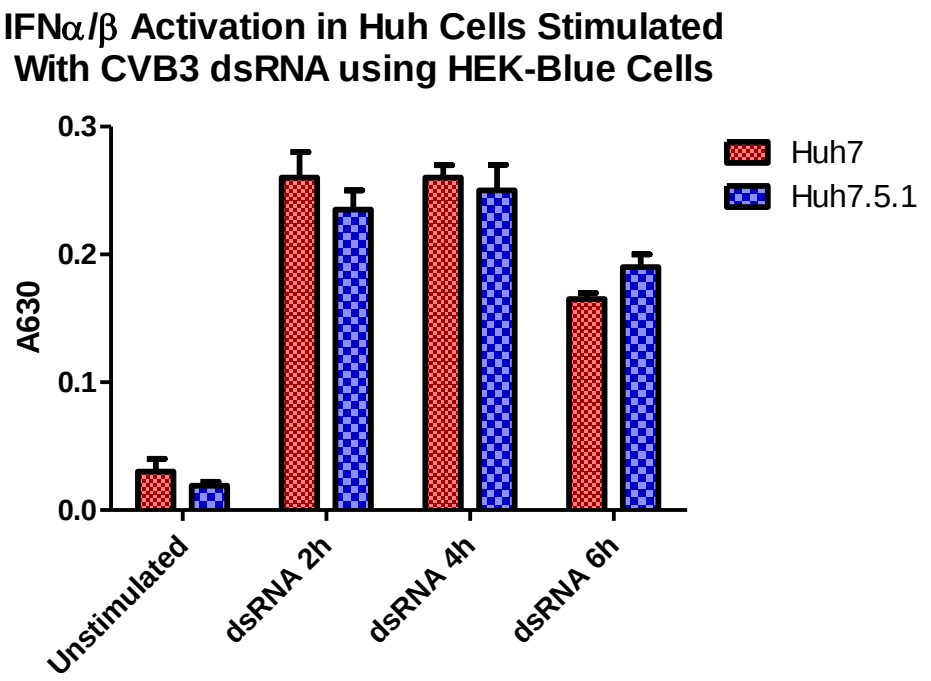

Figure 5.10 - IFN α/β response in RF-RNA (dsRNA). Supernatant from HUH stimulations with 10µg of dsRNA, for 2, 4 and 6 hours was added to HEK IFN α/β reporter cells and incubated for 24 hours. Quanti-Blue was added and the levels of SEAP measured using a spectrophotometer at 630nm. The SEAP levels correspond to the expression levels of IFNα/β.

The dsRNA stimulations show an 8.5 fold increase in IFNα/β expression over the unstimulated for both the 2 and 4 hour time points in the Huh7 cells, with the Huh7.5.1 having slightly lower IFNα/β levels, but a higher increase in terms of comparison to the unstimulated at over 10 times the unstimulated value. The 6 hour time point however shows a larger difference with a 5.5 fold increase for the Huh7 cells and much larger 10 fold increase for the Huh7.5.1. This gain complements the cytokine assay data and shows further evidence that RIG-I is not essential to CVB3 dsRNA IFN α/β response

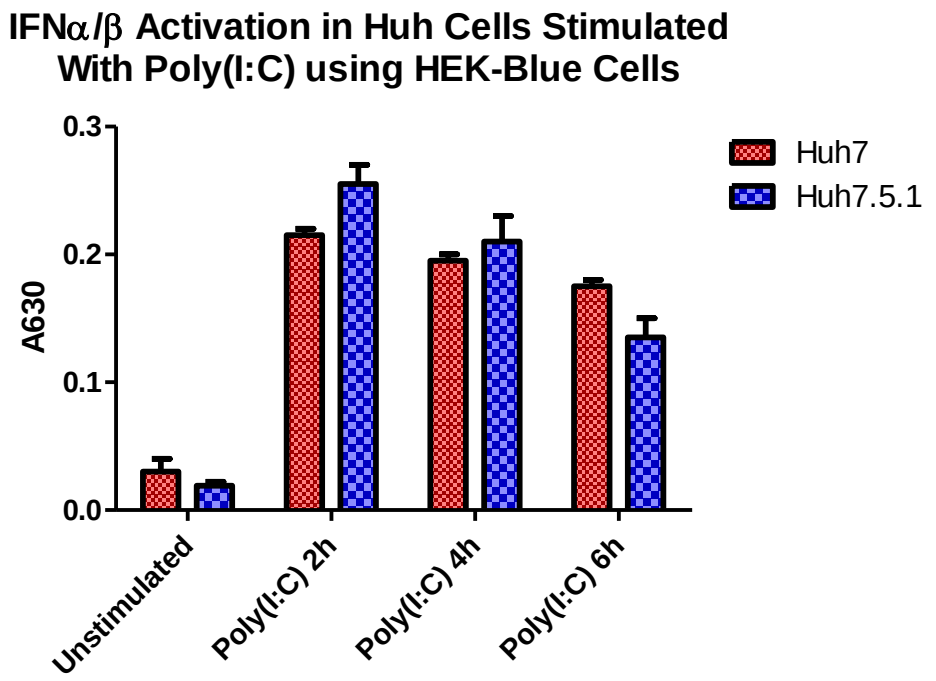

Figure 5.11 - IFN α/β response in Poly IC stimulations. Supernatant from HUH stimulations with 10µg of Poly(I:C), for 2, 4 and 6 hours was added to HEK IFN α/β reporter cells and incubated for 24 hours. Quanti-Blue was added and the levels of SEAP measured using a spectrophotometer at 630nm. The SEAP levels correspond to the expression levels of IFNα/β.

The Poly(I:C) results are similar to the dsRNA results, although slightly lower. This data confirms that RIG-I does not appear to be involved in the recognition of Poly(I:C).

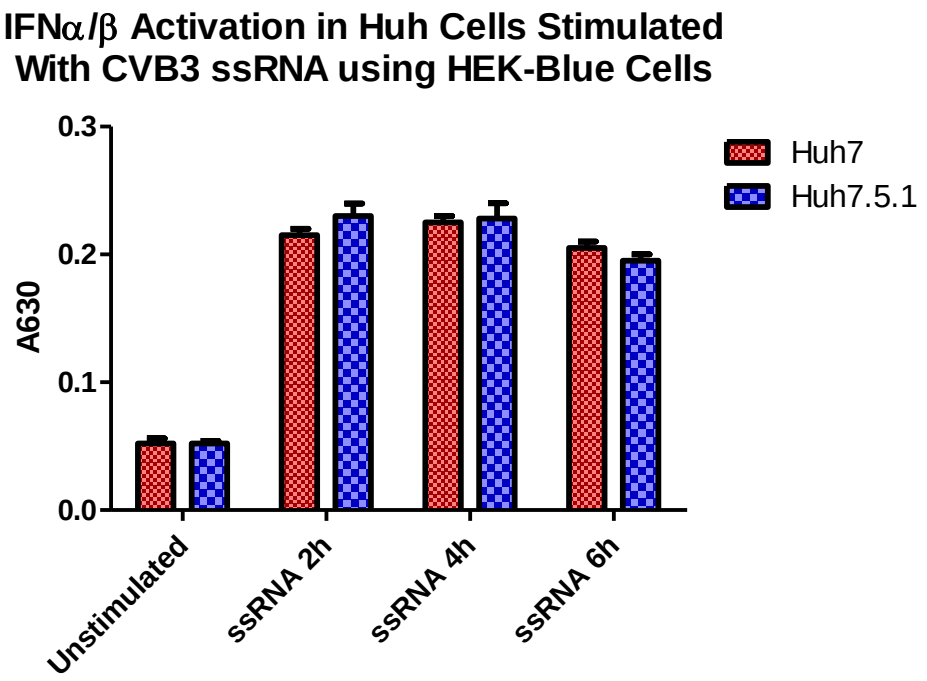

Figure 5.12 - IFN α/β response in CVB3 ssRNA stimulations. Supernatant from HUH stimulations with 10µg of CVB3 ssRNA, for 2, 4 and 6 hours was added to HEK IFN α/β reporter cells and incubated for 24 hours. Quanti-Blue was added and the levels of SEAP measured using a spectrophotometer at 630nm. The SEAP levels correspond to the expression levels of IFNα/β.

As with the IFNβ results from the cytokine assay, the IFNα/β expression levels as detected through the HEK-Blue cells show very little difference between the Huh7 and Huh7.5.1. This confirms that RIG-I does not play a role in CVB3 ssRNA recognition and is incapable of creating an immune response.

Since RIG-I was shown to be ineffective in CVB3 and CBV3 RNA recognition, IFVA ssRNA was also used to stimulate HUH cells for different time points as a control (figure 5.13).

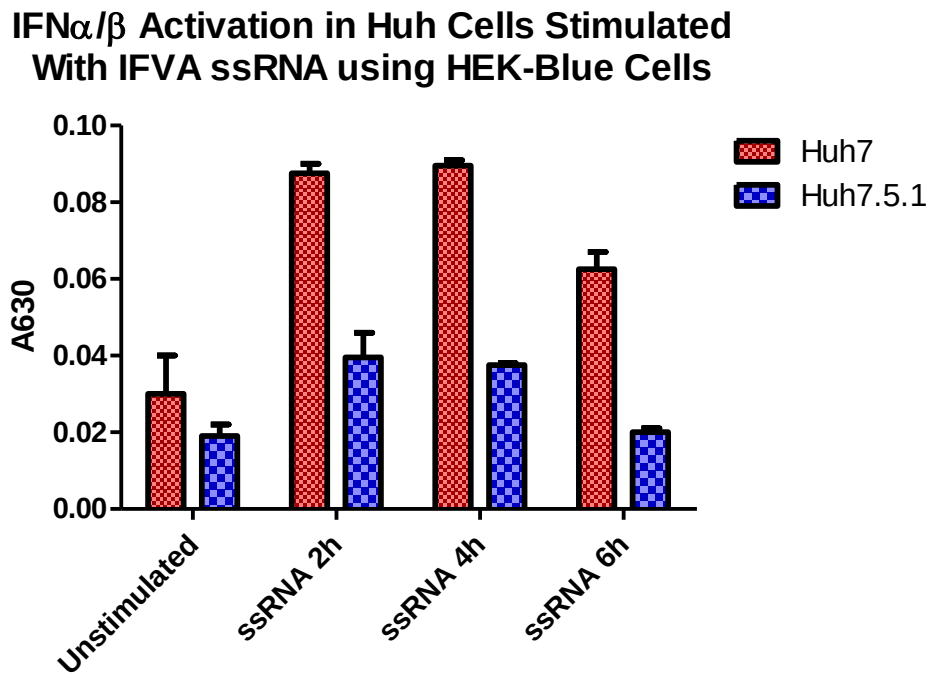

Figure 5.13 - IFN α/β response in IFVA ssRNA stimulations. Supernatant from HUH stimulations with 10µg of IFVa ssRNA for 2, 4 and 6 hours was added to HEK IFN α/β reporter cells and incubated for 24 hours. Quanti-Blue was added and the levels of SEAP measured using a spectrophotometer at 630nm. The SEAP levels correspond to the expression levels of IFNα/β.

As expected since IFVA ssRNA is a ligand for RIG-I, the data showed that there is an obvious difference between the two cell lines. The IFNα/β response is diminished in Huh7.5.1 cells since there is no functional RIG-I.

5.3: Discussion

The IFN-β production in Huh7 cells and Huh7.5.1 cells are the most significant results here. Huh7.5.1 cells have an inactivating mutation in RIG-I that leads to a defect in IFN production. The major effect of the absence of a working RIG-I pathway is an impaired response to IFVA ssRNA showing no IRF3 signalling and diminished IFNα/β production. However when CVB3 and CVB3 ssRNA or RF-RNA were used there was no major difference in IFNα/β production or in signalling, as IRF3 and P-IκB production remained unaffected.

As stated earlier there is the possibility that the VPg group that usually prevents RIG-I binding ssRNA in Picornaviruses is removed during Coxsackievirus replication. Whether this occurs or not is still debatable, however regardless of this it does not play a role in RLR recognition of ssRNA as neither the whole virus, nor the isolated ssRNA create an immune response through RIG-I. As the isolated ssRNA is not bound by RIG-I it would seem likely that it is a structural trait of the RNA, not another factor created ii the life cycle of the virus, that prevents RIG-Is binding, thus it would seem likely that it is the VPg group preventing RIG-I creating an immune response to Coxsackievirus. Neither of the dsRNA intermediates create a response through RIG-I either, suggesting that the structures are too long for RIG-I to bind. It also suggests that the nascent ssRNA in the RI is not a suitable ligand for RIG-I.

This evidence supports the hypothesis that RIG-I does not create an innate immune response to Picornaviruses, particularily Coxsackieviruses and suggests that as with other Picornaviruses the VPg end group prevents Coxsackievirus recognition.

CHAPTER 6: RLR DIMERISATION

6.1: Introduction

Once a viral ligand has been detected and bound by RIG-I and MDA5, both signal downstream through their CARDs to activate IRF3/7 and NF-κB indirectly, via the protein intermediate MAVS [329]. After interaction with RIG-I and MDA5, MAVS goes on to recruit and activate a variety of other proteins, including TRAF2, TRAF3, and TRAF6 [330-332]. These TRAF proteins then signal further downstream to the IκB kinase (IKK) family members, to activate the transcription factors IRF3/7 and NF-κB, and initiate an immune response.

RIG-I, MDA5, and LGP2 have been proposed to homo- and heterodimerise upon viral ligand detection. This process involves the C-terminal RD, which is important for controlling RLR-mediated IFN responses. RIG-I has two states; an inactive (closed) one and an active (open) one. In the inactive state, the CARDs and the helicase domain are repressed by the RD. Once a viral ligand binds to the RD, a conformational change occurs, converting RIG-I to the active state. This results in the dimerisation of RIG-I and the initiation of downstream signalling via the CARDs. Without the RD, RIG-I constitutively activates downstream signalling, whilst over-expression of the RD inhibits the antiviral response [333].

Dimerisation of the RLRs is essential for them to function correctly. LGP2 has been suggested as a negative regulator of the RIG-I- and MDA5-mediated antiviral response, as its over-expression inhibits virus-induced IRF3 and NF-κB activation [334-336]. LGP2 has been proven to be a regulator for RIG-I- and MDA5-dependent signalling via its RD. Although it was previously thought that LGP2 inhibits dimerisation of RIG-I

and its interaction with MAVs, it has now been shown that LGP2 augments MDA5-dependent signalling [337].

Recently it has been shown that MAVS requires homo-dimerisation through its CARD domain as part of its requirements for signalling [338], it would seem very possible that the same is true of RIG-I and MDA5 both through their CARD domains as well. It is already established that TLRs form homodimers or heterodimers in order to induce signalling [108] as well as NLRs forming oligomers in the form of the inflammasome. Oligomerisation of PRRs appears to be a crucial role in the induction of an immune response in creating signalling platforms. To establish whether the same is true of the RLRs, immunoprecipitation was used in order to determine whether MDA5 or RIG-I formed homodimers, and whether they also formed heterodimers with each other or LGP2.

To test whether RIG-I, MDA5, and LGP2 homo- or heterodimerise together, immunoprecipitation experiments were performed. Immunoprecipitation is a technique used to precipitate a protein out of a lysate using an antibody specific for that protein coupled with beads specific for the antibody. The technique can be used to isolate and concentrate a particular protein, as well as determine if dimerisation between two proteins has occurred.

In this project, RIG-I, MDA5, or LGP2 antibodies were used to precipitate out their respective protein, and western blotting was then used to detect a different protein, i.e. precipitate out MDA5 and then perform western blotting to detect LGP2.

RIG-I is 110 KDa, MDA5 is 117 KDa, while LGP2 is smaller and is around 60 KDa. Thus a dimer of RIG-I should be roughly 200 KDa, as should an MDA5 dimer, while a RIG-I/MDA5 with LGP2 dimer should be around 170 KDa. The results obtained are in

three sets, those precipitated for RIG-I, MDA5 and LGP2 and each set contains a control which is a boiled sample. Each precipitation/gel contains an unstimulated sample and CVB3 stimulations at 1, 2, 4 and 6 hours.

6.2: Results

6.2.1: MDA5 Homodimerisation

Cardiac cells were stimulated with CVB3 for 1, 2, 4, or 6 hours, or left unstimulated, and an MDA5 Goat pAb was used to precipitate MDA5 out of the cell lysate. The western blot results after incubating with MDA5 Rabbit pAb and detecting using polyclonal Swine anti-Rabbit Ig HRP are shown in Figure 6.1.

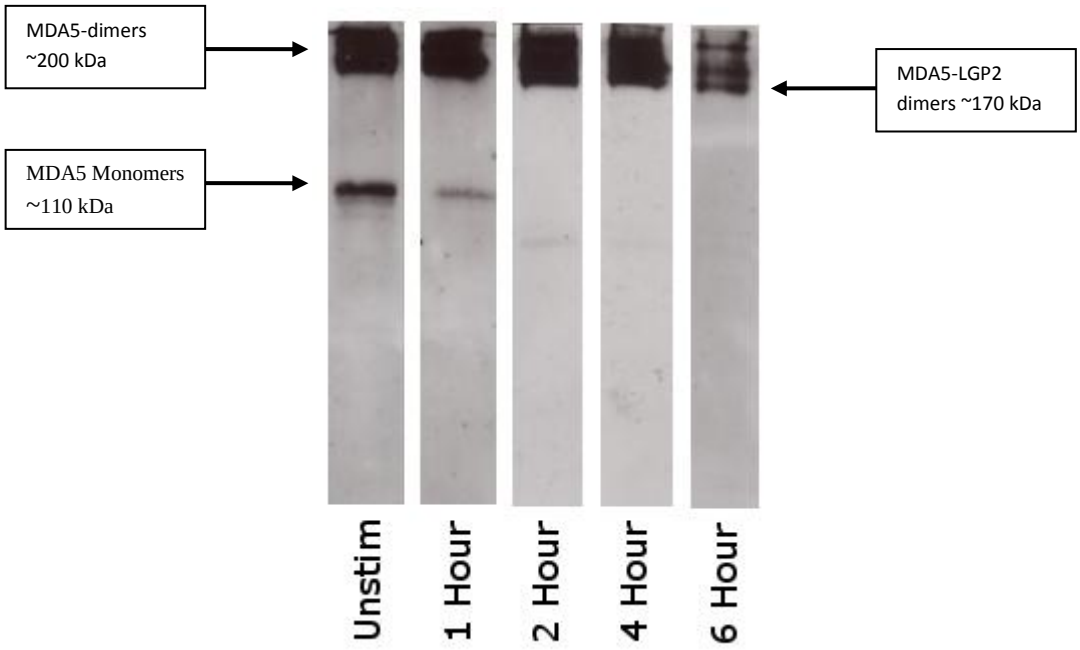

Figure 6.1 - Homodimerisation of MDA5. Cardiac cells were stimulated with CVB3 for 1, 2, 4, or 6 hours, or left unstimulated, and the cell lysate was pre-cleared twice with PAS beads. Incubation with MDA5 Goat pAb and PAS beads followed, to precipitate MDA5 out of the lysate. The resulting pellets were washed in lysis buffer and analysed using SDS-PAGE (using X2 SDS-PAGE Non-Reducing Sample Buffer) and western blotting with MDA5 Rabbit pAb primary antibody followed by polyclonal Swine anti-Rabbit Ig HRP. Enhanced chemiluminescence was used to visualise the protein bands. kDa: kiloDalton.

The gel where the cell lysate was precipitated for MDA5 and subsequent western blot performed for MDA5 shows bands around 200 kDa for all the time points suggesting that MDA5 does indeed form a dimer. There are also bands around 170kDa which could be an MDA5-LGP2 dimer as well as a band at around 110kDa which is most likely the MDA5 monomer.

As a control cardiac cells were stimulated with CVB3 for 1, 2, 4, or 6 hours, or left unstimulated, and an MDA5 Goat pAb was used to precipitate MDA5 out of the cell lysate. The samples were analysed via reducing conditions as a control to determine if the dimer could be disrupted. Western blot results after incubating with MDA5 Rabbit pAb and detecting using polyclonal Swine anti-Rabbit Ig HRP are shown in Figure 6.2.

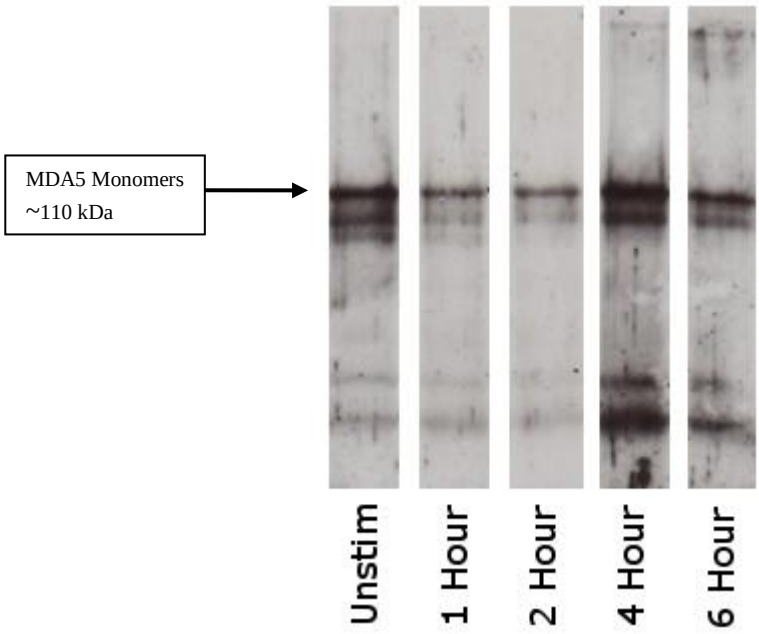

Figure 6.2 - Homodimerisation of MDA5 under reducing conditions. Cardiac cells were stimulated with CVB3 for 1, 2, 4, or 6 hours, or left unstimulated, and the cell lysate was pre-cleared twice with PAS beads. Incubation with MDA5 Goat pAb and PAS beads followed, to precipitate MDA5 out of the lysate. The resulting pellets were washed in lysis buffer and analysed using SDS-PAGE (using X2 SDS-PAGE -Reducing Sample Buffer) and western blotting with MDA5 Rabbit pAb primary antibody followed by polyclonal Swine anti-Rabbit Ig HRP. Enhanced chemiluminescence was used to visualise the protein bands. kDa: kiloDalton.

The data showed that the 200 kDa dimer was disrupted and broke down into monomers with a Mw of 110 kDa.

6.2.2: MDA5 – LGP2 Interactions

Western blotting was performed using a LGP2 Rabbit pAb followed by a polyclonal Swine anti-Rabbit Ig HRP (Figure 6.3). Faint higher bands approximately 170 kDa can be seen, possibly suggesting the presence of a MDA5- LGP2 dimer. A strong band of 60 kDa was also seen, which is most likely the LGP2 monomers.

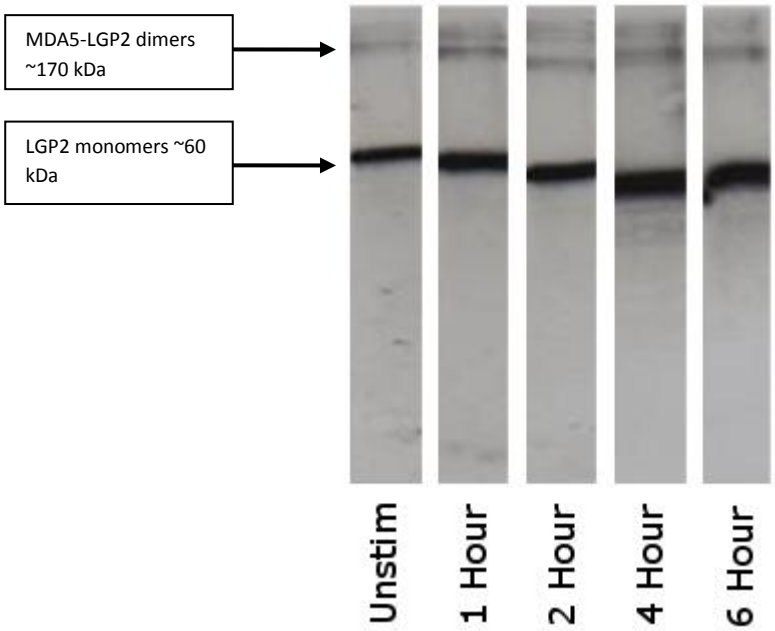

Figure 6.3 - Association between MDA5 and LGP2. Cardiac cells were stimulated with CVB3 for 1, 2, 4, or 6 hours, or left unstimulated, and the cell lysate was pre-cleared twice with PAS beads. Incubation with MDA5 Goat pAb and PAS beads followed, to precipitate MDA5 out of the lysate. The resulting pellets were washed in lysis buffer and analysed using SDS-PAGE (using X2 SDS-PAGE Non-Reducing Sample Buffer) and western blotting with LGP2 Rabbit pAb primary antibody followed by polyclonal Swine anti-Rabbit Ig HRP. Enhanced chemiluminescence was used to visualise the protein bands. kDa: kiloDalton

6.2.3: RIG-I Homodimerisation

Cardiac cells were stimulated with CVB3 for 1, 2, 4, or 6 hours, or left unstimulated, and a RIG-I Goat pAb was used to precipitate RIG-I out of the cell lysate. The western blot results after incubating with RIG-I Rabbit pAb and detecting using polyclonal Swine anti-Rabbit Ig HRP are shown in Figure 6.4. A boiled control using X2 SDS-PAGE Reducing Sample Buffer was performed to illustrate that reducing conditions disrupt protein structure (figure 6.5).

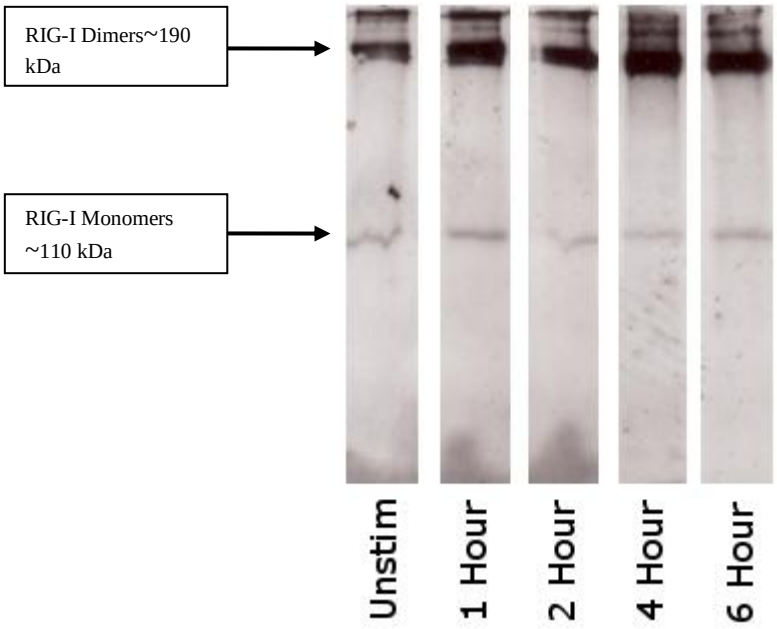

Figure 6.4 - Homodimerisation of RIG-I. Cardiac cells were stimulated with CVB3 for 1, 2, 4, or 6 hours, or left unstimulated, and the cell lysate was pre-cleared twice with PAS beads. Incubation with RIG-I Goat pAb and PAS beads followed, to precipitate RIG-I out of the lysate. The resulting pellets were washed in lysis buffer and analysed using SDS-PAGE (using X2 SDS-PAGE Non-Reducing Sample Buffer) and western blotting with RIG-I Rabbit pAb primary antibody followed by polyclonal Swine anti-Rabbit Ig HRP. Enhanced chemiluminescence was used to visualise the protein bands. kDa: kiloDalton.

In this instance it was shown that bands of around 190 kDa were present at all time points after stimulation with CVB3 suggesting the presence of a RIG-I dimer. RIG-I even appears to be a dimer in unstimulated cells, which is not consistent with a study performed by Cui *et al.*, 2008. A band at around 110 kDa showing RIG-I monomers can also be seen.

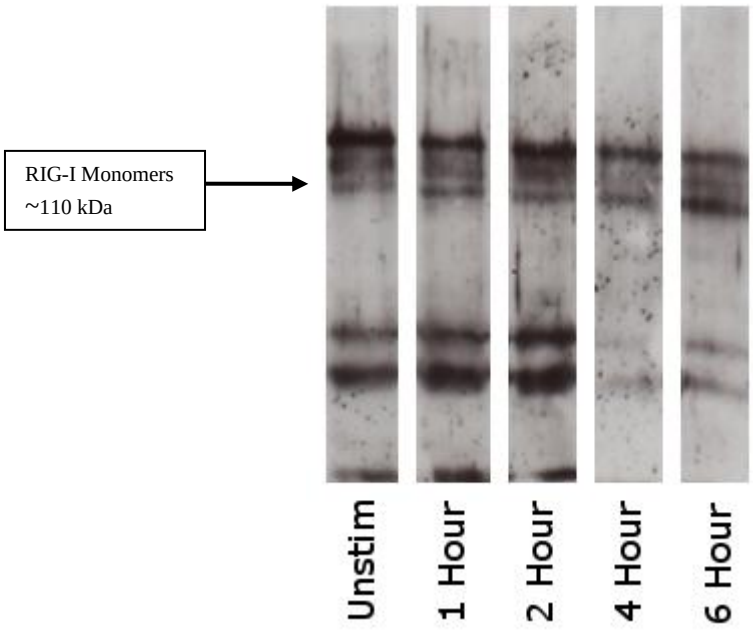

Figure 6.5 - Homodimerisation of RIG-I under reducing conditions.. Cardiac cells were stimulated with CVB3 for 1, 2, 4, or 6 hours, or left unstimulated, and the cell lysate was pre-cleared twice with PAS beads. Incubation with RIG-I Goat pAb and PAS beads followed, to precipitate RIG-I out of the lysate. The resulting pellets were washed in lysis buffer and analysed using SDS-PAGE (using X2 SDS-PAGE -Reducing Sample Buffer) and western blotting with RIG-I Rabbit pAb primary antibody followed by polyclonal Swine anti-Rabbit Ig HRP. A boiled control using X2 SDS-PAGE Reducing Sample Buffer was also performed. Enhanced chemiluminescence was used to visualise the protein bands. kDa: kiloDalton.

As expected under reducing conditions the RIG-I dimer is disrupted and we can detect RIG-I monomers as seen in Figure 6.5.

6.2.4: RIG-I – LGP2 Interactions

The association between LGP2 and RIG-I can be seen in Figure 6.6, showing the western blot results after incubating with LGP2 Rabbit pAb and detecting using polyclonal Swine anti-Rabbit Ig HRP.

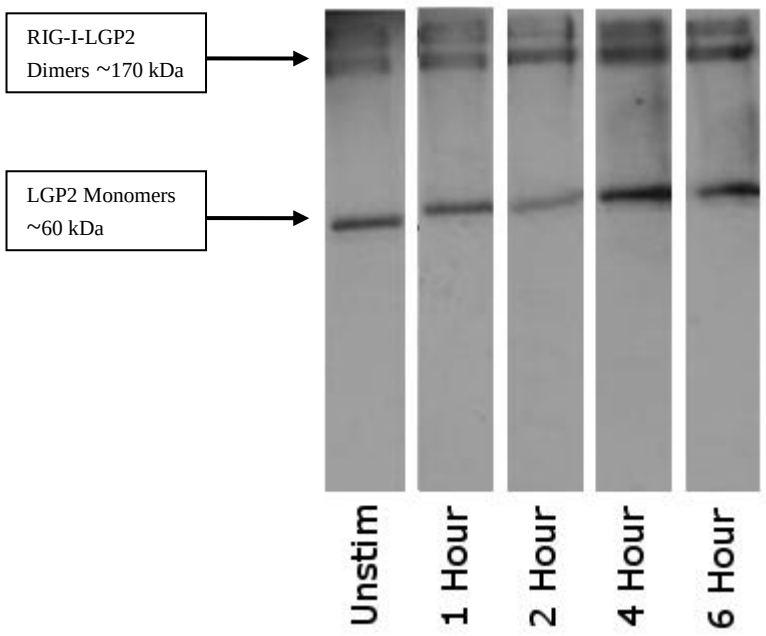

Figure 6.6 - Association between RIG-I and LGP2. Cardiac cells were stimulated with CVB3 for 1, 2, 4, or 6 hours, or left unstimulated, and the cell lysate was pre-cleared twice with PAS beads. Incubation with RIG-I Goat pAb and PAS beads followed, to precipitate RIG-I out of the lysate. The resulting pellets were washed in lysis buffer and analysed using SDS-PAGE (using X2 SDS-PAGE Non-Reducing Sample Buffer) and western blotting with LGP2 Rabbit pAb primary antibody followed by polyclonal Swine anti-Rabbit Ig HRP. Enhanced chemiluminescence was used to visualise the protein bands. kDa: kiloDalton.

The gel shows a band around 170 kDa which is the RIG-I –LGP2 heterodimer as well as a 60 kDa, which is an LGP2 monomer. Thus verifying LGP2 and RIG-I associations.

6.2.5: LGP2 Homodimerisation

In order to determine whether LGP2 also homodimerises, cardiac cells were stimulated with CVB3 for 1, 2, 4, or 6 hours, or left unstimulated, and an LGP2 Goat pAb was used to precipitate LGP2 out of the cell lysate. The western blot results after incubating with LGP2 Rabbit pAb and detecting using polyclonal Swine anti-Rabbit Ig HRP can be seen in Figure 6.7.

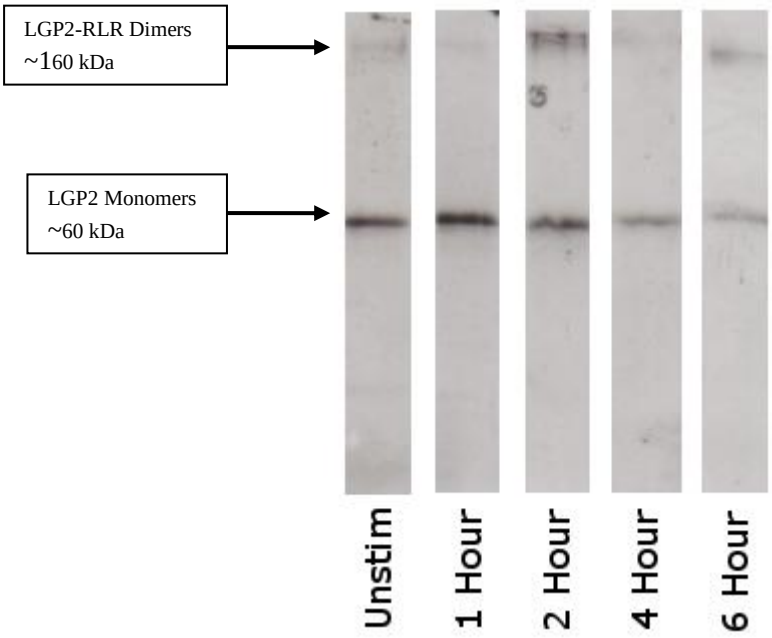

Figure 6.7 - Dimers and Monomers of LGP2. Cardiac cells were stimulated with CVB3 for 1, 2, 4, or 6 hours, or left unstimulated, and the cell lysate was pre-cleared twice with PAS beads. Incubation with LGP2 Goat pAb and PAS beads followed, to precipitate LGP2 out of the lysate. The resulting pellets were washed in lysis buffer and analysed using SDS-PAGE (using X2 SDS-PAGE Non-Reducing Sample Buffer) and western blotting with LGP2 Rabbit pAb primary antibody followed by polyclonal Swine anti-Rabbit Ig HRP. Enhanced chemiluminescence was used to visualise the protein bands. kDa: kiloDalton.

The results showed that there were two bands for each time point, one at around 170 kDa which is most likely an LGP2 heterodimer with either RIG-I or MDA5. The other band is around 60 kDa showing LGP2 monomers at all time points. It should be noted that while LGP2 appears to dimerise with RIG-I and MDA5 it clearly does not under these conditions homodimerise.

Samples were also run under reducing conditions see figure 6.8. The results showed that the LGP2-RLR heterodimer was disrupted under reducing conditions and broke down into monomers and smaller fragments.

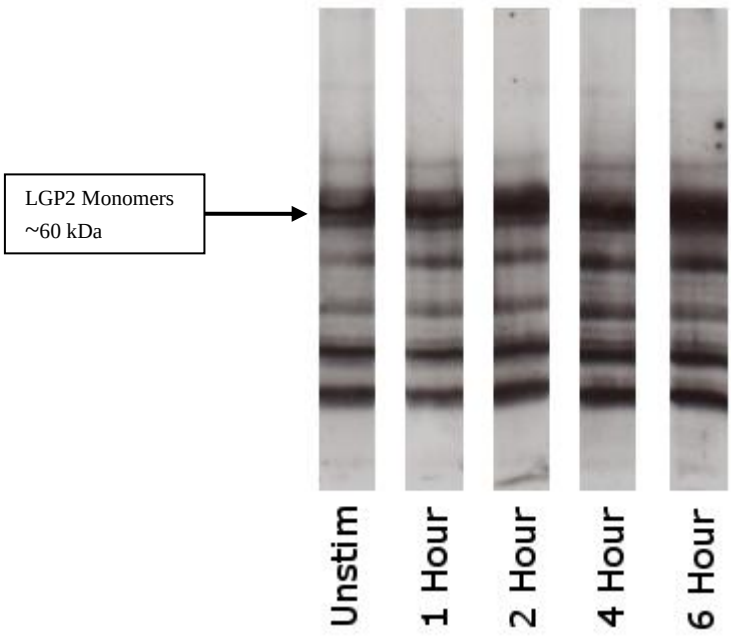

Figure 6.8 - Monomers of LGP2. Cardiac cells were stimulated with CVB3 for 1, 2, 4, or 6 hours, or left unstimulated, and the cell lysate was pre-cleared twice with PAS beads. Incubation with LGP2 Goat pAb and PAS beads followed, to precipitate LGP2 out of the lysate. The resulting pellets were washed in lysis buffer and analysed using SDS-PAGE (using X2 SDS-PAGE -Reducing Sample Buffer) and western blotting with LGP2 Rabbit pAb primary antibody followed by polyclonal Swine anti-Rabbit Ig HRP. Enhanced chemiluminescence was used to visualise the protein bands. kDa: kiloDalton.

6.2.6: LGP2 – MDA5 Interactions

Heterodimerisation between LGP2 and MDA5 appears to occur at all time points, indicated by the bands appearing near the 170 kDa mark. The bands around the 110 kDa mark imply that MDA5 monomers are also present. It seems that only a percentage of LGP2 is required to associate with MDA5, as MDA5 appears as a monomer as well. Treatment with SDS could have disrupted the bond between LGP2 and MDA5, thereby allowing the detection of MDA5 monomers.

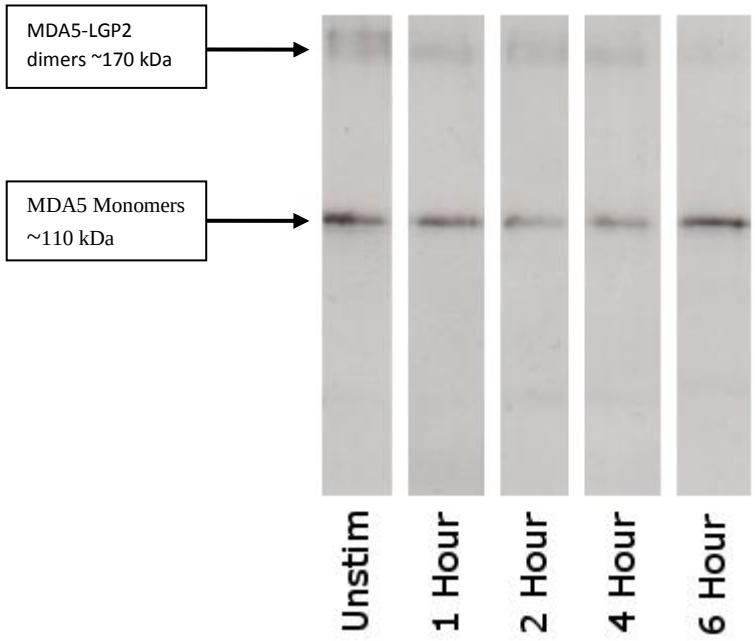

Figure 6.9 - Association between LGP2 and MDA5. Cardiac cells were stimulated with CVB3 for 1, 2, 4, or 6 hours, or left unstimulated, and the cell lysate was pre-cleared twice with PAS beads. Incubation with LGP2 Goat pAb and PAS beads followed, to precipitate LGP2 out of the lysate. The resulting pellets were washed in lysis buffer and analysed using SDS-PAGE (using X2 SDS-PAGE Non-Reducing Sample Buffer) and western blotting with MDA5 Rabbit pAb primary antibody followed by polyclonal Swine anti-Rabbit Ig HRP. Enhanced chemiluminescence was used to visualise the protein bands. kDa: kiloDalton.

6.2.7: LGP2 – RIG-I Interactions

Similarly, heterodimerisation between LGP2 and RIG-I can be seen at all time points, indicated by the top bands near the 170 kDa mark. Monomers of RIG-I can also be seen, as indicated by the bands around the 110 kDa mark.

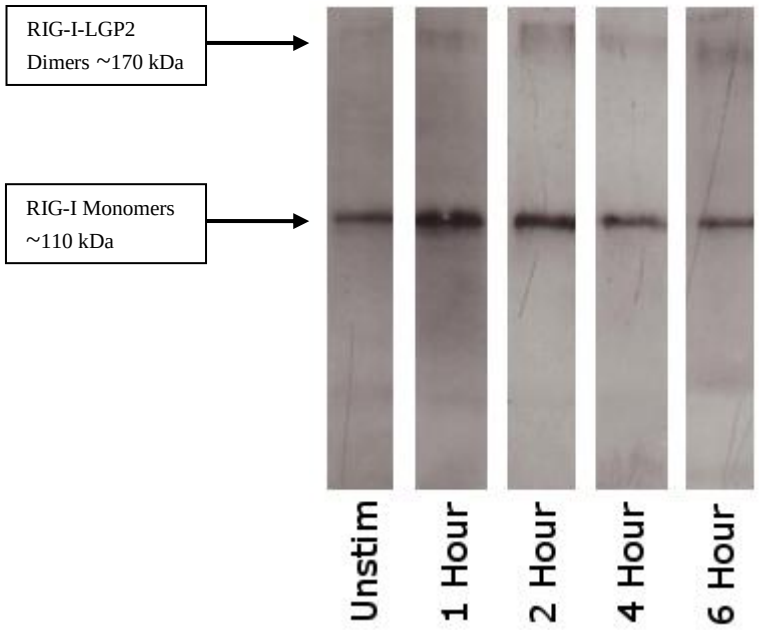

Figure 6.10 - Association between LGP2 and RIG-I. Cardiac cells were stimulated with CBV3 for 1, 2, 4, or 6 hours, or left unstimulated, and the cell lysate was pre-cleared twice with PAS beads. Incubation with LGP2 Goat pAb and PAS beads followed, to precipitate LGP2 out of the lysate. The resulting pellets were washed in lysis buffer and analysed using SDS-PAGE (using X2 SDS-PAGE Non-Reducing Sample Buffer) and western blotting with RIG-I Rabbit pAb primary antibody followed by polyclonal Swine anti-Rabbit Ig HRP. Enhanced chemiluminescence was used to visualise the protein bands. kDa: kiloDalton.

6.3: Discussion

Both MDA5 and RIG-I are capable of forming homodimers as well as heterodimers with LGP2. It would appear that in the native state both RIG-I and MDA5 form heterodimers with LGP2, possibly to prevent signalling without the presence of a pathogen. Upon CVB3 infection the MDA5-LGP2 dimer no longer occurs and an MDA5-MDA5 homodimer forms that can cause a signalling cascade. As RIG-I does not recognise the virus it remains as a heterodimer with LGP2 at all time points and does not form a homodimer. It should be noted that there is no evidence of LGP2 forming a homodimer. There also does not appear to be any cleavage of the RLRs even at the 6 hour time point.

The function and mechanism of LGP2 in innate immunity is still puzzling. So far, it is known that the LGP2 RD can regulate RIG-I and MDA5-dependent signalling. This study aimed to determine whether the RLRs dimerise. It can be seen that RIG-I and MDA5 exist primarily as homodimers, but also as monomers, in cardiac cells, whilst LGP2 exists as a monomer. RIG-I and MDA5 can also heterodimerise with a percentage of LGP2. The perplexing question is that although heterodimers between LGP2 and RIG-I or MDA5 are present in the LGP2 immunoprecipitations, in the MDA5 or RIG-I immunoprecipitations, LGP2 presence is only detected as a monomer. These results could be due to the higher affinity of the LGP2 RD with the other RLRs, enabling it to bind and precipitate RIG-I or MDA5, whereas MDA5 or RIG-I have a lower affinity, and may therefore not be able to bind a detectable percentage of higher LGP2 aggregates.

There are both advantages and disadvantages to using immunoprecipitation in order to determine interaction between two molecules. The proteins pulled through will be in

their native state and concentration and due to the small quantities of protein involved, procedures such as mass spectrometry are not possible. Western blotting is highly specific so still gives an exact result as to whether the two proteins interact. The downside is that it only detects stable interactions and does not elucidate whether the interactions are direct or whether other proteins have been pulled through in the complex. However, by working out the Rf (relative mobility) of the proteins it is possible to determine the molecular weight of the complex and this determine the likely components. In order to make sure unspecific binding to the sepharose beads was not occuring pre-clears were performed and removes the posibility of non-specific binding to the beads.

It still needs to be determined whether these are direct interactions occuring. Due to the molecular weights being detected it would seem likely however other small moleculaes may be in the complex and aid interaction between the RLRs. An interesting route for further study would be to determine the specific proteins in the complex precipitated and to explore the nature of interaction between the RLRs.

Overall, this study concludes that LGP2 and RIG-I or MDA5 associate in cardiac cells, and that there is a synergistic mechanism of RLR association for viral detection.

CHAPTER 7: DISCUSSION

Coxsackieviruses can cause serious infection particularly in children leading to severe inflammatory disorders of the heart, pancreas and CNS. The main disorders associated with CVB3 are myocarditis, pancreatitis, aseptic meningitis and encephalitis as well as complications that can occur such as myocarditis leading to chronic dilated cardiomyopathy in persistent infections [12;339]. Myocarditis occurs due to persistent infection causing an immune response that damages the cells, with lesions that occur on the heart tissue being due to viral lesion and the immune response [340]. Pancreatitis is similarly caused by both the viral factors and the hosts immune response [341]. Understanding the immune response therefore is crucial to developing a way of preventing the damage caused by the host immune response, as well as clearing the infection.

The immune system, consisting of two main branches of immunity (innate and acquired), defends the human body against invading pathogens. Innate immunity is the first line of defence against pathogens, and responds rapidly to invading microbes. It does this via pattern recognition receptors (PRRs) which can distinguish self from non-self, and recognise certain microbial components, termed pathogen-associated molecular patterns (PAMPs), to initiate an appropriate immune response. Recognition of PAMPs by PRRs leads to the rapid activation of latent transcription factors (such as NF-κB and IRF3) to stimulate the expression of antimicrobial genes and the production of type I interferons (IFN) [342].

The Toll-like receptors (TLRs) are an important class of PPRs. The 13 currently known members within the TLR family recognise a wide range of different PAMPs, and

initiate appropriate downstream signalling (via two different pathways: the MyD88-dependent pathway; and the MyD88-independent (TRIF-dependent) pathway) to activate the innate and adaptive immune response. Several TLRs are important for the recognition of different viruses, including TLR2, TLR3, TLR4, TLR7/8, and TLR9.

Along with the TLRs, several new TLR-independent PRRs have been discovered, including the Retinoic-acid Inducible Gene-I (RIG-I)-Like Receptor (RLR) family. There are three known members: RIG-I [343], Melanoma Differentiation-Associated gene 5 (MDA5) [344], and Laboratory of Genetics and Physiology 2 (LGP2) [345]. The RLRs detect cytoplasmic viral RNA during viral replication, and preferentially recognise different viruses, triggering the host's Interferon response.

RIG-I has been shown to detect a number of both positive and negative stranded viruses, as well as several different viral PAMPs, whilst MDA5 has been shown to be critical for Picornaviridae detection, including CVB3. Despite the wealth of research on identifying the RLR ligands, the precise PAMPs recognised by each RLR are, as yet, still undetermined.

The structure of Coxsackieviruses is relatively simple, consisting of a viral capsid containing the single positive stranded RNA genome [346]. The nucleic acid takes on several forms throughout the viral life cycle.

The native state of the RNA genome is a single stranded positive sense RNA and therefore would most likely to be recognised by TLRs 7 or 8 and RIG-I [108;109;347;348]. However for RIG-I, the all important 5'ppp group at the end of the ssRNA is replaced or blocked by the CVB3 VPg [349;350]. There is evidence that the VPg molecule can be removed by the hosts "unlinking enzyme" so RIG-Is involvement

cannot be ruled out completely. TLR 7 and 8 have already been shown to be crucial in CVB3 mediated inflammatory response in the myocardium by Triantafilou *et al* [351].

Two forms of dsRNA are also present during the CVB3 life cycle. The first is the replicative intermediate (RI), a positive sense ssRNA to which 6 to 8 nascent negative strands are attached, which form double stranded sections where the main full length RNA and nascent chains join. VPg molecules are usually found on the end of the nascent chains so the RI is unlikely to be recognised by RIG-I. The second form is the replicative form (RF), a dsRNA intermediate with one full copy of both a positive and negative chain attached [352;353]. The RF seems the most likely ligand in CVB3 for MDA5 recognition. Finberg *et al* [354] showed the importance of MDA5 and the RLR adaptor molecule MAVS in the Type I IFN response to CVB3 in mice but did not reveal the specific RNA structure which MDA5 recognises.

It has been shown that RIG-I recognizes single-stranded RNA (ssRNA) containing a terminal 5 -triphosphate (ppp), as well as linear dsRNA no longer than 23 nucleotides. MDA5 recognition is less clear, since it does not sense viral genomic ssRNA. It seems to recognise long strands of dsRNA but the mechanism by which this occurs has not been revealed. Pichlmair *et al* [289] using mainly biochemical methods had suggested that MDA5 senses high order structured RNA containing ssRNA and dsRNA, however that fails to explain why MDA5 can sense Poly:I:C, which is a synthetic long dsRNA or dsRNA viruses such as Reoviruses [286] or why it cannot sense Picornavirus genomic ssRNA that contains highly ordered secondary structures and tertiary RNA structures in the 3’ and 5’UTR regions. The inherent problem with the study by Pichlmair *et al* is that they rely on immunoprecipitations with a dsRNA-specific antibody in order to isolate RNA/MDA5 complexes. Using this method they demonstrated that infected cells

contained not only dsRNA but also ssRNA of high molecular weight, which was found to be immunostimulatory. The problem is that such biochemical isolations rely exclusively on the specificity of the antibody used and they are prone to artefactual associations. Under these conditions, weak or transient receptor-ligand associations might be lost and artefactual associations might be retained. Therefore although Pichlmair *et al* have given us a clue on what the MDA5 ligand might be, by saying that it is most likely an RNA web rather than simply long molecules of dsRNA, they have left us with a lot of questions regarding the exact MDA5 ligand.

In this regard, this project aims to enhance the current knowledge on whether the RNA helicase RIG-I or MDA5 is the primary detector of Coxsackieviruses. Is it simply the double stranded structure of the RNA or are there other structures within the RNA that are required for recognition? How important a role does MDA5 play in the immune response to CAV9 and CVB3? Does RIG-I play any role in Coxsackievirus recognition? Do the RLRs oligomerise or co-localise with the virus during infection?

The goal of the present study was to determine whether RIG-I or MDA5 participate in the induction of type I IFN in response to Coxsackievirus infection and to determine the specific RNA ligand that was recognized and activated these sensors using non-invasive methods.

Coxsackieviruses Group A (CAV) and Group B (CVB) are positive ssRNA viruses therefore in addition to their ssRNA genome there are also substantial amounts of cytosolic dsRNA produced during the replicative life cycle of these positive ssRNA viruses. Thus during a CAV or CVB infection, there is a pool of viral RNA that trigger the host's innate immune response, raising the question of which viral RNA species is responsible for MDA5 activation. In this study, for the first time, viral ssRNA as well as

the replicative intermediate dsRNA (RF) and the high order replicative intermediate (RI), which is basically a dsRNA RF with a nascent ssRNA viral strand, were isolated.

A negative ssRNA virus such as Influenza A virus was also used as a control since it is well established that RIG-I acts as a sensor triggering interferon production in the presence of negative ssRNA virus such as Influenza A virus [285].

The experiments showed that there was no interaction of MDA5 with the positive sense genomic ssRNA. However MDA5 recognised the dsRNA produced during the CVA and CVB replication as well as RI-RNA which has a dsRNA core, highlighting the importance of dsRNA in MDA5 recognition. Using fluorescent imaging methods, the association of MDA5 with the replicative form of enteroviruses was visualised. This is the first report of the visualization of dsRNA and MDA5, which provides unique evidence between the relationship of viral dsRNA and MDA5 and proves without a doubt that the dsRNA replicative intermediate form of positive sense ssRNA viruses is the effective agonist recognised by MDA5.

Furthermore when synthetic dsRNA was used with either 5'OH ends or 5' ppp ends they both elicited IFNα/β response, however dsRNA with 5'OH ends was more immunostimulatory in HEK/MDA5 cells revealing that MDA5 could have a higher affinity for 5'OH dsRNA.

It seems that MDA5 is an essential sensor of the innate response that unlike TLRs or RIG-I is not involved in the initial steps of ssRNA viral infection but detects and activates the interferon response only when the RNA viruses begin to replicate generating replicative intermediates thus posing a threat for the host cell.

A very recent study by Peisley *et al* supports our findings of dsRNA viral recognition by MDA5. This study revealed the MDA5 mechanism of ligand recognition. They have shown MDA5 assembly into oligomers composed of segmental arrangement of MDA5 dimers along the length of dsRNA [355]. They propose a role of ATP hydrolysis as a conformational switch for MDA5 activation and signalling.

These new insights should pave the way for the development of future antiviral therapeutics. An increased understanding of the complex mechanisms of viral host defence will eventually helps us design new targets for viral infections.

To verify these findings Huh7 and Huh7.5.1 cells were used to determine the role of RIG-I in infection by CVB3. Huh7.5.1 have a mutation within the RIG-I gene so the RIG-I pathway is inactive in the cell line. Huh7 have a working RIG-I pathway and both Huh7 and Huh7.5.1 cells have an otherwise full active set of PRRs including functional MDA5.

CBV3 ssRNA and dsRNA as well as synthetic dsRNA poly(I:C) was used to stimulate Huh cells. What is clear from this data is that despite RIG-Is ability to recognise Influenza ssRNA and create an immune response it can't recognise CVB3 ssRNA or dsRNA. This confirms that RIG-I does not contribute in the IFNα/β host response during an infection with Picornaviridae.

Pattern recognition receptors have a well established tendency towards forming dimeric or oligomeric structures within the cell, both in hetero and homo form. TLRs form homodimers, with the exception of TLR2 which forms a heterodimer with either TLR1 or TLR6, to create a strong signalling platform to recruit MyD88, TRIF, TRAM and TIRAP [108]. Recruitment and dimerisation both occur through the TIR domain on the TLRs and downstream molecules. It is the binding of their ligand that causes

dimerisation of TLRs and brings together the TIR domains creating a stable platform for interaction with downstream factors [116].

NLRs form larger oligomeric structures called inflammasomes with other molecules such as ASC, binding through PYDs or CARDs depending on the NLR. As with TLRs, binding their ligands causes conformational changes in NLRs resulting in the nuclear binding domain becoming available for ATP or NTP binding which in turn frees the CARD/PYD for oligomerisation [356].

In the RLR pathway both RIG-I and MDA5 form complexes with MAVS through their CARD domains and MAVS has been shown to form a homodimer, again through the CARD domain [357]. As with TLRs and NLRs binding of the RLRs to their ligands causes conformational change and this releases the CARD domains for homotypic interactions with other CARD domains [358;359].

While CARD-CARD interactions have been shown for RLRs with MAVS, there is little in terms of evidence as to dimers or oligomers forming between the RLRs. Homodimers (or oligomers) in CARD containing receptors has already been shown to be possible through the NLR inflammasomes and MAVS. And in many PRRs dimerisation has been shown to be a crucial step in creating a stable signalling platform for downstream signalling upon ligand binding. Therefore it would seem likely that once the RLRs have bound their specific PAMP a dimer would form and create a binding platform for MAVS and perhaps other signalling accessory molecules as well. As well as homodimers, as can be seen through TLR2, it may also be possible for heterodimers between the RLRs to occur.

Immunoprecipitation was used to determine whether the RLRs formed complexes with themselves or other the RLRs by precipitating for a particular RLR and then running the

precipitate through gel electrophoresis and probing for either the same RLR or a different one. If MDA5 or RIG-I forms a homodimer then a band will appear at approximately twice the known molecular weight of that RLR, while a heterodimer with LGP2 would form a band at a slightly lower molecular weight as LGP2 has a lower molecular weight.

The results showed clearly that for MDA5, a heterodimer with LGP2 exists in the unstimulated state. Upon infection with CVB3 this heterodimer disappears and is replaced by an MDA5 homodimer. RIG-I differs to MDA5 in that while it forms a heterodimer with LGP2, this does not disappear upon CVB3 infection. There is also some evidence that RIG-I is capable of forming a homodimer, however it appears that the RIG-I-LGP2 dimer predominates. Precipitates for LGP2 show that while LGP2 can form a dimer with RIG-I and MDA5, it does not appear to homodimerise.

Through this data it can be proposed that LGP2 is bound to both RIG-I and MDA5 in an inactive state, perhaps keeping them inactive as negative regulation in the absence of infection. With the presence of a ligand LGP2 releases the RLR (in this case MDA5 in the presence of CVB3 dsRNA) allowing it to homodimerise and form a signalling platform through which it can interact with MAVS and initiate an immune response. As LGP2 does not contain a CARD domain it must dimerise using a different method and could suggest that the same is true of RIG-I and MDA5 allowing the CARDs to remain free for MAVS binding. Further work needs to be carried out to determine the exact nature of the dimers being formed.

Overall it can be seen that MDA5 forms a crucial part of the innate immune response to CVB3 alongside the TLRs and NLRs. The idea of a trinity of PRRs seems very valid in the case of CVB3 infection with MDA5 being crucial in the Type- IFN response, while

TLRs 4, and 7/8 are responsible for the main cytokine response and TLR3 for part of the Type-I IFN response and also the Type-II IFN response. The NLRs respond by inducing caspase-1 to cleave molecules such as Pro-IL-1β into IL-1β creating a further step in the immune response. CVB3 requires a complement of PRRs from the 3 family members of the trinity to create a full immune response.

This study has clearly shown that of the RLRs it is MDA5 that responds to and recognises CVB3. It has also shown that MDA5 specifically binds to the dsRNA of CVB3 that is formed during viral replication and known as the Replicative Form. End structures such as the 5'ppp group preferred as a ligand by RIG-I are not favoured by MDA5 and it is most likely that the most crucial structural factor in MDA5 binding is the presence of long double stranded RNA. There is also clear evidence to suggest that LGP2 acts in a regulatory role by forming a dimer with RIG-I or MDA5 in a cells natural state and releases them upon ligand binding allowing signalling activation.

Further work to be carried out include deterining the exact way in which the RLRs dimerise. If LGP2 does not contain a CARD region nthen how does it dimerise with MDA5 and RIG-I? Are there other molecules that form a part of the receptor complex and would it be possible to run further tests on precipitate to determine the exact contents and the proteins present? It would also be of great interest to determine MDA5s role within myocarditis. In a disease where the damage contributation largely comes from presistant inflmmation would preventing MDA5 from binding CVB or the dsRNA intermediate alleviate some of the damage caused by the infection? Or would it simply prevent viral recognition and inhibit the immune response from protecting the host from the virus. Mouse models could be a fascinating step forward in understanding MDA5s role in disease.

Recognition of CVB by TLRs and RLRs is becoming well understood, but to better understand the relationship between the PRRs in creating an innate immune response, CVB3s recognition by NLRs should be explored.

A model can be suggested where Coxsackieviruses infect the host cell by inserting positive-sense ssRNA into the cytoplasm. During replication of its RNA a dsRNA intermediate occurs that acts as a ligand for MDA5. MDA5 in an inactive heterodimer with LGP2 undergoes a conformational change once bound to the dsRNA intermediate and is released from LGP2, allowing it form a homodimer. This creates a stable platform for the recruitment of MAVS and further downstream signalling to occur leading to the expression of Type-I IFNs and the expression of ISGs. Along with the response from TLRs and NLRs this forms crucial part of the innate immune response to Coxsackieviruses.

CHAPTER 8: APPENDIX

X10 PBS

- 100 g NaCl
- 2.5 g KCl
- 14.4 g Na_2HPO_4 (or 18.0 g $Na_2HPO_4\,2H_2O$)
- 2.5 g KH_2PO_4
- Add distilled water to 1000 ml

For PBS Tween add 10 ml of Tween 20 and rinse tip in buffer.

X1 PBS

- 50 ml from X10 stock
- Raise to 500 ml with distilled water (add 450 ml).

X2 PBS

- 100 ml from X10 stock
- Raise to 500 ml with distilled water (add 400 ml).

4% PFA

- 8.0 g of formaldehyde to 80ml distilled water
- Heat to 60°C in fume hood
- Add a few drops of 1 M NaOH to help dissolve (until clear).
- Top up to 100 ml with distilled water.
- Once the solid has dissolved, cool to RT and add 100 ml of X2 PBS.

X1 PBS/0.02%BSA/0.02%NaN_3/0.02%saponin

- 0.02% = 0.02g in 100 ml
- In 500 ml 0.1 needed.
- 0.1 g of each added to 500 ml (sodium azide, saponin and albumin bovine serum)

10% SDS

- 10 g SDS
- In 100 ml of distilled water

0.5 M Tris-HCl pH 6.8 (500 ml)

- 30.28 g Tris
- 500 ml distilled water
- pH to 6.8 using concentrated HCl

1.5 M Tris-HCl pH 8.8 (500 ml)

- 90.85 g Tris
- 500 ml distilled water
- pH to 8.8 using concentrated HCl

X2 Reducing sample buffer

- For 40 ml use 20 ml 0.5 M Tris pH 6.8
- 16 ml 10% SDS
- 10 g Glycerol
- 4ml 14.3 M β-mercaptoethanol
- Small spatula full of bromophenol blue

10% Resolving Gel (for 2 gels)

- 4.02 ml distilled water
- 2.5 ml 1.5 M Tris-HCl pH 8.8
- 100 µl 10% SDS
- 3.33 ml acrylamide/bis (wear gloves)

To polymerise add:

- 50 µl 10% APS
- 5 µl TEMED

4% Stacking Gel (for 2 gels)

- 6.1 ml distilled water
- 2.5 ml 0.5 M Tris-HCl pH 6.8
- 100 µl 10% SDS
- 1.3 ml acrylamide/bis

To polymerise add:

- 100 µl 10% APS
- 30 µl TEMED

X2 Transfer buffer

- 4.88 g Tris
- 20 ml 10% SDS
- 400ml isopropanol
- pH to 8.3 with acetic acid
- Make up to 1000 ml distilled water

Running Buffer

- 100 ml x10 Running buffer
- Make up to 1000 ml with distilled water

PBS Tween (2 litres)

- 200 ml x10 PBS in 1000 ml beaker.
- Top up to 1000 ml with distilled water.
- Add 2 ml of PBS Tween 20, dropping the tips into the PBS and using magnetic stirrer until mixed.
- Decant 500 ml into another 1000 ml beaker and top both up to 1000 ml.

Blocking Reagent

- 2 g Milk powder
- In 40 ml PBS Tween

Stripping Buffer

- 1.4 ml Mercaptoethanol (10 0mM)
- 40 ml 10% SDS (2%)
- 1.52 g Tris-HCl (62.5 mM) pH 6.7
- Top up to 200 ml with PBS-Tween.

NET Buffer (100 ml) pH 8.0

- 6.056 g Tris-HCl (500 mM)
- 8.768 g NaCl (1.5 M)
- 1.86 g EDTA (50 mM)
- Make up to 100 ml with dH_2O

10mM Iodoacetamide (50ml)

- 92.5mg (0.0925g) in 50ml dH_2O

10% (w/v) NP-40 (50 ml)

- 5 g in 50 ml dH_2O

PMSF Stock (100 ml)

- 1.74 g PMSF in 100 ml ethanol

Lysis Buffer (50 ml)

- 5 ml NET buffer
- 500 µl Iodoacetamide
- 5 ml NP-40
- 25 µl PMSF
- 2 Protease Tablets (We used 20 µl protease inhibitor)
- Make up to 50 ml with dH_2O.

Protein A – Sepharose

- 0.1 g in 1ml lysis buffer
- Leave for atleast one hour to swell or overnight (in fridge).

X2 Non-Reducing Sample Buffer

- 20 ml 0.5 M Tris pH 6.8
- 16 ml 10% SDS
- 10 g Glycerol
- Small spatula full of bromophenol blue

Lysis buffer for RNA Extraction

- 1.5 g TrisHCl (50 mM)
- 2.0 g NaCl (140 mM)
- 0.074 g $MgCl_2$ (1.5 mM)
- 1.25 ml V/V NP4O (0.5%)
- In 250 ml distilled water.
- pH to 8.0

Digestion buffer for T1 enzyme

- 50 mM TrisHCl – 0.6 g
- 1 mM EDTA - 0.037 g
- In 100 ml dH_2O
- pH 7.5

8.1: Abbreviations:

5'ppp - 5'triphosphate

AIM2 - Absent in Melanoma-2

AP - Alkaline Phosphatase

ASC - Apoptosis-associated Speck-like protein containing CARD

BDV - Borna Disease Virus

BIR - Baculovirus Inhibitor Repeat

CAR - Coxsackie-Adenovirus Receptor

CARD - Caspase Recruitment Domain

CBA - Cytometric Bead Array

CCHFV - Crimean Congo Hemorrhagic Gever Virus

CHO - Chinese Hamster Ovary

CNS - Central Nervous System

CT - C-Terminal

CTD - D-terminal Domain

CVA - Coxsackievirus A

CVB - Coxsackievirus B

DAF - Decay Accelerating Factor

DAMP - Danger Associated Molecular Pattern

DAP - Diaminopimelic Acid

DC - Dendritic Cell

DD - Death Domain

dsRNA - double stranded RNA

ECL - Electrochemiluminescence

EMCV - Ecephalomyocarditis virus

ER - Endoplasmic Reticulum

ERK - Extracellular signal Related Kinases

FADD - Fas-Associated Death Domain

FCS - Fetal Calf Serum

FITC - Fluorescein Isothiocyanate

HCV - Hepatitis Virus C

HEK - Human Embryonic Kidney

HRP - Horseradish Peroxidase

HTNV - Hantaan Virus

HUH - Human Hepatocellular

IFN - Interferon

IFVA - Influenzavirus A

IG - Immunoglobulin

IL - Interleukin

IKK - IκB Kinase

IRAK - IL-1 Receptor-Associated Kinase

IRF - Interferon Regulatory Factor

ISG - Interferon-induced Genes

JNK - Jun Kinases

kDa - kiloDalton

LGP2 - Lboratory of Genetics and Physiology 2

LLC - Lewis Lung Carcinoma

LPS - Lipopolysaccharide

LRR - Leucine Rich Repeats

LTA - Lipotechoic Acid

MAPK - Mitogen Activated Protein kinase

MAVS - Mitochondrial AntiViral Signalling

MDA5 - Melanoma Differentiation Associated-gene 5

MDP - Muramyl Dipeptide

MHC - Major Histocompatibility Complex

MyD88 - Myeloid Differentiation primary response gene-88

NBD - Nucleotide Binding Domain

NDV - Newcastle Disease Virus

NEMO - NF-κB Essential Modulator

NF-κB - Nuclear Factor kappa-light-chain enhancer of activated B cells

NLR - Nod-Like Receptor

NOD - Nucleotide-binding Oligomerisation Domain-containing

NT - N-Terminal

P-IκB - phospho-IκB

PAMP - Pathogen Associated Molecular Pattern

PAS - Protein A Sepharose

PBS - Phosphate Buffered Saline

PE - Phycoerythrin

PKR - Protein Kinase R

PMT - Photomultiplier Tube

PRR - Pattern Recognition Receptor

PYD - Pyrin Domain

RD - Rhabdo-myosarcoma or Regulatory Domain

RF - Replicative Form (dsRNA)

RI - Replicative Intermediate (dsRNA)

RIG-I - Retinoic-acid Inducible Gene-I

RIP - Receptor-Interacting Protein

RLR - RIG-Like Receptor

ROS - Reactive Oxygen Species

RSV - Respiratory Syncitial Virus

RT - Room Temperature

SCR - Short Consensus Repeats

SDS-PAGE - Sodium Dodecyl Sulphate Polyacrylamide Gel Electrophoresis

SEAP - Secreted Embryonic Alkaline Phosphatase

SeV - Sendai Virus

ssRNA - single stranded RNA

STING - Stimulator of Interferon Genes

T-IκB - Total-IκB

TAK - TGF-β Activated Kinase

TBK - TANK-Binding Kinase

TC - Tissue Culture

TIM - TRAF Interacting Motif

TIR - Toll-Interleukin-1 Receptor

TIRAP - TIR-domain containing Adaptor Protein

TLR - Toll-Like Receptor

TNF - Tumour Necrosis Factor

TRADD - TNFR-Associated Death Domain

TRAF - TNF Receptor Associated Factor

TRAM - TRIF Related Adaptor Molecule

TRIF - TIR domain-containing adaptor-inducing Interferon β

UPS - Ubiquitin/Proteosome Sytem

VP - Viral Protein

VPg - Viral Protein genome-linked

VSV - Vesicular Stomatitis Virus

wt - Wild Type

References

1. Rahman, M. Introduction to Flow Cytometry. http://www.abdserotec.com/uploads/Flow-Cytometry.pdf . 1-3-2006. 20-4-2012.

2. Kerestes, A. J. Coxsackievirus. http://maptest.rutgers.edu/drupal/?q=node/449 . 5-5-2011. 16-7-0012.

3. Manavalan,B., Basith,S. & Choi,S. (2011) Similar Structures but Different Roles - An Updated Perspective on TLR Structures *Front Physiol* **2,** 41.

4. Semwoerere, D. and Weeks, E. R. Confocal Microscopy. Encyclopedia of Biomaterials and Biomedical Engineering. http://www.physics.emory.edu/~weeks/lab/papers/ebbe05.pdf . 2005. 20-4-2012.

5. Dalldorf,G. & Sickles,G.M. (1948) An Unidentified, Filtrable Agent Isolated From the Feces of Children With Paralysis *Science* **108,** 61-62.

6. Tracy,S., Chapman,N.M., Romero,J. & Ramsingh,A.I. (1996) Genetics of coxsackievirus B cardiovirulence and inflammatory heart muscle disease *Trends in Microbiology* **4,** 175-179.

7. Tracy,S., Chapman,N.M., Romero,J. & Ramsingh,A.I. (1996) Genetics of coxsackievirus B cardiovirulence and inflammatory heart muscle disease *Trends in Microbiology* **4,** 175-179.

8. MELNICK,J.L., SHAW,E.W. & CURNEN,E.C. (1949) A virus isolated from patients diagnosed as non-paralytic poliomyelitis or aseptic meningitis *Proc. Soc. Exp. Biol. Med.* **71,** 344-349.

9. Knipe,D.M. & Howley,P.M. (2006) *Fields Virology*. Lippincott Williams and Wilkins.

10. Romero,J.R. (2008) Pediatric group B coxsackievirus infections *Group B Coxsackieviruses* **323,** 223-239.

11. Knipe,D.M. & Howley,P.M. (2006) *Fields Virology*. Lippincott Williams and Wilkins.

12. Kaplan,M.H., Klein,S.W., McPhee,J. & Harper,R.G. (1983) Group B Coxsackieviruses infections in infants younger than three months of age: A serious childhood illness. *Rev. Infect. Dis.* **5,** 1019-1032.

13. Daley,A.J., Isaacs,D., Dwyer,D.E. & Gilbert,G.L. (1998) A cluster of cases of neonatal coxsackievirus B meningitis and myocarditis *Journal of Paediatrics and Child Health* **34,** 196-198.

14. Bowles,N.E., Richardson,P.J., Olsen,E.G.J. & Archard,L.C. (1986) Detection of Coxsackie-B-Virus-Specific Rna Sequences in Myocardial Biopsy Samples

from Patients with Myocarditis and Dilated Cardiomyopathy *Lancet* **1,** 1120-1124.

15. Tracy,S., Chapman,N.M., Romero,J. & Ramsingh,A.I. (1996) Genetics of coxsackievirus B cardiovirulence and inflammatory heart muscle disease *Trends in Microbiology* **4,** 175-179.

16. Ukimura,A. et al. (1997) Intracellular viral localization in murine coxsackievirus-B3 myocarditis - Ultrastructural study by electron microscopic in situ hybridization *American Journal of Pathology* **150,** 2061-2074.

17. Knipe,D.M. & Howley,P.M. (2006) *Fields Virology*. Lippincott Williams and Wilkins.

18. Daley,A.J., Isaacs,D., Dwyer,D.E. & Gilbert,G.L. (1998) A cluster of cases of neonatal coxsackievirus B meningitis and myocarditis *Journal of Paediatrics and Child Health* **34,** 196-198.

19. Martino,T.A., Liu,P. & Sole,M.J. (1994) Viral-Infection and the Pathogenesis of Dilated Cardiomyopathy *Circulation Research* **74,** 182-188.

20. Bowles,N.E. et al. (1989) End-Stage Dilated Cardiomyopathy - Persistence of Enterovirus Rna in Myocardium at Cardiac Transplantation and Lack of Immune-Response *Circulation* **80,** 1128-1136.

21. Tam,P.E. (2006) Coxsackievirus myocarditis: Interplay between virus and host in the pathogenesis of heart disease *Viral Immunology* **19,** 133-146.

22. Knipe,D.M. & Howley,P.M. (2006) *Fields Virology*. Lippincott Williams and Wilkins.

23. Huber,S. & Ramsingh,A.I. (2004) Coxsackievirus-induced pancreatitis *Viral Immunology* **17,** 358-369.

24. Mena,I., Fischer,C., Gebhard,J.R., Perry,C.M., Harkins,S. & Whitton,J.L. (2000) Coxsackievirus infection of the pancreas: Evaluation of receptor expression, pathogenesis, and immunopathology *Virology* **271,** 276-288.

25. Feuer,R., Pagarigan,R.R., Harkins,S., Liu,F., Hunziker,I.P. & Whitton,J.L. (2005) Coxsackievirus targets proliferating neuronal progenitor cells in the neonatal CNS *Journal of Neuroscience* **25,** 2434-2444.

26. Knipe,D.M. & Howley,P.M. (2006) *Fields Virology*. Lippincott Williams and Wilkins.

27. Knipe,D.M. & Howley,P.M. (2006) *Fields Virology*. Lippincott Williams and Wilkins.

28. Curry,S., Chow,M. & Hogle,J.M. (1996) The poliovirus 135S particle is infectious *Journal of Virology* **70,** 7125-7131.

29. Muckelbauer,J.K. et al. (1995) The Structure of Coxsackievirus B3 at 3.5 Angstrom Resolution *Structure* **3,** 653-667.

30. Tuthill,T.J., Bubeck,D., Rowlands,D.J. & Hogle,J.M. (2006) Characterization of early steps in the poliovirus infection process: Receptor-decorated liposomes induce conversion of the virus to membrane-anchored entry-intermediate particles *Journal of Virology* **80,** 172-180.

31. Curry,S., Chow,M. & Hogle,J.M. (1996) The poliovirus 135S particle is infectious *Journal of Virology* **70,** 7125-7131.

32. Tuthill,T.J., Bubeck,D., Rowlands,D.J. & Hogle,J.M. (2006) Characterization of early steps in the poliovirus infection process: Receptor-decorated liposomes induce conversion of the virus to membrane-anchored entry-intermediate particles *Journal of Virology* **80,** 172-180.

33. Knipe,D.M. & Howley,P.M. (2006) *Fields Virology*. Lippincott Williams and Wilkins.

34. Tuthill,T.J., Bubeck,D., Rowlands,D.J. & Hogle,J.M. (2006) Characterization of early steps in the poliovirus infection process: Receptor-decorated liposomes induce conversion of the virus to membrane-anchored entry-intermediate particles *Journal of Virology* **80,** 172-180.

35. Hafenstein,S. et al. (2007) Interaction of decay-accelerating factor with coxsackievirus B3 *Journal of Virology* **81,** 12927-12935.

36. Bowles,N.E., Richardson,P.J., Olsen,E.G.J. & Archard,L.C. (1986) Detection of Coxsackie-B-Virus-Specific Rna Sequences in Myocardial Biopsy Samples from Patients with Myocarditis and Dilated Cardiomyopathy *Lancet* **1,** 1120-1124.

37. Knipe,D.M. & Howley,P.M. (2006) *Fields Virology*. Lippincott Williams and Wilkins.

38. Bowles,N.E., Richardson,P.J., Olsen,E.G.J. & Archard,L.C. (1986) Detection of Coxsackie-B-Virus-Specific Rna Sequences in Myocardial Biopsy Samples from Patients with Myocarditis and Dilated Cardiomyopathy *Lancet* **1,** 1120-1124.

39. Knipe,D.M. & Howley,P.M. (2006) *Fields Virology*. Lippincott Williams and Wilkins.

40. Knipe,D.M. & Howley,P.M. (2006) *Fields Virology*. Lippincott Williams and Wilkins.

41. Mapoles,J.E., Krah,D.L. & Crowell,R.L. (1985) Purification of A Hela-Cell Receptor Protein for Group-B Coxsackie-Viruses *Journal of Virology* **55,** 560-566.

42. Martino,T.A. et al. (2000) The coxsackie-adenovirus receptor (CAR) is used by reference strains and clinical isolates representing all six serotypes of

coxsackievirus group B and by swine vesicular disease virus *Virology* **271,** 99-108.

43. Noutsias,M. et al. (2001) Human coxsackie-adenovirus receptor is colocalized with integrins alpha(v)beta(3) and alpha(v)beta(5) on the cardiomyocyte sarcolemma and upregulated in dilated cardiomyopathy - Implications for cardiotropic viral infections *Circulation* **104,** 275-280.

44. Cohen,C.J., Shieh,J.T.C., Pickles,R.J., Okegawa,T., Hsieh,J.T. & Bergelson,J.M. (2001) The coxsackievirus and adenovirus receptor is a transmembrane component of the tight junction *Proceedings of the National Academy of Sciences of the United States of America* **98,** 15191-15196.

45. Coyne,C.B. & Bergelson,J.M. (2005) CAR: A virus receptor within the tight junction *Advanced Drug Delivery Reviews* **57,** 869-882.

46. Coyne,C.B. & Bergelson,J.M. (2005) CAR: A virus receptor within the tight junction *Advanced Drug Delivery Reviews* **57,** 869-882.

47. Bergelson,J.M. et al. (1998) The murine CAR homolog is a receptor for coxsackie B viruses and adenoviruses *Journal of Virology* **72,** 415-419.

48. Tomko,R.P., Xu,R.L. & Philipson,L. (1997) HCAR and MCAR: The human and mouse cellular receptors for subgroup C adenoviruses and group B coxsackieviruses *Proceedings of the National Academy of Sciences of the United States of America* **94,** 3352-3356.

49. Coyne,C.B. & Bergelson,J.M. (2005) CAR: A virus receptor within the tight junction *Advanced Drug Delivery Reviews* **57,** 869-882.

50. Kim,J.S., Lee,S.H., Cho,Y.S., Choi,J.J., Kim,Y.H. & Lee,J.H. (2002) Enhancement of the adenoviral sensitivity of human ovarian cancer cells by transient expression of coxsackievirus and adenovirus receptor (CAR) *Gynecologic Oncology* **85,** 260-265.

51. Nicholsonweller,A., Burge,J., Fearon,D.T., Weller,P.F. & Austen,K.F. (1982) Isolation of A Human-Erythrocyte Membrane Glycoprotein with Decay-Accelerating Activity for C-3 Convertases of the Complement-System *Journal of Immunology* **129,** 184-189.

52. Shafren,D.R., Bates,R.C., Agrez,M.V., Herd,R.L., Burns,G.F. & Barry,R.D. (1995) Coxsackieviruses B1, B3, and B5 Use Decay-Accelerating Factor As A Receptor for Cell Attachment *Journal of Virology* **69,** 3873-3877.

53. Shafren,D.R., Dorahy,D.J., Ingham,R.A., Burns,G.F. & Barry,R.D. (1997) Coxsackievirus A21 binds to decay-accelerating factor but requires intercellular adhesion molecule 1 for cell entry *Journal of Virology* **71,** 4736-4743.

54. Ward,T., Pipkin,P.A., Clarkson,N.A., Stone,D.M., Minor,P.D. & Almond,J.W. (1994) Decay-Accelerating Factor Cd55 Is Identified As the Receptor for Echovirus-7 Using Celics, A Rapid Immune-Focal Cloning Method *Embo Journal* **13,** 5070-5074.

55. Powell,R.M., Schmitt,V., Ward,T., Goodfellow,I., Evans,D.J. & Almond,J.W. (1998) Characterization of echoviruses that bind decay accelerating factor (CD55): evidence that some haemagglutinating strains use more than one cellular receptor *Journal of General Virology* **79,** 1707-1713.

56. Shieh,J.T.C. & Bergelson,J.M. (2002) Interaction with decay-accelerating factor facilitates coxsackievirus B infection of polarized epithelial cells *Journal of Virology* **76,** 9474-9480.

57. Selinka,H.C., Wolde,A., Sauter,M., Kandolf,R. & Klingel,K. (2004) Virus-receptor interactions of coxsackie B viruses and their putative influence on cardiotropism *Medical Microbiology and Immunology* **193,** 127-131.

58. Knipe,D.M. & Howley,P.M. (2006) *Fields Virology*. Lippincott Williams and Wilkins.

59. Orthopoulos,G., Triantafilou,K. & Triantafilou,M. (2004) Coxsackie B viruses use multiple receptors to infect human cardiac cells *Journal of Medical Virology* **74,** 291-299.

60. Milstone,A.M., Petrella,J.E., Sanchez,M.D., Mahmud,M., Whitbeck,J.C. & Bergelson,J.M. (2005) Interaction with coxsackievirus and adenovirus receptor, but not with decay-accelerating factor (DAF), induces a-particle formation in a DAF-binding coxsackievirus B3 isolate *Journal of Virology* **79,** 655-660.

61. Nemerow,G.R. (2000) Cell receptors involved in adenovirus entry *Virology* **274,** 1-4.

62. Rossmann,M.G., He,Y.N. & Kuhn,R.J. (2002) Picornavirus-receptor interactions *Trends in Microbiology* **10,** 324-331.

63. Milstone,A.M., Petrella,J.E., Sanchez,M.D., Mahmud,M., Whitbeck,J.C. & Bergelson,J.M. (2005) Interaction with coxsackievirus and adenovirus receptor, but not with decay-accelerating factor (DAF), induces a-particle formation in a DAF-binding coxsackievirus B3 isolate *Journal of Virology* **79,** 655-660.

64. Hafenstein,S. et al. (2007) Interaction of decay-accelerating factor with coxsackievirus B3 *Journal of Virology* **81,** 12927-12935.

65. Hafenstein,S. et al. (2007) Interaction of decay-accelerating factor with coxsackievirus B3 *Journal of Virology* **81,** 12927-12935.

66. Hafenstein,S. et al. (2007) Interaction of decay-accelerating factor with coxsackievirus B3 *Journal of Virology* **81,** 12927-12935.

67. Bergelson,J.M., Mohanty,J.G., Crowell,R.L., John,N.F.S., Lublin,D.M. & Finberg,R.W. (1995) Coxsackievirus B3 Adapted to Growth in Rd Cells Binds to Decay-Accelerating Factor (Cd55) *Journal of Virology* **69,** 1903-1906.

68. Selinka,H.C. et al. (2002) Comparative analysis of two coxsackievirus B3 strains: Putative influence of virus-receptor interactions on pathogenesis *Journal of Medical Virology* **67,** 224-233.

69. Shieh,J.T.C. & Bergelson,J.M. (2002) Interaction with decay-accelerating factor facilitates coxsackievirus B infection of polarized epithelial cells *Journal of Virology* **76,** 9474-9480.

70. Shafren,D.R., Williams,D.T. & Barry,R.D. (1997) A decay-accelerating factor-binding strain of coxsackievirus B3 requires the coxsackievirus-adenovirus receptor protein to mediate lytic infection of rhabdomyosarcoma cells *Journal of Virology* **71,** 9844-9848.

71. Tomko,R.P., Xu,R.L. & Philipson,L. (1997) HCAR and MCAR: The human and mouse cellular receptors for subgroup C adenoviruses and group B coxsackieviruses *Proceedings of the National Academy of Sciences of the United States of America* **94,** 3352-3356.

72. Bergelson,J.M. et al. (1997) Isolation of a common receptor for coxsackie B viruses and adenoviruses 2 and 5 *Science* **275,** 1320-1323.

73. Coyne,C.B. & Bergelson,J.M. (2005) CAR: A virus receptor within the tight junction *Advanced Drug Delivery Reviews* **57,** 869-882.

74. Rossmann,M.G., He,Y.N. & Kuhn,R.J. (2002) Picornavirus-receptor interactions *Trends in Microbiology* **10,** 324-331.

75. Coyne,C.B. & Bergelson,J.M. (2005) CAR: A virus receptor within the tight junction *Advanced Drug Delivery Reviews* **57,** 869-882.

76. He,Y. et al. (2001) Interaction of coxsackievirus B3 with the full length coxsackievirus-adenovirus receptor *Nat. Struct. Biol.* **8,** 874-878.

77. Cunningham,K.A., Chapman,N.M. & Carson,S.D. (2003) Caspase-3 activation and ERK phosphorylation during CVB3 infection of cells: influence of the coxsackievirus and adenovirus receptor and engineered variants *Virus Research* **92,** 179-186.

78. Hafenstein,S. et al. (2007) Interaction of decay-accelerating factor with coxsackievirus B3 *Journal of Virology* **81,** 12927-12935.

79. Clarkson,N.A. et al. (1995) Characterization of the Echovirus-7 Receptor - Domains of Cd55 Critical for Virus Binding *Journal of Virology* **69,** 5497-5501.

80. Knipe,D.M. & Howley,P.M. (2006) *Fields Virology*. Lippincott Williams and Wilkins.

81. Knipe,D.M. & Howley,P.M. (2006) *Fields Virology*. Lippincott Williams and Wilkins.

82. Cornell,C.T., Kiosses,W.B., Harkins,S. & Whitton,J.L. (2006) Inhibition of protein trafficking by coxsackievirus B3: Multiple viral proteins target a single organelle *Journal of Virology* **80,** 6637-6647.

83. De Jong,A.S. et al. (2006) The coxsackievirus 2B protein increases efflux of ions from the endoplasmic reticulum and Golgi, thereby inhibiting protein

trafficking through the Golgi *Journal of Biological Chemistry* **281,** 14144-14150.

84. van Kuppeveld,F.J., De Jong,A.S., Melchers,W.J. & Willems,P.H. (2005) Enterovirus protein 2B po(u)res out the calcium: a viral strategy to survive? *Trends Microbiol.* **13,** 41-44.

85. Cornell,C.T., Mosses,W.B., Harkins,S. & Whitton,L. (2007) Coxsackievirus B3 proteins directionally complement each other to downregulate surface major histocompatibility complex class I *Journal of Virology* **81,** 6785-6797.

86. Kemball,C.C., Harkins,S., Whitmire,J.K., Flynn,C.T., Feuer,R. & Whitton,J.L. (2009) Coxsackievirus B3 Inhibits Antigen Presentation In Vivo, Exerting a Profound and Selective Effect on the MHC Class I Pathway *Plos Pathogens* **5**.

87. Knipe,D.M. & Howley,P.M. (2006) *Fields Virology*. Lippincott Williams and Wilkins.

88. Feuer,R., Mena,I., Pagarigan,R., Slifka,M.K. & Whitton,J.L. (2002) Cell cycle status affects coxsackievirus replication, persistence, and reactivation in vitro *Journal of Virology* **76,** 4430-4440.

89. Luo,H.L. et al. (2003) Ubiquitin-dependent proteolysis of cyclin D1 is associated with coxsackievirus-induced cell growth arrest *Journal of Virology* **77,** 1-9.

90. Si,X.N., Gao,G., Wong,J., Wang,Y.H., Zhang,J.C. & Luo,H.L. (2008) Ubiquitination Is Required for Effective Replication of Coxsackievirus B3 *Plos One* **3**.

91. Si,X. et al. (2005) Pyrrolidine dithiocarbamate reduces coxsackievirus B3 replication through inhibition of the ubiquitin-proteasome pathway *J. Virol.* **79,** 8014-8023.

92. Luo,H., Zhang,J., Cheung,C., Suarez,A., McManus,B.M. & Yang,D. (2003) Proteasome inhibition reduces coxsackievirus B3 replication in murine cardiomyocytes *Am. J. Pathol.* **163,** 381-385.

93. Esfandiarei,M. et al. (2004) Protein kinase B/Akt regulates coxsackievirus B3 replication through a mechanism which is not caspase dependent *Journal of Virology* **78,** 4289-4298.

94. Luo,H.L. et al. (2002) Coxsackievirus B3 replication is reduced by inhibition of the extracellular signal-regulated kinase (ERK) signaling pathway *Journal of Virology* **76,** 3365-3373.

95. Opavsky,M.A. et al. (2002) Enhanced ERK-1/2 activation in mice susceptible to coxsackievirus-induced myocarditis *J. Clin. Invest* **109,** 1561-1569.

96. Tran,S.E., Holmstrom,T.H., Ahonen,M., Kahari,V.M. & Eriksson,J.E. (2001) MAPK/ERK overrides the apoptotic signaling from Fas, TNF, and TRAIL receptors *J. Biol. Chem.* **276,** 16484-16490.

97. Knipe,D.M. & Howley,P.M. (2006) *Fields Virology*. Lippincott Williams and Wilkins.

98. Janeway,C.A., Jr. (1989) Approaching the asymptote? Evolution and revolution in immunology *Cold Spring Harb. Symp. Quant. Biol.* **54 Pt 1,** 1-13.

99. Anderson,K.V., Jurgens,G. & Nusslein-Volhard,C. (1985) Establishment of dorsal-ventral polarity in the Drosophila embryo: genetic studies on the role of the Toll gene product *Cell* **42,** 779-789.

100. Gay,N.J. & Keith,F.J. (1991) Drosophila Toll and IL-1 receptor *Nature* **351,** 355-356.

101. Lemaitre,B., Nicolas,E., Michaut,L., Reichhart,J.M. & Hoffmann,J.A. (1996) The dorsoventral regulatory gene cassette spatzle/Toll/cactus controls the potent antifungal response in Drosophila adults *Cell* **86,** 973-983.

102. Medzhitov,R., Preston-Hurlburt,P. & Janeway,C.A., Jr. (1997) A human homologue of the Drosophila Toll protein signals activation of adaptive immunity *Nature* **388,** 394-397.

103. Rock,F.L., Hardiman,G., Timans,J.C., Kastelein,R.A. & Bazan,J.F. (1998) A family of human receptors structurally related to Drosophila Toll *Proc. Natl. Acad. Sci. U. S. A* **95,** 588-593.

104. Poltorak,A. et al. (1998) Genetic and physical mapping of the Lps locus: identification of the toll-4 receptor as a candidate gene in the critical region *Blood Cells Mol. Dis.* **24,** 340-355.

105. Takeuchi,O. et al. (1999) TLR6: A novel member of an expanding toll-like receptor family *Gene* **231,** 59-65.

106. Chuang,T.H. & Ulevitch,R.J. (2000) Cloning and characterization of a sub-family of human toll-like receptors: hTLR7, hTLR8 and hTLR9 *Eur. Cytokine Netw.* **11,** 372-378.

107. Chuang,T. & Ulevitch,R.J. (2001) Identification of hTLR10: a novel human Toll-like receptor preferentially expressed in immune cells *Biochim. Biophys. Acta* **1518,** 157-161.

108. Kawai,T. & Akira,S. (2010) The role of pattern-recognition receptors in innate immunity: update on Toll-like receptors *Nat. Immunol.* **11,** 373-384.

109. Kawai,T. & Akira,S. (2011) Toll-like receptors and their crosstalk with other innate receptors in infection and immunity *Immunity.* **34,** 637-650.

110. Keogh,B. & Parker,A.E. (2011) Toll-like receptors as targets for immune disorders *Trends Pharmacol. Sci.* **32,** 435-442.

111. Akashi-Takamura,S. & Miyake,K. (2008) TLR accessory molecules *Curr. Opin. Immunol.* **20,** 420-425.

112. Akira,S., Uematsu,S. & Takeuchi,O. (2006) Pathogen recognition and innate immunity *Cell* **124,** 783-801.

113. Blasius,A.L. & Beutler,B. (2010) Intracellular toll-like receptors *Immunity.* **32,** 305-315.

114. Beutler,B.A. (2009) TLRs and innate immunity *Blood* **113,** 1399-1407.

115. InvivoGen. PRR-signalling-2011. http://www.invivogen.com/docs/PRR-signaling-2011.pdf . 2011. 14-7-2012.

116. Kang,J.Y. & Lee,J.O. (2011) Structural biology of the Toll-like receptor family *Annu. Rev. Biochem.* **80,** 917-941.

117. Botos,I., Segal,D.M. & Davies,D.R. (2011) The structural biology of Toll-like receptors *Structure.* **19,** 447-459.

118. Creagh,E.M. & O'Neill,L.A. (2006) TLRs, NLRs and RLRs: a trinity of pathogen sensors that co-operate in innate immunity *Trends Immunol.* **27,** 352-357.

119. Broz,P. & Monack,D.M. (2011) Molecular mechanisms of inflammasome activation during microbial infections *Immunol. Rev.* **243,** 174-190.

120. Broz,P. & Monack,D.M. (2011) Molecular mechanisms of inflammasome activation during microbial infections *Immunol. Rev.* **243,** 174-190.

121. Broz,P. & Monack,D.M. (2011) Molecular mechanisms of inflammasome activation during microbial infections *Immunol. Rev.* **243,** 174-190.

122. Stutz,A., Golenbock,D.T. & Latz,E. (2009) Inflammasomes: too big to miss *J. Clin. Invest* **119,** 3502-3511.

123. Kersse,K., Bertrand,M.J., Lamkanfi,M. & Vandenabeele,P. (2011) NOD-like receptors and the innate immune system: Coping with danger, damage and death *Cytokine Growth Factor Rev.*

124. Latz,E. (2010) The inflammasomes: mechanisms of activation and function *Curr. Opin. Immunol.* **22,** 28-33.

125. Martinon,F., Burns,K. & Tschopp,J. (2002) The inflammasome: a molecular platform triggering activation of inflammatory caspases and processing of proIL-beta *Mol. Cell* **10,** 417-426.

126. Davis,B.K., Wen,H. & Ting,J.P. (2011) The inflammasome NLRs in immunity, inflammation, and associated diseases *Annu. Rev. Immunol.* **29,** 707-735.

127. Broz,P. & Monack,D.M. (2011) Molecular mechanisms of inflammasome activation during microbial infections *Immunol. Rev.* **243,** 174-190.

128. Kersse,K., Bertrand,M.J., Lamkanfi,M. & Vandenabeele,P. (2011) NOD-like receptors and the innate immune system: Coping with danger, damage and death *Cytokine Growth Factor Rev.*

129. Kersse,K., Bertrand,M.J., Lamkanfi,M. & Vandenabeele,P. (2011) NOD-like receptors and the innate immune system: Coping with danger, damage and death *Cytokine Growth Factor Rev.*

130. Davis,B.K., Wen,H. & Ting,J.P. (2011) The inflammasome NLRs in immunity, inflammation, and associated diseases *Annu. Rev. Immunol.* **29,** 707-735.

131. Davis,B.K., Wen,H. & Ting,J.P. (2011) The inflammasome NLRs in immunity, inflammation, and associated diseases *Annu. Rev. Immunol.* **29,** 707-735.

132. Broz,P. & Monack,D.M. (2011) Molecular mechanisms of inflammasome activation during microbial infections *Immunol. Rev.* **243,** 174-190.

133. Stutz,A., Golenbock,D.T. & Latz,E. (2009) Inflammasomes: too big to miss *J. Clin. Invest* **119,** 3502-3511.

134. Horvath,G.L., Schrum,J.E., De Nardo,C.M. & Latz,E. (2011) Intracellular sensing of microbes and danger signals by the inflammasomes *Immunol. Rev.* **243,** 119-135.

135. Martinon,F., Burns,K. & Tschopp,J. (2002) The inflammasome: a molecular platform triggering activation of inflammatory caspases and processing of proIL-beta *Mol. Cell* **10,** 417-426.

136. Faustin,B. et al. (2007) Reconstituted NALP1 inflammasome reveals two-step mechanism of caspase-1 activation *Mol. Cell* **25,** 713-724.

137. Broz,P. & Monack,D.M. (2011) Molecular mechanisms of inflammasome activation during microbial infections *Immunol. Rev.* **243,** 174-190.

138. Horvath,G.L., Schrum,J.E., De Nardo,C.M. & Latz,E. (2011) Intracellular sensing of microbes and danger signals by the inflammasomes *Immunol. Rev.* **243,** 119-135.

139. Horvath,G.L., Schrum,J.E., De Nardo,C.M. & Latz,E. (2011) Intracellular sensing of microbes and danger signals by the inflammasomes *Immunol. Rev.* **243,** 119-135.

140. Stutz,A., Golenbock,D.T. & Latz,E. (2009) Inflammasomes: too big to miss *J. Clin. Invest* **119,** 3502-3511.

141. Horvath,G.L., Schrum,J.E., De Nardo,C.M. & Latz,E. (2011) Intracellular sensing of microbes and danger signals by the inflammasomes *Immunol. Rev.* **243,** 119-135.

142. Broz,P. & Monack,D.M. (2011) Molecular mechanisms of inflammasome activation during microbial infections *Immunol. Rev.* **243,** 174-190.

143. Stutz,A., Golenbock,D.T. & Latz,E. (2009) Inflammasomes: too big to miss *J. Clin. Invest* **119,** 3502-3511.

144. Davis,B.K., Wen,H. & Ting,J.P. (2011) The inflammasome NLRs in immunity, inflammation, and associated diseases *Annu. Rev. Immunol.* **29,** 707-735.

145. Horvath,G.L., Schrum,J.E., De Nardo,C.M. & Latz,E. (2011) Intracellular sensing of microbes and danger signals by the inflammasomes *Immunol. Rev.* **243,** 119-135.

146. Davis,B.K., Wen,H. & Ting,J.P. (2011) The inflammasome NLRs in immunity, inflammation, and associated diseases *Annu. Rev. Immunol.* **29,** 707-735.

147. Horvath,G.L., Schrum,J.E., De Nardo,C.M. & Latz,E. (2011) Intracellular sensing of microbes and danger signals by the inflammasomes *Immunol. Rev.* **243,** 119-135.

148. Kersse,K., Bertrand,M.J., Lamkanfi,M. & Vandenabeele,P. (2011) NOD-like receptors and the innate immune system: Coping with danger, damage and death *Cytokine Growth Factor Rev.*

149. Kersse,K., Bertrand,M.J., Lamkanfi,M. & Vandenabeele,P. (2011) NOD-like receptors and the innate immune system: Coping with danger, damage and death *Cytokine Growth Factor Rev.*

150. Horvath,G.L., Schrum,J.E., De Nardo,C.M. & Latz,E. (2011) Intracellular sensing of microbes and danger signals by the inflammasomes *Immunol. Rev.* **243,** 119-135.

151. Davis,B.K., Wen,H. & Ting,J.P. (2011) The inflammasome NLRs in immunity, inflammation, and associated diseases *Annu. Rev. Immunol.* **29,** 707-735.

152. Horvath,G.L., Schrum,J.E., De Nardo,C.M. & Latz,E. (2011) Intracellular sensing of microbes and danger signals by the inflammasomes *Immunol. Rev.* **243,** 119-135.

153. Latz,E. (2010) The inflammasomes: mechanisms of activation and function *Curr. Opin. Immunol.* **22,** 28-33.

154. Kersse,K., Bertrand,M.J., Lamkanfi,M. & Vandenabeele,P. (2011) NOD-like receptors and the innate immune system: Coping with danger, damage and death *Cytokine Growth Factor Rev.*

155. Davis,B.K., Wen,H. & Ting,J.P. (2011) The inflammasome NLRs in immunity, inflammation, and associated diseases *Annu. Rev. Immunol.* **29,** 707-735.

156. Latz,E. (2010) The inflammasomes: mechanisms of activation and function *Curr. Opin. Immunol.* **22,** 28-33.

157. Horvath,G.L., Schrum,J.E., De Nardo,C.M. & Latz,E. (2011) Intracellular sensing of microbes and danger signals by the inflammasomes *Immunol. Rev.* **243,** 119-135.

158. Horvath,G.L., Schrum,J.E., De Nardo,C.M. & Latz,E. (2011) Intracellular sensing of microbes and danger signals by the inflammasomes *Immunol. Rev.* **243,** 119-135.

159. Latz,E. (2010) The inflammasomes: mechanisms of activation and function *Curr. Opin. Immunol.* **22,** 28-33.

160. Stutz,A., Golenbock,D.T. & Latz,E. (2009) Inflammasomes: too big to miss *J. Clin. Invest* **119,** 3502-3511.

161. Horvath,G.L., Schrum,J.E., De Nardo,C.M. & Latz,E. (2011) Intracellular sensing of microbes and danger signals by the inflammasomes *Immunol. Rev.* **243,** 119-135.

162. Horvath,G.L., Schrum,J.E., De Nardo,C.M. & Latz,E. (2011) Intracellular sensing of microbes and danger signals by the inflammasomes *Immunol. Rev.* **243,** 119-135.

163. Davis,B.K., Wen,H. & Ting,J.P. (2011) The inflammasome NLRs in immunity, inflammation, and associated diseases *Annu. Rev. Immunol.* **29,** 707-735.

164. Kersse,K., Bertrand,M.J., Lamkanfi,M. & Vandenabeele,P. (2011) NOD-like receptors and the innate immune system: Coping with danger, damage and death *Cytokine Growth Factor Rev.*

165. Broz,P. & Monack,D.M. (2011) Molecular mechanisms of inflammasome activation during microbial infections *Immunol. Rev.* **243,** 174-190.

166. Broz,P. & Monack,D.M. (2011) Molecular mechanisms of inflammasome activation during microbial infections *Immunol. Rev.* **243,** 174-190.

167. Latz,E. (2010) The inflammasomes: mechanisms of activation and function *Curr. Opin. Immunol.* **22,** 28-33.

168. Stutz,A., Golenbock,D.T. & Latz,E. (2009) Inflammasomes: too big to miss *J. Clin. Invest* **119,** 3502-3511.

169. Davis,B.K., Wen,H. & Ting,J.P. (2011) The inflammasome NLRs in immunity, inflammation, and associated diseases *Annu. Rev. Immunol.* **29,** 707-735.

170. Horvath,G.L., Schrum,J.E., De Nardo,C.M. & Latz,E. (2011) Intracellular sensing of microbes and danger signals by the inflammasomes *Immunol. Rev.* **243,** 119-135.

171. Latz,E. (2010) The inflammasomes: mechanisms of activation and function *Curr. Opin. Immunol.* **22,** 28-33.

172. Horvath,G.L., Schrum,J.E., De Nardo,C.M. & Latz,E. (2011) Intracellular sensing of microbes and danger signals by the inflammasomes *Immunol. Rev.* **243,** 119-135.

173. Horvath,G.L., Schrum,J.E., De Nardo,C.M. & Latz,E. (2011) Intracellular sensing of microbes and danger signals by the inflammasomes *Immunol. Rev.* **243,** 119-135.

174. Kersse,K., Bertrand,M.J., Lamkanfi,M. & Vandenabeele,P. (2011) NOD-like receptors and the innate immune system: Coping with danger, damage and death *Cytokine Growth Factor Rev.*

175. Broz,P. & Monack,D.M. (2011) Molecular mechanisms of inflammasome activation during microbial infections *Immunol. Rev.* **243,** 174-190.

176. Kersse,K., Bertrand,M.J., Lamkanfi,M. & Vandenabeele,P. (2011) NOD-like receptors and the innate immune system: Coping with danger, damage and death *Cytokine Growth Factor Rev.*

177. Magalhaes,J.G., Sorbara,M.T., Girardin,S.E. & Philpott,D.J. (2011) What is new with Nods? *Curr. Opin. Immunol.* **23,** 29-34.

178. Kersse,K., Bertrand,M.J., Lamkanfi,M. & Vandenabeele,P. (2011) NOD-like receptors and the innate immune system: Coping with danger, damage and death *Cytokine Growth Factor Rev.*

179. Ting,J.P., Duncan,J.A. & Lei,Y. (2010) How the noninflammasome NLRs function in the innate immune system *Science* **327,** 286-290.

180. Kersse,K., Bertrand,M.J., Lamkanfi,M. & Vandenabeele,P. (2011) NOD-like receptors and the innate immune system: Coping with danger, damage and death *Cytokine Growth Factor Rev.*

181. Ting,J.P., Duncan,J.A. & Lei,Y. (2010) How the noninflammasome NLRs function in the innate immune system *Science* **327,** 286-290.

182. Ting,J.P., Duncan,J.A. & Lei,Y. (2010) How the noninflammasome NLRs function in the innate immune system *Science* **327,** 286-290.

183. Kersse,K., Bertrand,M.J., Lamkanfi,M. & Vandenabeele,P. (2011) NOD-like receptors and the innate immune system: Coping with danger, damage and death *Cytokine Growth Factor Rev.*

184. Magalhaes,J.G., Sorbara,M.T., Girardin,S.E. & Philpott,D.J. (2011) What is new with Nods? *Curr. Opin. Immunol.* **23,** 29-34.

185. Magalhaes,J.G., Sorbara,M.T., Girardin,S.E. & Philpott,D.J. (2011) What is new with Nods? *Curr. Opin. Immunol.* **23,** 29-34.

186. Yu,M. et al. (1997) Cloning of a gene (RIG-G) associated with retinoic acid-induced differentiation of acute promyelocytic leukemia cells and representing a new member of a family of interferon-stimulated genes *Proc. Natl. Acad. Sci. U. S. A* **94,** 7406-7411.

187. Zhang,X., Wang,C., Schook,L.B., Hawken,R.J. & Rutherford,M.S. (2000) An RNA helicase, RHIV -1, induced by porcine reproductive and respiratory

syndrome virus (PRRSV) is mapped on porcine chromosome 10q13 *Microb. Pathog.* **28,** 267-278.

188. Yoneyama,M. & Fujita,T. (2009) RNA recognition and signal transduction by RIG-I-like receptors *Immunol. Rev.* **227,** 54-65.

189. Kang,D.C., Gopalkrishnan,R.V., Wu,Q., Jankowsky,E., Pyle,A.M. & Fisher,P.B. (2002) mda-5: An interferon-inducible putative RNA helicase with double-stranded RNA-dependent ATPase activity and melanoma growth-suppressive properties *Proc. Natl. Acad. Sci. U. S. A* **99,** 637-642.

190. Cui,Y. et al. (2001) The Stat3/5 locus encodes novel endoplasmic reticulum and helicase-like proteins that are preferentially expressed in normal and neoplastic mammary tissue *Genomics* **78,** 129-134.

191. Ireton,R.C. & Gale,M., Jr. (2011) RIG-I Like Receptors in Antiviral Immunity and Therapeutic Applications *Viruses.* **3,** 906-919.

192. Kato,H., Takahasi,K. & Fujita,T. (2011) RIG-I-like receptors: cytoplasmic sensors for non-self RNA *Immunol. Rev.* **243,** 91-98.

193. Kato,H., Takahasi,K. & Fujita,T. (2011) RIG-I-like receptors: cytoplasmic sensors for non-self RNA *Immunol. Rev.* **243,** 91-98.

194. Kawasaki,T., Kawai,T. & Akira,S. (2011) Recognition of nucleic acids by pattern-recognition receptors and its relevance in autoimmunity *Immunol. Rev.* **243,** 61-73.

195. Kato,H., Takahasi,K. & Fujita,T. (2011) RIG-I-like receptors: cytoplasmic sensors for non-self RNA *Immunol. Rev.* **243,** 91-98.

196. Kawasaki,T., Kawai,T. & Akira,S. (2011) Recognition of nucleic acids by pattern-recognition receptors and its relevance in autoimmunity *Immunol. Rev.* **243,** 61-73.

197. Schmidt,A., Rothenfusser,S. & Hopfner,K.P. (2012) Sensing of viral nucleic acids by RIG-I: From translocation to translation *Eur. J. Cell Biol.* **91,** 78-85.

198. Wilkins,C. & Gale,M., Jr. (2010) Recognition of viruses by cytoplasmic sensors *Curr. Opin. Immunol.* **22,** 41-47.

199. Peisley,A. et al. (2011) Cooperative assembly and dynamic disassembly of MDA5 filaments for viral dsRNA recognition *Proc. Natl. Acad. Sci. U. S. A* **108,** 21010-21015.

200. Hornung,V. et al. (2006) 5'-Triphosphate RNA is the ligand for RIG-I *Science* **314,** 994-997.

201. Pichlmair,A. et al. (2006) RIG-I-mediated antiviral responses to single-stranded RNA bearing 5'-phosphates *Science* **314,** 997-1001.

202. Kato,H., Takahasi,K. & Fujita,T. (2011) RIG-I-like receptors: cytoplasmic sensors for non-self RNA *Immunol. Rev.* **243,** 91-98.

203. Wilkins,C. & Gale,M., Jr. (2010) Recognition of viruses by cytoplasmic sensors *Curr. Opin. Immunol.* **22,** 41-47.

204. Schmidt,A., Rothenfusser,S. & Hopfner,K.P. (2012) Sensing of viral nucleic acids by RIG-I: From translocation to translation *Eur. J. Cell Biol.* **91,** 78-85.

205. Yoneyama,M. & Fujita,T. (2009) RNA recognition and signal transduction by RIG-I-like receptors *Immunol. Rev.* **227,** 54-65.

206. Wilkins,C. & Gale,M., Jr. (2010) Recognition of viruses by cytoplasmic sensors *Curr. Opin. Immunol.* **22,** 41-47.

207. Yoneyama,M. & Fujita,T. (2009) RNA recognition and signal transduction by RIG-I-like receptors *Immunol. Rev.* **227,** 54-65.

208. Kawasaki,T., Kawai,T. & Akira,S. (2011) Recognition of nucleic acids by pattern-recognition receptors and its relevance in autoimmunity *Immunol. Rev.* **243,** 61-73.

209. Schmidt,A., Rothenfusser,S. & Hopfner,K.P. (2012) Sensing of viral nucleic acids by RIG-I: From translocation to translation *Eur. J. Cell Biol.* **91,** 78-85.

210. Wilkins,C. & Gale,M., Jr. (2010) Recognition of viruses by cytoplasmic sensors *Curr. Opin. Immunol.* **22,** 41-47.

211. Schmidt,A., Rothenfusser,S. & Hopfner,K.P. (2012) Sensing of viral nucleic acids by RIG-I: From translocation to translation *Eur. J. Cell Biol.* **91,** 78-85.

212. Wilkins,C. & Gale,M., Jr. (2010) Recognition of viruses by cytoplasmic sensors *Curr. Opin. Immunol.* **22,** 41-47.

213. Ireton,R.C. & Gale,M., Jr. (2011) RIG-I Like Receptors in Antiviral Immunity and Therapeutic Applications *Viruses.* **3,** 906-919.

214. Schmidt,A., Rothenfusser,S. & Hopfner,K.P. (2012) Sensing of viral nucleic acids by RIG-I: From translocation to translation *Eur. J. Cell Biol.* **91,** 78-85.

215. Kawasaki,T., Kawai,T. & Akira,S. (2011) Recognition of nucleic acids by pattern-recognition receptors and its relevance in autoimmunity *Immunol. Rev.* **243,** 61-73.

216. Schmidt,A., Rothenfusser,S. & Hopfner,K.P. (2012) Sensing of viral nucleic acids by RIG-I: From translocation to translation *Eur. J. Cell Biol.* **91,** 78-85.

217. Murali,A. et al. (2008) Structure and function of LGP2, a DEX(D/H) helicase that regulates the innate immunity response *J. Biol. Chem.* **283,** 15825-15833.

218. Ireton,R.C. & Gale,M., Jr. (2011) RIG-I Like Receptors in Antiviral Immunity and Therapeutic Applications *Viruses.* **3,** 906-919.

219. Cui,Y. et al. (2001) The Stat3/5 locus encodes novel endoplasmic reticulum and helicase-like proteins that are preferentially expressed in normal and neoplastic mammary tissue *Genomics* **78,** 129-134.

220. Wilkins,C. & Gale,M., Jr. (2010) Recognition of viruses by cytoplasmic sensors *Curr. Opin. Immunol.* **22,** 41-47.

221. Kawasaki,T., Kawai,T. & Akira,S. (2011) Recognition of nucleic acids by pattern-recognition receptors and its relevance in autoimmunity *Immunol. Rev.* **243,** 61-73.

222. Yoneyama,M. & Fujita,T. (2009) RNA recognition and signal transduction by RIG-I-like receptors *Immunol. Rev.* **227,** 54-65.

223. Jiang,X. et al. (2012) Ubiquitin-Induced Oligomerization of the RNA Sensors RIG-I and MDA5 Activates Antiviral Innate Immune Response *Immunity.* **36,** 959-973.

224. Jiang,X. et al. (2012) Ubiquitin-Induced Oligomerization of the RNA Sensors RIG-I and MDA5 Activates Antiviral Innate Immune Response *Immunity.* **36,** 959-973.

225. Kato,H., Takahasi,K. & Fujita,T. (2011) RIG-I-like receptors: cytoplasmic sensors for non-self RNA *Immunol. Rev.* **243,** 91-98.

226. Seth,R.B., Sun,L., Ea,C.K. & Chen,Z.J. (2005) Identification and characterization of MAVS, a mitochondrial antiviral signaling protein that activates NF-kappaB and IRF 3 *Cell* **122,** 669-682.

227. Kawai,T. et al. (2005) IPS-1, an adaptor triggering RIG-I- and Mda5-mediated type I interferon induction *Nat. Immunol.* **6,** 981-988.

228. Xu,L.G., Wang,Y.Y., Han,K.J., Li,L.Y., Zhai,Z. & Shu,H.B. (2005) VISA is an adapter protein required for virus-triggered IFN-beta signaling *Mol. Cell* **19,** 727-740.

229. Meylan,E. et al. (2005) Cardif is an adaptor protein in the RIG-I antiviral pathway and is targeted by hepatitis C virus *Nature* **437,** 1167-1172.

230. Yoneyama,M. & Fujita,T. (2009) RNA recognition and signal transduction by RIG-I-like receptors *Immunol. Rev.* **227,** 54-65.

231. Baril,M., Racine,M.E., Penin,F. & Lamarre,D. (2009) MAVS dimer is a crucial signaling component of innate immunity and the target of hepatitis C virus NS3/4A protease *J. Virol.* **83,** 1299-1311.

232. Onoguchi,K. et al. (2010) Virus-infection or 5'ppp-RNA activates antiviral signal through redistribution of IPS-1 mediated by MFN1 *PLoS. Pathog.* **6,** e1001012.

233. Hou,F., Sun,L., Zheng,H., Skaug,B., Jiang,Q.X. & Chen,Z.J. (2011) MAVS forms functional prion-like aggregates to activate and propagate antiviral innate immune response *Cell* **146,** 448-461.

234. Yoneyama,M. & Fujita,T. (2009) RNA recognition and signal transduction by RIG-I-like receptors *Immunol. Rev.* **227,** 54-65.

235. Kato,H., Takahasi,K. & Fujita,T. (2011) RIG-I-like receptors: cytoplasmic sensors for non-self RNA *Immunol. Rev.* **243,** 91-98.

236. Schmidt,A., Rothenfusser,S. & Hopfner,K.P. (2012) Sensing of viral nucleic acids by RIG-I: From translocation to translation *Eur. J. Cell Biol.* **91,** 78-85.

237. Wang,Y., Swiecki,M., McCartney,S.A. & Colonna,M. (2011) dsRNA sensors and plasmacytoid dendritic cells in host defense and autoimmunity *Immunol. Rev.* **243,** 74-90.

238. Kawasaki,T., Kawai,T. & Akira,S. (2011) Recognition of nucleic acids by pattern-recognition receptors and its relevance in autoimmunity *Immunol. Rev.* **243,** 61-73.

239. Wang,Y., Swiecki,M., McCartney,S.A. & Colonna,M. (2011) dsRNA sensors and plasmacytoid dendritic cells in host defense and autoimmunity *Immunol. Rev.* **243,** 74-90.

240. Belgnaoui,S.M., Paz,S. & Hiscott,J. (2011) Orchestrating the interferon antiviral response through the mitochondrial antiviral signaling (MAVS) adapter *Curr. Opin. Immunol.* **23,** 564-572.

241. Yoneyama,M. & Fujita,T. (2009) RNA recognition and signal transduction by RIG-I-like receptors *Immunol. Rev.* **227,** 54-65.

242. Wang,Y., Swiecki,M., McCartney,S.A. & Colonna,M. (2011) dsRNA sensors and plasmacytoid dendritic cells in host defense and autoimmunity *Immunol. Rev.* **243,** 74-90.

243. Wang,J.P., Cerny,A., Asher,D.R., Kurt-Jones,E.A., Bronson,R.T. & Finberg,R.W. (2010) MDA5 and MAVS mediate type I interferon responses to coxsackie B virus *J. Virol.* **84,** 254-260.

244. Wang,Y., Swiecki,M., McCartney,S.A. & Colonna,M. (2011) dsRNA sensors and plasmacytoid dendritic cells in host defense and autoimmunity *Immunol. Rev.* **243,** 74-90.

245. Yoneyama,M. & Fujita,T. (2009) RNA recognition and signal transduction by RIG-I-like receptors *Immunol. Rev.* **227,** 54-65.

246. Barral,P.M., Sarkar,D., Fisher,P.B. & Racaniello,V.R. (2009) RIG-I is cleaved during picornavirus infection *Virology* **391,** 171-176.

247. Barral,P.M. et al. (2007) MDA-5 is cleaved in poliovirus-infected cells *J. Virol.* **81,** 3677-3684.

248. Yoneyama,M. & Fujita,T. (2009) RNA recognition and signal transduction by RIG-I-like receptors *Immunol. Rev.* **227,** 54-65.

249. Kowalinski,E. et al. (2011) Structural basis for the activation of innate immune pattern-recognition receptor RIG-I by viral RNA *Cell* **147,** 423-435.

250. Kowalinski,E. et al. (2011) Structural basis for the activation of innate immune pattern-recognition receptor RIG-I by viral RNA *Cell* **147,** 423-435.

251. Kowalinski,E. et al. (2011) Structural basis for the activation of innate immune pattern-recognition receptor RIG-I by viral RNA *Cell* **147,** 423-435.

252. Lu,C. et al. (2010) The structural basis of 5' triphosphate double-stranded RNA recognition by RIG-I C-terminal domain *Structure.* **18,** 1032-1043.

253. Kowalinski,E. et al. (2011) Structural basis for the activation of innate immune pattern-recognition receptor RIG-I by viral RNA *Cell* **147,** 423-435.

254. Kowalinski,E. et al. (2011) Structural basis for the activation of innate immune pattern-recognition receptor RIG-I by viral RNA *Cell* **147,** 423-435.

255. Schmidt,A., Rothenfusser,S. & Hopfner,K.P. (2012) Sensing of viral nucleic acids by RIG-I: From translocation to translation *Eur. J. Cell Biol.* **91,** 78-85.

256. Li,X. et al. (2009) Structural basis of double-stranded RNA recognition by the RIG-I like receptor MDA5 *Arch. Biochem. Biophys.* **488,** 23-33.

257. Belgnaoui,S.M., Paz,S. & Hiscott,J. (2011) Orchestrating the interferon antiviral response through the mitochondrial antiviral signaling (MAVS) adapter *Curr. Opin. Immunol.* **23,** 564-572.

258. Schönborn J, Oberstrass J, Breyel E, Tittgen J, Schumacher J, and Lukacs N. Monoclonal antibodies to double-stranded RNA as probes of RNA structure in crude nucleic acid extracts. Nucleic Acids Res 19, 2993-3000. 1991.

259. Richards,O.C., Hey,T.D. & Ehrenfeld,E. (1981) Two forms of VPg on poliovirus RNAs *J Virol* **38,** 863-871.

260. Richards,O.C., Hey,T.D. & Ehrenfeld,E. (1987) Poliovirus snapback double-stranded RNA isolated from infected HeLa cells is deficient in poly(A) *J Virol* **61,** 2307-2310.

261. Spector, D. H. and Baltimore, D. Polyadenylic acid on Poliovirus RNA. J.Virol 15, 1418-1431. 1975.

262. Protocol Online. Immunofluorescence. http://www.protocol-online.org/prot/Immunology/Immunofluorescence/ . 30-7-2011. 20-4-2012.

263. USBiological. Immunofluorescence General Protocol. http://www.usbio.net/misc/Immunofluorescence . 30-11-2011. 20-4-2012.

264. Protocol Online. Flow Cytometry (FCM). http://www.protocol-online.org/prot/Cell_Biology/Flow_Cytometry__FCM_/index.html . 30-7-2011. 20-4-2012.

265. Flow Cytometry Facility, UC Berkeley. Introduction. http://biology.berkeley.edu/crl/flow_cytometry_basic.html . 2011. 20-4-2012.

266. Invitrogen. Introduction to Flow Cytometry. http://probes.invitrogen.com/resources/education/tutorials/4Intro_Flow/player.html . 8-8-2011. 20-4-2012.

267. Caprette, D. R. Introduction to SDS-PAGE. Department of Biochemistry and Cell Biology, Rice University. http://www.ruf.rice.edu/~bioslabs/studies/sds-page/gellab2.html . 2011. 20-4-2012.

268. Campbell, M. A. SDS-PAGE (PolyAcrylamide Gel Electrophoresis). Department of Biology, Davidson College. http://www.bio.davidson.edu/courses/genomics/method/SDSPAGE/SDSPAGE.html . 2001. 20-4-2012.

269. Schmieg, F. Principles of Polyacrylamide Gel Electrophoresis (PAGE). Department of Biological Sciences, University of Delaware. http://www.udel.edu/biology/fschmieg/411acrylamide.htm . 2011. 20-4-2012.

270. abcam. WESTERN BLOTTING - A BEGINNER'S GUIDE. http://www.abcam.com/ps/pdf/protocols/WB-beginner.pdf . 2011. 20-4-2012.

271. Campbell, M. A. Western Blot Procedure. Department of Biology, Davidson College. http://www.bio.davidson.edu/courses/genomics/method/Westernblot.html . 2001. 20-4-2012.

272. abcam. IMMUNOPRECIPITATION (IP) PROTOCOL. http://www.abcam.com/ps/pdf/protocols/Immunoprecipitation%20protocol%20(IP).pdf . 2011.

273. Thermo Scientific. Immunoprecipitation (IP). http://www.piercenet.com/browse.cfm?fldID=E5049863-D59D-B7A5-D057-E23F7B22AD44 . 2011. 20-4-2012.

274. Amos,W.B. & White,J.G. (2003) How the confocal laser scanning microscope entered biological research *Biol. Cell* **95,** 335-342.

275. Cox,G. (2002) Biological Confocal Microscopy *Materials Today* **5,** 34-41.

276. Pulli,T., Koskimies,P. & Hyypia,T. (1995) Molecular Comparison of Coxsackie A virus serotypes *Virology* **212,** 30-38.

277. Akira,S. (2001) Toll-like receptors and innate immunity *Adv. Immunol.* **78,** 1-56.

278. Takeuchi O & Akira S (2008) MDA5/RIG-I and virus recognition *Curr Opin Immunol.* **20,** 17-22.

279. Triantafilou,K. et al. (2005) TLR8 and TLR7 are involved in the host's immune response to Human Parechovirus 1 *Eur J Immunol* **35,** 2416-2423.

280. Triantafilou,K. et al. (2005) Human cardiac inflammatory responses triggered by Coxsackie B Viruses are mainly Toll-like receptor (TLR) 8-dependent *Cellul Microbiol* **7,** 1117-1126.

281. Wang, J. P, Cerny, A., Asher, D. R, Kurt-Jones, E. A, Bronson, R. T., and Finberg, R. W. MDA5 and MAVS mediate type I interferon responses to coxsackie B virus. J.Virol 84, 254-260. 2010.

282. Takeuchi,O. & Akira,S. (2009) Innate immunity to virus infection *Immunol Rev* **227,** 75-86.

283. Kato H et al. (2006) Differential roles of MDA5 and RIG-I helicases in the recognition of RNA viruses *Nature* **441,** 101-105.

284. Loo, Y. M., Fornek, J., Crochet, N., Bajwa, G., Perwitasari, O., Martinez-Sobrido, L., Akira, S., Gill, M. A., García-Sastre, A., Katze, M. G., and Gale, M. Jr. DISTINCT RIG-I AND MDA5 SIGNALING BY RNA VIRUSES IN INNATE IMMUNITY. J.Virol 82, 335-345. 2008.

285. Pichlmair A et al. (2007) RIG-I-mediated antiviral responses to single-stranded RNA bearing 5'-phosphates. *Science* **314,** 997-1001.

286. Kato,H. et al. (2008) Length-dependent recognition of double-stranded ribonucleic acids by retinoic acid-inducible gene-I and melanoma differentiation-associated gene 5 *J. Exp Med* **205,** 1601-1610.

287. Hornung,V. et al. (2006) 5'-Triphosphate RNA is the ligand for RIG-I *Science* **314,** 994-997.

288. Rehwinkel,J. et al. (2010) RIG-I detects viral genomic RNA during negative-strand RNA virus infection *Cell* **140,** 397-408.

289. Pichlmair,A. et al. (2009) Activation of MDA5 requires higher-order RNA structures generated during virus infection. *J. Virol* **83,** 10761-10769.

290. Triantafilou,K. & Triantafilou,M. (2004) Coxsackievirus B4-induced cytokine production in pancreatic cells is mediated through TLR4 *J Virol* **78,** 11313-11320.

291. Richer, M. J., Fang, D., Shanina, I., and Horwitz, M. S. Toll-like receptor 4-induced cytokine production circumvents protection conferred by TGF-beta in coxsackievirus-mediated autoimmune myocarditis. Clin Immunol 121, 339-349. 2006.

292. Richards,O.C., Hey,T.D. & Ehrenfeld,E. (1987) Poliovirus snapback double-stranded RNA isolated from infected HeLa cells is deficient in poly(A) *J Virol* **61,** 2307-2310.

293. Bao, G., Rhee, W. J., and Tsourkas, A. Fluorescent Probes for Live-Cell RNA Detection. Annu Rev Biomed Eng 11, 25-47. 2009.

294. Giles R.V, Spiller D.G, Grzybowski J, Clark R E, Nicklin P, and Tidd D.M. Selecting optimal oligonucleotide composition for maximal antisense effect following streptolysin O-mediated delivery into human leukaemia cells. Nucleic Acids Res 26, 1567-1575. 1998.

295. Meylan E, Curran J, Hofmann K, Moradpour D, Binder M, Bartenschlager R, and Tschopp J. 110. Cardif is an adaptor protein in the RIG-I antiviral pathway and is targeted by hepatitis C virus. Nature 437, 1167-1172. 2005.

296. Tracy,S., Chapman,N.M., Romero,J. & Ramsingh,A.I. (1996) Genetics of coxsackievirus B cardiovirulence and inflammatory heart muscle disease *Trends in Microbiology* **4,** 175-179.

297. Benzi, L. R. GIRARDI HEART (human, heart). http://bioinformatics.istge.it/cldb/cl1468.html . 20-8-2011. 26-4-0012.

298. Ireton,R.C. & Gale,M., Jr. (2011) RIG-I Like Receptors in Antiviral Immunity and Therapeutic Applications *Viruses.* **3,** 906-919.

299. Kato,H., Takahasi,K. & Fujita,T. (2011) RIG-I-like receptors: cytoplasmic sensors for non-self RNA *Immunol. Rev.* **243,** 91-98.

300. Wang,J.P., Cerny,A., Asher,D.R., Kurt-Jones,E.A., Bronson,R.T. & Finberg,R.W. (2010) MDA5 and MAVS Mediate Type I Interferon Responses to Coxsackie B Virus *Journal of Virology* **84,** 254-260.

301. Barral,P.M., Sarkar,D., Fisher,P.B. & Racaniello,V.R. (2009) RIG-I is cleaved during picornavirus infection *Virology* **391,** 171-176.

302. Barral,P.M. et al. (2007) MDA-5 is cleaved in poliovirus-infected cells *J. Virol.* **81,** 3677-3684.

303. Knipe,D.M. & Howley,P.M. (2006) *Fields Virology*. Lippincott Williams and Wilkins.

304. Kato,H., Takahasi,K. & Fujita,T. (2011) RIG-I-like receptors: cytoplasmic sensors for non-self RNA *Immunol. Rev.* **243,** 91-98.

305. Kawasaki,T., Kawai,T. & Akira,S. (2011) Recognition of nucleic acids by pattern-recognition receptors and its relevance in autoimmunity *Immunol. Rev.* **243,** 61-73.

306. Kawasaki,T., Kawai,T. & Akira,S. (2011) Recognition of nucleic acids by pattern-recognition receptors and its relevance in autoimmunity *Immunol. Rev.* **243,** 61-73.

307. Schmidt,A., Rothenfusser,S. & Hopfner,K.P. (2012) Sensing of viral nucleic acids by RIG-I: From translocation to translation *Eur. J. Cell Biol.* **91,** 78-85.

308. Wilkins,C. & Gale,M., Jr. (2010) Recognition of viruses by cytoplasmic sensors *Curr. Opin. Immunol.* **22,** 41-47.

309. Knipe,D.M. & Howley,P.M. (2006) *Fields Virology*. Lippincott Williams and Wilkins.

310. Schmidt,A., Rothenfusser,S. & Hopfner,K.P. (2012) Sensing of viral nucleic acids by RIG-I: From translocation to translation *Eur. J. Cell Biol.* **91,** 78-85.

311. Hornung,V. et al. (2006) 5'-Triphosphate RNA is the ligand for RIG-I *Science* **314,** 994-997.

312. Pichlmair,A. et al. (2006) RIG-I-mediated antiviral responses to single-stranded RNA bearing 5'-phosphates *Science* **314,** 997-1001.

313. Kato,H., Takahasi,K. & Fujita,T. (2011) RIG-I-like receptors: cytoplasmic sensors for non-self RNA *Immunol. Rev.* **243,** 91-98.

314. Schmidt,A., Rothenfusser,S. & Hopfner,K.P. (2012) Sensing of viral nucleic acids by RIG-I: From translocation to translation *Eur. J. Cell Biol.* **91,** 78-85.

315. Yoneyama,M. & Fujita,T. (2009) RNA recognition and signal transduction by RIG-I-like receptors *Immunol. Rev.* **227,** 54-65.

316. Wang,J.P., Cerny,A., Asher,D.R., Kurt-Jones,E.A., Bronson,R.T. & Finberg,R.W. (2010) MDA5 and MAVS Mediate Type I Interferon Responses to Coxsackie B Virus *Journal of Virology* **84,** 254-260.

317. Kato,H. et al. (2006) Differential roles of MDA5 and RIG-I helicases in the recognition of RNA viruses *Nature* **441,** 101-105.

318. Loo,Y.M. et al. (2008) Distinct RIG-I and MDA5 signaling by RNA viruses in innate immunity *J. Virol.* **82,** 335-345.

319. Pichlmair,A. et al. (2006) RIG-I-mediated antiviral responses to single-stranded RNA bearing 5'-phosphates *Science* **314,** 997-1001.

320. Kato,H. et al. (2008) Length-dependent recognition of double-stranded ribonucleic acids by retinoic acid-inducible gene-I and melanoma differentiation-associated gene 5 *J. Exp. Med.* **205,** 1601-1610.

321. Kato,H. et al. (2008) Length-dependent recognition of double-stranded ribonucleic acids by retinoic acid-inducible gene-I and melanoma differentiation-associated gene 5 *J. Exp. Med.* **205,** 1601-1610.

322. JCRB. JCRB0403 [HuH-7]. http://cellbank.nibio.go.jp/celldata/jcrb0403.htm . 13-12-2007. 29-4-2012.

323. Sumpter,R., Jr. et al. (2005) Regulating intracellular antiviral defense and permissiveness to hepatitis C virus RNA replication through a cellular RNA helicase, RIG-I *J. Virol.* **79,** 2689-2699.

324. Yoneyama,M. & Fujita,T. (2009) RNA recognition and signal transduction by RIG-I-like receptors *Immunol. Rev.* **227,** 54-65.

325. Triantafilou,K. et al. (2005) Human cardiac inflammatory responses triggered by Coxsackie B viruses are mainly Toll-like receptor (TLR) 8-dependent *Cellular Microbiology* **7,** 1117-1126.

326. Wang,J.P., Cerny,A., Asher,D.R., Kurt-Jones,E.A., Bronson,R.T. & Finberg,R.W. (2010) MDA5 and MAVS mediate type I interferon responses to coxsackie B virus *J. Virol.* **84,** 254-260.

327. Triantafilou,K. et al. (2005) Human cardiac inflammatory responses triggered by Coxsackie B viruses are mainly Toll-like receptor (TLR) 8-dependent *Cellular Microbiology* **7,** 1117-1126.

328. Rehwinkel,J. et al. (2010) RIG-I detects viral genomic RNA during negative-strand RNA virus infection *Cell* **140,** 397-408.

329. Kawai,T. et al. (2005) IPS-1, an adaptor triggering RIG-I- and Mda5-mediated type I interferon induction *Nat. Immunol.* **6,** 981-988.

330. Oganesyan,G. et al. (2006) Critical role of TRAF3 in the Toll-like receptor-dependent and -independent antiviral response *Nature* **439,** 208-211.

331. Xu,L.G., Wang,Y.Y., Han,K.J., Li,L.Y., Zhai,Z. & Shu,H.B. (2005) VISA is an adapter protein required for virus-triggered IFN-beta signaling *Mol. Cell* **19,** 727-740.

332. Saha,S.K. et al. (2006) Regulation of antiviral responses by a direct and specific interaction between TRAF3 and Cardif *EMBO J.* **25,** 3257-3263.

333. Cui,S. et al. (2008) The C-terminal regulatory domain is the RNA 5'-triphosphate sensor of RIG-I *Mol. Cell* **29,** 169-179.

334. Rothenfusser,S. et al. (2005) The RNA helicase Lgp2 inhibits TLR-independent sensing of viral replication by retinoic acid-inducible gene-I *J. Immunol.* **175,** 5260-5268.

335. Saito,T. et al. (2007) Regulation of innate antiviral defenses through a shared repressor domain in RIG-I and LGP2 *Proc. Natl. Acad. Sci. U. S. A* **104,** 582-587.

336. Komuro,A. & Horvath,C.M. (2006) RNA- and virus-independent inhibition of antiviral signaling by RNA helicase LGP2 *J. Virol.* **80,** 12332-12342.

337. Komuro,A. & Horvath,C.M. (2006) RNA- and virus-independent inhibition of antiviral signaling by RNA helicase LGP2 *J. Virol.* **80,** 12332-12342.

338. Baril,M., Racine,M.E., Penin,F. & Lamarre,D. (2009) MAVS dimer is a crucial signaling component of innate immunity and the target of hepatitis C virus NS3/4A protease *J. Virol.* **83,** 1299-1311.

339. Knipe,D.M. & Howley,P.M. (2006) *Fields Virology*. Lippincott Williams and Wilkins.

340. Ukimura,A. et al. (1997) Intracellular viral localization in murine coxsackievirus-B3 myocarditis - Ultrastructural study by electron microscopic in situ hybridization *American Journal of Pathology* **150,** 2061-2074.

341. Huber,S. & Ramsingh,A.I. (2004) Coxsackievirus-induced pancreatitis *Viral Immunology* **17,** 358-369.

342. Takeuchi,O. & Akira,S. (2007) Recognition of viruses by innate immunity *Immunol. Rev.* **220,** 214-224.

343. Yoneyama,M. et al. (2004) The RNA helicase RIG-I has an essential function in double-stranded RNA-induced innate antiviral responses *Nat. Immunol.* **5,** 730-737.

344. Kang,D.C., Gopalkrishnan,R.V., Wu,Q., Jankowsky,E., Pyle,A.M. & Fisher,P.B. (2002) mda-5: An interferon-inducible putative RNA helicase with double-stranded RNA-dependent ATPase activity and melanoma growth-suppressive properties *Proc. Natl. Acad. Sci. U. S. A* **99,** 637-642.

345. Rothenfusser,S. et al. (2005) The RNA helicase Lgp2 inhibits TLR-independent sensing of viral replication by retinoic acid-inducible gene-I *J. Immunol.* **175,** 5260-5268.

346. Knipe,D.M. & Howley,P.M. (2006) *Fields Virology*. Lippincott Williams and Wilkins.

347. Hornung,V. et al. (2006) 5'-Triphosphate RNA is the ligand for RIG-I *Science* **314,** 994-997.

348. Pichlmair,A. et al. (2006) RIG-I-mediated antiviral responses to single-stranded RNA bearing 5'-phosphates *Science* **314,** 997-1001.

349. Knipe,D.M. & Howley,P.M. (2006) *Fields Virology*. Lippincott Williams and Wilkins.

350. Wilkins,C. & Gale,M., Jr. (2010) Recognition of viruses by cytoplasmic sensors *Curr. Opin. Immunol.* **22,** 41-47.

351. Triantafilou,K. et al. (2005) Human cardiac inflammatory responses triggered by Coxsackie B viruses are mainly Toll-like receptor (TLR) 8-dependent *Cellular Microbiology* **7,** 1117-1126.

352. Knipe,D.M. & Howley,P.M. (2006) *Fields Virology*. Lippincott Williams and Wilkins.

353. Negishi,H. et al. (2008) A critical link between Toll-like receptor 3 and type II interferon signaling pathways in antiviral innate immunity *Proc. Natl. Acad. Sci. U. S. A* **105,** 20446-20451.

354. Wang,J.P., Cerny,A., Asher,D.R., Kurt-Jones,E.A., Bronson,R.T. & Finberg,R.W. (2010) MDA5 and MAVS Mediate Type I Interferon Responses to Coxsackie B Virus *Journal of Virology* **84,** 254-260.

355. Peisley,A. et al. (2011) Cooperative assembly and dynamic disassembly of MDA5 filaments for viral dsRNA recognition *Proc. Natl. Acad. Sci. U. S. A* **108,** 21010-21015.

356. Kersse,K., Bertrand,M.J., Lamkanfi,M. & Vandenabeele,P. (2011) NOD-like receptors and the innate immune system: Coping with danger, damage and death *Cytokine Growth Factor Rev.*

357. Baril,M., Racine,M.E., Penin,F. & Lamarre,D. (2009) MAVS dimer is a crucial signaling component of innate immunity and the target of hepatitis C virus NS3/4A protease *J. Virol.* **83,** 1299-1311.

358. Cui,Y. et al. (2001) The Stat3/5 locus encodes novel endoplasmic reticulum and helicase-like proteins that are preferentially expressed in normal and neoplastic mammary tissue *Genomics* **78,** 129-134.

359. Ireton,R.C. & Gale,M., Jr. (2011) RIG-I Like Receptors in Antiviral Immunity and Therapeutic Applications *Viruses.* **3,** 906-919.

Triantafilou,K., Vakakis,E., Kar,S., Richer,E.A., Evans,G.L. & Triantafilou,M. (2012) Visualisation of direct interaction of MDA5 and the dsRNA replicative intermediate form of positive strand RNA viruses. *Journal of cell science.*